Vol.: 49(2)
June, 2025
ISSN: 0250-4758
Online ISSN: 0973-970X

IJVP-2025

# INDIAN JOURNAL OF VETERINARY PATHOLOGY

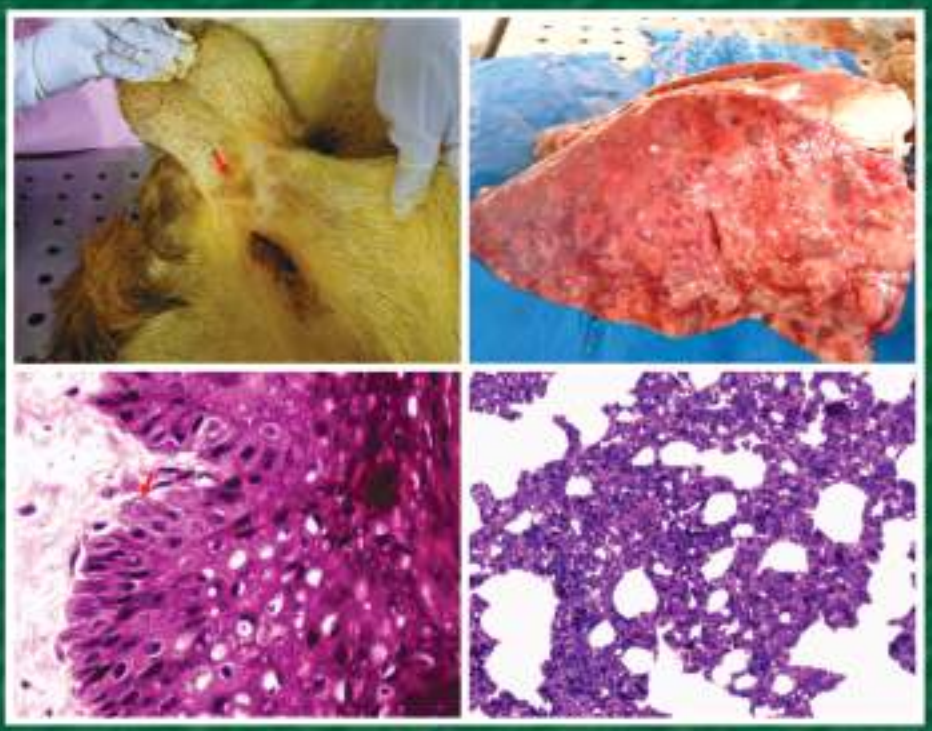

INDIAN ASSOCIATION OF VETERINARY PATHOLOGISTS
(Registered under article 21 of Societies Act 1860)

*Visit us at:* **www.iavp.org**
*Journal available at:* **www.indianjournals.com**

Vol. 49 (2)
June, 2025
ISSN: 0250-4758

# INDIAN JOURNAL OF VETERINARY PATHOLOGY



**Department of Veterinary Pathology, College of Veterinary Science,**
**Sri Venkateswara Veterinary University, Tirupati-517502, Andhra Pradesh**
Mobile: +91-9441185383; E-mail: 7aakumar@gmail.com

# INDIAN JOURNAL OF VETERINARY PATHOLOGY





## Membership Fee and Subscription of Journal

- Individual life membership — Rs. 3,000/- (India) — US$ 600/- (Foreign)
- Individual Annual Membership (for foreign only) — US $ 60/- (with free online access; no hard copy of journal)
- Library, Institutions, etc. (Annual) — Rs. 12,000/- (India) — US$ 400/- (Foreign)
- Individual Patron of IAVP — Rs. 1,00,000/- (Life member - paid patron for 5 years)
- Govt./Non-Govt./Corporate/ Institution Patrons — Rs. 5,00,000/ (for 5 years)

## Advertisement Tariff

| | Black and White | Full Colour |
|---|---|---|
| Regular full page | Rs. 4,000 | Rs. 6,000 |
| Regular half page | Rs. 2,000 | Rs. 3,000 |
| Inside front & back cover page | – | Rs. 10,000 |
| Back cover page | – | Rs. 15,000 |

**Note:**

- Those submitting advertisement for two/four/six issues of the IJVP will be extended 15%/20%/25% discounts, respectively, on the above rates.
- The membership fee must be paid through Cash/Online/Crossed cheque or DD in favour of Treasurer "Indian Association of Veterinary Pathologists" payable at SBI, CARI Branch, Bareilly.

# Contents

INDIAN JOURNAL OF VETERINARY PATHOLOGY

# INDIAN ASSOCIATION OF VETERINARY PATHOLOGISTS
## (Estd. 1974)



**Cover Page Photo (Clockwise) : Sheep Pox :** Photograph showing multiple raised firm circular nodules on the skin at the base of scrotum (Left top), lungs showing multiple and confluent greyish, round, firm nodules with hyperaemic borders (Right top), photomicrograph of skin showing intracytoplasmic eosinophilic inclusions in the hyperplastic epithelial cells (Left bottom) and lungs showing subacute interstitial pneumonia (Right bottom).

*Indian J. Vet. Pathol., 49(2) : 107-121, 2025: DOI: https://doi.org/10.56093/sds1m252*

REVIEW ARTICLE

# The future of Veterinary Pathologists in current scenario of artificial intelligence

**C. Balachandran**
Tamil Nadu Veterinary and Animal Sciences University, Chennai, India

**Address for Correspondence**
*C. Balachandran, Retired Professor of Veterinary Pathology, Former Vice-Chancellor, Tamil Nadu Veterinary and Animal Sciences University, Chennai, India, E-mail: balachandran.path@gmail.com*

*Received: 13.4.2025; Accepted: 20.5.2025*

**How to cite this article :** Balachandran, C. 2025. The future of Veterinary Pathologists in current scenario of artificial intelligence. Indian J. Vet. Pathol., 49(2) : 107-121.

*We are in an era of rapid change and Veterinary Pathology can and will remain one of the leading biomedical discipline, provided recognize forces around and maintain our currency*[1].

Veterinary Pathology is the branch of pathology concerned with the investigation of disease and disease processes in non-human species. Veterinary pathology is a multifaceted field within veterinary medicine that focuses on diagnosing diseases in animals, a foundational discipline for maintaining animal health and, by extension, human health. Veterinary pathology encompasses diagnostic, research, and preclinical facets, each serving a critical role in understanding and managing animal diseases. Diagnostic veterinary pathology is concerned with the examination of tissues, body fluids, and organs to diagnose diseases in animals. Veterinary pathologists play a crucial role in identifying and characterizing diseases, aiding in treatment decisions and disease management. Research veterinary pathology relates to investigating the mechanisms, causes, and treatments of diseases in animals contributing to advancing veterinary medicine, developing new therapies, and understanding disease processes. Preclinical veterinary pathology plays crucial role on assessing the safety and efficacy of pharmaceuticals, chemicals, and other interventions in animals before they are applied clinically minimizing risks to animal and human health. It underpins all aspects of clinical disease management in veterinary medicine and is essential to biomedical research, human and animal drug development and animal health surveillance, which protects human food supplies.

Veterinary Pathologists are veterinary surgeons who usually have post-graduate training in clinical or anatomic pathology. Veterinary anatomic pathology is concerned with the investigation of pathological changes in tissues, and veterinary clinical pathology is concerned with the investigation of changes in body fluid or cellular samples. Veterinary pathologists tend to specialize in particular species groups, including laboratory animals, small domestic animals, large domestic animals, fish, exotic species and birds, also veterolegal cases. We are a group with tremendously diverse interests and expertise that includes basic and clinically applied research, drug discovery and preclinical toxicologic testing, diagnostic testing and quality assurance, public health and governmental policy, public outreach, and education.

Our diversity of interests is both a strength and a challenge[2]. The veterinary pathology discipline is experiencing dramatic changes. The diagnostic techniques used by veterinary pathologists are incorporating new methodologies with a focus on molecular detection, digitalisation and the incorporation of digital analysis and artificial intelligence. New technologies are also being used in research pathology, to understand the pathogenesis of disease and to be in line with the 3Rs[3].

As per FAO, animal diseases can have a devastating impact on animal production, livestock and its products trade, food security, livelihoods and consequently, on the overall process of economic and social development, emphasizing veterinary pathologists' role in disease diagnosis and control.

**Diagnosis**

*Future research in veterinary pathology should focus on the development of low-cost, high-accuracy diagnostic tools and the integration of AI to aid in rapid and precise diagnoses*[4].

The bases for diagnosis of diseases are history, clinical signs, physical examination and using appropriate laboratory tests. Role of Veterinary Pathologists changing rapidly, and they play vital role in finding anatomical changes *viz.* i. necropsy (Gk: *Nekros*-Dead; *opsis*-Sight) diagnosis and ii. microscopical findings in spontaneous diseases and reading experimentally induced lesions in laboratory animals. Pathologists should develop the art of differential diagnosis and help clinicians for prognosis. There is a call for

international guidelines for veterinary tumour pathology. The authors felt that this initiative (a continuation of efforts published in veterinary pathology journal in 2011) will facilitate collaboration and reproducibility between pathologists and institutions, increase case numbers, and strengthen clinical research findings, thus ensuring continued progress in veterinary oncologic pathology and improving patient care. Synoptic reporting as opposed to narrative reporting will facilitate reporting specific pieces of prognostically relevant data in a discrete[5].

Third dimension being impact of molecular biology, veterinary pathologist felt it e.g. neoplasms, altered genes, rearrangements of genes, surface receptors like identifying lymphoid tumours, T or B cell lineages, intracellular markers, neoplasms producing polypeptide hormones or histologically relevant receptors cannot be identified morphologically. Further developments in future will reflect on advances in tissue handling, technology, application of molecular biology in pathology and greater use of telepathology in teaching, quality assurance and continuing veterinary education for professional development. Hence, veterinary pathology is increasingly integrated and interdependent. Making final diagnosis by veterinary pathologists involve microbiologists, parasitologists, toxicologists, radiologists, immunologists and clinicians. We should be aware of local settings like small holdings or farms-Dairy, sheep/goat or large highly commercialized poultry/dairy farms. Hence, diagnosis starts from local investigation to the involvement of District/State/University laboratories, national referral laboratories. Identification of markers and developing relevant diagnostics, treatment protocols and vaccines are important in veterinary medicine. Poultry disease diagnosis is complicated since most diseases are multifactorial. In poultry, the market adopts various strategies for preventing the diseases rather than treatment.

**Electron microscopy**

Ultrastructural studies also provide information on presence of viruses and their structure which will help in identifying the virus. Morphology of other organisms are discernible in detail[6].

**Histochemistry**

Special stains can bring about the features of causative organisms such as Gram's staining for bacteria acid fast-tubercle bacilli, silver stain for leptospires, GG and PAS for fungi[7] and so on.

**Immunohistochemistry (IHC)**

Under the action of invisible ultra violet light (350-400 nm wavelength) acting as an exciting light, the different cellular components re-emit variable lengths of visible light waves according to their molecular density. Primary Ab to specific cell components (Ag) are exposed to secondary Ab directed against the primary Ab. The secondary Ab is linked to peroxidase or avidin biotin peroxidase complexes. The peroxidase catalyzes a reaction in presence of dye which precipitates on the complex. Ag-Ab binding is demonstrated with a coloured histochemical reaction visible by light microscopy or flurochromes with UV light. The use of immunoperoxidase staining is rapidly expanding with the increasing number of new commercially and non-commercially available specific Ab. The choice of Ab depends on the nature and amount of the available specimen and the intended differential diagnosis. Molecular markers, antibody against organism can identify the pathogens *in situ* and location can also be identified-intra- and/or extracellular[8].

**IHC: Molecular tumour markers**

Markers against intermediate filaments identify type of cells (Cytokeratin-Epithelium; Vimentin-Fibroblasts; Desmin-Muscle; Glial fibrillary acidic protein-GFAP-Glial cells; Neurofilaments-Neural origin-These just identify the cells not the tumour), malignancy (Caveolin-Adenocarcinoma of mammary gland[9], Ki67, hormone receptor markers ER, PR, recurrence/metastasis-CSC[10], PCNA[11], Caspase 3-Apoptotic marker, TWIST 1-Metastatic marker (Upregulates N-cadherin and downregulates E-cadherin expression Induce metastasis, angiogenesis, EMT and chromosomal instability, Negatively associated with p53 protein); Cathepsin D-Metastatic marker-E-cadherin, proteolytic action by degrading the cysteine cathepsin inhibitor cystatin C-Attacks basement membrane, digest extracellular matrix, liberates growth factors, increase angiogenesis and results in metastasis, proapoptotic-Bax, antiapoptotic-BCL2, arginase-1-Hepatic tumour etc.[12,13].

IHC markers in different types of the tumours: Mammary tumor: Ki-67, CK 7, 18, 5, 8, ER, HER 2, Bcl-2, p63; Pancreatic cancer: CK19, Colo-rectal cancer: CK 7, 20; Stomach cancer: SMA, CD 34; Oral cancer: EGP-40; Bladder cancer: CK 7, 20, 14, GATA-3; Liver tumor: GP-73, TAG-72; Kidney tumor: PAX-2, 8, CD-10.

Epithelial-mesenchymal transition is the loss of epithelial characteristics and the acquisition of a mesenchymal phenotype in epithelial cells. Apart from reversible change during embryogenesis and wound healing, it also occurs in malignancy for the acquisition of invasive properties. Cells lose expression of epithelial markers like cytokeratins and E-cadherin and acquire a mesenchymal phenotype, expressing vimentin, N-cadherin[14].

**Cancer stem cells**

Cancer stem cell (CSC) theory: In this model, cancers can be considered an abnormal organ in which the bulk of tumour growth is provided by a small population of

cells, CSCs, that divide asymmetrically to produce more CSCs and a non-tumorigenic population of cancer cells. This asymmetric division is thought to contribute to the heterogeneity of solid tumours. CSCs can be considered to be cells that have the ability to self-renew and are capable of asymmetric cell division. Osteosarcoma: Embryonic stem cells (ESCs)-Oct4, Nanog and STAT3 and the mesenchymal stem cell (MSC) marker Stro-1[11,15].

Solid cancer consists of heterogeneous cells that contain a subpopulation of tumour cells with stem cell properties, including self-renewal capacity, differentiation potential, tumorigenicity in immunodeficient mice, and resistance to chemotherapy and radiation. Such tumour cells, termed CSCs or tumour-initiating cells (TICs), are generated either from mutational events in normal tissue stem cells or from the acquisition of stem cell properties by differentiated cells; these tumour cells exist at the apex of a hierarchy of cancer tissues. In various cancers such as skin, liver, and glioblastoma, CSCs are organized as tree-like hierarchies. CSCs have been shown to drive tumour initiation, recurrence, and metastasis. Morphologically, canine mammary mixed tumours comprise epithelial components, including luminal and/or myoepithelial cells and mesenchymal cells such as osteoblasts and chondrocytes. However, the cellular origin of mammary mixed tumours remains unclear. Based on comparisons of DNA alterations, the cellular components in most mixed tumours are thought to share a common origin, such that the various cell types observed in mixed tumours may originate from common CSCs[16]. A triple immunohistochemistry was done using $CD44^+$ $CD24^-$ and ESA in canine mammary tumour to identify CSC[10]. Use of sphere-forming assay, surface markers, CD24, 44 expression and Aldeflour assay (ALDHA) in CSC in canine mammary tumour was reported[17]. Each molecular mammary tumor subtype corresponds with a different histological type, grade, tumor aggressiveness, and prognosis. This helps to standardize treatment options and to estimate prognosis, but it is still not very precise and further studies are needed[18].

**Experimental pathology/Toxicological pathology/Biomedical research**

Animal models have been fundamental in preclinical and biomedical research for revealing key biochemical and physiologic processes, clarifying disease mechanisms, and translating biomedical discoveries into effective clinical treatments for human disease. Animal models have been critical in the development of history's most seminal breakthroughs in medicine. Although the use of animals in research is widespread and has advanced the understanding of human disease, concerns about the limitations of preclinical animal research and its ability (or often inability) to reliably predict clinical trial success have received considerable attention. Too frequently, historical precedent, availability and funding drive selection of animal models, rather than critical analysis of the model system, and how it can answer the research question[19].

**Gene editing technology**

Gene editing process involves the deletion, insertion, or modification of specific DNA sequences in the genome, allowing the host machinery to repair or modify this defect. Knockouts, knockins, and other manipulations can be generated with this technology. Base editing introduces precise, single nucleotide substitutions in a DNA or RNA strand. Prime editing, a recent technique, unlike base editing, not limited to transition substitutions and allows a broader range of mutations, including insertions and deletions. Prime editors utilize an engineered reverse transcriptase fused to a Cas9 nickase (nicks the DNA strand at precise locations) and a prime editing guide RNA (pegRNA) to introduce edits.

**CRISPR-based diagnostics (nucleic acid detection)**

A common gene editing tool called clustered regularly interspaced short palindromic repeat (CRISPR) is based on the adaptive immune system of bacteria. CRISPR and CRISPR-associated (CRISPR-Cas) adaptive immune systems contain programmable endonucleases that can be leveraged for CRISPR-based diagnostics (CRISPRDx). CRISPR-cas (Caspase) is a low cost, less complex and easy for multiple edits system. It comprises two components i. a guide RNA (gRNA) and ii. Cas9 nuclease, which together form a ribonucleoprotein (RNP) complex. The presence of a specific protospacer adjacent motif (PAM) in the genomic DNA is required for the gRNA to bind to the target sequence. The Cas9 nuclease then makes a double strand break in the DNA (denoted by the scissors). Endogenous repair mechanisms triggered by the double strand break may result in gene knockout via a frameshift mutation or knock-in of a desired sequence if a DNA template is present. The Cas protein is a pair of molecular scissors and gRNA is the GPS that guides it to the appropriate site. In prokaryotes, the gRNA guides the nuclease to viral DNA, but as a biotechnological tool, the design specifications of the gRNA can be altered to target any organism's genome at virtually any location.

Currently, CRISPR-Cas systems can be divided, according to evolutionary relationships, into two classes, six types and several subtypes. The classes of CRISPR-Cas system are defined by the nature of the ribonucleoprotein effector complex: class 1 systems are characterized by a complex of multiple effector proteins, and class 2 systems encompass a single crRNA-binding protein. The design of crRNAs for the different effector proteins used in CRISPR diagnostics follow the same principles as those of other CRISPR applications. Among the diverse CRISPR systems, class 2 systems have primarily been applied for diagnostics, as these systems are simpler to reconstitute.

They include enzymes with collateral activity, which serves as the backbone of many CRISPR-based diagnostic assays. Class 1 systems (such as the type III effector nuclease Csm6 or Cas10) have also been engineered for diagnostics, either in combination with components of the class 2 system or with the native type III complex[20,21,22].

While some Cas enzymes target DNA, single effector RNA-guided RNases, such as Cas13a, can be reprogrammed with CRISPR RNAs (crRNAs) to provide a platform for specific RNA sensing. Upon recognizing its RNA target, activated Cas13a engages in "collateral" cleavage of nearby non-targeted RNAs. This crRNA-programmed collateral cleavage activity allows Cas13a to detect the presence of a specific RNA *in vitro* by nonspecific degradation of labeled RNA.

***Uses:*** CRISPR and similar gene editing tools have been suggested as potential treatments and cures for a variety of conditions including monogenic diseases (cystic fibrosis), metabolic disease (type 2 diabetes), cancer (melanoma), infectious diseases, septic shock, and neurodegenerative diseases (Alzheimer's disease). Challenges: unexpected challenges that sometimes arise that require new approaches and technologies in animal model development and utilization, as illustrated by COVID-19 caused by severe acute respiratory syndrome coronavirus 2 (SARS-CoV2). Institutional research enterprises were largely postponed, supply chains were disrupted, and personal protective equipment was scarce. Opportunities: New types of animal models were developed and new research techniques (single cell transcript analysis) were applied to advance studies on SARS-CoV2 cellular predilection, pathogenesis and therapies[23]. Neurodegeneration Initiative (iNDI) for Alzheimer's Disease and related dementia; potential cell therapies - triple-knockout, hypoimmunogenic 'off-the-shelf' T cells-immunotherapy in multiple disorders while evading any immune response; Development of precise transgenic mouse models for disease progression and therapeutic research in a relatively short span of time[22].

CRISPR gene editing is useful in humanization of mouse models (by replacing specific mouse genome sequences with the human equivalent) which are more physiologically relevant systems than their conventional transgenic counterparts, and key to understanding and treating human diseases and can solve the most difficult of life sciences problems and enable explore dimensions of the genome that have not been studied hitherto. Thus, CRISPR technology is promising in human therapeutics, agricultural biology, biofuels, and basic scientific research.

Modified version of CRISPR is now used for exploring epigenomics as CRISPR complex that is capable of acetylating histone proteins at precise locations dictated by the complex's gRNA has been developed and can correlate relationship between epigenetic markers and gene expression. CRISPR-edited cells are effective tools to generate disease models. CRISPR-based editing of induced pluripotent stem cells (iPSCs) provides a versatile bandwidth to generate isogenic disease models with genetically matched controls allowing high throughput modeling of complex diseases involving multiple genes and mutations[22]. Experimental models on veterinary diseases using cell cultures or molecular technologies e.g. organoid technology, infancy stage. The progress from 2D to 3D culture systems and the incorporation of stem cells into organoids. Insights on experimental and diagnostic pathology given[3].

***Advantages:*** The CRISPR-based diagnostic (CRISPR-Dx), providing rapid DNA or RNA detection with attomolar sensitivity and single-base mismatch specificity. Cas13a-based molecular detection platform has been used to detect specific strains of viruses, distinguish pathogenic bacteria, and genotype human DNA. The reaction reagents can be lyophilized for cold-chain independence and long-term storage, and readily reconstituted on paper for field applications. CRISPR-Dx open new avenues for rapid, robust and sensitive detection of biological molecules. Disadvantages: The sample preparation requires a separate step, and incubation temperatures higher than room temperature necessitate heating devices.

**Zoonotic disease: Rudolf Virchow coined term zoonosis who is father of cellular pathology**

A zoonotic disease is a disease or infection that can be transmitted naturally from vertebrate animals to humans or from humans to vertebrate animals. More than 60% of human pathogens are zoonotic in origin. This includes a wide variety of bacteria, viruses, fungi, protozoa, parasites, and other pathogens. Factors such as climate change, urbanization, animal migration and trade, travel and tourism, vector biology, anthropogenic factors, and natural factors have greatly influenced the emergence, re-emergence, distribution, and patterns of zoonoses. Most humans are in contact with animals in a way or another. As time goes on, there are more emerging and re-emerging zoonotic diseases.

**One health/medicine/pathology-Public health-Comparative pathology**

One Health concerns with human, animal, plant and environment. The American Medical Association and the American Veterinary Medical Association have recently approved resolutions supporting 'One Medicine' or 'One Health' that bridge the two professions. The concept is far from novel. Rudolf Virchow, the Father of Modern Pathology, and Sir William Osler, the Father of Modern Medicine, were outspoken advocates of the concept. The concept in its modern iteration was re-articulated

in the 1984 edition of Calvin Schwabe's Veterinary Medicine and Human Health. The veterinary and medical pathology professions are steeped in a rich history of 'One Medicine,' but they have paradoxically parted ways. The time has come for not only scientists but also all pathologists to recognize the value in comparative pathology, the consequences of ignoring the opportunity and, most importantly, the necessity of preparing future generations to meet the challenge inherent in the renewed momentum for 'One Medicine.' The impending glut of new genetically engineered mice creates an urgent need for prepared investigators and pathologists[24-26].

**Epigenetics and genetics**

The genomes of several animal species have been sequenced and annotated, including dogs, cats and horses. These resources have allowed us to employ genome-wide association mapping to identify genetic abnormalities in inbred animals with simple disease traits that have helped inform similar diseases and normal development in humans. These breakthroughs have in turn resulted in the development of diagnostic tests for the genetic traits, which has potential for reducing disease prevalence. Genetic screening has also revealed associations with specific loci for complex diseases. Further investigation of these loci may lead us to discover causative genes and develop relevant diagnostic tests. Despite the rapid advances in genomic mapping, many challenges remain. For example, we are just beginning to explore epigenetic patterns in animals but lack important tools, such as promoter arrays. We also need more information on cancer genomes in animals.

**Nano-engineering/Nanotechnology**

Nanoparticles defined as particles which measure 1-100 nm, allow unique interaction with biological systems at the molecular level. The burgeoning field of biomedical engineering has rapidly morphed from basic research into translational medicine, with the application of engineering principles to cancer diagnostics, drug delivery, imaging, and infectious disease detection, to name a few application. This field, together with genomic analysis, has ushered in personalized medicine in humans. Application of nanoengineering tools has just begun in veterinary medicine, but the goal of personalized medicine for pet animals is likely to come sooner rather than later. As pathologists, we hold a unique position where we can be both leaders and an integral member of multidisciplinary teams in the charge toward personalized medicine.

There is a critical need for novel immunopotentiators and delivery vehicles capable of eliciting humoral, cellular and mucosal immunity. Various vaccine adjuvants and delivery vehicles are being developed that are approximately nanoscale in size. PLGA and CaP coupled NDV inactivated vaccines elicited stronger and prolonged immune responses in comparison to commercial live vaccine. Nanotechnology and anticancer effects: Effect of aqueous nano-neem leaf extract against mammary tumour was impressive[27] and that of solid nano-lipid curcumin was encouraging against hepatocarcinogenesis[28] in rats.

**Nanotechnology-based strategies for rapid detection**

The advancements in nanotechnology offer innovative solutions to improve current diagnostic strategies for managing infectious diseases. The nanomaterials (1 and 100 nm) have tunable optical, magnetic, electrical, thermal, and biological properties and can be engineered with different shapes, sizes, chemical compositions and surface functionalities. These properties enable them to be exploited for improving the detection of biological molecules or whole pathogens. Nanomaterials, namely Quantum dots (QDs), Gold nanoparticles (GNPs), and Magnetic nanoparticles (MNPs), have been extensively used in developing various *in vitro* diagnostics due to their unique optical, magnetic, electrical and thermal properties. Nanodiagnostics have various detection modalities like fluorescence, surface-enhanced Raman, magnetic, electrochemical, colorimetric, and thermal. Advantages: The nanodiagnostics is rapid, precise, and economical. Disadvantages: Limited use for the clinical samples.

**Regenerative medicine**

Regenerative medicine is the replacement or regeneration of human/animal cells, tissue or organs to restore or establish normal function which is an emerging multidisciplinary field that aims to restore, maintain or enhance tissues and hence organ functions. Regenerative medicine is considered to have the potential for developing new treatments for previously untreatable, or difficult to treat diseases. Regeneration of tissues can be achieved by the combination of living cells, which will provide biological functionality and materials, which act as scaffolds to support cell proliferation. Nanotechnology is not only an excellent tool to produce material structures that mimic the biological ones but also holds the promise of providing efficient delivery systems.

Clinical application of regenerative medicine e.g. replacement of skin for burns patients, wounds, pressure sores or diabetic foot ulcers. Also bone and cartilage regeneration, bladder repair, vascular tissue engineering, the use of stem cells in tissue regeneration, repair of damaged heart muscle following heart attack, restoration of peripheral nerve or spinal cord following injury, regeneration of pancreatic tissue to produce insulin for people with diabetes, to replace lost organ function the stabilization and maintenance of the viability of tissue prior to regeneration, control of environmental contaminants, interfaces between tissues and devices, such as the artificial retina the fate of biomaterials and

implant materials within the environment of the body. Check for biocompatibility and stability.

**Diagnostic Imaging**

The introduction of powerful advanced techniques, such as imaging flow cytometry and histology-directed imaging mass spectrophotometry, is yielding new insights into disease pathogenesis. As dedicated instruments become more commonplace and cost-effective, it will only be a matter of time before these technologies enter the diagnostic realm, the opportunity that these modalities represent. Pinpoint accuracy for infectious disease diagnosis, novel insights into biochemical pathways that lead to pathology - the possibilities are endless.

**Human-wildlife boundaries/conflict**

Human activity continues to encroach upon uninhabited areas perturbing ecosystems and wildlife populations. A consequence of bringing human populations into close contact with previously isolated wild species is the interspecies transmission of infectious disease. Recently seen outbreaks of Ebola and Zika viruses in humans, viruses that have previously been largely restricted to wildlife. Conversely, viruses that are typically considered pathogens of domestic animals, such as canine distemper, have spread into native wildlife, with devastating effects. Technologic advances, such as hydrofracking, have allowed for the increased utilization of previously inaccessible natural resources. Yet, these come at a health cost to animals and humans. Wildlife species are sentinels of environmental changes, the proverbial "canary in the coal mine." The emergence and spread of fungal diseases, such as *Pseudogymnoascus destructans* and chytridiomycosis *(Batrachochytrium dendrobatidis)*, emphasizes our need to be continually and actively vigilant at screening wildlife for environmental changes that may affect human and animal health. Veterinary pathologists will continue to play a vital and prominent role in identification and investigation of these diseases.

**Diagnostics**

Diagnostics can be used in various contexts - testing of symptomatic individuals, at-risk presymptomatic individuals, confirmatory testing, differential diagnosis, testing of patients with previous exposure, surveillance at sites of outbreaks and environmental monitoring (Foundation for Innovative New Diagnostics (FIND). The use case determines the way in which diagnostic tests are used optimally. Different Platforms for Veterinary Diagnostic Kits: Serological diagnostic assays, Nucleic acid-based diagnostic assays a. Hybridization methods, b. Amplification methods, Novel and high-throughput assays, a. Microarray, b. Peptide nucleic acid and aptamers, c. Biosensors, d. Next-generation sequencing-based methods, e. POC diagnostics[29-31] and f. Patented diagnostic technologies.

**Lateral Flow Assays**

Lateral flow assays (LFAs) are point-of-care (POC) devices currently used for qualitative and semi-quantitative diagnosis in non-laboratory settings. The parts of a LFA include sample application pad, conjugate pad, nitrocellulose membrane and adsorption pad. Nitrocellulose membrane is imprinted with test and control lines[32]. Pre-immobilized reagents on the LFA become active upon flow of liquid sample and buffer inducing immune complex formation. Since one of the reagents is coupled with a reporter dye such as colored latex or colloidal gold, concentration of this tagged reagent in a narrow zone exhibits itself as a colored line. Advantages: Single step assay, rapid, user friendly, no instrumentation required and long term stability. Disadvantages: Low sensitivity, qualitative and difficult to optimize.

**Enzyme Linked Immunosorbent Assay (ELISA)**

ELISA is one of the most commonly used protein-based assays to detect the presence of an antibody or an antigen in a sample. Different ELISA platforms are available for detection of antigen or antibody. The immune capture or sandwich ELISA uses capture and detecting antibodies (either specific MAbs or polyclonal antibodies) and is used for antigen detection. The Competitive ELISA (cELISA) is used to detect or quantify antibody/antigen using a competitive method[33]. The cELISA for detection of specific antibodies has largely replaced the Indirect (iELISA) for large-scale screening and sero-surveillance. Advantages include that it is a rapid, scalable and specific assay, very useful for mass screening, qualitative or quantitative means and objective result interpretation. Limitations are that these, highly variable, needs skilled personnel, stability of reagents and needs specific equipment such as ELISA reader.

**Polymerase chain reaction (PCR)**

PCR is an enzymatic amplification method that permits amplification of an exact DNA fragment from a complex pool of DNA[29,34]. PCR can be performed using DNA from various sources including tissues, microbes, fluid samples, swabs, semen etc. Only trace amounts of DNA is required for PCR. Advantages: Quick, reliable, sensitive, relatively easy and specific. Limitations: Need for equipment, aerosol contamination leading to false positive results, possibility of cross reactivity and non-specific amplification.

**Quantitative real time PCR**

Real time PCR (qRT-PCR) has become a handy tool for disease diagnosis, identification of species, quantifying gene expression and monitoring viral loads during therapy. A DNA binding dye for real-time detection allows PCR amplification to be monitored. However, the DNA binding dyes does not distinguish between signals generated by either specific or non-

specific products. Thus, any mispriming events that lead to spurious bands observed on electrophoretic gels will generate false positive signal when a generic DNA binding dye is used for real-time detection[35,36].

Real-time systems for PCR were improved by probe-based, rather than intercalator-based, PCR product detection. The fluorogenic probe is an oligonucleotide with both a reporter fluorescent dye and a quencher dye attached. While the probe is intact, the proximity of the quencher greatly reduces the fluorescence emitted by the reporter dye. If the target sequence is present in the template, the probe anneals downstream from one of the primer sites and is cleaved by the 5' nuclease activity of *Taq* DNA polymerase as this primer is extended. This cleavage of the probe separates the reporter dye from quencher dye, increasing the reporter dye signal. Cleavage removes the probe from the target strand, allowing primer extension to continue to the end of the template strand. Thus, inclusion of the probe does not inhibit the overall PCR process. Additional reporter dye molecules are cleaved from their respective probes with each cycle, affecting an increase in fluorescence intensity proportional to the amount of amplicon produced. The advantage of fluorogenic probes over DNA binding dyes is that specific hybridization between probe and target is required to generate fluorescent signal. Thus, with fluorogenic probes, non-specific amplification due to mis-priming or primer-dimer artifact does not generate signal. Another advantage of fluorogenic probes is that they can be labeled with different, distinguishable reporter dyes. By using probes labeled with different reporters, amplification of two distinct sequences can be detected in a single PCR reaction. The disadvantage of fluorogenic probes is that different probes must be synthesized to detect different sequences. Advantages: Quantitative, no post PCR processing, TaqMan probe eliminated nonspecific amplification, UDG eliminates carry over contamination, real time, large range of quantitation and more sensitive than PCR[37,38]. Limitations: Costly equipment needed, and presence of PCR inhibitors. Use of qRT-PCR methods for diagnosis of some of the animal and poultry viruses. In situ PCR was also used in rabies diagnosis[39].

**Isothermal Amplification assays**

Isothermal amplification-based tests are generally being used in the detection of pathogen genomes from clinical samples. DNA polymerases with strand displacement activity or DNA polymerases combined with strand displacement enzymes and proteins are being used in the isothermal amplification of DNA/RNA. Isothermal amplification assays with higher temperature requires thermostable reverse transcriptase[40]. There are seven types of isothermal assays for the detection of animal and poultry viruses, of which LAMP is most used.

**Loop Mediated Isothermal Amplification (LAMP)**

It is a widely applied modification of PCR which avoids the need for the expensive thermal cycler and allows the technique to be carried at field level. This methodology uses an auto cycling strand displacement DNA synthesis approach that is done in isothermal condition within a short period of time. In addition, the results of the LAMP can be detected visually and does not require post PCR methodologies. Advantages: Does not require a thermal cycler and can be carried out in a water bath, does not require post amplification procedures for result visualization, results are available in an hour, sensitivity is higher than the regular PCR and tolerance to inhibitory substances. Limitations: Size of the target sequence should not be more than 300 bp, more chances of carry over contamination and need for high strand displacement enzyme[41].

**Imaging flow cytometry (IFC)**

This platform combines the workflow of flow cytometry and fluorescent microscopy. IFC can be used for analyzing the morphology and fluorescence information of not only a single cell but also a population of cells. Morphological and spatial information at single-cell resolution can be obtained using IFC[42]. IFC has been used to study apoptosis in relation to alterations of nuclear morphology and structure, cell cycle progression based on chromatin condensation, protein and molecule translocation and/or colocalization in different cellular compartments, and cytoskeleton structures. Thus, IFC can be a better tool for oncology. Due to the high throughput nature of IFA, analysis of rare cell types like leukemia circulating in blood can be identified. Advantages: Thousands of morphological and spatial properties can be measured from each individual cell. IFC has the capacity to image non-adherent or dissociated cells, hence, bodily fluids like blood, whose structures can be distorted by placement onto a slide. Limitations: Currently the technology is in preliminary stages and requires costly equipment; User-friendly, robust, and standardized workflows that can facilitate machine learning is essential.

**Microarray**

Microarray technology is a general laboratory approach that involves binding an array of thousands to millions of known nucleic acid fragments to a solid surface referred to as a "chip". The chip is then bated with DNA or RNA isolated from a study sample (cells or tissue, organisms). The steps involve isolation/ preparation, hybridization, washing and image analysis. Main types are spotted arrays, in-situ arrays and self-assembled arrays. It may be gene expression microarray and tissue microarray (TMA) and also cDNA based microarray and oligonucleotide based microarray[35,43,44]. Microarray is useful in infectious organisms/toxin and

also lymphoma cell identification and in ALL. Normal or apparently healthy samples are used along with affected tissue to compare the results.

**Next generation sequencing (NGS)**

NGS also referred to High-thorough put sequencing encompasses all modern sequencing technologies that can sequence large number of genes or whole genome in short time, simultaneously at an affordable cost. The generations of sequencing include: First Generation - Sanger sequencing; Second generation - Pyrosequencing; Third generation - Single molecule fluorescent sequencing, Nanopore; Fourth generation - genomic analysis directly in the cell. While whole genome sequencing of individual microorganisms/isolates was once the primary target for microbial NGS technologies, the substantial increase in throughput has led to the adoption of metagenomic sequencing approaches for disease diagnosis. This possibility to rapidly identify the entire microbial content of a target sample provides a unique and novel strategy for pathogen detection and identification. Compared to the targeted approaches such as PCR or qPCR, metagenomic approaches are less biased and require no prior knowledge of the pathogen involved. In addition, metagenomic data also allows for the detection and identification of antibiotic resistance genes and virulence factors that can be used to guide treatment options and improve antibiotic stewardship. As NGS technology matures, it has the potential to be used in routine diagnosis clinically[45].

**Proteomics**

Protein expression represents the accumulation or end product of genetic information. DNA is transcribed into RNA which is then translated into proteins often phosphorylated the global understanding can be both qualitative and quantitative and can western blotting, immunohistochemistry and various novel non-candidate proteomic approaches. Proteomics, the main tool for proteome research, is a relatively new and extremely dynamically evolving branch of science, focused on the evaluation of gene expression at proteome level. Proteome is a set of proteins in a given time and space, as its composition may vary from tissue to tissue or even from cell to cell. A protein, the basic unit of a proteome, is a molecule composed of single amino acids, further forming secondary, tertiary, and quaternary three-dimensional structures. The rapid development of proteomics was made possible by progress in analytical instrumentation, especially in mass spectrometry (MS) with the introduction of new, cutting-edge types of mass spectrometers and improvements of soft ionization techniques. Although the amino acid sequence is defined by the appropriate gene, the genetic information itself cannot provide the complete information about a protein. In contrast to the stable, rigid, single-dimensional genomic information based on a combination of four nucleotides, the information encoded in proteins is not exclusively limited to the amino acid sequence. Thus, protein expression in a two-dimensional polyacrylamide gel electrophoresis (2D) is a technique used to separate proteins by both their isoelectric point (pl; in the first dimension) and by their mass (second dimension)[46].

**Biomarker**

A biomarker is a characteristic one that is objectively measured and evaluated as an indicator of normal biologic or pathogenic processes or pharmacological responses to a therapeutic intervention. It may be also defined as an *in vivo* derived molecule present at levels deviating significantly from the average in association with specific conditions of health. A biomarker is a characteristic that is objectively measured and evaluated as an indicator of normal biologic or pathogenic processes or pharmacological responses to a therapeutic intervention (FDA). It may be also defined as an *in vivo* derived molecule present at levels deviating significantly from the average in association with specific conditions of health[47].

**Biosensor**

Biosensor recognizes a target biomarker, characteristic for particular pathogen, via an immobilized sensing element called bioreceptor (monoclonal antibody, RNA, DNA, glycan, lectin, enzyme, tissue, and whole cell). The bioreceptor is a crucial component as its biochemical properties assure high sensitivity and selectivity of the biomarker detection and permit to avoid interferences from other microorganisms or molecules present in the tested sample. The specific biochemical interaction between the biomarker and the bioreceptor is converted into a measurable signal by the transductor signal recording and display should, then, allow qualitative and quantitative pathogen identification. There are two principal challenges to develop a biosensor for pathogen detection: (i) elaboration of a bioassay for biomarker detection, and (ii) improving the robustness of the bioassay to adapt it for applications in field and/or on complex biological samples. Indeed, many bioassays that work well on the bench with purified biomarker molecules fail to detect them in complex media like blood or serum. Different sensing strategies based on DNA receptors, glycan, aptamers and antibodies are presented. Besides devices still at development level some are validated according to standards of the World Organization for Animal Health and are commercially available. Especially, paper-based platforms proposed as an affordable, rapid and easy to perform sensing systems for implementation in field condition are included. In addition, diagnostics of infection disease require high sensitivity since pathogens might spread rapidly before that any clinical sign appears in animals. e.g. *E. coli*, avian

influenza, mycoplasma and other pathogen mastitis, foot and mouth disease, blue tongue, *Clostridium perfringens* toxins[48].

**Emerging diseases**

An emerging disease is a new infection or infestation resulting from the evolution or change of an existing pathogenic agent, a known infection or infestation spreading to a new geographic area or population, or a previously unrecognized pathogenic agent or disease diagnosed for the first time and which has a significant impact on animal or public health (OIE, WOAH). A known or endemic disease is considered to be re-emerging, if it shifts its geographical setting, expands its host range, or significantly increases its prevalence. Otherwise, emerging diseases are diseases that appear in a population for the first time e.g. Avian influenza, african swine fever, lumpy skin disease in cattle or that may have existed previously but are rapidly increasing in incidence or geographic range and re-emergence is the reappearance of a known disease after a significant decline in incidence e.g. glanders.

Most (75%) emerging infectious diseases (EID) are caused by zoonotic pathogens. Factors contributing to EID include population growth, spread in health care facilities, aging population, global travel, and changing vector habitats related to climate change. Environmental changes, human and animal demography, pathogen changes and changes in farming practice are among the factors that lead to emerging diseases. Social and cultural factors such as food habits and religious beliefs play a role too. Re-emergence may happen because of a breakdown in public health measures for diseases that were once under control and can also happen when new strains of known disease-causing organisms appear. Emerging diseases have economic repercussions well beyond their immediate health costs. They may impede trade and travel or cause disproportionate alarm. The answer to the international threat from these diseases is through well-coordinated global surveillance and response.

**Digital pathology - Rudolf Virchow - Father of modern cellular pathology (1858)**

Digital pathology is a transformative approach to pathology that involves the digitization of pathology information, including slides and data. It encompasses the acquisition, management, sharing, and interpretation of pathology data in a digital environment. Slide scanners consist of 4 components i. light source, ii. robotics to move the slide holder, iii. 1 or several objectives, and iv. an associated camera to capture the images (Digitized by high resolution charge-coupled device-CCD camera). Magnifications (Objective lens 2x to 100x). 40x for haematopoietic tumours and subtle cellular changes and 100x for cytological diagnosis. Use of 20x to 1000x objectives and file size doubling mag. 400 MB to 1.6 GB. Scanning time: 5 to 20 minutes. One of the important advantages of digital pathology is that pathological AI-based models can be easily used during the diagnostic process and collection and management of pathologic big data. Pathological big data can be used for learning various AI diagnostic models needed for pathological diagnosis and can be used as various educational materials. Histopathological processing, paraffin embedding, sectioning and staining need to be standardized[49].

Digital pathology helps in quantitative analysis of the WSI, can identify and quantify specific cell types quickly and accurately and can quantitatively evaluate histological features, morphological patterns, and biologically relevant regions of interest (e.g. tumoral or peritumoral areas, relationships between different immune cell populations, areas of expression, presence of metastasis). The challenges of digital pathology include expensive equipment, data security, etc., Real-time reporting demands a fast transfer of data. Strong connections between the internet, laboratory information systems and electronic medical records are necessary for clinical implementation and require new systems of storage due to large file sizes.

Benefits of digital pathology include improved quality, productivity, and innovation. Pathologists are faced with a workforce shortage, and digital technology adoption offers solutions to enhance analysis and collaboration[49-51]. Digital microscopy (DM) can be further separated into robotic microscopy, region of interest (ROI) digital microscopy, or whole-slide imaging (WSI). Visualization of the sample on a computer is the common thread that links these modalities, but they differ in how much of the slide is available for viewing (individual fields, ROIs, or the entire slide) and whether the image is stored (static telepathology, WSI, or ROI scans) or viewed in "real-time" (robotic microscopy)[52].

Digital pathology benefits patient by rapid reference for expert advice on diagnoses, improves laboratory workflow and connectivity and increases flexibility and efficiency of the workforce, helping creation of digital training resources for specialists, improving pathology profession by slide sharing and can combine AI for advancement of pathology services[53].

**Telepathology**

Telepathology, since 2015, as a subset of teleconsulting, is pathology interpretation performed at a distance. Teleconsulting gained prominence during the COVID-19 pandemic as veterinary clinics looked for alternatives to in-person consultation. Telepathology following significant advances in information technology and telecommunications coupled with the pandemic led to unprecedented sophistication, accessibility, and use

of telepathology in human and veterinary medicine. Furthermore, telepathology can connect veterinary practices to distant laboratories and provide support for underserved animals and communities. Despite the widespread use of digital microscopy in large veterinary diagnostic laboratories. But, there is a significant gap in validation of WSI for primary diagnosis and underutilization of telepathology to support postmortem examinations conducted in the field indicating a potential area for service development. Telepathology involves the acquisition of cytologic, hematologic, histologic, or macroscopic images for transmission along telecommunication pathways for diagnosis, consultation, education, and research. This process can include *static* telepathology, also known as offline or store and-forward, and *dynamic* or "real-time" pathology[49].

**Bioinformatics**

Bioinformatics is application of techniques from computer science to problems from biology. Bioinformatics is a key discipline that combines computer science, mathematics, statistics, engineering, and biology to help answer biological issues. To designate the study of informatics processes in biotic systems, Hogeweg and Hesper introduced the word "bioinformatics" in 1970. A field of science that uses computers, databases, math, and statistics to collect, store, organize, and analyze large amounts of biological, medical, and health information. Information may come from many sources, including genetic and molecular research studies, patient statistics, tissue specimens, clinical trials, and scientific journals. It is also called as computational biology. Bioinformatics is conceptualizing biology in terms of macromolecules (in the sense of physical-chemistry) and then applying "informatics" techniques (derived from disciplines such as applied maths, computer science, and statistics) to understand and organize the information associated with these molecules, on a large-scale. Since the publication of the *Haemophilus influenzae* genome, complete sequences for nearly 300 organisms have been released, ranging from 450 genes to over 100,000. As a result of this surge in data, computers have become indispensable to biological research. Such an approach is ideal because of the ease with which computers can handle large quantities of data and probe the complex dynamics observed in nature. Bioinformatics, the subject of the current review, is often defined as the application of computational techniques to understand and organise the information associated with biological macromolecules[54]. Bioinformatics involves structural bioinformatics, drug designing, phylogenetics, computational biology, and gene prediction[55].

**Aims of bioinformatics**

1. Organize biological data in an easy-to-use format that allows biologists and researchers to save and access current data.
2. Create software tools to aid in data analysis and management.
3. To analyze and interpret the results in a biologically meaningful manner using these biological data.
4. To aid pharmaceutical industry researchers in better understanding protein structure those contribute to the development of medicines.
5. In order to enable and assist physicians in understanding the gene architecture that will aid in the recognition and diagnosis of diseases like cancer. The execution of BLAST is fast and reliable, whose search from the query sequence (Query) is compared to the database to be used[56].

***In silico* analysis**

This is also known as computational therapeutics, computational pharmacology. Of scientific experiments or research, conducted or produced by means of computer modelling or computer simulation "in silico analysis of the human genome".

Drug discovery: Pharmacology over the past 100 years has had a rich tradition of scientists with the ability to form qualitative or semiquantitative relations between molecular structure and activity *in cerebro*. To test these hypotheses they have consistently used traditional pharmacology tools such as *in vivo* and *in vitro* models. Computational (in silico) methods have been developed and applied to pharmacology hypothesis development and testing. These in silico methods include databases, quantitative structure-activity relationships, pharmacophores, homology models and other molecular modeling approaches, machine learning, data mining, network analysis tools and data analysis tools that use a computer. In silico methods are primarily used alongside the generation of *in vitro* data both to create the model and to test it. Such models have seen frequent use in the discovery and optimization of novel molecules with affinity to a target, the clarification of absorption, distribution, metabolism, excretion and toxicity properties as well as physicochemical characterization[57].

**Docking**

Docking is a molecular modeling technique designed to find the proper fit between a ligand and its binding site (receptor). Dock pose: A ligand molecule can bind with a receptor in a multiple positions, conformations, and orientations.

**Artificial intelligence**

Artificial intelligence (AI) is intelligence manifested by machines, as opposed to the natural intelligence demonstrated by humans and animals. Machines mimic cognitive function associated with the human mind *viz.*, learning and problem assessment. AI was invented as an academic discipline in 1959. AI is intelligence manifested by machines and has developed into subfields five; i.

Machine learning (ML): ML is the process of utilizing mathematical models of data to make computer learn without direct instruction given. ii. DL (Deep learning) is a promising subfield of machine learning, composed of multiple layers, uses raw data as input, and improves the representations of data. Deep learning algorithms are classified into categories; Convolutional neural network (CNN), Restricted Boltzmann Machines, Auto encoder and Sparse Codingta. iii. Natural language processing (NLP): A subfield of AI concerned with enabling computers to process, understand, and generate human language, iv. Natural language generation (NLG): A subfield of NLP that involves generating humanlike text from structured data. NLG is commonly used for tasks such as chatbots, automated writing, and content generation. v. Computer Vision: The field of AI that deals with enabling computers to interpret and understand visual information from the world, such as images and videos[58-62].

**Bioinspired ML in bioinformatics and applications**

The exponential growth in the size and rate of capture of biomedical data during the "big data" age is posing a challenge to traditional analysis methods. DL, a subset of machine learning methods with biological origins, promises to use massive data sets to find hidden patterns and make precise predictions. ML has a lot of potential for the analysis of biological data sets, as is known. Building complex models that reveal their underlying structure theoretically enabling greater exploitation of the accessibility of increasingly large and high-dimensional data sets. The learned models include advanced properties, enhanced interpretability, and a better knowledge of the structure of biological data[63].

Livestock farming is utilizing AI-based technology to improve cattle welfare and productivity where sensors, cameras and data analytics, are being used by farmers to monitor their livestock's feeding habits, behavior, fertility and the spread of illnesses. Disease diagnosis, predictive analytics, therapy optimization, remote monitoring, behavior analysis and data-driven research are just a few examples of how AI is being employed in animal healthcare[64].

The incorporation of AI-supported surgical robots in veterinary diagnostics has shown promising results in enhancing precision and reducing human error. Exploring the use of machine learning algorithms to predict disease outbreaks and developing standardized protocols for diagnostic procedures are also crucial areas for future study[4]. Integration of AI and ML in veterinary pathology holds great promise. AI algorithms can assist in analyzing necropsy data, identifying patterns, and detecting anomalies that may be overlooked by human observers. This can lead to more accurate diagnoses and a more efficient necropsy process[65].

AI accelerates the pace of veterinary research and drug development. ML algorithms can analyze complex veterinary data and identify potential drug candidates. This expedites the discovery process and contributes to developing novel therapies for various veterinary conditions. The prospects of AI in veterinary science are undeniably transformative, redefining animal healthcare. AI offers a spectrum of benefits from rapid and precise diagnostics to personalized treatment plans and proactive disease management. However, embracing this future requires careful navigation of ethical considerations and a collaborative synergy between human expertise and AI capabilities.

We can tap the transformative potential of AI and ensure a future of improved animal health and well-being. As we unleash AI in veterinary science, a new era of compassionate, data-driven and efficient animal care emerges, promising a healthier future for our animal companions[66].

In recent years, the emergence of AI has led to a new direction in biomedical research, especially in translational research with great potential, promising to revolutionize science. AI is applicable in antimicrobial resistance (AMR) research, cancer research, drug design, vaccine development, epidemiology, disease surveillance, and genomics. The potential impact of various aspects of AI in veterinary clinical practice and biomedical research, as a key tool for addressing pressing global health challenges across various domains were discussed[67].

AI applied on veterinary education in two different cases showed need for further study, improvement and caution. One on suturing skills of veterinary students[68] and another on examination on evaluation of the knowledge level and consistency[69]. In a swine production and machine learning study, a balanced accuracy of 85.3% on any disease in the first system and balanced accuracies (average prediction accuracy on positive and negative samples) of 58.5%, 58.7%, 72.8% and 74.8% on porcine reproductive and respiratory syndrome, porcine epidemic diarrhea virus, influenza A virus, and *Mycoplasma hyopneumoniae* in the second system, respectively, using the six most important predictors in all cases. These models provide daily infection probabilities that can be used by veterinarians and other stakeholders to more timely support preventive and control strategies on farms[70].

**Implementation framework that can support veterinary practices in adopting AI[71]**

1. Establish an AI implementation team consisting of stakeholders across the organization.
2. Ensure appropriate training of team members to understand AI basics.

3. Define the use case or purpose of the AI system.
4. Determine data needs, availability, and quality.
5. Develop or procure the appropriate model.
6. Consider ethical and legal obligations.
7. Create an implementation plan (a) Training and engagement; (b) Ongoing monitoring.
8. Manage change.
9. Stay relevant.

**AI applications in veterinary medicine**

Epidemiology and population health: To collect and analyze massive amounts of data, perform disease surveillance tasks, and predict disease outbreaks. Livestock production: Disease detection, behavior recognition, environmental management, and growth evaluation, to score teat ends and lameness in dairy cows, predict calving based on behavior and assess meat quality in production animals. Image analysis in tissue and cytological samples-Storage and archiving. Clinically to predict the need for surgery and survivability in colicking horses by using history and clinical information. NN: Predict the onset of chronic kidney disease within 12 months in cats with 88% accuracy. NNs: Classification of the severity of canine ulcerative keratitis based on corneal photographs. To perform the time-intensive task of converting written medical records to digital documents or searching digital documents for keywords or phrases. AI and ML are also used in biomedical and translational research settings and 3D printing of biological materials[72].

**AI applications in veterinary pathology**

***Image analysis:*** AI analyzes images, aiding pathologists in identifying abnormalities and diagnosing diseases, including tumor detection, cell classification, and quantification of features. Identify subtle patterns and abnormalities that may not be apparent to the human eye; reduce interpretation variability by standardizing analysis methods and criteria; reduce workload and improve turnaround times; able to reduce fatigue by reducing the need for laborious or repetitive tasking e.g. mitotic figures or cell counts, measuring nuclear or cell diameters), or searching for fine details like binucleated or multinucleated cells amongst neoplastic mononuclear cell populations. Pattern recognition: AI recognizes patterns, aiding pathologists in identifying disease trends, correlations, and biomarkers, particularly useful for research uncovering disease mechanisms. Diagnostic assistance: AI systems can serve as diagnostic aids, providing pathologists with second opinions and assisting in decision-making. Predictive modeling: AI can help predict disease using patient history, lab results, and imaging, helping pathologists anticipate progression and tailor treatments for better outcomes. AI-based telepathology systems can overcome geographical barriers by enabling remote consultation and diagnosis[58].

**AI offers five crucial benefits to veterinary pathologists**

1. *Enhanced accuracy:* AI algorithms can analyze large volumes of data with high precision, leading to more accurate diagnoses and prognoses.
2. *Time savings:* AI automates repetitive tasks, allowing pathologists to process samples and interpret results more quickly.
3. *Improved productivity:* With AI handling routine tasks, veterinary pathologists can devote more time to complex cases, research endeavors, and professional development.
4. *Consistency:* AI ensures consistency in diagnostic interpretation by standardizing analysis methods and criteria. This consistency is particularly valuable in multicenter studies and longitudinal research projects, where uniformity is essential for accurate comparisons and conclusions.
5. *Expanded knowledge base:* AI facilitates the aggregation and analysis of vast amounts of data from diverse sources, leading to the discovery of new disease markers, therapeutic targets, and treatment strategies[58].

**Ethics in AI**

Ethical issues for veterinary AI are accuracy and reliability, over diagnosis, transparency, data security, trust and distrust, autonomy of clients, information overload and skill erosion, responsibility of AI-influenced outcomes, environmental effects. Ethical guidance is in the interest of ethicists, veterinarians, clinic owners, veterinary bodies and regulators, clients, technology developers and AI researchers[73].

**Future prospects, perspectives, contributions of Veterinary Pathology/gists**

Work as a veterinary pathologist in interdisciplinary biomedical research teams offers exciting opportunities to impact human and animal health. Projects and discoveries may be directly translatable to the clinic in terms of improved diagnostic strategies or novel therapeutics, truly making a difference in many lives. Future comparative veterinary pathologists will continue to play important roles in identifying and researching emerging diseases and pandemics, critically assessing and developing models to meet these and other challenges. The recent SARS-CoV2 pandemic illustrates the need for new models and approaches for emerging diseases, as well as roles for comparative pathologists in developing and interpreting the models to develop and qualify vaccines and other interventions with rigor and efficiency. When global events impact society, as in 2020, pathology provides mission critical insights into feasible solutions. With these challenges come significant opportunities for pathologists to advance our roles and opportunities in biomedical research and pharmaceutical drug development, and beyond[23].

Virtual microscopy is increasingly applied in all fields of pathology and poses a unique chance to improve the performance of pathologists as diagnosticians, researchers, and teachers, despite all current minor weaknesses. Major advantages of DP and WSI include remote and off-site access to digitalized slides, easy handling, improved ergonomics, and quantitative measurements. Although digital veterinary pathology is in its fledgling stage, automated image analysis will improve in the next decade and will certainly facilitate and broaden the pathologist's work by providing higher reproducibility and reliability of qualitative and quantitative diagnoses. These innovations will inevitably influence the pathologist's routine workflow regardless of whether we are skeptics or promotors of digital pathology. Current and future pathologists should therefore learn and be taught information technologies and image editing to keep up with the inevitable digitization of their profession[49].

In the field of veterinary and toxicologic pathology (few publications, acceptance of regulatory authorities, GLP), evidence for acceptable diagnostic concordance of DM is largely lacking and further validation study publications are needed, especially for specific applications in our fields[50]. There are gaps in the literature on the use and validation of telepathology in veterinary medicine despite the widespread use of DM by private veterinary diagnostic laboratories[52].

**Consensus statements and standardization of testing (One Pathology)**

New guidelines for our vast array of assays, such as cytologic/histopathologic tumor grading, clonality assays and reporting, and flow cytometric methods. These guidelines should be grounded in evidence-based medicine and have a built-in plan for re-evaluation. American Society of Veterinary Clinical Pathology has given guidelines and consensus statements for several diagnostic activities, including reference interval establishment, prognostic markers in cancer, flow cytometric reporting in canine hematopoietic neoplasia, immunocytochemical staining, and viscoelastic-based hemostasis testing etc. Similarly, cytologic and histologic grading schemes have been proposed for various tumors. Importantly, these guidelines are the culmination of efforts of multiple investigators and truly represent a global approach ("One Pathology"). Their frequency of citation and routine application during diagnostic testing attests to the usefulness of these guidelines.

**Recommendations to Veterinary Pathologists**

1. Training on statistical analysis and experimental design that helps in data analysis.
2. Developing skill in the use of micro-computational resources designed to allow them to collect and interpret large bodies of data.
3. Develop and standardize a) a discipline-wise nomenclature for all lesions, and b) terms for semiquantitative expression of lesion severity.
4. Using quantitative methods in morphology to provide as secure a quantitative base as possible for lesion occurrence, size, degree of organ involvement, severity of lesion etc[1].

To meet increased pressures councils like ICVP, ACVP, ECVP, JCVP, RCVP etc. to update knowledge by

1. Conducting annual education programme-Continuing education on one topic.
2. Training programmes for speciality groups.
3. Short courses including laboratory techniques and methods to complement diagnostic process.
4. To share spontaneously occurring lesions including experimentally induced.

Scope of employment for veterinary pathologists is wide, Dept Animal Husbandry - Veterinary Assistant Surgeons (Specialist post - IAVP propose to Governments), Teaching profession Universities - Assistant Professor - Professor), Lab animal facilities: Institutes (Central), CROs, pharmaceuticals - Veterinary Officers/Researchers/ preclinical toxicology/drug discovery National-ICAR/ ICMR - Scientists, Fisheries, Self-employment, private organizations - Lab and abroad etc.

Considering various opportunities available as discussed veterinary pathologists need to develop day one skills, necropsy, gross pathology, histopathology, clinical pathology, veterolegal cases, wild animal pathology, one health, zoonotic diseases, aquatic animal pathology, molecular methods to imbibe methods in currency like digital pathology, telepathology, AI, drug discovery and in future. These skills will immensely help veterinary pathologists in getting employed.

*Machine Learning and Veterinary Pathology: Be Not Afraid!* [58].

## REFERENCES


1. Shadduck JA. 1989. Editorial: Future directions in veterinary pathology. *Vet Pathol* **26:** 353-355.
2. Stokol T. 2016. Veterinary Pathology - A path forward with new directions and opportunities. *Front Vet Sci* **3:** 76.
3. Salguero FJ. 2024. Editorial: Insights in veterinary experimental and diagnostic pathology. *Front Vet Sci* **11:** 1437289.
4. Orakpoghenor O. 2024. Problems in veterinary pathology: A focus on diagnosis. *European J Sci Res Rev* **1:** 103-111.
5. Meuten DJ, Moore FM and Donovan TA. 2021. International guidelines for veterinary tumour pathology: A call to action. *Vet Pathol* **58:** 766-794.
6. Hemalatha S, Manohar BM, Chandramohan A, Balachandran C and Sundararaj A. 2006. Ultrastructural changes of infectious bursal disease in chicken. *Indian J Vet Pathol* **30:** 77-78.
7. Lakshman M, Nagamalleswari Y and Balachandran C. 2010.

Cutaneous mycotic granuloma (Dermatomycosis) in fowl - A pathomorphological observations. *Indian J Vet Pathol* **33:** 204-206.
8. Hemalatha S, Manohar BM and Balachandran C. 2009. Sequential immunodetection of infectious bursal disease virus antigen in experimental chicken. *Indian J Vet Pathol* **33:** 82-84.
9. Debiprasanna Das, Balachandran C, Hemalatha S and George RS. 2011. Diagnostic and prognostic significance of expression of caveolin-1, c-erbb2 and brca1 in canine mammary neoplasms. Paper presented in XXVIII IAVP Conference, Chennai.
10. Anjankumar KR, Sudhakar Rao GV, Balachandran C, Murali Manohar B, Dhananjaya Rao G, Uzama S and Shammi M. 2014. Immunohistochemical expression of CD 44, CD24 and ESA in canine mammary tumours. *J Cell Tissue Res* **14:** 4193-4199.
11. Thangathurai R and Balachandran C. 2017. Pathomorphology and prognostic survival analysis of bitches with recurrent and metastatic mammary tumours. *Indian Vet J* **94:** 51-53.
12. Kaszak I, Ruszczak A, Kanafa S, Kacprzak K, Król M and Jurka P. 2018. Current biomarkers of canine mammary tumors. *Acta Vet Scand* **60:** 66.
13. Gherman L, Isachesku E, Zanoaga O, Braicu C and Berindan IN. 2024. Molecular markers in canine mammary tumors. *Acta Veterinaria-Beograd* **74:** 159-182.
14. Ramesh R, Anand Kumar CT, Balachandran C and Shafiuzama M. 2017. Identification of metastatic potential of mammary tumour in dogs. Presented in Asian Veterinary Pathology Congress-XXXIV IAVP Conference, Bengaluru.
15. Wilson H, Huelsmeyer M, Chun R, Young KM, Friedrichs K and Argyle DJ. 2008. Isolation and characterisation of cancer stem cells from canine osteosarcoma. *The Vet J* **175:** 69-75.
16. Zhou H, Tan L, Liu B and Guan XY. 2023. Cancer stem cells: Recent insights and therapies. *Biochem Pharmacol* **209:** 115441.
17. Michishita M. 2020. Understanding of tumourigenesis in canine mammary tumours based on cancer stem cell research. *The Vety J* **265:** 105-560.
18. Kaszak I, O Witkowska-Piłaszewicz, Domrazek K and Jurka P. 2022. The novel diagnostic techniques and biomarkers of canine mammary tumors. *Vet Sci* **9:** 526.
19. Kelly DF. 2007. Pathology-Global challenges in education: Veterinary Pathology in the United Kingdom: Past, Present, and Future. *JVME* **34:** 383-389.
20. Kaminski MM, Abudayyeh OO, Gootenberg J, Zhang F and Collins JJ. 2021. CRISPR-based diagnostics. *Nature Biomed Eng* **5:** 643-656.
21. Peipei L, Wang L, Yang J, Di LJ and Li J. 2021. Applications of the CRISPR-Cas system for infectious disease diagnostics. *Exp Rev Mol Diagnos* **21:** 723-732.
22. Synthego CRISPR ebook 2021. CRISPR 101: Your guide to understanding CRISPR. Publisher Synthego. pp. 1-20.
23. Hoenerhoff MJ, Meyerholz DK, Brayton C and Beck AP. 2021. Challenges and Opportunities for the Veterinary Pathologist in Biomedical Research. *Vet Pathol* **58:** 258-265.
24. Cardiff RD, Ward JM and Barthold SW. 2008. 'One medicine - one pathology': are veterinary and human pathology prepared? *Lab Invest* **88:** 18-26.
25. Rahman T, Abdus Sobur Md, Saiful Islam, Samina Ievy, Md Jannat Hossain, Mohamed E El Zowalaty, Taufiquer Rahman AMM and Hossam M Ashour. 2020. Zoonotic Diseases: Etiology, Impact, and Control. *Microorganisms* **8:** 1405.
26. Grange ZL, Goldstein T and Johnson CK. 2021. "Ranking the risk of animal to human spillover for newly discovered viruses". *Proc Natl Aca Sci USA* **118**.
27. Chavhan SG, Balachandran C, Nambi AP, Dhinakar Raj G and Vairamuthu S. 2023. Assessment of anticarcinogenic potential of neem *(Azadirachta indica)* leaf extract loaded calcium nanoparticles against experimentally induced mammary carcinogenesis in rats. *Toxicol Inter* **30:** 659-674.
28. Madhav Nilakanth Mugale and Balachandran C. 2020. Haematological protective effect of raw extract and nano-*Eclipta alba*-treated rats in experimentally induced hepato carcinogenesis. *Comp Clin Oncol*.
29. Hamond C, Martins G and Loureiro. 2014. Urinary PCR as an increasingly useful tool for an accurate diagnosis of leptospirosis in livestock. *Vet Res Comm* **38:** 81-5.
30. Bergmann M, Zablotski Y, Rieger A, Speck S, Truyen U and Hartmann K. 2021. Comparison of four commercially available point-of-care tests to detect antibodies against canine distemper virus in dogs. *Vet J* **273:** 105-693.
31. Walter-Weingärtner J and Bergmann M. 2021. Comparison of eight commercially available faecal Point-of-Care tests for detection of canine parvovirus antigen. *Viruses* **13:** 2080.
32. Koczula KM and Gallotta A. 2016. Lateral flow assays. *Essays Biochem* **60:** 111-20.
33. Zhao J, Zhu J and Wang Y. 2022. A simple nanobody-based competitive ELISA to detect antibodies against African swine fever virus. *Virol Sin* **37:** 922-933.
34. Green MR and Sambrook J. 2018. The Basic Polymerase Chain Reaction (PCR). *Cold Spring Harb Protoc*.
35. Rhind M. 2002. Veterinary oncological pathology-Current and future perspectives. *The Vety J* **163:** 7-18.
36. Singh C and Roy Chowdhuri S. 2016. Quantitative real-time PCR: Recent advances. *Methods Mol Biol* **1392:** 161-76.
37. Jozwik A and Fryman T. 2005. Comparison of the immunofluorescence assay with RT-PCR and Nested PCR in the diagnosis of canine distemper. *Vet Res Comm* **29:** 347-359.
38. Fagbohun OA, Jarikre TA and Alaka OO. 2020. Pathology and molecular diagnosis of canine parvoviral enteritis in Nigeria: case report. *Comp Clin Path* **29:** 887-893.
39. Ezhil Praveena P, Jayakumar R, Balachandran C, Thirumurugan G, Dhinakar Raj G and Murali Manohar B. 2007. Detection of rabies virus genes by in-situ polymerase chain reaction. *Vet Res Comm* **31:** 775-781.
40. Yan L, Zhou J and Zheng Y. 2014. Isothermal amplified detection of DNA and RNA. *Mol Biosyst* **10:** 970-1003.
41. Maan S, Maan NS and Batra K. 2016. Reverse transcription loop-mediated isothermal application assays for rapid identification of eastern and western strains of blue tongue virus in India. *J Virolo Mds* **234:** 65-74.
42. Doan M, Vorobjev I and Rees P. 2018. Diagnostic potential of imaging flow cytometry. *Trends Biotechnol* **36:** 649-652.
43. Govidarajan R, Duraiyan J, Kaliyappan K and Murugesan P. 2012. Microarray and its applications. *J Phar Bioallied Sci* **4**.
44. Sagar A. 2022. DNA microarray-Definition, Principle, Procedure, Types. Microbe Notes.
45. Satam H, Joshi K and Mangrolia U. 2023. Review. Next-Generation Sequencing Technology: Current Trends and Advancements. *Biology* **12:** 997.
46. Kumaraguruparan R, Karunagara D, Balachandran C, Murali Manohar B and Nagini S. 2006. Of humans and canines: A comparative evaluation of heat shock and apoptosis-associated proteins in mammary tumors. *Clinica Chimica Acta* **365:** 168-176.
47. Tambor V and Fučíková AR. 2009. Application of proteomics in biomarker discovery: a primer for the clinician. *Physiol Res/ Academia Scientiarum Bohemoslovaca* 2009.
48. Vidic J, Manzano M, Chang C and Jaffrezic-Renaul N. 2017. Advanced biosensors for detection of pathogens related to livestock and poultry. *Vet Res* **48:** 11-22.

49. Bertram CA and Klopfleisch R. 2017. The pathologist 2.0: An update on digital pathology in veterinary medicine. *Vet Pathol* **54:** 756-766.
50. Bertram CA, Stathonikos N and Donovan TA. 2022. Validation of digital microscopy: Review of validation methods and sources of bias. *Vet Pathol* **59:** 26-38.
51. Zuraw A and Aeffner F. 2022. Whole-slide imaging, tissue image analysis, and artificial intelligence in veterinary pathology: An updated introduction and review. *Vet Pathol*.
52. Rogers L, Galezowski A and Ganshorn H. 2024. The use of telepathology in veterinary medicine: a scoping review. *J Vet Diag Inves* **36:** 490-497.
53. Battazza A, Brasileiro FCS and Tasaka A. 2024. Integrating telepathology and digital pathology with artificial intelligence: An inevitable future. *Vety World* **17:** 1667-1671.
54. Luscombe LM, Greenbaum D and Gerstein M. 2001. What is Bioinformatics. A proposed definition and overview of the field. *Method Inform Med* **40:** 346-58.
55. Sharma MK, Dhar MK and Kaul S. 2012. Bioinformatics: An introduction and overview. *Intl J Engg Res Dev* **3:** 88-99.
56. Diniz IWJS and Canduri F. 2017. Bioinformatics: an overview and its applications. *Genetics Molec Res* **16:** 1601-9645.
57. Ekins S, Mestres J and Testa B. 2007. In silico pharmacology for drug discovery: methods for virtual ligand screening and profiling. *British J Pharmacol* **152:** 9-20.
58. La Perle KMD. 2019. Machine Learning and Veterinary Pathology: Be Not Afraid! *Vet Pathol* **56:** 506-507.
59. Kour S, Agrawal R, Sharma N, Tikoo A, Pande N and Sawhney A. 2022. Artificial intelligence and its application in animal disease diagnosis. *J Anim Res* **12:** 1-10.
60. Amaral CI, Langohr IM, Giaretta PR and Ecco R. 2024. Digital pathology and artificial intelligence in veterinary medicine. *Braz J Vet Pathol* **17:** 147-151.
61. Appleby RB and Basran PS. 2022. Artificial intelligence in veterinary medicine. *JAVMA* **260:** 819-824.
62. Burti S, Banzato T, Coghlan S, Wodzinski M, Bendazzoli M and Zotti A. 2024. Artificial intelligence in veterinary diagnostic imaging: Perspectives and limitations. *Res Vet Sci* **175:** 105-317.
63. Mandal AK, Sarma PKD and Dehuri S. 2023. *The Open Bioinformatics Journal*.
64. AlZubi AA and Al-Zu'bi M. 2023. Application of artificial intelligence in monitoring of animal health and welfare. *Indian J Anim Res* pp. 1-6.
65. Orakpoghenor O and Terfa AJ. 2024. Necropsy as an important diagnostic step in veterinary pathology: The past, present, and future perspectives. *Res Vet Sci Med* **4:** 1-4.
66. Sharun K, Banu SA, Mamachan M, Abualigah L, Pawde AM and Dhama K. 2024. Unleashing the future: Exploring the transformative prospects of artificial intelligence in veterinary science. *J Exp Biol Agri Sci* **12:** 297-317.
67. Akinsulie OC, Idris I, Aliyu VA and Shahzad S. 2024. The potential application of artificial intelligence in veterinary clinical practice and biomedical research. *Front Vet Sci* **11:** 1347550.
68. Kuzminsky J and Philips H. 2023. Reliability in performance assessment creates a potential application of artificial intelligence in veterinary education: evaluation of suturing skills at a single institution. *AJVR* pp. 1-11.
69. Coleman MC and Moore JN. 2024. Two artificial intelligence models underperform on examinations in a veterinary curriculum. *JAVMA* **262:** 692-697.
70. Halev A and Martinez-Lopez B. 2023. Infection prediction in swine populations with machine learning. *Scientific Reports* **13:** 17738.
71. Basran P and Appleby RP. 2024. What's in the box. A toolbox for safe deployment of artificial intelligence in veterinary medicine. *JAVMA* **262:** 1090-1098.
72. Hennessey E, DiFazio M, Hennessey R and Nicky Cassel N. 2022. Artificial intelligence in veterinary diagnostic imaging: A literature review. *Vet Radiol Ultrasound* **63:** 851-870.
73. Coghlan S and Quinn T. 2023. Ethics of using artificial intelligence (AI) in veterinary medicine. AI & Society Published on May 2023.

*Indian J. Vet. Pathol., 49(2) : 122-126, 2025: DOI: https://doi.org/10.56093/yykr6r11*

RESEARCH ARTICLE

# Prevalence of Ovarian Pathologies in Sheep of Andhra Pradesh: Insights into Reproductive Health

**K. Vishnu[1*], N. Sailaja, A. Nasreen[2] and D. Rani Prameela[3]**

Department of Veterinary Pathology, College of Veterinary Science Tirupati, Sri Venkateswara Veterinary University, Andhra Pradesh, [1]Veterinary Dispensary Mannur, Palakkad, Department of Animal Husbandry, Kerala, [2]Veterinary Clinical Complex, College of Veterinary Science Tirupati, [3]State Level Disease Diagnostic Laboratory, Tirupati

**Address for Correspondence**

*K. Vishnu, Veterinary Surgeon, Veterinary Dispensary Mannur, Palakkad, Department of Animal Husbandry, Kerala, India, E-mail: vishnuk0207@gmail.com*

*Received: 25.1.2025; Accepted: 3.4.2025*

## ABSTRACT

This study investigates the prevalence and characteristics of ovarian pathologies in sheep, focusing on reproductive efficiency's impact on productivity. A total of 212 ovaries from 106 sheep were examined using gross, cytological and histopathological techniques. Of these, 62.26% were normal, while 37.73% exhibited pathological abnormalities, comprising 18.39% neoplastic and 19.34% non-neoplastic conditions. Granulosa cell tumors were the most common neoplastic condition (7.55%), followed by adenomas (4.72%) and hemangiosarcomas (1.89%). Histopathological analysis revealed distinct features, such as Call-Exner bodies in granulosa cell tumors and papillary projections in adenomas. Among the non-neoplastic conditions, follicular cysts were the most prevalent (6.13%), followed by folliculoids (3.77%) and embedded corpus luteum (2.36%). Microscopically, these lesions demonstrated consistent features, such as granulosa cell absence in follicular cysts and fibrous connective encapsulation in embedded corpus luteum. The study highlights significant variations in pathological prevalence between left and right ovaries, with the right ovary more commonly affected. These findings align with existing literature, supporting their diagnostic validity and emphasizing the impact of ovarian abnormalities on reproductive health. By identifying and characterizing these conditions, this research contributes to improved diagnostic accuracy and the development of strategies to enhance reproductive efficiency in small ruminants, ultimately supporting rural livelihoods and food security.

**Keywords:** Follicular cyst, granulosa cell tumor, ovaries, reproductive efficiency

## INTRODUCTION

Livestock production represents one of the fastest-growing agricultural subsectors in developing countries, playing a pivotal role in the economic framework of India[1]. Among various livestock categories, small ruminants hold particular importance for ensuring livelihood security, especially for resource-constrained farmers[2]. These animals serve as a viable alternative to crop farming, contributing to subsistence, economic growth, and food security. Indigenous small ruminant breeds, such as sheep and goats are integral to the rural economy, providing multifaceted benefits through products like wool, meat, milk, skins, and manure. Their adaptability to arid, semi-arid and mountainous regions makes them livelihoods of small and marginal farmers as well as landless laborers[3].

Sheep and goats have been a cornerstone of Indian farming systems for centuries, offering significant economic and environmental benefits compared to larger livestock species. However, the productivity of these animals is heavily influenced by reproductive efficiency, a critical determinant of successful small ruminant production. Reproductive disorders, including infertility, irregular estrous cycles, abortions, fetal mummification and the birth of weak or stillborn offspring, pose substantial challenges. Without timely diagnosis and effective management, these conditions can escalate into widespread epidemics, adversely affecting herd productivity and economic returns[4]. Early detection and control of reproductive diseases rely on advanced diagnostic methods such as ultrasonography, radiology, laboratory analyses, and abattoir investigations. Abattoir studies are particularly valuable in assessing the reproductive health, providing insights into genital tract abnormalities, ovarian cyclicity, and seasonal breeding patterns[5]. This is especially relevant in the context of indiscriminate slaughter practices, which often include gravid animals, due to inadequate ante-mortem examinations. Such practices not only exacerbate prenatal losses but also hinder the ability to meet the growing demand for affordable and high-quality meat[6]. Studies on the female reproductive tract of small ruminants have further highlighted these concerns, revealing a 14.19% prevalence

**How to cite this article :** Vishnu, K., Sailaja, N., Nasreen, A. and Prameela, D.R. 2025. Prevalence of Ovarian Pathologies in Sheep of Andhra Pradesh: Insights into Reproductive Health. Indian J. Vet. Pathol., 49(2) : 122-126.

of ovarian abnormalities, of which 10.48% were neoplastic and the remaining were non-neoplastic[7].

In Andhra Pradesh, small ruminants play a crucial role in rural livelihoods, yet there is limited data on reproductive wastage, seasonal breeding behaviors, ovarian activity and reproductive tract pathologies. Abattoir investigations provide a vital approach in estimating these losses and addressing the underlying challenges. By identifying and mitigating reproductive inefficiencies, such studies can substantially enhance small ruminant production and thereby contribute to food security in rural communities.

## MATERIALS AND METHODS

The study was conducted between June and November 2022. A total of 212 ovaries were collected from 106 sheep of various age groups from slaughterhouses in and around Tirupati, as well as from necropsied animals at the Department of Veterinary Pathology, College of Veterinary Science, Tirupati, and field mortalities. Necropsies were performed according to standard protocols[8].

Impression smears were prepared by making incisions on the ovaries, fixing the smears in 70% methanol, and staining them with Giemsa stain for cytological examination[9]. For histological evaluation, the ovaries underwent gross examination, followed by fixation in 10% neutral buffered formalin. After fixation, the tissues were rinsed in running tap water for a specific duration to remove excess fixative, then processed through a graded series of alcohols for dehydration, cleared in xylene and embedded in paraffin. Thin sections (4-5 μm) were obtained using a Leica manual rotary microtome and carefully mounted onto glass slides. The mounted sections were then deparaffinized, rehydrated through a descending series of alcohol concentrations, and stained with hematoxylin and eosin (H&E) following standard protocols[10].

## RESULTS

In the present study, a total of 212 ovaries from 106 sheep were examined, regardless of age group or breed. Of the 212 ovaries, 132 (62.26%) were normal, while 80 (37.73%) exhibited various pathological lesions. Among the affected ovaries, 39 (18.39%) were neoplastic and 41 (19.34%) were non-neoplastic conditions (Table 1). The prevalence of pathological lesions varied between the left and right ovaries depending on the specific condition, but the right ovaries were found more affected (55%) compared to the left ovaries (45%).

**Table 1.** Prevalence (%) of various pathological conditions in sheep ovaries.

| S. No. | Name of the Pathological Condition | No. of Cases | Prevalence (%) |
|---|---|---|---|
| 1. | Granulosa cell tumour | 16 | 7.55 |
| 2. | Follicular cyst | 13 | 6.13 |
| 3. | Adenoma | 10 | 4.72 |
| 4. | Folliculoid | 8 | 3.77 |
| 5. | Embedded corpus luteum | 5 | 2.36 |
| 6. | Hemangiosarcoma | 4 | 1.89 |
| 7. | Lymphangiectasia | 4 | 1.89 |
| 8. | Luteinized cyst | 3 | 1.41 |
| 9. | Endometriosis | 3 | 1.41 |
| 10. | Adenocarcinoma | 2 | 0.94 |
| 11. | Fibroma | 2 | 0.94 |
| 12. | Clear cell carcinoma | 2 | 0.94 |
| 13. | Angioleiomyoma | 2 | 0.94 |
| 14. | Cystic corpus luteum | 2 | 0.94 |
| 15. | Parovarian cyst | 2 | 0.94 |
| 16. | Hemangiopericytoma | 1 | 0.47 |
| 17. | Ovarian hypoplasia | 1 | 0.47 |
| 18. | Normal ovaries | 132 | 62.26 |
| | Total | 212 | 100 |

Granulosa cell tumor was the most common condition (7.55%), followed by follicular cysts (6.13%), adenomas (4.72%) (Fig. 3), folliculoid lesions (3.77%), embedded corpus luteum (2.36%), hemangiosarcoma (1.89%), lymphangiectasia (1.89%), luteinized cysts (1.41%), endometriosis (1.41%), adenocarcinoma (0.94%), fibroma (0.94%), clear cell carcinoma (0.94%), angioleiomyoma (0.94%), cystic corpus luteum (0.94%), parovarian cysts (0.94%) and the least prevalent conditions were hemangiopericytoma (0.47%) and ovarian hypoplasia (0.47%). Except for follicular cysts (Fig. 1), parovarian cysts (Fig. 2), and hypoplastic ovaries, other conditions did not show any significant gross lesions.

### Prevalence of the ovine ovarian neoplastic conditions

This study identified eight distinct neoplastic conditions, comprising one sex cord tumor, three epithelial tumors, and four mesenchymal tumors. Granulosa cell tumors were the most frequent, accounting for 7.55% of cases (Fig. 3). Histopathology revealed the characteristic intrafollicular radial arrangements of tumor cells encircling the central eosinophilic structures, known as Call-Exner bodies. Adenomas were the second most common, representing 4.72% of cases (Fig. 4). Microscopically, two types of adenomatous conditions were observed, cystadenomas in the ovarian stroma

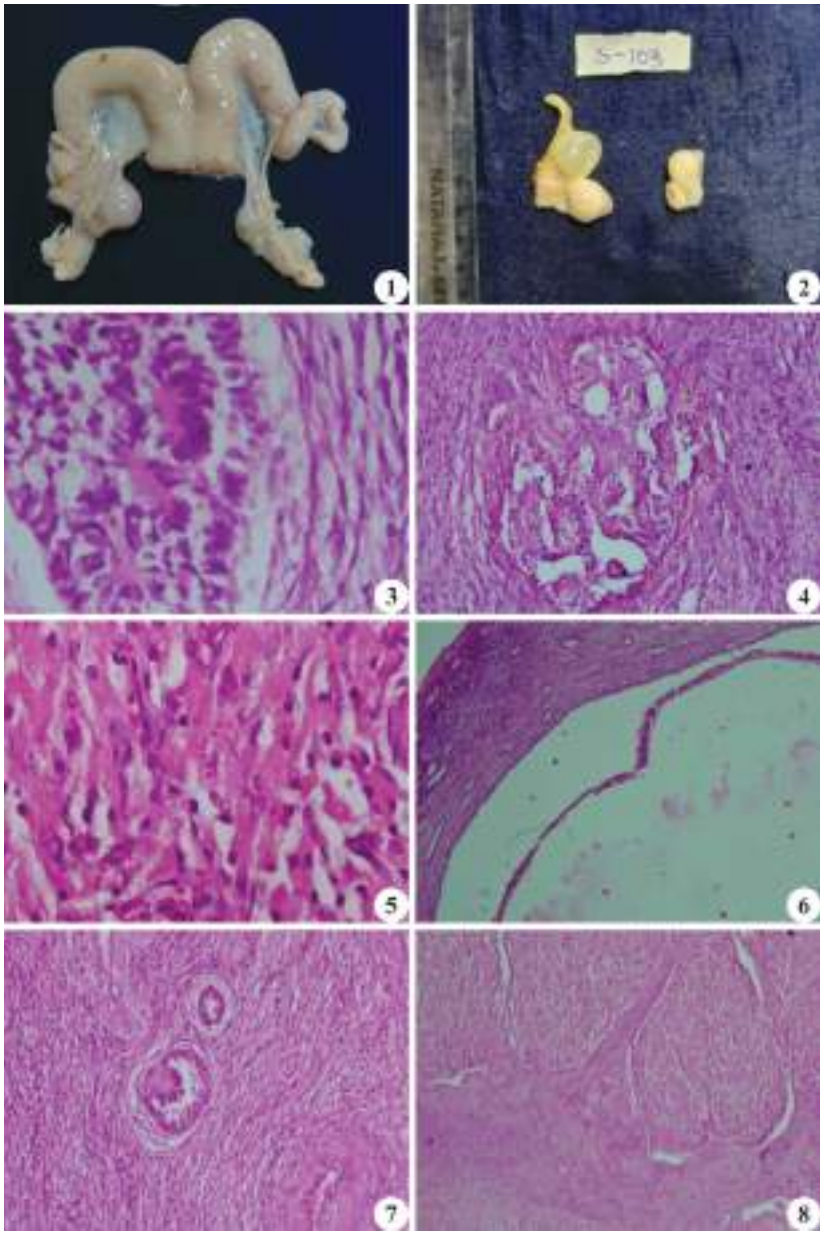

**Fig. 1.** Follicular Cyst: A thin-walled cyst containing transparent fluid, bulging outward from the surface of the left ovary. This structure often represents an anovulatory follicle, which has failed to rupture and release an oocyte; **Fig. 2.** Parovarian Cyst: A thin-walled cystic structure located near the posterior end of the ovary. Parovarian cysts are non-functional remnants of embryological structures; **Fig. 3.** Granulosa Cell Tumor: Neoplastic granulosa cells forming Call-Exner bodies, arranged in a distinctive rosette pattern around eosinophilic material. Histological staining (H&E x40) highlights these features, which are typical of this ovarian tumor type; **Fig. 4.** Adenoma: Neoplastic epithelial cells project into the cystic space, supported by collagenous fibers. The histological section (H&E x10) reveals a benign tumor commonly seen in the ovarian stroma; **Fig. 5.** Hemangiosarcoma: Vascular endothelial tumour with proliferated endothelial cells form cleft-like structures, supported by thin collagen fibers. Some clefts contain red blood cells (RBCs), while others are devoid of RBCs. (H&E x40); **Fig. 6.** Follicular Cyst: A cyst lined by an extremely thin layer of granulosa cells with a compressed thecal layer. The cystic space is highlighted in the low-magnification histological image (H&E x4); **Fig. 7.** Folliculoid: Structures resembling ovarian follicles found embedded in the ovarian stroma. These folliculoid formations are observed in the histological section (H&E x10); **Fig. 8.** Embedded corpus luteum: Connective tissue fibers traversed into the luteal tissue and divided it into a number of lobes (H&E x10).

and cystadenomas of the rete ovarii. In both conditions, neoplastic cells and collagen fibers projected into the lumen of the cystic spaces, with the cystic walls lined by thick collagenous fibers. Hemangiosarcomas accounted for 1.89% of cases (Fig. 5), characterized histologically by multifocal areas of proliferated and thickened blood vessels, with undifferentiated endothelial cells infiltrating the ovarian stroma. Hemangiopericytomas that revealed fingerprint appearance of pericyte were the least common neoplasm, with a prevalence of 0.47%.

**Prevalence of the ovine ovarian non neoplastic conditions**

Among non-neoplastic ovarian conditions, follicular cysts were the most prevalent, accounting for 6.13% of cases. Macroscopically, these cysts appeared as thin-walled, tense structures filled with clear, colorless fluid, measuring 5-8 mm in diameter, and causing ovarian enlargement due to their presence in the cortex (Fig. 1). Microscopically, the cysts lacked ova, with the stratum granulosum either intact, absent, or reduced to a single layer. Desquamated granulosa cells were frequently observed within the cystic lumen (Fig. 6).

The second most common condition was folliculoids, observed in 3.77% of cases. These were characterized by eosinophilic material within follicle-like structures lined by one to two layers of granulosa-like cells. The granulosa-like cells were polygonal, with large, oval to round nuclei, scant cytoplasm, and a colloid-type morphology (Fig. 7).

Embedded corpus luteum was the third most prevalent non-neoplastic condition, observed in 2.36% of cases. Microscopically, it appeared as a thick fibrous connective tissue layer encapsulating the corpus luteum and separating it from the surrounding ovarian stroma (Fig. 8). The least prevalent condition was ovarian hypoplasia, with a prevalence of 0.47% in this study.

## DISCUSSION

In the present study, pathological abnormalities were identified in 80 out of 212 ovaries examined from 106 sheep, resulting in an overall prevalence of 37.73%. One study reported a significantly lower prevalence of ovarian pathology in sheep[11] compared to our findings, while other cited literature aligns more closely with our results[12]. A slightly higher prevalence has also been reported in some studies[7]. These findings suggest a prevalence range of 4.95% to 39.87%, with our study positioned at the higher end of this spectrum. This elevated prevalence may be attributed to the inclusion of aged and infertile sheep, whose genital tracts were collected from slaughterhouses[7].

Interestingly, the high incidence of abnormalities in the right ovary may be associated with its greater follicular activity compared to the left[13]. Among the pathological conditions observed, neoplastic abnormalities had a prevalence of 18.39%, which is notably higher than the prevalence reported by other researchers[7,14]. The significant variation in these findings could be attributed to differences in sample populations or environmental factors.

Granulosa cell tumors were the most prevalent neoplastic condition observed, consistent with previous reports highlighting their common occurrence in ovine ovaries. Microscopically, our findings revealed proliferating neoplastic cells and collagen fibers projecting into the ovarian lumen, with the cystic wall lined by thick collagenous fibers. These characteristics align with descriptions provided by other authors[15,16], further affirming the accuracy of our diagnostic observations.

Adenoma emerged as the second most prevalent neoplastic condition in this study, manifesting in two distinct types. The first type of tumor exhibited multibranched papillae that arose multicentrically, often filling the lumen of the cyst. These papillae were covered by a single or multilayered epithelium of columnar or cuboidal cells overlying connective tissue stalks[15]. The second type was characterized by proliferated papillae consisting of connective tissue stalks lined by single or multiple layers of cuboidal or columnar epithelial cells[16].

In this study, several less common neoplastic conditions were identified, including adenocarcinoma (0.94%), clear cell carcinoma (0.94%), hemangiosarcoma (1.89%), fibroma (0.94%), angioleiomyoma (0.94%), and hemangiopericytoma (0.47%). These findings are consistent with previously reported microscopic lesions in similar and other domestic species[15,16,17,18,19].

Follicular cysts were the most prevalent non-neoplastic condition identified in this study, with a prevalence rate of 6.13%. Some studies reported prevalence rates approximately half of our findings[20], while others showed rates with closely comparable figures, supporting the validity of our results[14]. Microscopically, the cysts did not contain ova, and the stratum granulosum layer was present. In some cases, however, the stratum granulosum layer was absent. Similar microscopic findings have also been reported by other authors in studies on ewes[21].

Folliculoid was the second most prevalent non neoplastic condition with a prevalence of 3.77%. Microscopically, eosinophilic material was present in the follicle-like structure, which was lined by 1-2 layers of granulosa cell like cells and formed colloid type folliculoids[7,22].

A total of five cases of embedded corpus luteum were noticed in this study, which had a prevalence rate of 2.36%. A thick fibrous connective tissue layer was observed entrapping the corpus luteum from the surrounding ovarian stroma during histopathological examination[24].

In this study, the prevalence of less common non-neoplastic conditions was as follows: luteinized cyst (1.41%), cystic corpus luteum (0.94%), parovarian cyst (0.94%), lymphangiectasia (1.89%), endometriosis (1.41%) and ovarian hypoplasia (0.47%). These conditions were

among the least prevalent. A similar pattern of low prevalence has also been reported in other studies[12,20]. However, variations in the occurrence of these conditions have been noted among different domestic animals. The microscopic features of these lesions observed in this study align with descriptions in the existing literature, further confirming the consistency of these pathological characteristics across studies[23,25,26,27].

In conclusion, this study identified pathological abnormalities in 37.73% of examined sheep ovaries, with granulosa cell tumors as the most common neoplastic condition (18.39%). Variations in prevalence across studies reflect differences in sample populations or environmental factors. Microscopic features aligned with previous reports, confirming consistency in pathological presentations. Findings emphasize the importance of understanding ovarian abnormalities in sheep to improve diagnostic and reproductive health strategies.

## ACKNOWLEDGEMENT

The authors extend their gratitude to the Head and staff of the Department of Veterinary Pathology, College of Veterinary Science, Tirupati for providing the facilities necessary to conduct this study.

## REFERENCES

1. Kumar V. 2022. Trend and Composition of Export of Livestock Products in the Context of the WTO Regime. *Indian J Agri Mar* **36:** 96-234.
2. Singh VK, Suresh A, Gupta DC and Jakhmola RC. 2005. Common property resources rural livelihood and small ruminants in India: A review. *Indian J Anim Sci* **75:** 1027-1036.
3. Naqvi SM, De K and Gowane GR. 2013. Sheep production system in arid and semi-arid regions of India. *Ann Arid Zone* **52:** 265-274.
4. Beena V, Pawaiya RVS, Gururaj K, Singh DD, Mishra AK, Gangwar NK and Kumar A. 2017. Molecular etiopathology of naturally occurring reproductive diseases in female goats. *Vet World* **10:** 964.
5. Abera T. 2018. Abattoir and Clinical Study of Small Ruminant Female Reproductive Disorders. *Livestock Res Results* **:** 519-527.
6. Ugwu PC, Njoga EO, Njoga UJ, Aronu CJ, Atadiose EO, Okoli CE and Abonyi FO. 2023. Indiscriminate slaughter of pregnant goats for meat in Enugu, Nigeria: Causes, prevalence, implications and waysout. *PloS One* **18:** e0280524.
7. Kankhedia PC. 2005. Occurrence and pathology of various conditions of female genital tract in sheep. Master of Veterinary Science Dissertation approved by Rajasthan Agricultural University, Bikaner.
8. Strafuss A. 1987. Necropsy Procedures and basic diagnostic methods for practicing veterinarians.
9. Benjamin MM. 1978. Outline of Veterinary Clinical Pathology, 3rd edn: 299-309.
10. Bancroft DJ and Cook CH. 1994. Fundamentals of normal histology and histopathology. Manual of histopathological techniques and their diagnostic application, Edinburgh. *Chur Living* 1-17.
11. Karadas E and Timurkaan N. 1999. Pathomorphologic investigations on the genital system of ewes I. Ovarium and oviduct. *Turkish J Vet Anim Sci* **23:** 557-565.
12. Moghaddam A and Gooraninejad S. 2007. Abattoir survey of gross abnormalities of the ovine genital tracts in Iran. *Small Rum Res* **73:** 259-261.
13. Stevenson JS. 2019. Spatial relationships of ovarian follicles and luteal structures in dairy cows subjected to ovulation synchronization: Progesterone and risks for luteolysis, ovulation, and pregnancy. *J Dairy Sci* **102:** 5686-5698.
14. Silva RM, Macedo J, Lacerda MS, Azevedo JPM, Ferreira Júnior JA, Cerqueira RB and Pedroso PMO. 2021. Lesions of the sheep reproductive system found in a slaughterhouse in the state of Bahia, Brazil. *Pes Vet Brasil* **40:** 955-962.
15. Moulton JE. 1978. Tumors in domestic animals. University of California Press 2nd edn: 547-551.
16. Meuten DJ. 2002. Tumors in domestic animals. John Wiley and Sons 5th edn: 547-575.
17. Jangir BL, Chaudhary RN, Gupta RP and Sharma S. 2017. A case report of ovarian haemangiosarcoma in a dog. *Indian J Vet Pathol* **41:** 140-142.
18. Seaman WJ. 1985. Canine ovarian fibroma associated with prolonged exposure to mibolerone. *Toxicol Pathol* **13:** 177-180.
19. Strickland KC. 2020. Ovary and Peritoneal Washings. Practical Cytopathology: Frequently Asked Questions 161-184.
20. Sharma A, Kumar P, Singh M and Vasishta NK. 2014. Reproductive health status of north western Himalayan Gaddi sheep: An abattoir study. *Open Vet J* **4:** 103-106.
21. Jarad AS, Faraj Majeed AS, Aboud QM, Hasan MS, Farhan WH and Aboud AE. 2021. Pathological Study of Reproductive Tracts of Awassi Ewes in Fallujah, Iraq. *Indian J Forens Med Toxicol* **15:** 14-17.
22. Sastry GA and Rama Rao P. 2001. Veterinary Pathology, Chapter II, Special Pathology 421-430.
23. Dharani P, Kumar R, Nair MG, Lakkawar AW, Murugavel K and Varshney KC. 2019. Pathomorphological studies of the ovaries in goats. *J Entom Zoo Studies* **7:** 322-25.
24. Dawood KE. 2010. Pathological abnormalities of the reproductive tracts of ewes in Basra, Iraq. *Vet Rec* **166:** 205.
25. Jubb KVF, Kennedy PC and Palmer N. 2012. Pathology of domestic animals. Academic press 2nd edn: 456-497.
26. Stock RJ and Tobon H. 1977. Lymphangiectasia of the uterus. *Obst Gynecol* **50:** 630-633.
27. Zachary JF and McGavin MD. 2012. Pathologic Basis of Veterinary Disease **5:** 456-478.

*Indian J. Vet. Pathol., 49(2) : 127-130, 2025: DOI: https://doi.org/10.56093/1skt0c21*

RESEARCH ARTICLE

# Pathological study on an outbreak of sheep pox in a Mecheri sheep flock

**M. Sasikala*, J. Selvaraj[1], N. Babu Prasath[2], P. Ponnusamy[3] and T. Arulkumar[4]**
Department of Veterinary Pathology, Veterinary College and Research Institute, Namakkal-637 002, Tamil Nadu Veterinary and Animal Sciences University, Chennai-600 051, [1&2]Department of Veterinary Pathology, VCRI, Orathanadu, Thanjavur-614 625, [3]Department of Veterinary Microbiology, VCRI, Orathanadu, Thanjavur-614 625, [4]Veterinary Clinical Complex, VCRI, Orathanadu, Thanjavur-614 625

**Address for Correspondence**
*M. Sasikala, Assistant Professor, Department of Veterinary Pathology, Veterinary College and Research Institute, Namakkal -637 002, Tamil Nadu Veterinary and Animal Sciences University, Chennai-600 051, India, E-mail: vetsasi.pathologist@gmail.com*

*Received: 15.2.2025; Accepted: 3.4.2025*

## ABSTRACT

In the present article, the pathology of sheep pox in a Mecheri sheep flock has been described. Six adult sheep carcasses from an organized sheep farm were presented for necropsy. Affected sheep had clinical signs of pyrexia, conjunctivitis, laboured breathing, loss of appetite and raised firm nodules in the hairless areas all over the body. On necropsy, skin over the groin, ventral abdomen and inner thigh revealed multiple, round, firm, elevated grey-coloured nodules. Lung lobes revealed many reddish-brown circular areas. Microscopically, hyperplasia with hydropic degeneration of the lining epithelium was observed in tissues of skin, lip, rumen and reticulum. Eosinophilic intracytoplasmic inclusions also seen in hyperplastic epithelial cells of the above tissues. Trachea showed mucosal congestion with subacute tracheitis, epithelial hyperplasia with intracytoplasmic inclusions and lungs showed interstitial pneumonia. Tissues with lesions were subjected to polymerase chain reaction and were found to be positive for ITRs of the sheep pox virus with an amplicon size of 289 bp. The disease was diagnosed as sheep pox on the basis of gross pathology, histopathology and confirmation by molecular methods.

**Keywords:** Mecheri sheep, pathology, sheep pox, Tamil Nadu

## INTRODUCTION

In India, sheep pox is a contagious disease of sheep affecting all age groups and is endemic in Indian subcontinent. It is economically important viral disease of sheep which causes heavy economic losses in outbreaks due to heavy mortality, abortions and loss of market value of the affected animals[1]. Mortality rate of up to 50% in a fully susceptible flock and as high as 100% in young lambs has been reported[2,3]. Mild infections are common in indigenous breeds. However, symptoms may be more severe in lambs, animals under stress and those with concurrent infections and or animals from areas where sheep pox is not endemic[4,5].

Sheep pox is caused by sheep pox virus, a member of the genus *Capripox virus* of the family *Poxviridae*[6]. The other members of the genus are goat pox virus and lumpy skin disease virus (LSDV) of cattle. Although the geographic distribution of sheep pox, goat pox and lumpy skin disease is different, the viruses are indistinguishable by conventional serology and barely distinguishable by restriction endonuclease analysis[7]. Strains of sheep pox and goat pox virus are not considered to be host-specific and although the majority of strains show a host preference, but preferably a single strain may cause disease in both sheep and goats. Goats may get mild infection with sheep strains, which can then cause severe disease when transmitted back to sheep. Similarly, sheep may become infected with virulent goat strains[2]. It has been proposed that both sheep pox and goat pox be described as a single disease called capripox[8]. The present study describes the pathology of an outbreak of sheep pox in an organized sheep breeding farm in Thanjavur district of Tamil Nadu.

**How to cite this article :** Sasikala, M., Selvaraj, J., Prasath, N.B., Ponnusamy, P. and Arulkumar, T. 2025. Pathological study on an outbreak of sheep pox in a Mecheri sheep flock. Indian J. Vet. Pathol., 49(2) : 127-130.

## MATERIALS AND METHODS

Six carcasses of sheep of different ages (4 months - 3 years) were brought for post-mortem examination from an organized sheep farm during the month of January 2016 (mid-winter season) to the Department of Veterinary Pathology, Veterinary College and Research Institute, Orathanadu, Thanjavur, Tamil Nadu with the clinical history of pyrexia, conjunctivitis, loss of appetite, depression, abortion, raised firm nodules in the hairless areas, prostration and laboured breathing followed by death. The farm had a flock strength of 58 animals and were maintained in closed pen system with open grazing time of 6 to 8 hours.

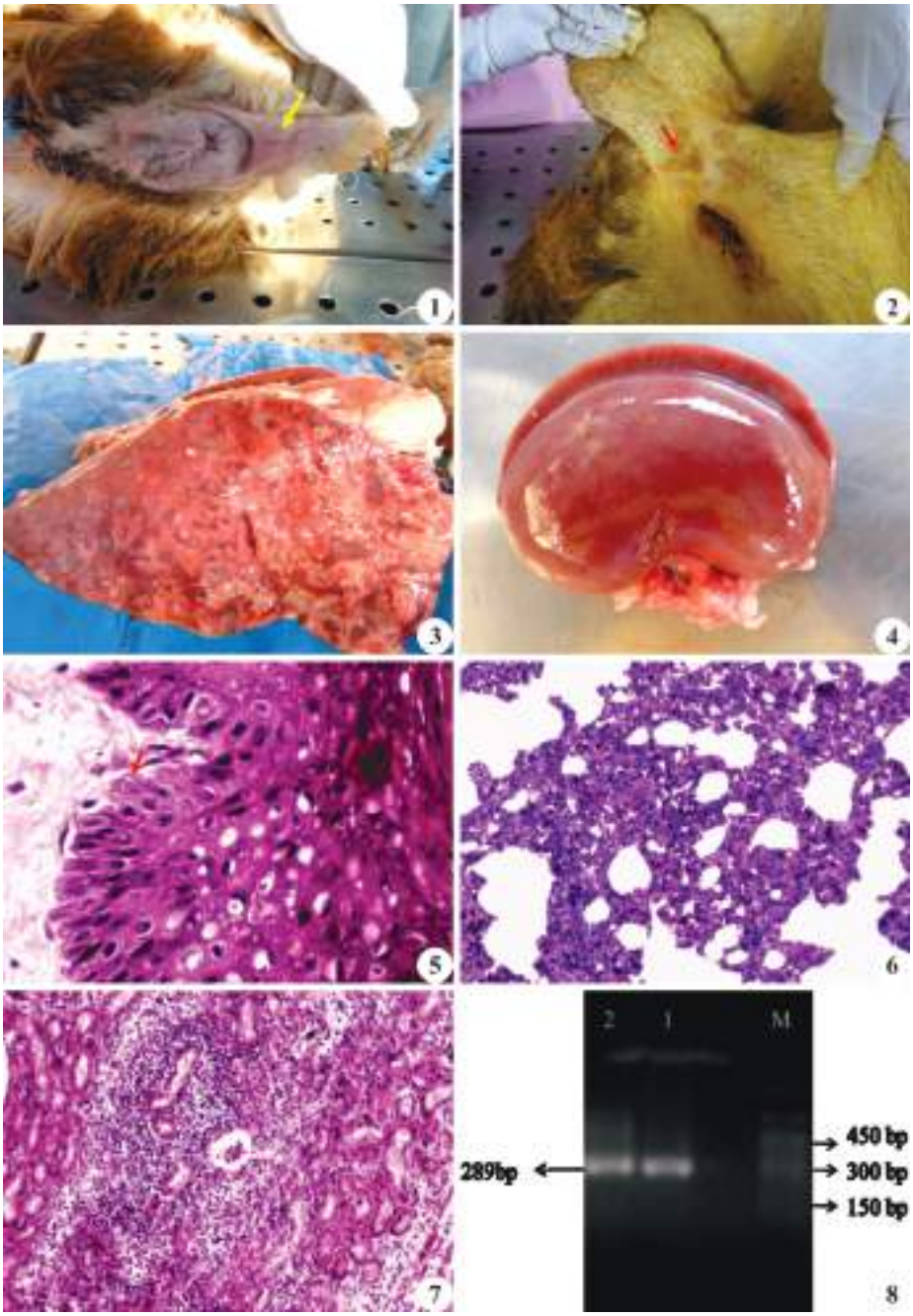


**Fig. 1.** Raised, firm, circular nodules on underside of the tail; **Fig. 2.** Multiple, raised, firm, circular nodules on skin at the base of the scrotum; **Fig. 3.** Lungs: Multiple and confluent greyish, round, firm nodules with hyperaemic borders; **Fig. 4.** Kidney: Cortical surface showing multifocal, greyish spots; **Fig. 5.** Skin: Intracytoplasmic eosinophilic inclusions in the hyperplastic epithelial cells (H&E x400); **Fig. 6.** Lungs: Subacute interstitial pneumonia (H&E x100); **Fig. 7.** Kidney: Subacute interstitial nephritis (H&E x100); **Fig. 8.** Agarose gel electrophoresis showing amplicons specific to sheep pox virus for 289 bp of the inverted terminal repeats gene. Lane M: DNA marker; Lane 1 & 2: Representative positive field samples.

Sick animals were segregated from apparently healthy animals and housed in a separate enclosure away from the main stock. Clinical signs, mortality and morbidity were recorded.

Necropsy was performed as per the standard procedure and gross lesions were recorded. The representative tissue pieces from the skin, lungs, kidney, spleen, liver, heart, trachea, rumen and reticulum were collected in 10% neutral buffered formalin. The tissues were processed as per standard histological technique[9]. The tissue sections were cut at 3-5µ thickness and stained by the Haematoxylin and Eosin staining technique. Samples of infected lung tissue and other organs showing lesions collected in sterile container and heart blood swab

were sent to Department of Veterinary Microbiology, Veterinary College and Research Institute, Orathanadu for identification of etiological agent. The DNA was extracted and the PCR was carried out to amplify inverted terminal repeats of sheep pox virus with a forward primer, InS-1.1 (5′-AGAAACGAGGTCTCGAAGCA-3′) and a reverse primer, InS-1.1′ (5′-GGAGGTTGCTGGAAATGTGT-3′) to get an amplicon size of 289 bp length of the inverted terminal repeats (ITRs) of sheep pox virus[10].

## RESULTS

The outbreak of sheep pox was recorded during mid-winter season. The overall morbidity and mortality were 56% and 11%, respectively and the severity was more in adults. On external examination, the skin of lips, ventral neck, sternum, abdomen, inner thigh, inguinal region and underside of the tail also revealed multiple, elevated, greyish, round, firm areas of about 5-8 mm diameter (Figs. 1 & 2). Scab formation was noticed in the udder, sternum and ventral abdomen of a few animals. Subcutaneous tissue of the above cutaneous lesions revealed congestion and areas of ecchymosis. The nodular lesions extended into the mucosa of mouth, dental pad, pharynx, larynx, rumen, reticulum, abomasum and vagina with generalized lymphadenopathy. The spleen was congested. Dorsal aspect of the tip of tongue revealed severe erosions and it was covered with yellow strands of necrotic debris. Trachea showed ulcerations with hyperaemic borders. Lungs revealed multiple, confluent, greyish, round, firm nodules of 3-8 mm diameter with hyperaemic borders (Fig. 3). Moderate to severe pulmonary oedema and endocardial haemorrhages were also observed. Liver and kidneys revealed multifocal, greyish spots of 1-2 mm diameter (Fig. 4).

On microscopic examination, skin revealed thickening of dermis with lympho-macrophage infiltration. Epidermis revealed hyperplasia, acanthosis, areas of parakeratosis and hyperkeratosis, necrosis and reepithelialisation. Epithelial cells of skin and labia showed hydropic changes with intracytoplasmic eosinophilic inclusion bodies (Fig. 5). Hair follicular epithelium also revealed epithelial proliferation with intracytoplasmic inclusions. Sebaceous gland revealed sebaceous adenitis. Lungs showed sub-acute interstitial pneumonia (Fig. 6) with areas of emphysema and pleuritis. Trachea showed mucosal congestion with sub-acute tracheitis and epithelial hyperplasia with intracytoplasmic eosinophilic inclusions. Rumen and reticulum revealed epithelial hyperplasia with intracytoplasmic eosinophilic inclusions. Liver showed cell swelling of hepatocytes with periportal fibrosis. Kidneys revealed sub-acute interstitial nephritis (Fig. 7). Lymph node revealed lymphoid depletion with multifocal areas of haemorrhage. The lung and skin tissues were found to be positive by PCR for inverted terminal repeats (ITRs) of the sheep pox viral proteins with the amplicon size of 289 bp (Fig. 8).

## DISCUSSION

An outbreak of sheep pox was recorded in Mecheri sheep flock in Thanjavur district of Tamil Nadu. The overall morbidity and mortality were 56% and 11%, respectively. Similar morbidity and mortality patterns owing to sheep pox have been reported earlier in different breeds of sheep[11,12]. It has also been described that the indigenous sheep are more resistant to sheep pox while exotic breeds are considered highly susceptible[8]. Although, Mecheri sheep is an indigenous breed, the severity of disease was more in the present outbreak.

The gross and histopathological findings recorded in the present study were in accordance with earlier findings[13]. The pox lesions dispersed over the body surface especially on hairless areas and lesions in visceral organs especially pneumonia might have caused increased mortality[14]. Moreover, the findings of sheep pox viral inclusion bodies in affected tissues of infected animals demonstrated through histopathology were further confirmed by PCR for the sheep pox virus, were comparable with earlier documented evidences[10].

Environmental contamination as a result of the virus getting excreted in the nasal secretions, milk, urine[15] and the improper husbandry practices with high stocking densities in the endemic areas increases the close contact between the affected and susceptible animals for the spread of infection. In the present outbreak, higher mortality was observed in adult females than in males and the outbreak was recorded in winter when cold stress and fodder scarcity acts as an important predisposing factor. It has been suggested that the sheep pox shows seasonal trends[16,17] and therefore the disease might have precipitated in the presence of the above factors. Therefore, the sheep farmers must keep a strict vigil on sheep pox among animals in susceptible areas by quarantine of new animals before introduction into herds, immediate implementation of mass vaccination, segregation of morbid animals and proper disposal of affected animals to prevent any further losses.

The present study underlines the clinico-pathological features of sheep pox outbreak in the Thanjavur district of Tamil Nadu in which the sheep pox emerges as one of the major economic hazard to the sheep farmers.

## REFERENCES

1. OIE (Office International des Epizooties). 2008. Sheep and goat pox. In: Terrestrial Animal Health Code. World Organization for Animal Health, Paris, France.
2. Bhanuprakash V, Moorthy ARS, Krishnapa G, Sirinivasa GRN

and Indrani BK. 2005. An epidemiological study of sheep pox infection in Karanataka State, India. *Rev Sci Tech* **24:** 909-920.
3. Beard PM, Sugar S and Bazarragchaa A. 2010. Description of two outbreaks of capripox virus disease in Mongolia. *Vet Micro* **142:** 427-431.
4. Buller RM, Arif BM and Black DN. 2005. Poxviridae in Virus Taxonomy: Eighth Report of the International Committee on the Taxonomy of viruses. Elsevier Academic Press. Oxford. pp-117.
5. Tullman ER, Afonso CL and Lu Z. 2002. The Genomes of Sheep pox and Goat pox viruses. *J Virol* **76:** 6054-6061.
6. Murphy FA, Faquet CM, Bishop DHL, Ghabrial SA, Jarvis AW, Martelli GP, Mayo MA and Summers MD. 1995. Virus taxonomy: 6th report of the International Committee on Taxonomy of Viruses. *Arch Viro Supp* **10:** 85-86.
7. Gershon PD and Black DN. 1988. A comparison of the genomes of capripoxvirus isolates of sheep, goats and cattle. *J Virol* **164:** 341-349.
8. Heine HG, Stevens MP, Foord AJ and Boyle DB. 1999. A capripoxvirus detection PCR and antibody ELISA based on the major antigen P32, the homolog of the vaccinia virus H3L gene. *J Immunol Meth* **227:** 187-196.
9. Bancroft JD, Stevens A and David RT. 1992. Theory and practice of histological techniques, 4th Edn., Churchill Livingstone, London. pp: 303.
10. Mangana-Vougiouka O, Markoulatos P, Koptopoulos G, Nomikou K, Bakandritsos N and Papadopoulos P. 2000. Sheep poxvirus identification from clinical specimens by PCR, cell culture, immunofluorescence and agar gel immunoprecipitation assay. *Mol Cell Probes* **14:** 305-310.
11. Mondal B, Hosamani M, Dutta TK, Senthilkumar VS, Rathore R and Singh RK. 2004. An outbreak of sheep pox on a sheep breeding farm in Jammu, India. *Rev Sci Tech* **2:** 943-949.
12. Roy P, Purushothaman V, Sreekumar C, Tamizharasan S and Chandramohan A. 2008. Sheep pox disease outbreaks in Madras Red and Mechery breeds of indigenous sheep in Tamil Nadu, India. *Res Vet Sci* **85:** 617-621.
13. Sharma R, Patil RD, Parimoo HA, Thakur D and Katoch VC. 2013. Clinico-Pathology of Sheep Pox disease in Himachal Pradesh, India. *Ruminant Sci* **2:** 127-130.
14. Kitching RP. 2007. Diseases of Sheep, 4th Edn.
15. Bhanuprakash V, Indrani BK, Hosamani M and Singh RK. 2006. The current status of sheep pox disease. *Comp Immunol Micro Infect Dis* **29:** 27-60.
16. Murthy DK and Singh PP. 1971. Epidemiological studies on an outbreak of sheep pox in a mixed flock in Uttar Pradesh. *Indian J Anim Sci* **41:** 1072-1079.
17. Eroksuz Y, Bulut H, Gulacti I and Ceribasi AO. 2008. Seasonal distribution of sheep pox cases in lambs in Eastern Turkey. *J Anim Vet Adv* **7:** 638-642.

*Indian J. Vet. Pathol., 49(2) : 131-141, 2025: DOI: https://doi.org/10.56093/d6h1y272*

RESEARCH ARTICLE

# Amelioration of bleomycin-induced epithelial-mesenchymal transition in pulmonary fibrosis by baicalein in mice

**D.K. Sharma, N.D. Singh*, G.D. Leishangthem and H.S. Banga**
Department of Veterinary Pathology, College of Veterinary Science, Guru Angad Dev Veterinary and Animal Sciences University, Ludhiana, Punjab, India

**Address for Correspondence**
*N.D. Singh, Professor, Department of Veterinary Pathology, College of Veterinary Science, Guru Angad Dev Veterinary and Animal Sciences University, Ludhiana, Punjab, India, E-mail: nitindevsingh@gadvasu.in*

*Received: 14.2.2025; Accepted: 25.4.2025*

## ABSTRACT

Epithelial-mesenchymal transition (EMT) play a vital role in pulmonary fibrosis. The present study investigates the ameliorative effect of baicalein, a bioactive flavonoid present in the dry roots of *Scutellariabaicalensis Georgi*, on bleomycin-inducedpulmonary fibrosis and subsequent EMT. Mice were given a single intratracheal instillation of saline containing bleomycin @ 1 mg/kg b.wt. Baicalein in different doses of 0.1, 1.0 and 10 mg/kg b.wt was given intraperitoneally daily for 8 weeks. Baicalein was effective in attenuating the BLM induced Pulmonary fibrosis through suppression of oxidative stress, inflammation, histological as well as ultrastructural damages and EMT, especially during the chronic stage injury. This study will provide additional knowledge on the ameliorative effect of baicalein during the later stages of lung injury where the EMT starts and this may help in the therapeutic or management of clinical chronic lung injury associated pulmonary fibrosis.

**Keywords:** Baicalein, bleomycin, chronic lung injury, epithelial-mesenchymal transition

## INTRODUCTION

Idiopathic pulmonary fibrosis (IPF) is a chronic progressive and fatal lung disease of unknown etiology. Its prognosis is poor and the outcome is even worse than in many malignant diseases, and the exact pathophysiological mechanisms for the development of which are not fully understood[1]. There is a general consensus that this disease is due to the combination of alveolar epithelial cell injury which is followed by the release of proinflammatory/fibrotic cytokines, inflammatory cell infiltration, epithelial-mesenchymal transition (EMT) and excessive deposition of extracellular matrix in the lung[2]. Most of patients present at an advanced stage of the disease. Treatment options for pulmonary fibrosis are limited. Anti-inflammatory drugs such as prednisone may carry symptomatic relief, but they do not appear to halt progression of fibrosis, and their beneficial effects in IPF remain in question. Cytotoxic drugs (cyclophosphamide, azathioprim, etc.) have not been shown to improve lungs function or life expectancy and may be associated with harmful side effects.

Animal models play an important role in the investigation of diseases, and many models are established to examine pulmonary pathobiology. Chronic diseases are more difficult to model. The situation with IPF is even more complicated since the etiology and natural history of the disease is unclear and no single trigger is known that is able to induce "IPF" in animals. Different models of pulmonary fibrosis have been developed over the years. Most of them mimic some, but never all features of human IPF, especially the progressive and irreversible nature of the condition. Common methods include radiation damage, instillation of bleomycin, silica or asbestos, and transgenic mice or gene transfer employing fibrogenic cytokines. So far, the standard agent for induction of experimental pulmonary fibrosis in animals is bleomycin. Bleomycin is a chemotherapeutic antibiotic, produced by the bacterium "*Streptomyces verticillus*". Its use in animal models of pulmonary fibrosis is based on the fact that fibrosis is one of the major adverse drug effects of bleomycin in human cancer therapy. This

**How to cite this article :** Sharma, D.K., Singh, N.D., Leishangthem, G.D. and Banga, H.S. 2025. Amelioration of bleomycin-induced epithelial-mesenchymal transition in pulmonary fibrosis by baicalein in mice. Indian J. Vet. Pathol., 49(2) : 131-141.

happens by chelation of metal ions, and reaction of the formed pseudoenzyme with oxygen, which leads to the production of DNA-cleaving superoxide and hydroxide free radicals. An overproduction of reactive oxygen species can lead to an inflammatory response causing pulmonary toxicity, activation of fibroblasts and subsequent fibrosis. Bleomycin as an agent to induce experimental lung fibrosis has been reported long ago in laboratory animals[3].

The last two decades have markedly improved the knowledge about the underlying mechanisms of pulmonary fibrosis and helped to identify potential targets for novel therapies. Various therapeutic agents like

antibiotics, corticosteroids, and antioxidants have been used as therapeutic agents, but they lead to other problem like antibiotic sensitivity, immunosuppression etc. Hence, nowadays herbal drugs are preferred which have no side effects. Herbal medicines can be used as one of the dietary supplement. There are many different systems of traditional medicine, and the philosophy and practices of each are influenced by the prevailing conditions, environment, and geographic area within which it first evolved, however, a common philosophy is a holistic approach to life, equilibrium of the mind, body, and the environment, and an emphasis on health rather than on disease. Traditional Chinese medical herbs are the most important components of the traditional Chinese medicine (TCM) system, which have been reported to cure infectious diseases, in the form of hot water extracts, for almost 2,000 years. In traditional Chinese herb medicine, the root of *Scutellariabaicalensis Georgi* was usually gathered before Tomb-Sweeping Day and decocted for the purpose of "cleansing heart" and "removing toxins," for example, cough with yellow sputum, jaundice, swelling and pain of eye, and so on. Baicalein (BAIC) is a bioactive flavonoid, which is widely used in Chinese herbal medicine. Evidence has shown that BAIC has many pharmacological effects, including antiallergic, antioxidant, antiapoptotic, antiviral, anti-inflammatory, antitumor, and neuroprotective effects and a modulatory effect on the immune system[4].

**Table 1.** Hematology of mice of different groups 8 weeks post-treatment.

| Groups | Hb (g/dL) (Mean±SE) | TLC (x10³/µl) (Mean±SE) | DLC | |
|---|---|---|---|---|
| | | | Neutrophil | Mononuclear Cells |
| SHAM | 10.92±0.29$^{c}$ | 10.18±0.12$^{a}$ | 33.46±1.35$^{a}$ | 66.46±1.41$^{a}$ |
| BLEO | 6.90±0.18$^{b}$ | 10.40±1.34$^{a}$ | 37.78±0.79$^{a}$ | 62.22±0.88$^{a}$ |
| BLEO/BAIC/0.1 | 7.65±0.62$^{b}$ | 9.92±1.11$^{a}$ | 35.52±1.11$^{a}$ | 64.48±1.47$^{a}$ |
| BLEO/BAIC/1.0 | 8.10±0.27$^{bc}$ | 8.39±0.34$^{a}$ | 37.67±1.09$^{a}$ | 62.33±1.01$^{a}$ |
| BLEO/BAIC/10 | 9.95±0.25$^{bc}$ | 8.22±0.28$^{a}$ | 34.92±1.03$^{a}$ | 65.08±0.96$^{a}$ |

The values (Mean±SE) in a column having different superscript differ significantly from each other at 5% level of significance. The values (Mean±SE) in a column having same superscript do not differ significantly from each other at 5% level of significance.

## MATERIALS AND METHODS

### Animals and Treatments

The study protocol was approved by the Institutional Animal Ethics Committee (IAEC) of Guru Angad Dev Veterinary and Animal Sciences University (GADVASU), Ludhiana. Male albino mice (n=30, 4-6 weeks age), were obtained from Disease free small animal house, Central Research Institute, Kasauli, Himachal Pradesh and housed in the small animal house of GADVASU. All mice received humane care. After the acclimatization period of 7 days, the animals were weighed again and, 30 male albino mice were randomly divided into five experimental groups (6 animals each) and named as per the challenge and treatment: SHAM/PBS (saline-only/control group), BLM (bleomycin @ 1 mg/kg bwt treated group), BLM/BAIC/0.1 (bleomycin @ 1 mg/kg bwt + baicalein (0.1 mg/kg bwt), BLM/BAIC/1 (bleomycin @ 1 mg/kg bwt + baicalein (1 mg/kg bwt) and BLM/BAIC/10 (bleomycin @ 1 mg/kg bwt + baicalein (10 mg/kg bwt). Mice received a single intratracheal instillation of saline containing bleomycin sulfate @ 1 mg/kg bwt (Sigma, USA) in a volume of 50 µl in all groups, except vehicle group. Baicalein (Sigma, USA) in three different doses (0.1, 1.0, 10 mg/kg bwt) was given intraperitoneally daily for 8 weeks. All the mice were sacrificed after 8 weeks by ketamine and xylazine overdose.

### Collection of Blood and Bronchoalveolar lavage (BAL) fluid

The blood was withdrawn by cardiac puncture after sacrificing the animal and it was collected in EDTA vials for the hematological parameter estimations *viz.* hemoglobin concentration (Hb) and total leucocyte count (TLC). The collection of bronchoalveolar lavage was done three times through a tracheal cannula which was attached to 1 ml syringe with 0.5 mL of PBS in each animal from the left lung. Bronchoalveolar lavage fluid (BALF) was processed to get cell pellets and supernatants as described earlier[5]. TLC and DLC were performed of the cell pellets of BALF with a hemocytometer and the smears were stained with Leishman stain. The supernatant of BALF was collected and stored at -80°C for estimation of other parameters like protein concentration, TNF-$\alpha$ and IL-6.

**Table 2.** Lung W/D weight ratio and Protein concentration in bronchoalveolar lavage fluid (BALF) in different groups of mice 8 weeks post treatment.

| Groups | Lung W/D Weight Ratio (Mean±SE) | Protein Concentration in BALF (µg/ml) (Mean±SE) |
|---|---|---|
| SHAM | 3.04±0.17$^{ab}$ | 406.65±9.08$^{ab}$ |
| BLEO | 6.89±0.62$^{d}$ | 1114.60±112.58$^{f}$ |
| BLEO/BAIC/0.1 | 4.89±0.46$^{c}$ | 925.95±45.55$^{e}$ |
| BLEO/BAIC/1.0 | 4.08±0.45$^{bc}$ | 910.75±36.88$^{e}$ |
| BLEO/BAIC/10 | 3.73±0.22$^{abc}$ | 730.43±17.79$^{d}$ |

The values (Mean±SE) in a column having different superscript differ significantly from each other at 5% level of significance. The values (Mean±SE) in a column having same superscript do not differ significantly from each other at 5% level of significance.

**Wet to Dry Lung Weight Ratio**

The similar lobe of the right lung from each animal was collected after sacrificing and was weighed immediately after its excision, which was termed as wet weight. After weighing the lung lobes were dried at 60$^{O}$C for 72 h, and weighed again to get the dry weight. This wet dry (W/D) lung weight ratio was calculated as an indicator of pulmonary edema.

**Estimation of protein in bronchoalveolar lavage fluid**

Commercially available BCA Protein Assay Kit (Thermo Scientific, USA) was used to estimate protein in BALF as per manufacturer's instruction.

**Histopathological studies**

After the BAL fluid collection, the tissue samples from the lungs were collected and were fixed in 10% neutral buffered formalin and were further processed and embedded in paraffin. Five μm thick sections were stained with hematoxylin and eosin. To ascertain fibrosis and collagen deposition Masson Trichrome and Picro-sirius red staining were also done respectively. The slides were viewed and photomicrographs were taken by microscope attached with camera (BX 61, Olympus Corporation, Japan). Histopathologically, the lung injury was assessed experimentally by blind experts and was graded semi-quantitatively using modified Ashcroft's scoring method[10] with a score range of 0-8 score. For Picro-sirius red staining, the slides were stained with picro-sirius red stain (0.1% Sirius red in aqueous saturated picric acid) for 1 hour followed by washing with acidified water (0.5% glacial acetic acid), dehydration and mounting with DPX. Collagen was red in colour while non-collagen components were orange. The images were analyzed using Image J (Fiji) software (http://fiji.sc). The intensity of the picrosirius red positive area was expressed as percentage area (μm$^2$).

**Estimation of Lipid peroxidation and Superoxide dismutase in lung homogenates**

The lung tissue (10 mg) was homogenised in 1 ml of ice-cold phosphate buffered saline (pH 7.4), using a tissue homogenizer with a teflon pestle at 4$^{O}$C. The resultant tissue homogenates were used for measurements of Total protein, Lipid peroxidation (LPO) and Superoxide dismutase (SOD) activity. Total proteins were estimated using commercially available BCA Protein Assay Kit (Thermo Scientific, USA) as per manufacturer's protocol. LPO was calculated and denoted in terms of MDA (malondialdehyde) production, by the thiobarbituric acid (TBA) method as described with slight modifications. Briefly, 1 ml of tissue homogenate were incubated at 37$^{O}$C for 2 hours after which 1 ml of 10% w/v trichloroacetic acid was added to each sample. The mixture was mixed thoroughly and centrifuged at 2000 rpm for 10 min. To 1 ml of supernatant after centrifugation, an equal volume of 0.67% w/v TBA was added and kept in boiling water bath for 10 min. The samples were cooled down and then diluted with 1 ml of distilled water. The absorbance was read at 535 nm. The amount of LPO was expressed in nanomoles of MDA formed per gram of wet tissue. SOD activities were estimated as per the method described[6]. It basically involves generation of superoxide by autoxidation of pyrogallol and the inhibition of superoxide-dependent reduction of the tetrazolium dye, 3-(4-5 dimethyl thiazol 2-yl) 2, 5 diphenyl tetrazolium bromide (MTT), to its formazan, which was measured at 570 nm.

**Table 3.** MPO activity in different groups of mice at 8 weeks post treatment.

| Groups | MPO (mμ/ml) |
|---|---|
| SHAM | 54.30±1.72$^{a}$ |
| BLEO | 164.50±8.71$^{cde}$ |
| BLEO/BAIC/0.1 | 145.42±3.96$^{bcd}$ |
| BLEO/BAIC/1.0 | 137.31±11.80$^{bcd}$ |
| BLEO/BAIC/10 | 103.74±18.47$^{b}$ |

The values (Mean±SE) in a column having different superscript differ significantly from each other at 5% level of significance. The values (Mean±SE) in a column having same superscript do not differ significantly from each other at 5% level of significance.

**Estimation of Myeloperoxidase (MPO) activity**

Myeloperoxidase Colorimetric Activity Assay Kit (SIGMA ALDRICH, St. Louis, USA) was used to measure myeloperoxidase (MPO) activity in the lung homogenates using as per the manufacturers instructions. The absorbance was measure at 412 nm using microplate reader.

**Estimation of cytokines by ELISA**

Mouse IL-6 and Mouse TNF-α ELISA Kit (Krishgen Biosystem) and Mouse TGF-β ELISA kit (YH Bioresearch Laboratory) were used to measure Interleukin-6 (IL-6), Tumor necrotic factor-alpha (TNF-α) in BALF and transforming growth factor-β in lung homogenatesas

**Table 4.** LPO and SOD level in lung homogenates of different groups of mice at 1 and 8 weeks post treatment.

| Groups | LPO (nM/g) (Mean±SE) | SOD (U) (Mean±SE) |
|---|---|---|
| SHAM | 1.05±0.25$^{a}$ | 4.75±0.15$^{g}$ |
| BLEO | 2.00±0.00$^{cde}$ | 2.81±0.32$^{bcd}$ |
| BLEO/BAIC/0.1 | 1.51±0.13$^{abc}$ | 2.89±0.14$^{cd}$ |
| BLEO/BAIC/1.0 | 1.71±0.33$^{cd}$ | 3.10±0.26$^{de}$ |
| BLEO/BAIC/10 | 1.15±0.13$^{ab}$ | 3.94±0.15$^{f}$ |

The values (Mean±SE) in a column having different superscript differ significantly from each other at 5% level of significance. The values (Mean±SE) in a column having same superscript do not differ significantly from each other at 5% level of significance.

per the manufacturer instructions.

**Estimation of collagen by hydroxyproline Assay**

Hydroxyproline (HYP) assay was undertaken to estimate the collagen content in the lung homogenates.Briefly, 100 µl of lung homogenate were hydrolyzed with equal amount of concentrated HCl in a pressure-tight, teflon capped vial at 120$^{O}$C for 3 hours followed by clarification with activated charcoal. 10 µl of each hydrolyzed sample were then transferred to a 96-well plate and the liquid portion of the sample was evaporated to dryness under vacuum. Hydroxyproline standard (1 mg/ml) was used to prepare the standard curve. Chloramine T reagent (100 µl) was added to each sample and standard and the incubated at room temperature for 5 min. After this DMAB reagent was added (100µl) and the plate was incubated at 60$^{O}$C for 90 min. The absorbance of each sample was read at 560 nm using a microplate reader.

**Table 5.** TNF-$\alpha$ and IL-6 level in BALF of different groups of mice at 1 and 8 weeks post treatment.

| Groups | TNF-$\alpha$ (Mean±SE) | IL-6 (Mean±SE) |
|---|---|---|
| BLEO | 612.02±18.56$^{g}$ | 154.58±12.29$^{d}$ |
| BLEO/BAIC/0.1 | 562.24±25.42$^{f}$ | 140.71±13.68$^{cd}$ |
| BLEO/BAIC/1.0 | 458.77±13.11$^{e}$ | 124.82±8.58$^{bc}$ |
| BLEO/BAIC/10 | 281.74±7.85$^{d}$ | 72.00±4.43$^{a}$ |

The values (Mean±SE) in a column having different superscript differ significantly from each other at 5% level of significance. The values (Mean±SE) in a column having same superscript do not differ significantly from each other at 5% level of significance.

**Immunohistochemistry (IHC)**

Immunohistochemical analysis for epithelial and mesenchymal markers (E-cadherin and alpha-smooth muscle actin) was performed. Briefly, 5-µm paraffin sections on poly-L-lysine coated slides were rehydrated. After antigen retrieval (heat induced) and blocking of endogenous peroxidase in tissue slides, the slides were incubated with primary antibodies to mouse monoclonal alpha-smooth muscle actin ($\alpha$-SMA) (Abcam, UK) and to rabbit polyclonal E-cadherin (Gentex, USA) which was followed by incubation with secondary antibody (ABC, Universal, Vector). The colour was developed using diaminobenzidine (DAB) substrate and counter stained with hematoxylin. In negative control, tissue sections were processed without application of primary antibody. Semi-quantitative immunohistochemical analysis was performed using scoring pattern[7] as per Lomas *et al* (2012) with a score range of 0-5 where 0 (0 Positives staining cells (%), no expression), 1 (<1 %, Negligible expression), 2 (1 to 10%, Scanty expression), 3 (10 to 33%, Low-moderate expression), 4 (33 to 66%, Moderate expression) and 5 (>66, Extensive expression).

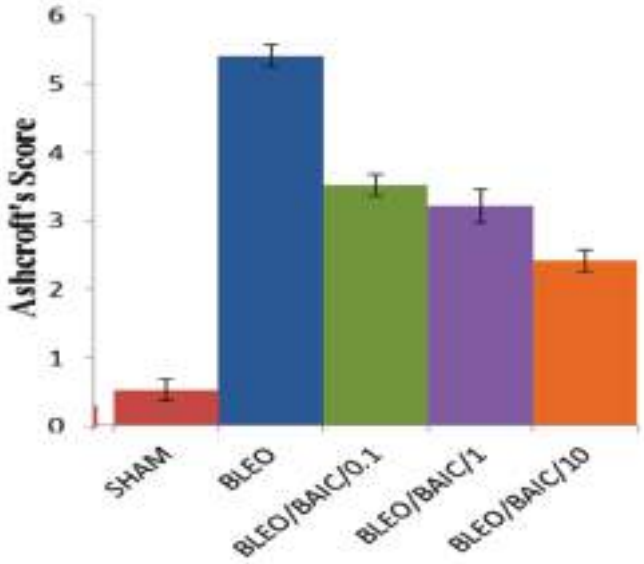


**Fig. 1.** Ashcroft's scoring scale for assessment of histological changes of different groups of mice 8 weeks post treatment.

**Ultrastructural examination of lung tissue**

After sacrificing the animals, lung tissues were removed and dissected at size of 1 mm$^{3}$ and were fixed in Karnovsky's fixative for 6 hours at 40$^{O}$C. The tissues were processed for transmission electron microscopy as described earlier[8]. After several washings, the 1 mm$^{3}$ lung tissues were post fixed in 1% osmium tetraoxide for 1 hour at 40$^{O}$C followed by dehydration at various grade of acetone (30-100% acetone) for 30 min each at 40$^{O}$C and the clearing was done with 2 changes of toluene for 30 min at room temperature. The tissues were further processed and embedded in pure epoxy resin to make blocks. Ultrathin sections (70 nm) were mounted on the copper grid of 300 meshe size and stained with uranyl acetate and lead citrate. The sections were visualized with Tecnai 200Kv transmission electron microscope (Tecnai, Fei Electron Optics) at Elecron Microscopy acility at All India Institute of Medical Sciences (AIIMS), New Delhi.

**Statistical Methods**

Data generated from various experiments were presented as Mean ± SE. All the grouped data was evaluated using SPSS/10.0 software. One-way analysis of variance (ANOVA) was used to detect differences among groups and the means were compared by Duncan's and LSD post hoc test and a value of $P \leq 0.05$ was taken as significant.

## RESULTS

**Effect of baicalein on hematology in bleomycin (BLM) induced lung injury**

In the present study, mean values of hemoglobin at 8 weeks in different groups was lowered in BLM group (6.90±0.18 g/dL), the Hb value was improved by baicalein

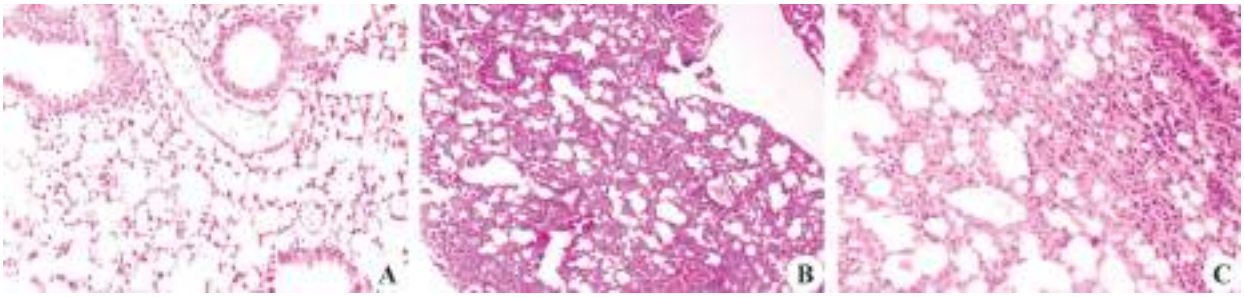


**Fig. 2A.** SHAM: Lung: Showing normal histology with normal bronchi and alveolar epithelium (H&E x100). **B.** BLEO/8 week post treatment: Lung: Showing severely damaged lung architecture with inflammatory cells infiltration, fibrosis, collagen deposition and decreased alveolar spaces with edematous changes (H&E x100). **C.** BLEO/BAIC/10/8 week post treatment: Lung: Moderate fibrin deposition with reduction in inflammatory cells infiltration, edema with improved lung architecture compare to BLEO/8 week (H&E x100).

in BLM/BAIC/0.1 group (7.65±0.62 g/dL), BLM/BAIC/1.0 group (8.10±0.27 g/dL), BLM/BAIC/10 group (9.95±0.25 g/dL) with inclined dose rate and maximum effect was seen at highest dose rate where, the mean value of the group was comparable to SHAM group (10.92±0.29 g/dL) demonstrating the preventive effect of baicalein @ 10 mg/kg dose rate (Table 1).

Similar trend was seen in the pattern of TLC in the animals, where the TLC decreased by baicalein treatment in different groups *viz*. SHAM, BLM, BLM/BAIC/0.1, BLM/BAIC/1.0 and BLM/BAIC/10 i.e. (10.18±0.12×$10^3$/µl), (10.40±1.34×$10^3$/µl), (9.92±1.11×$10^3$/µl), (8.39±0.34×$10^3$/µl) and (8.22± 0.28×$10^3$/µl) which signalled that baicalein had a protective effect (Table 1).

**Baicalein attenuated bleomycin induced pulmonary edema and microvascular permeability**

The wet/dry (W/D) lung weight ratio was calculated as an indicator of pulmonary edema. In the present study the BLM group (6.89±0.62) showed increased mean

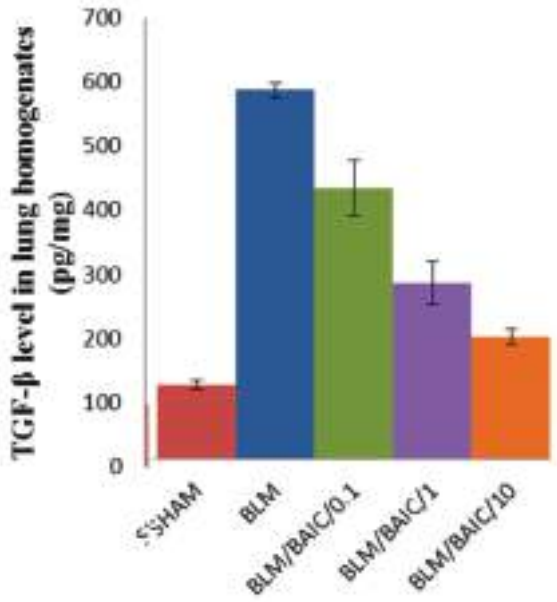


**Fig. 3.** TGF-β levels in lung homogenates of different groups of mice at 8 weeks post treatment.

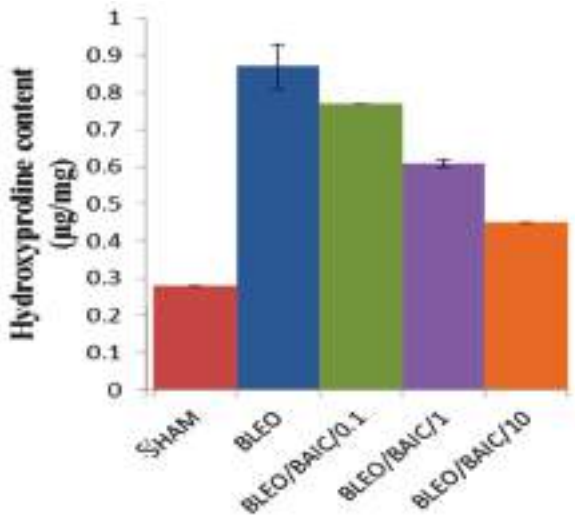


**Fig. 4.** Mean values for hydroxyproline content in lung homogenates of different groups of mice at 1 and 8 weeks post treatment.

wet/dry (W/D) lung weight ratio, while SHAM group (3.04±0.17) and BLM/BAIC/10 group (3.73±0.22) showed comparable values. The animals revealed dose dependent fall in the mean wet/dry (W/D) lung weight ratio in the BLM/BAIC/0.1 (4.89±0.46) and BLM/BAIC/1.0 (4.08±0.45) groups, which further supported that baicalein @ 10 mg/kg attenuated bleomycin induced lung edema. Mean values of wet-to-dry lung weight ratio are presented in Table 2.

The total protein concentration in Bronchio-alveolar Lavage fluid (BALF) was used as a measure to ascertain the microvascular permeability in the present study. The total protein concentration in BALF of BLM group (1114.60±112.58 µg/ml) was significantly ($p<0.05$) higher as compared to that of SHAM (406.65±9.08 µg/ml). But baicalein treatment BLM/BAIC/10 group (730.43±17.79 µg/ml) showed significant decline in total protein concentration as compared to that of BLM group. The improvement was seen in BLM/BAIC/0.1 and BLM/BAIC/1.0 groups also but maximum improvement was seen in highest dose group. Hence, this showed that BAIC at maximum dose was able to maintain vascular

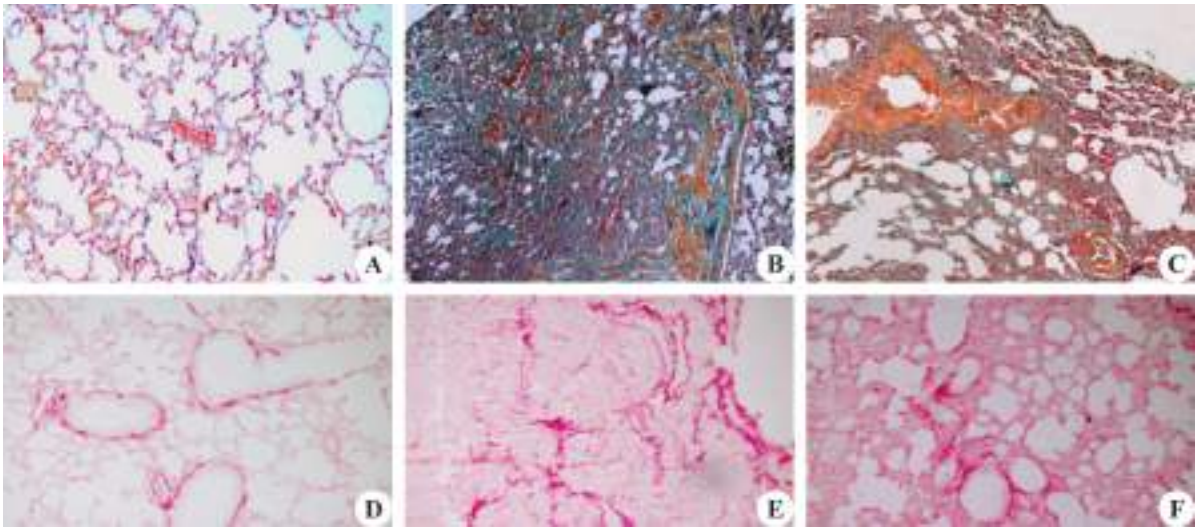


**Fig. 5A.** SHAM: Lung: Showing normal histology with normal alveolar architecture (Masson's trichrome x100). **B.** BLEO/8 week post treatment: Lung: Massive deposition of collagen fibers (green color stained areas) with thickening of alveolar septa and in interstitial areas depicting pulmonary fibrosis (Masson's trichrome x200). **C.** BLEO/BAIC10/8 week post treatment: Lung: Moderate pulmonary fibrosis with decreased deposition of collagen in baicalein treated group (Masson's trichrome x200). **D.** SHAM: Lung: Normal architecture of bronchioles and alveoli (Picro-Sirius red x100). **E.** BLEO/8 week post treatment: Lung: Massive deposition of collagen fibers (red color stained areas) with thickening of alveolar septa and in interstitial areas depicting pulmonary fibrosis (Picro-Sirius red x100). **F.** BLEO/BAIC/10/8 week post treatment: Lung: Moderate pulmonary fibrosis with decreased deposition of collagen in interstitial area (Picro-Sirius red x100).

permeability in lungs. The mean protein concentration values in BALF for different groups are presented in Table 2.

**Baicalein attenuated pulmonary inflammatory cells infiltration**

Meanvalues of TLC were measured in BALF of all the groups and it was observed that there was massive increase in the Total Leukocyte Count of BALF in BLM (4.25±0.52×$10^3$/µl) group compared to SHAM (0.60±0.05×$10^3$/µl) group. TLC value of BLM/BAIC/0.1 (3.32±0.40×$10^3$/µl) and BLM/BAIC/1.0 (2.45±0.28×$10^3$/µl) groups were comparable to each other but significant drop in TLC was seen in BLM/BAIC/10 group (1.65±0.08×$10^3$/µl). This proved the anti-inflammatory action of baicalein. Mean value of TLC alteration are presented in Fig. 3a. Moreover, the percentage of mononuclear cells in mice showed increase in the percentage of mononuclear cells in BALF which were 64.67±2.27 in BLM group, 61.40±2.20 in BLM/BAIC/0.1 group, 57.60±1.93 in BLM/BAIC/1.0 group and percentage was subsidized to 54.67±1.30 in BLM/BAIC/10 group. This further showed that baicalein @ 10 mg/kg bwt was able to make balance in DLC of BALF.

Myeloperoxidase (MPO) activity was measured as an indicator of inflammatory cells accumulation especially macrophages in the chronic stage. Mean values of MPO activity in lung homogenates of mice in SHAM group (54.30±1.72 mu/ml) and BLEO/BAIC/10 (103.74±18.47 mu/ml) showed comparable difference but the difference was significant from mean values of BLM (164.50±8.71 mu/ml), BLM/BAIC/0.1 (145.42±3.96 mu/ml) and BLM/BAIC/1.0 (137.31±11.80 mu/ml) groups (Table 3). These all findings suggested that baicalein was able to limit the infiltration of inflammatory cells mainly macrophages in lungs.

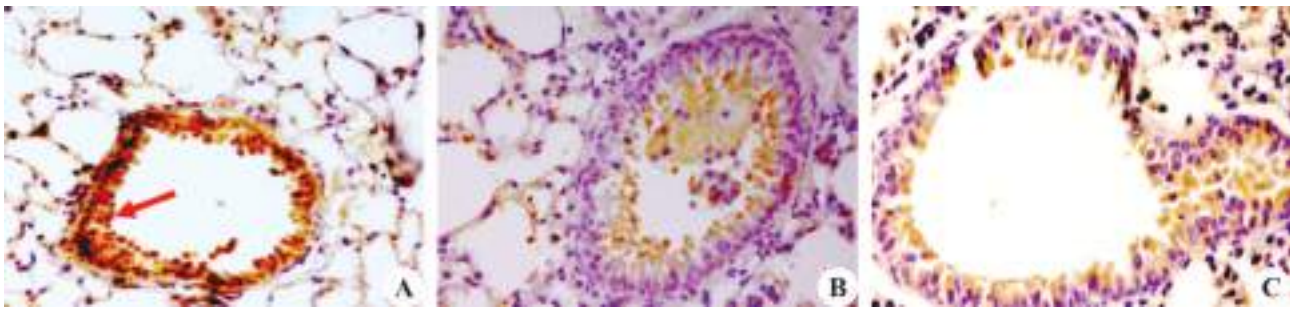


**Fig. 6A.** SHAM/1 week post treatment: Lung: Bronchial and alveolar epithelial cells distinctly expressing E-cadherin (Arrow) (IHC x200). **B.** BLEO/8 week post treatment: Lung: Expression of E-cadherin was seen only on the tip of bronchial epithelial cells (IHC x200). **C.** BLEO/BAIC/10/8 week post treatment: Lung: Restoration of E-cadherin expression in the bronchial epithelial cells (IHC x200).

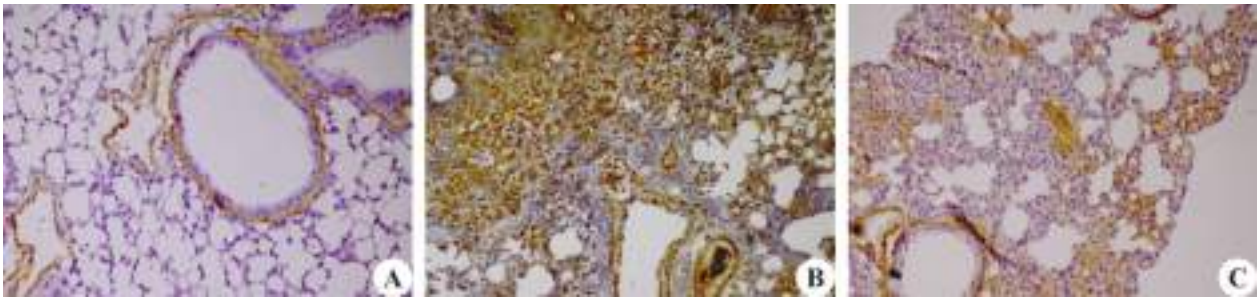

**Fig. 7A.** SHAM: Lung: Alpha-smooth muscle actin (α-SMA) normally expressed in the bronchial as well as vascular smooth muscles (IHC x100). **B.** BLEO/8 week post treatment: Lung: Increased immunolocalization of α-SMA in the myofibroblasts present in the alveolar interstitial area (IHC x100). **C.** BLEO/BAIC/10/8 week post treatment: Lung: BAIC treatment restored the expression of α-SMA in vascular endothelial area and decreased expression of α-SMA in the alveolar interstitial area (IHC x100).

**Baicalein attenuated bleomycin induced oxidative stress**

The lung malondialdehyde (MDA) level of the mice in BLM group rose to 2.00±0.00 nM MDA/g while it was significantly decreased in BLM/BAIC/10 group (1.15±0.13 nM MDA/g) which was comparable to control (SHAM) group (1.05±0.25 nM MDA/g). Baicalein also lowered the level of MDA in BLM/BAIC/0.1 (1.51±0.13 nM MDA/g) and BLM/BAIC/1.0 (1.71±0.33 nM MDA/g) groups (Table 4). This specifies that baicalein reduces the increased level of Lipid peroxidation (LPO) by bleomycin.

Further, the Superoxide Dismutase (SOD) level also decreased significantly in BLM group (2.81±0.32 U) in contrast to (SHAM) group (4.75±0.15 U). But it was raised in animals treated with baicalein in a dose dependent manner BLM/BAIC/0.1 (2.89±0.14 U), BLM/BAIC/1.0 (3.10±0.26 U) and BLM/BAIC/10 (3.94±0.15 U). Thus, it hence showed that baicalein reversed the bleomycin-induced decrease in the superoxide dismutase activity (Table 4).

**Baicalein attenuated bleomycin induced inflammatory cytokines production**

Interleukin-6 (IL-6) and Tumor necrotic factor-alpha (TNF-α) level were estimated in BALF. The level of IL-6 was significantly increased in BLM (154.58±12.29 pg/mg) group as compared to SHAM (71.34±2.34 pg/mg). In contrast to this, BLM/BAIC/10 (72.00±4.43 pg/mg) showed marked reduction in the IL-6 level (Table 5). Further, TNF-α in BLM (612.02±18.56 pg/mg) was higher than SHAM (58.44±4.43 pg/mg) while BLM/BAIC/10 (281.74±7.85 pg/mg) showed reduction in the level of TNF-α level (Table 5).

**Baicalein attenuated bleomycin induced histopathological changes**

Pulmonary morphological changes as assessed by Ashcroft's scoring scale showed reduction of the score in BAIC treated group when compared to that of BLM group (Fig. 1). Significant and consistent lesions in lung sections of different groups were categorized according to Ashcroft's (a numerical fibrotic scale) lung injury assessment scale from 0 to 8. The animals sacrificed showed infiltration of inflammatory cells mainly mononuclear cells along with edematous changes, deposition of collagen fibers, fibrosis in the sub-pleural areas in BLM group which was reduced by baicalein treatment (Fig. 2A-C).

**Baicalein attenuated bleomycin induced pulmonary fibrosis**

To determine the effect of baicalein on bleomycin induced pulmonary fibrosis, TGF-β level and hydroxyproline assays in lung homogenates along with Masson's trichrome and Picro Sirius red staining were performed. As TGF-β1 plays most important role in the development of pulmonary fibrosis, we determined the effect of BAIC on the levels and expression of TGF-β1. In the present study, the level of TGF-β was increased in BLM (573.75±12.31 pg/mg) group as compared to SHAM (114.97±6.82 pg/mg). BAIC treatment resulted in the reduction in the expression and levels of TGF-β in lung (Fig. 3). Further, the collagen content in the lung homogenates was examined by a hydroxyproline assay which showed increase in collagen content in lungs. Collagen content of BLM group (0.87±0.06 μg/mg) was raised which was decreased by baicalein in BLM/BAIC/10 group (0.45±0.00 μg/mg) and was comparable to SHAM

**Table 6.** Score range of E-cadherin and alpha-smooth muscle actin expression in different groups of mice 8 weeks post treatment.

| Groups | Score of E-Cadherin expression (Mean±SE) | Score of alpha-smooth muscle actin expression (Mean±SE) |
|---|---|---|
| SHAM | 4.66±0.21$^{c}$ | 1.83±0.16$^{a}$ |
| BLEO | 2.16±0.16$^{a}$ | 4.66±0.21$^{cd}$ |
| BLEO/BAIC/10 | 3.66±0.21$^{b}$ | 2.16±0.16$^{b}$ |

The values (Mean±SE) in a column having different superscript differ significantly from each other at 5% level of significance. The values (Mean±SE) in a column having same superscript do not differ significantly from each other at 5% level of significance.

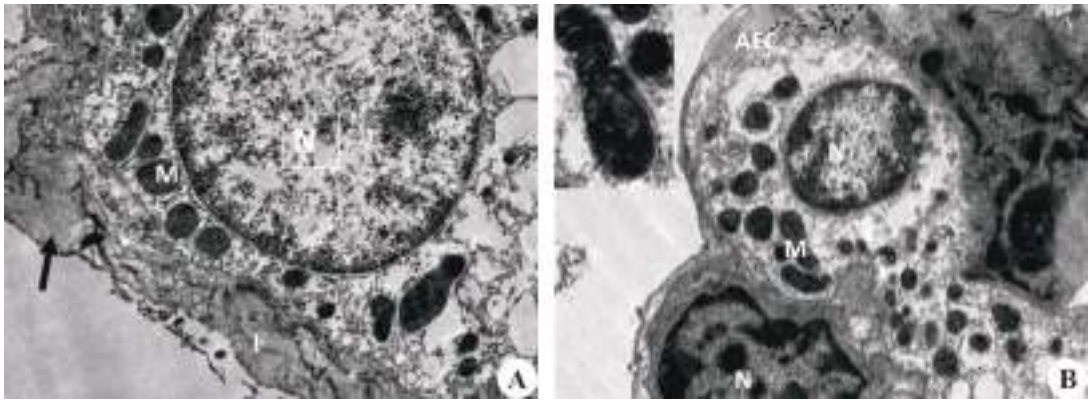


**Fig. 8A.** BLEO/8 week post treatment: Lung: Type 2 alveolar epithelial cells with swollen mitochondria and surrounded by deposition of collagen fibers (arrow) (Bar = 1μm) (N = nucleus, F = collagen fibers, M = mitochondria). **B.** BLEO/BAIC/10/8 week post treatment: Lung: Type 2 alveolar epithelial cells showing restoration of mitochondrial damage with fine cristae in mitochondria (inset) (Bar = 1μm) (N = nucleus, AEC = alveolar epithelial cell, M = mitochondria).

group (0.28±0.00 μg/mg). Collagen deposition was also decelerated by baicalein in BLM/BAIC/0.1 (0.77±0.00 μg/mg) and BLM/BAIC/1.0 (0.61±0.01 μg/mg) groups. Hence, this signifies that baicalein can control collagen deposition in lungs (Fig. 4).

Moreover, by Masson's trichrome and Picro Sirius red staining, there was a decreased fibrosis in baicalein treated groups. Score of picrosirius red stained section in % area was higher in BLM (11.29±1.38 $\mu m^2$) as compared to that of SHAM (0.41±0.06 $\mu m^2$) group. However, this was reduced in BLM/BAIC/10 group (6.44±1.66 $\mu m^2$) (Fig. 5A-F). The decrease was more pronounced in BLM/BAIC/10 group suggesting the antifibrotic role of baicalein in dose dependent manner.

**Baicalein restored bleomycin induced changes in the expression of e-cadherin and alpha-smooth muscle actin**

In the present study, to study the impressions of epithelial and mesenchymal markers, immunohistochemistry was done using primary antibodies against epithelial (e-cadherin) and mesenchymal marker (alpha-smooth muscle actin). There was reduced expression of epithelial marker e-cadherin in BLM group when compared to that of SHAM. In SHAM group the expression of E-Cadherin was observed in the cytoplasm of the bronchial and alveolar epithelial cells with a score of (4.66±0.21) whereas it was seen mainly on the tip of bronchial epithelial cells in BLM (2.16±0.16). However, the treatment with BAIC treatment restored the expression of e-cadherin in the epithelial cells (3.66±0.21) (Fig. 6A-C). Alpha-smooth muscle actin ($\alpha$-SMA) was normally expressed in the bronchial as well as vascular smooth muscles as observed in SHAM mice (1.83±0.16). However there was expression of $\alpha$-SMA in the alveolar interstitial areas in BLM mice (4.66±0.21) which was further reduced by baicalein treatment (2.16±0.16) (Fig. 7A-C). The scoring pattern of both immunohistochemical markers are given in Table 6.

**Baicalein restored bleomycin induced ultrastructural changes**

Transmission electron microscopy was performed to determine the ultra-morphological changes in bronchial and alveolar epithelial cells. The alveolar epithelial cells showed degeneration and complete loss of mitochondrial cristae along with presence of collagen fibers deposited around the alveolar epithelial cells, severe degeneration of alveolar epithelial cells was observed with loss of mitochondria as vacuolation in BLM group (Fig. 8A). The effects were ameliorated in BLM/BAIC/10 mg group where alveolar epithelial cells showed restoration of mitochondrial damage. The mitochondria showed fine cristae (Fig. 8B).

## DISCUSSION

Pulmonary fibrosis (PF) is a chronic lung disorder marked by damage to alveolar epithelial cells, inflammation, fibroblast proliferation, and extracellular matrix deposition, leading to scar formation. Key areas affected include the alveolar walls and surrounding connective tissue. This process results in decreased lung elasticity and reduced alveolar surface area, impairing gas exchange and pulmonary function. In research, a single intratracheal injection of bleomycin in mice is used to model lung injury that leads to pulmonary fibrosis[9].

Baicalein (BAIC), a bioflavonoid, has various pharmacological effects, including antioxidant, anti-inflammatory, and neuroprotective properties. It works by scavenging Reactive Oxygen Species and improving antioxidant status, thus modulating the immune system[9]. However, the effectiveness of BAIC against BLM-induced chronic lung injury and its impact on Epithelial Mesenchymal Transition (EMT) is not well understood. This study aims to investigate whether BAIC treatment can improve pulmonary fibrosis and EMT following BLM exposure.

In many organs including lung, EMT is involved in pathogenesis of fibrosis. Chronic lung inflammation is always accompanied with EMT, collagen deposition, and lung fibrosis[10]. Thus in the present study focus was given to bleomycin induced chronic lung injury and subsequent EMT. And it has been observed that BAIC treatment showed amelioration in the chronic lung injury and pulmonary fibrosis caused by BLM.

The significant decrease in hemoglobin, in the present study might be because heme proteins are liable to release iron when peroxides are present. Organic peroxides and hydrogen peroxide can be produced during the bleomycin reaction leading to iron release from haemeproteins resulting in decrease in hemoglobin concentration[11]. The hemoglobin level was improved in group BLEO/BAIC/10 and was comparable to control because of baicalein has a strong antioxidant activity which quench the peroxides present and might prevent the release of iron from the heme proteins[13], thereby improving the Hb level.

Bleomycin leads to altered lung fluid balance leading to increased permeability in the endothelium leading to pulmonary edema which is a pathophysiological hallmark of lung injury.

Increased pulmonary capillary permeability leads to edema by allowing more fluid and protein to enter the lung interstitium[14]. This type of pulmonary edema, characterized by high protein content, arises from less restricted plasma proteins moving across the capillary membrane. The severity of alveolar flooding during lung injury depends on factors like interstitial edema extent, alveolar epithelial injury, and the epithelium's ability to clear edema fluid[15].

Because of the increase in micro vascular permeability in lung injury, concomitant increases in lung micro vascular hydrostatic pressure (as might occur with aggressive volume resuscitation) will lead to even greater formation of pulmonary edema. The injury is triggered by the release of inflammatory cells, proinflammatory cytokines and ROS which ultimately damage the endothelial cells. In the present study, the damage to the endothelial cells might have led to permanent influx of protein and edematous fluid into the lung alveoli leading to increase in protein content and wet to dry lung ratios. In the present study baicalein in BLM/BAIC/10 group @ 10 mg bw I.P considerably reduces the pulmonary edema due to its anti-inflammatory, antioxidant activity[16]. Mechanistically, baicalein treatment appears to mitigate lung damage by suppressing accumulation of inflammatory cell, decreasing IL-6, TNF$\alpha$ and inactivating NFκB pathway which results in inactivation of pro-inflammatory genes, with release of the cytokines[17].

The TLC in BALF was increased due to increase in the number of mononuclear cells at 8 weeks as during any chronic inflammation the MNCs predominate[18]. In addition, the alveolar inflammatory cells have been regarded as a major source of the release of pro-inflammatory cytokines and chemokines, promoting inflammatory cell accumulation in tissues, as well as reactive oxygen species (ROS) formation[19]. Accordingly, the immune cell-derived inflammatory mediators play a critical role in the pathogenesis of pulmonary fibrosis[20]. The number of inflammatory cells in the BLM/BAIC/10 group decreased and showed that baicalein ameliorated the effect of bleomycin induced lung injury due to its anti-inflammatory effect[21]. These changes might be due to the fact that baicalein leads to impairment of reactive oxygen intermediates production, through scavenging reactive oxygen intermediates by antagonizing ligand-initiated $Ca^{2+}$ influx by baicalein that accounts for the inhibition of Mac-1-dependent leukocyte adhesion that confers the anti-inflammatory activity of baicalein[22], hence, reduced leukocyte infiltration which ultimately lead to reduced MPO activity post treatment of BLM. Importantly, the increased amount of pro-inflammatory cytokines (IL-6 and TNF-$\alpha$) in BALF of mice challenged by BLM was remarkably inhibited by BAIC. These findings suggest that the protective effect of BAIC in chronic lung injury may be, at least in part, attributed to the suppression of inflammatory cell sequestration and infiltration into lungs, in turn attenuating pro-inflammatory cytokine release.

Bleomycin binds to iron ($Fe^{2+}$), undergoes redox cycling and catalyzes the formation of ROS that plays a major role in the progression of pulmonary fibrosis by targeting DNA, protein and lipids with ultimate progression of lipid peroxidation[23]. In this study the decreased LPO production observed in BAIC treated group, might also be due to the iron chelating activity of BAIC and has been shown to possess relatively potent metal chelating properties[24]. SOD is a ubiquitous enzyme that catalyzes the dismutation of superoxide into oxygen and hydroperoxides thereby protecting the cells from detrimental superoxide anion[25]. A notable descend in the activities of SOD was observed in bleomycin-induced animals, which might be due to increased LPO and overproduction of ROS[26]. The activity of SOD was maintained to near normal values upon treatment with Baicalein. This may be due to the direct action of BAIC on superoxide, hydroxyl and alkoxyl radical coupled with its ability to attenuate LPO, which in turn reduces free radical generation and oxidative stress during BLM induced chronic lung injury.

Histopathological examination of the lungs showed infiltration of inflammatory cells along with edematous changes, deposition of collagen fibres, fibrosis in the sub-pleural areas in BLM group which was reduced by

baicalein treatment. The pulmonary fibrosis caused due to bleomycin was restored backed by BAIC due to the antifibrotic effect of BAIC as observed in the present study depicted by reduction in the deposition of collagen as shown by Masson's trichrome, picro-sirius red stained lung sections as well as hydroxyproline content in the lung. In BLM induced chronic lung injury TGF-β plays the most important role in pulmonary fibrosis. TGF-β, a potent fibrogenic cytokine is elevated after bleomycin administration in the epithelial cells, endothelial cells, alveolar macrophages and interstitial fibroblasts and thereby initiates inflammatory response, apoptosis of epithelial cell and proliferation of fibroblast along with collagen deposition and EMT[27]. It has been postulated that the initial activation of TGF-β is due to the initial inflammatory response and generation of ROS[28]. In this study, baicalein had reduced the expression of TGF-β along with the reduction of collagen deposition in interstitial regions which might be due to inhibition of the increased expression of TGF-β1 and p-Smad-2/3 in bleomycin-treated mice[29].

Epithelial-mesenchymal transition (EMT) is a physiological process in which epithelial cells acquire the motile and invasive characteristics of mesenchymal cells[30]. E-cadherin, a cell adhesion molecule, normally expressed by epithelial cells is repressed during EMT. During EMT, these cells leave the epithelial layer and migrate through the lining basement membrane followed by accumulation in the tissue interstitium where they eventually loss the epithelial markers and gain a mesenchymal phenotype[31]. In the present study, the expression of e-cadherin was suppressed in BLM mice which were restored with baicalein treatment. Further in the present study, BLM administered mice showed increased TGF-β with decreased expression of E-cadherin. This may be due to the fact that TGF-β represses E-cadherin production in epithelial cells[32].

Further, alpha smooth muscle actin (α-SMA), a contractile protein and actin isoform, are expressed mainly in smooth-muscle cells of blood vessels and plays an important role in fibrogenesis[33]. In the present study, besides vascular and bronchiolar smooth muscles, α-SMA expression was observed in the alveolar interstitial areas in BLM administered mice which was restored with baicalein treatment. α-SMA positive myofibroblasts have been demonstrated in type 2 EMT associated with tissue regeneration and organ fibrosis. This occurs due to destabilize interactions between epithelial cells and/or cell to extracellular matrix. Further, stressed and injured epithelium can give rise to myofibroblasts and thereby contribute to fibrogenesis[34]. Thus, it indicates that EMT plays an important role in bleomycin induced pulmonary fibrosis.

Ultrastructural studies showed injured and apoptotic epithelial cells in BLEO treated lung which was restored with baicalein treatment. Evidently, baicalein treatment is associated with the restoration of mitochondrial functions with mitochondrial ultrastructural changes in bronchial epithelia either due to 15-LOX inhibition, or by indirect mechanisms such as the reduction lipid peroxidation. Baicalein may limit apoptosis, possibly via the inhibition of both the extrinsic and intrinsic pathways of apoptosis, including the inhibition of TNF-α production and modulation of pro- and anti-apoptotic signaling elements[35].

## CONCLUSION

In conclusion, baicalein was effective in attenuating the BLM induced Pulmonary fibrosis through suppression of oxidative stress, inflammation, histological as well as ultrastructural damages and EMT especially during the chronic stage injury. This study will provide an additional knowledge on the ameliorative effect of baicalein during the later stages of lung injury where the EMT starts and this may help in the therapeutic or management of clinical chronic lung injury associated pulmonary fibrosis.

## ACKNOWLEDGEMENT

The author acknowledged the financial support provided by Science and Engineering Research Board (SERB), Department of Science and Technology, Government of India via project No. YSS/2014/000045. We also acknowledge the help provided by Sophisticated Analytical Instrument Facility, All India Institute of Medical Sciences, New Delhi for transmission electron microscopy.

## REFERENCES

1. Oruqaj G, Karnati S, Vijayan V, Kotarkonda LK, Boateng E, Zhang W, Ruppert C, Günther A, Shi W and Baumgart-Vogt E. 2015. Compromised peroxisomes in idiopathic pulmonary fibrosis, a vicious cycle inducing a higher fibrotic response via TGF-β signalling. *Proc Nat Acad Sci United States of America* **112:** 2048.
2. Serrano-Mollar A. 2012. Alveolar epithelial cell injury as an etiopathogenic factor in pulmonary fibrosis. *Arch Bronconeumol* **48:** 2.
3. Adamson IY and Bowden DH. 1974. The pathogenesis of bleomycin-induced pulmonary fibrosis in mice. *Am J Pathol* **77:** 185.
4. Mabalirajan U, Ahmad T, Leishangthem GD, Joseph DA, Dinda AK, Agrawal A and Ghosh B. 2010. Beneficial effects of high dose of L-arginine on airway hyperresponsiveness and airway inflammation in a murine model of asthma. *J Allergy Clin Immunol* **125:** 626.
5. Hübner RH, Gitter W, Mokhtari NEE, Mathiak M, Both M, Bolte H, Wolf SF and Bewig B. 2008. Standardized quantification of pulmonary fibrosis in histological samples. *Bio Tech* **44:** 507.
6. Madesh M and Balasubramanian KA. 1998. Microtitre plate assay for superoxide dismutase using MTT reduction by

superoxide. *Indian J Biochem Biophys* **35:** 184.
7. Lomas NJ, Watts KL, Akram KM, Forsyth NR and Spiteri MA. Idiopathic pulmonary fibrosis: immunohistochemical analysis provides fresh insights into lung tissue remodelling with implications for novel prognostic markers. *Int J Clin Exp Pathol* **5:** 58.
8. Leishangthem GD, Mabalirajan U, Singh VP, Agrawal A, Ghosh B and Dinda AK. 2013. Ultrastructural changes of airway in murine models of allergy and diet-induced metabolic syndrome. *ISRN Allergy*.
9. Mutsaers SE, Foster ML, Chambers RC, Laurent GJ and McAnulty RJ. 1998. Increased endothelin-1 and its localization during the development of bleomycin-induced pulmonary fibrosis in rats. *Am J Respir Cell Mol Biol* **18:** 611.
10. Shan H, Chen Y, Wang ZF, Mao-Ying QL, Mi WL, Jiang JW, Wu GC and Wang YQ. 2015. The Analgesic and Anti neuro inflammatory Effect of Baicalein in Cancer-Induced Bone Pain. *J Evid Based Comp Altern Med*.
11. Chen CM, Chou HC and Huang LT. 2015. Maternal Nicotine Exposure Induces Epithelial-Mesenchymal Transition in Rat Offspring Lungs. *Neonatol* **108:** 179.
12. Gutteridge JM and Hou YY. 1986. Iron complexes and their reactivity in the bleomyc in assay for radical-promoting loosely-bound iron. *Free Radic Res Commun* **2:** 143.
13. Liu W, Chen XL, Liu JH, Chen C and Ai J. 2009. The effect of baicalein on bleomycin-induced fibrosis in lungs of rats. *Chinese J Appl Physiol* **25:** 145.
14. Ware LB and Matthay MA. 2005. Clinical practice: acute pulmonary edema. *NEJM* **353:** 2788.
15. Ware LB and Matthay MA. 2001. Alveolar fluid clearance is impaired in the majority of patients with acute lung injury and the acute respiratory distress syndrome. *American Am J Respir Crit Care Med* **163:** 1376.
16. Gao Z, Huang K and Xu H. 2001. Protective effects of flavonoids in the roots of *Scutellariabaicalensis Georgi* against hydrogen peroxide-induced oxidative stress in HS-SY5Y cells. *Pharmacol Res* **43:** 173.
17. Ward PA. 2003. Acute lung injury: how the lung inflammatory response works. *Eur Respir J* **22:** 22.
18. Reutershan J, Basit A, Galkina EV and Ley K. 2005. Sequential recruitment of neutrophils into lung and bronchoalveolar lavage fluid in LPS-induced acute lung injury. *Am J Physiol* **289:** 807.
19. Agouridakis P, Kyriakou D, Alexandrakis MG, Prekates A, Perisinakis K, Karkavitsa N and Bouros D. The predictive role of serum and bronchoalveolar lavage cytokines and adhesion molecules for acute respiratory distress syndrome development and outcome. *Respir Res* **3:** 25.
20. Bhatia M and Moochhala SJ. 2004. Role of inflammatory mediators in the pathophysiology of acute respiratory distress syndrome. *J Pathol* **202:** 145.
21. Huang X, He Y, Chen Y, Wu P, Gui D, Cai H, Chen A, Chen M, Dai C, Yao D and Wang L. 2016. Baicalin attenuates bleomycin-induced pulmonary fibrosis via adenosine A2a receptor related TGF-β1 induced ERK1/2 signaling pathway. *BMC Pul Med* **16:** 132.
22. Shen YC, Chiou WF, Chou YC and Chen CF. 2003. Mechanisms in mediating the anti-inflammatory effects of baicalein and baicalein in human leukocytes. *Eur J Pharmacol* **465:** 171.
23. Martin WJ and Kachel DL. 1987. Bleomycin-induced pulmonary endothelial cell injury: evidence for the role of iron-catalyzed toxic oxygen-derived species. *J Lab Clin Med* **110:** 153.
24. Yoshino M and Murakami K. 1998. Interaction of iron with polyphenolic compounds: application to antioxidant characterization. *Anal Biochem* **257:** 40.
25. McCrod JM and Keele BB. 1971. An enzyme-based theory of obligate anaerobiosis: the physiological function of superoxide dismutase. *Proc Natl Acad Sci* **68:** 1024.
26. Iraz M, Erdogan H, Kotuk M, Yağmurca M, Kilic T, Ermis H, Fadillioğlu E and Yildirim Z. 2006. *Ginkgo biloba* inhibits bleomycin-induced lung fibrosis in rats. *Pharmacol Res* **53:** 310.
27. Andre PA, Prêle CM, Vierkotten S, Carnesecchi S, Donati Y, Chambers RC, Pache JC, Crestani B, Barazzone-Argiroffo C, Königshoff M, Laurent GJ and Irminger-Finger I. 2015. BARD1 mediates TGF-β signaling in pulmonary fibrosis.*Respir Res* **29:** 118.
28. Barcellos-Hoff MH and Dix TA. 1996. Redox-mediated activation of latent transforming growth factor-beta1. *Mol Endocrinol* **10:** 1077.
29. Gao Y, Lu J, Zhang Y, Chen Y, Gu Z and Jiang X. 2013. Baicalein attenuates bleomycin-induced pulmonary fibrosis in rats through inhibition of miR-21. *Pulm Pharmacol Ther* **26:** 649.
30. Paola N, Mina JB and Derek C. 2012. Radisky3 Epithelial-Mesenchymal Transition: General Principles and Pathological Relevance with Special Emphasis on the Role of Matrix Metallo proteinases. *CSH Perspect Biol* **4:** 1.
31. Kalluri R and Weinberg RA. The basics of epithelial-mesenchymal transition. *J Clin Invest* **119:** 1420.
32. Choi J, Park SY and Joo CK. 2007. Transforming growth factor-beta1 represses E-cadherin production via slug expression in lens epithelial cells. *IOVS* **48:** 2708.
33. Kawasaki Y, Imaizumi T, Matsuura H, Ohara S, Takano K, Suyama K, Hashimoto K, Nozawa R, Suzuki H and Hosoya M. 2008. Renal expression of alpha-smooth muscle actin and c-met in children with Henoch-Schonlein purpura nephritis. *Pediatr Nephrol* **23:** 913.
34. Lee K and Nelson CM. 2012. New insights into the regulation of epithelial-mesenchymal transition and tissue fibrosis. *Int Rev Cell Mol Biol* **294:** 171.
35. Mabalirajan U, Ahmad T, Rehman R, Leishangthem GD, Dinda AK, Agrawal A, Ghosh B and Sharma SK. 2013. Baicalein reduces airway injury in allergen and IL-13 induced airway inflammation. *PLoS One* **8:** e62916.

*Indian J. Vet. Pathol., 49(2) : 142-153, 2025: DOI: https://doi.org/10.56093/xd6m1h79*

RESEARCH ARTICLE

# Ameliorative effect of visnagin against colitis derived hepatoxicity by dextran sodium sulphate in C57BL/6 mice

**V. Sravathi, D. Madhuri*, Y. Ravi Kumar, B. Anil Kumar[1] and A. Vijaya Kumar[2]**
Department of Veterinary Pathology, College of Veterinary Science, PV Narsimha Rao Telangana Veterinary University, Rajendranagar, Hyderabad-500 030, Telangana, India, [1]Department of Pharmacology and Toxicology, [2]Department of Veterinary Public Health and Epidemiology

**Address for Correspondence**
*D. Madhuri, Professor & University Head, Department of Veterinary Pathology, College of Veterinary Science, PV Narsimha Rao Telangana Veterinary University, Rajendranagar, Hyderabad-500 030, Telangana, India, E-mail: madhurighanta@yahoo.co.in*

*Received: 3.1.2025; Accepted: 14.2.2025*

## ABSTRACT

The present study was conducted to investigate hepatic damage associated with Dextran sodium sulphate (DSS) induced ulcerative colitis (UC) and to evaluate the ameliorative effect of Visnagin (VIS) against this hepatic damage. Six groups of C57BL/6 male mice, each containing six animals *viz.* Group 1 (Normal), Group 2 (DSS @ 2% with 3 cycles of 5 day intervals diluted in distilled water administered orally), Group 3 (VIS @ 60 mg/kg b.wt., orally), Group 4 (VIS @ 30 mg/kg b.wt. and DSS), Group 5 (VIS @ 60 mg/kg b.wt. and DSS) and Group 6 (Dexamethasone sodium @ 1 mg/kg b.wt. IP and DSS). After the 31-day experimental period, organ weights, serum analysis, oxidative stress parameters, inflammatory cytokines, gross and histopathology and immunohistochemical analysis were evaluated on day 32. Group 2 mice (DSS only) showed significant increase in ALT, AST, MDA and nitrite levels, along with elevated pro-inflammatory cytokines levels. Conversely, significant decreases in total protein, albumin levels, antioxidant enzymes levels (SOD, CAT and GSH) and IL-10 concentrations were observed. Histopathological examination revealed severe degenerative changes in the livers of Group 2, with increased NF-κB immunoexpression and reduced Nrf2 protein expression. Groups 4 and 5 treated with VIS, showed dose-dependent improvements with moderate to mild changes attributed to VIS's anti-inflammatory and antioxidant properties likely through modulation of the Nrf2 signaling pathway. Group 6 treated with Dexamethasone, also showed improvement in all these parameters. In conclusion, VIS demonstrated notable anti-inflammatory and anti-oxidant properties against DSS-induced hepatotoxicity.

**Keywords:** Dextran sodium sulphate, hepatic damage, ulcerative colitis, visnagin

## INTRODUCTION

The gut-liver axis refers to the bidirectional relationship between the gastrointestinal tract and the liver, and it plays a crucial role in inflammatory bowel disease (IBD)[1]. Ulcerative colitis (UC), a subtype of IBD, is a chronic condition marked by persistent inflammation primarily affecting the colon's mucosal lining. This inflammation disrupts the integrity of the colon mucosa impairing the intestinal barrier function and leading to a range of gastrointestinal symptoms and complications[2]. In addition to the chronic, non-specific intestinal inflammation, IBD often presents with various extra intestinal manifestations which significantly contribute to the morbidity and mortality of affected patients. Among these extra intestinal manifestations, hepatobiliary disorders are relatively common, further complicating the clinical management of IBD[3]. Intestinal inflammation and microbial dysbiosis contribute to liver injury through excessive exposure to bacterial translocation, enteric antigens, toxins and inflammatory mediators which subsequently activate inflammatory signaling pathways such as the toll like receptors/nuclear factor kappa-light-chain-enhancer of activated B cell (TLR4/NF-κB) pathway. This process enhances the secretion of pro-inflammatory cytokines like tumor necrosis factor (TNF)-$\alpha$, interleukin (IL)-1$\beta$ and IL-6, thereby exacerbating liver damage and ultimately leading to chronic liver diseases[4]. The inflammatory cascade triggered by DSS results in liver damage characterized by hepatocyte apoptosis, fibrosis and altered liver function. Additionally, medications used to manage IBD can cause gastrointestinal and liver-related side effects[5]. Therefore, targeting inflammatory signaling pathways and regulation of the gut-liver axis present promising strategies for developing drugs to treat liver injury.

**How to cite this article :** Sravathi, V., Madhuri, D., Kumar, Y.R., Kumar, B.A. and Kumar, A.V. 2025. Ameliorative effect of visnagin against colitis derived hepatoxicity by dextran sodium sulphate in C57BL/6 mice. Indian J. Vet. Pathol., 49(2) : 142-153.

In response to emerging health risks, there is increasing interest in natural products for preventive and therapeutic measures. Visnagin {4-methoxy-7-methylfuro (3,2-g) chromen-5-one} is a funarochrome active compound extracted from the plant of *Ammi visnaga* has demonstrated widespread pharmacological actions including anti-cancer, anti-inflammatory, anti-oxidant, anti-microbial and other biological effects[6]. Previous studies indicate

that VIS prevents damage to renal epithelial cells through its diuretic action. Additionally, VIS has been reported to exhibit cardioprotective and vasodilatory effects[6,7] and to provide efficacy against hypertriglyceridemia, urolithiasis, reducing apoptosis in the follicular tissues of rat ovaries and diminishing inflammatory and oxidative responses in LPS-activated BV-2 microglial cells[8]. Pasari *et al.*[9] recently reported the role of Nrf2 in mediating the anti-inflammatory and antioxidant activities of VIS using a cerulein-induced acute pancreatitis model in mice. Their findings showed that VIS decreased the expression of pro-inflammatory cytokines in a dose-dependent manner. Notably, VIS enhanced antioxidant defenses by upregulating Nrf2 and reduced pancreatic inflammation by suppressing NF-κB expression in acinar cells. Furthermore, VIS inhibited the release of inflammatory cytokines in both pulmonary and intestinal tissues[9]. However, the effects of VIS on liver injury have not yet been analyzed. Therefore, in this study, we aimed to investigate the therapeutic potential of VIS against colitis induced liver injury.

**Table 1.** Ameliorative effect of VIS on serum biochemical parameters.

| Groups | ALT (IU/L) | AST (IU/L) | TP (g/dL) | Albumin (g/dL) |
|---|---|---|---|---|
| Group 1 | 53.59±0.42 | 58.86±3.44 | 7.12±0.17 | 3.50±0.11 |
| Group 2 | 84.60±0.50$^{###}$ | 235.60±6.15$^{###}$ | 3.76±0.05$^{###}$ | 1.60±0.13$^{###}$ |
| Group 3 | 53.37±0.91 | 59.59±2.70 | 7.23±0.07 | 3.55±0.11 |
| Group 4 | 78.17±0.40$^{***}$ | 212.90±2.80$^{***}$ | 4.67±0.12$^{***}$ | 2.25±0.10$^{**}$ |
| Group 5 | 73.31±0.60$^{***}$ | 194.80±1.07$^{***}$ | 5.72±0.08$^{***}$ | 2.53±0.10$^{***}$ |
| Group 6 | 64.98±0.50$^{***}$ | 165.90±1.42$^{***}$ | 6.51±0.08$^{***}$ | 2.90±0.13$^{***}$ |

## MATERIAL AND METHODS

### Reagents

Dextran sodium sulphate salt 500 was procured from Savvy Scientifics (CAT No. 99629) and Visnagin from Cayman Chemical Company, USA (CAT No. 34140). Kits for measuring Aspartate Transaminase (AST), Alanine Transaminase (ALT), total protein (TP) and albumin were purchased from Erba Diagnostics, USA. ELISA kits for TNF-$\alpha$, TGF-β, IL-1β, IL-6, NF-κB, IL-17 and LI-10 were acquired from Invitrogen, Thermo Fischer Scientific Ltd. Stains and chemicals for the histopathological study of tissues were obtained from HiMEDIA Laboratories Pvt. Ltd., Secunderabad, Telangana, Antibodies for NF-κB, Nrf2, COX-2 and caspase-3 used in immunohistochemical staining were sourced from M/s Santacruz Biotechnology, USA. The PolyExcel HRP/DAB detection system for

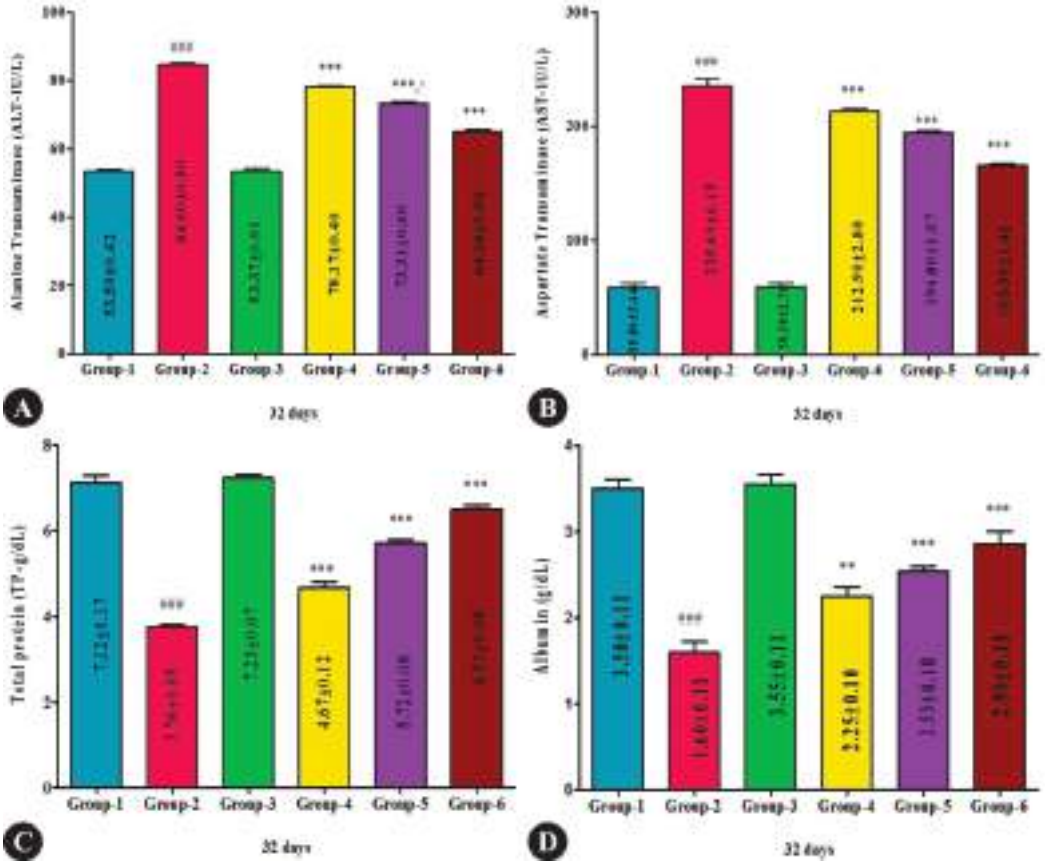


**Fig. 1.** Ameliorative effect of VIS on serum biochemical parameters. **A.** ALT. **B.** AST. **C.** Total Protein. **D.** Albumin.

**Table 2.** Effect of visnagin on Oxidative and antioxidant indices in liver of different groups of mice.

| Groups | TBARS (nM/mg protein) | Nitrite (µm/mg protein) | SOD (IU/mg protein) | GSH (µM/mg protein) | Catalase (IU/mg protein) |
|---|---|---|---|---|---|
| Group 1 | 15.44±2.17 | 10.03±0.41 | 29.75±0.86 | 47.76±4.30 | 15.03±0.70 |
| Group 2 | 59.14±2.64$^{###}$ | 46.00±1.49$^{###}$ | 9.45±0.71$^{###}$ | 14.17±0.83$^{###}$ | 4.31±0.31$^{###}$ |
| Group 3 | 16.88±1.25 | 11.60±0.30 | 32.16±1.99 | 45.30±1.90 | 14.52±0.61 |
| Group 4 | 33.07±1.22$^{*}$ | 25.41±0.44$^{***}$ | 14.89±0.33$^{*}$ | 25.17±0.80$^{**}$ | 7.91±0.40$^{*}$ |
| Group 5 | 22.76±1.85$^{***}$ | 15.90±0.84$^{***}$ | 22.88±1.19$^{***}$ | 34.86±1.30$^{***}$ | 9.87±0.80$^{***}$ |
| Group 6 | 20.66±1.21$^{***}$ | 13.04±0.32$^{***}$ | 25.14±0.61$^{***}$ | 38.38±1.07$^{***}$ | 10.25±1.04$^{***}$ |

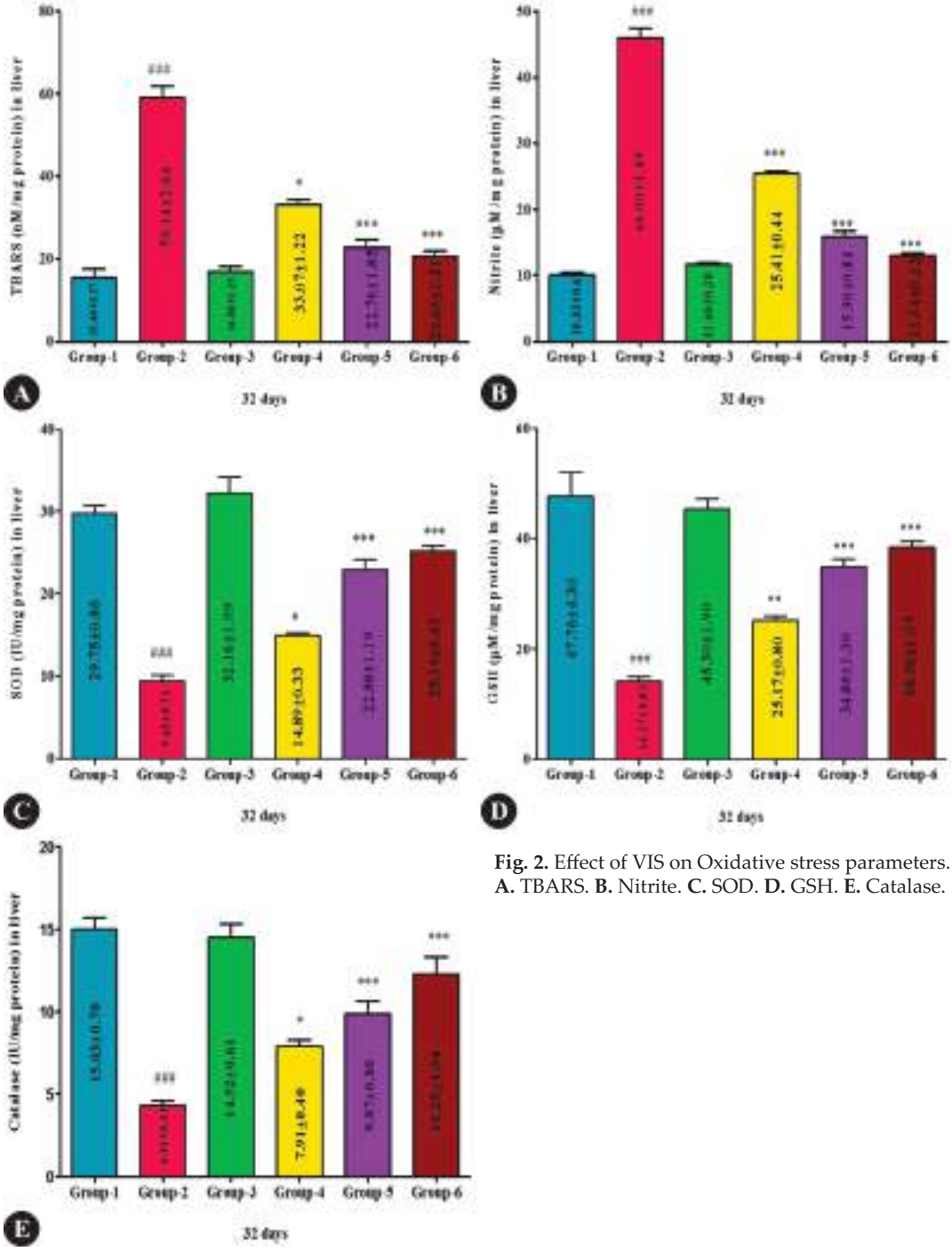


**Fig. 2.** Effect of VIS on Oxidative stress parameters. **A.** TBARS. **B.** Nitrite. **C.** SOD. **D.** GSH. **E.** Catalase.

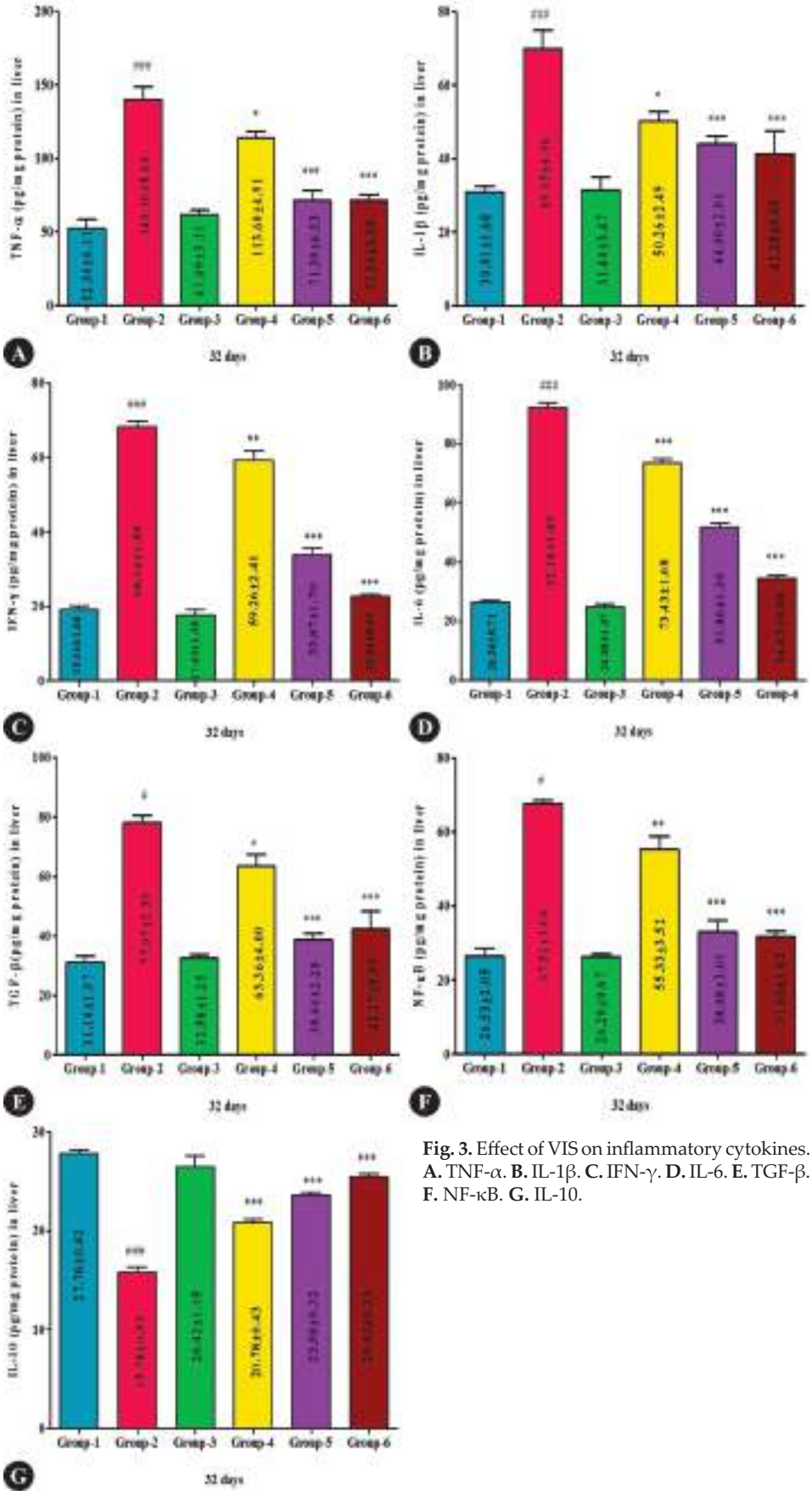


**Fig. 3.** Effect of VIS on inflammatory cytokines. **A.** TNF-α. **B.** IL-1β. **C.** IFN-γ. **D.** IL-6. **E.** TGF-β. **F.** NF-κB. **G.** IL-10.

**Table 3.** Effect of visnagin in pro-inflammatory and anti-inflammatory cytokine indices in liver of different groups of mice.

| Groups | TNF-$\alpha$ (pg/mg protein) | IL-1$\beta$ (pg/mg protein) | IFN-$\gamma$ (pg/mg protein) | IL-6 (pg/mg protein) | IL-10 (pg/mg protein) |
|---|---|---|---|---|---|
| Group 1 | 52.30±6.11 | 30.91±1.68 | 19.14±1.04 | 26.34±0.71 | 27.76±0.42 |
| Group 2 | 140.10±8.60$^{###}$ | 69.95±4.96$^{###}$ | 68.14±1.58$^{###}$ | 92.18±1.89$^{###}$ | 15.78±0.53$^{###}$ |
| Group 3 | 61.69±3.11 | 31.40±3.47 | 17.63±1.38 | 24.88±1.07 | 26.42±1.15 |
| Group 4 | 113.60±4.91$^{*}$ | 50.26±2.49$^{*}$ | 59.26±2.41$^{**}$ | 73.43±1.68$^{***}$ | 20.78±0.43$^{***}$ |
| Group 5 | 71.39±6.53$^{***}$ | 44.00±2.01$^{***}$ | 33.87±1.70$^{***}$ | 51.86±1.30$^{***}$ | 23.58±0.32$^{***}$ |
| Group 6 | 71.36±3.99$^{***}$ | 41.28±6.40$^{***}$ | 22.61±0.66$^{***}$ | 34.63±0.98$^{***}$ | 25.43±0.33$^{***}$ |

immunohistochemistry was procured from M/s PathnSitu Biotechnologies, USA.

**Study design**

36 male C57BL/6 mice (25-30 gms) were obtained from the M/S Jeeva life sciences Ltd. Hyderabad and were maintained in a controlled environment throughout the course of the experiment. Mice were provided with 7 days of acclimation period before the experiment began and allowed free access to sterile food and drinking water. The experimental protocol was reviewed and approved by Institutional Animal Ethics Committee, CVSc, Rajendranagar, Hyderabad (06/26/CVSc, Hyd. IAEC /2023). To assess the ameliorative effects of visnagin on liver injury caused by DSS induced colitis, the mice were randomly assigned to six experimental groups (n=6). The group 1 (sham control), group 2 (2% DSS with 3 cycles of 5 days' intervals, diluted in distilled water administered orally, group 3 *perse* (visnagin at 60 mg/kg b.wt), groups 4 and 5 (DSS + visnagin at 30 and 60 mg/kg b.wt respectively) and group 6 (standard drug, dexamethasone at 1 mg/kg b.wt) for 31 days. All mice were sacrificed on the 32$^{nd}$ day of the experimental period and liver samples were collected. A portion of liver tissue was preserved in 10% neutral buffer formalin (NBF) for histopathological examination while other portion was stored at -80$^{O}$C for further analysis.

**Biochemical analysis**

**Fig. 4.** Severe congestion of the liver observed in group 2 compared to other groups.

Approximately 0.5 mL of blood was collected from the retro-orbital plexus using a capillary tube and transferred into a plain serum vacutainer, allowing it to clot for 3-4 h. The blood samples were then centrifuged at 12,000 rpm for 15 min, serum was separated and stored at -20$^{O}$C. The serum samples were subsequently used to evaluate biochemical parameters (ALT, AST, TP & albumin) using Erba Mannheim biochemical kits following manufacturer's instructions on a semi-automatic ELISA reader.

**Tissue antioxidant profile**

Small pieces of liver tissue were collected and stored at -80$^{O}$C to analyze the organ's antioxidant profiles (GSH, SOD and Catalase) along with oxidative stress levels (TBARS and nitrite). For each gram of tissue sample, 10 mL of 0.2 M Tris HCl buffer was added and homogenized to make a 10% tissue homogenate for assessing oxidative stress parameters.

The tissue oxidation was measured by the reaction of the lipid peroxidation (LPO) end products like Malondialdehyde (MDA), with thiobarbituric acid (TBA) using a standard protocol[10]. Nitrite levels were measured according to the Griess Reagent Kit (Thermo Fisher Scientific Pvt. Ltd.). The activity of superoxide dismutase (SOD)[11], reduced glutathione (GSH)[12] and catalase[11] was measured to determine the antioxidant status of the liver tissue.

**Inflammatory cytokine assays**

The expression of pro-inflammatory (TNF-$\alpha$, TGF-$\beta$, IL-1$\beta$, IL-6, NF-$\kappa$B, IL-17) and anti-inflammatory (IL-10) cytokines in liver homogenate were measured by sandwich ELISA. The kits were procured from Invitrogen, Thermo Fischer Scientific Ltd. and the assay was performed following the protocol described by Sangomla *et al.* (2018).

**Gross, histopathological and scanning electron microscopic examination**

Experimental mice were sacrificed by cervical dislocation and detailed necropsy was carried out. Gross lesions if any were recorded in the liver and small slices of liver tissue were collected for histopathological

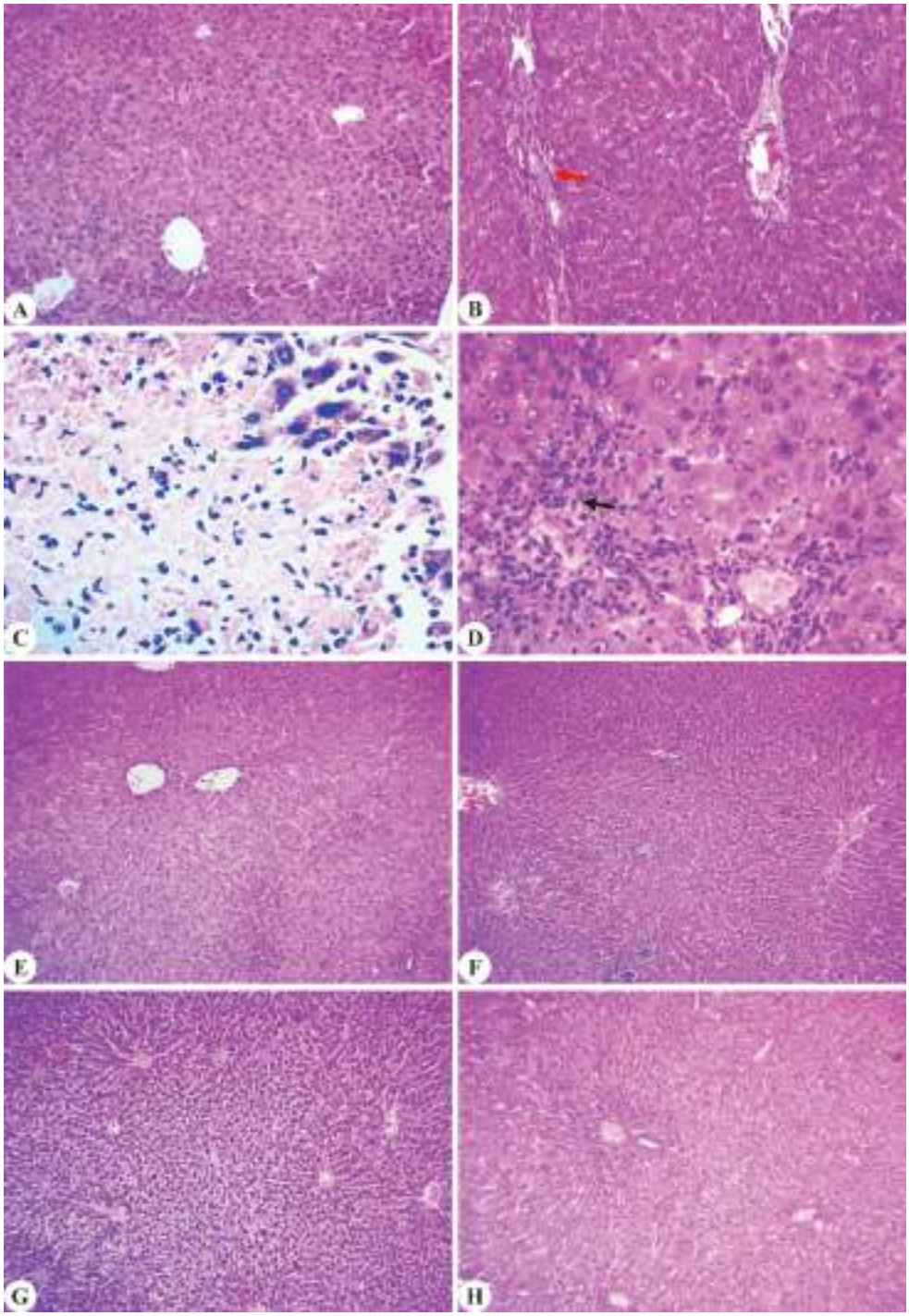


**Fig. 5.** Effect of VIS on histopathological changes. **A.** Control mice (G-1) Normal hepatic cord arrangement in the hepatic parenchyma (H&E X10). **B.** Severe proliferation of fibroblastic cells (H&E X10). **C, D.** Necrosis and haemorrhages in hepatic parenchyma with severe lymphocytic infiltration in DSS treated group (G-2) (H&E X40). **E.** Normal hepatic cord arrangement in the hepatic parenchyma in ameliorative group (G-3) (H&E X10). **F.** Low dose (G-4). **G.** High dose (G-5). **H.** Standard drug (G-6) moderate to mild changes from group 4 to 6 (H&E X10).

examination in 10% NBF. The samples were processed, sectioned (4 μm) and stained with hematoxylin and eosin as per the standard procedure[13].

**Immunohistochemistry**

Immunohistochemical analysis was carried out on formalin-fixed, paraffin-embedded sections of liver tissue with a thickness of 4 μm. Briefly, the tissue sections were incubated overnight at 4$^{O}$C with primary antibodies targeting NF-κB. After incubation, the sections were rinsed with phosphate-buffered saline (PBS) and treated

with a secondary antibody. They were then treated with Diaminobenzidine (DAB) and counter stained with hematoxylin and observed under optical microscope at 100x magnification[14].

**Statistical analysis and its interpretation**

The findings from current experiments are reported as mean ± SE values. Stastical analysis was performed using graph Pad Prism version 9.0 software (GraphPad Software, California, USA), which exposed to a one-way analysis of variance (ANOVA) applying Tukey's multiple comparison test. A P-value of less than 0.001 was considered statistically significant in each and every group[15].

## RESULTS

**Ameliorative effect of VIS on serum biochemical parameters**

Significantly (P<0.001) higher mean values of serum ALT and AST levels were recorded in the UC-induced group 2 compared to control group 1. Conversely, serum ALT and AST levels were significantly (P<0.01) ameliorated in VIS-treated groups 4 and 5, as well as standard-treated group 6, compared to group 2. Additionally, the values of ALT and AST in group 5 were significantly (P<0.05) lower than those in group 4. Moreover, a significant (P<0.001) decrease in serum TP and albumin concentrations was observed in group 2 compared to normal group 1. However, albumin levels significantly (P<0.01, P<0.001 and P<0.001, respectively) increased in groups 4, 5 and 6 compared to group 2. No significant difference was noticed between groups 5 and 6 as well as between control group 1 and 3 (Fig. 1A-D).

**Ameliorative effect of VIS on oxidative stress parameters**

Superoxide free radicals primarily released by nitrite and MDA, contribute significantly to oxidative stress. DSS administration caused a significant (P<0.001) rise in highly reactive MDA and nitrite mean values compared to normal group 1. However, treatment groups 4, 5 and the standard group 6 showed a significant (P<0.001) decrease in liver TBARS mean levels compared to group 2. Additionally, group 5 (high dose) displayed significantly (P<0.05) decrease in TBARS levels compared to group 4 (low dose) and group 5 mean values were insignificantly different from group 6. There were no significant variations between group 1 and group 3 (Fig. 2A, B).

The activity of antioxidant enzymes of SOD, CAT and GSH in DSS-treated group 2 were significantly (P<0.001) reduced as compared to the control group 1. In contrast, VIS-treated groups 4, 5 and the standard treated group 6 revealed a significant (P<0.001) increase compared to group 2. Group 5 showed significantly (P<0.05) greater improvement than group 4 in a dose-dependent manner. Additionally, SOD and CAT levels in mice from group 5 were comparable to those in group 6. No significant variation was found in the values between group 1 and *perse* group 3 (Fig. 2C-E).

**Ameliorative effect of VIS on inflammatory cytokines**

The concentration of pro-inflammatory cytokines (TNF-$\alpha$, IL-1$\beta$, IFN-$\gamma$, IL-6, TGF-$\beta$ and NF-Kb), in the liver tissue of DSS-treated group 2 was significantly (P<0.001) elevated compared to the untreated group 1. Conversely, treatment with VIS in groups 4, 5 and standard group 6 showed significant (P<0.05, P<0.001 and P<0.001, respectively) reductions compared to group 2, with group 5 exhibiting a more significant (P<0.05) reduction than group 4. Pro-inflammatory cytokine levels in group 5 were comparable to the standard group 6 with no significant difference. Group 3 revealed similar cytokine levels to the normal control group 1 indicating increased inflammatory markers in the DSS induced UC-mediated hepatic damage (Fig. 3A-F).

Additionally, the mean values of anti-inflammatory cytokine IL-10 levels were significantly (P<0.001) reduced in group 2 compared to group 1 and group 3 on the 32$^{nd}$ day of the experimental period. In contrast groups 4, 5 and 6 exhibited significantly (P<0.001) higher values compared to group 2 with group 5 showing significantly (P<0.05) more improvement than group 4 in a dose-dependent manner. Whereas, groups 5 and 6 exhibited almost non-significant mean values. No significant disparity was noticed between groups 1 and 3 (Fig. 4G).

**Ameliorative effect of VIS on Gross pathology**

Mice in group 1 and group 3 revealed grossly normal liver appearance. In contrast, group 2 mice showed severe congestion. Group 4 exhibited moderate congestion while groups 5 and 6 showed only mild congestion on the 32$^{nd}$ day of the experiment (Fig. 4).

**Ameliorative effect of VIS on histopathology**

To assess UC induced hepatic damage at cellular level, histopathological examination was done. Liver sections from group 1 and group 3 mice showed normal architecture including well defined hepatic cords, portal triad, sinusoidal space and central vein (CV) (Fig. 5A, E). In group 2 severe sinusoidal dilation and congestion of CV were evident. Hepatocytes showed necrosis, vacuolar degeneration with multifocal infiltration of MNCs (Black arrow) with pyknotic and karyorrhexis of nuclei along with swollen hepatocytes (Fig. 5C, D). Additionally, there was fibroblast proliferation in the hepatic parenchyma and distorted hepatic cords (Fig. 5B, red arrow). The liver section of VIS-treated groups 4 and 5 revealed moderate to mild degenerative changes indicating restoration of damaged hepatocytes (Fig. 5F, G). The liver sections of group 6 mice showed normal hepatic parenchyma with

only mild CV congestion (Fig. 5H).

**Ameliorative effect of VIS on immunohistochemical expression**

NF-κB is a key regulator of genes involved in the expression of pro-inflammatory mediators. Liver sections from groups 1 and 3 showed no immune reactivity for NF-κB protein (Fig. 6A, C). In contrast, sections from group 2 revealed strong positive immunoreactivity for NF-κB on the 32nd day of the experiment (Fig. 6B). Sections from group 4 showed moderate positive immunostaining for NF-κB protein indicated by moderate brown coloration in the sections while groups 5 and 6 exhibited mild positive immunostaining for NF-κB, indicating further reduction in the inflammation in these groups (Fig. 6D-F).

Nrf2 protein expression was assessed to evaluate the antioxidant enzyme activity in the liver. The expression of Nrf2 in group 2 showed a negative immunostaining (Fig. 6B) compared to group 1 and group 3 which showed intense positive immunostaining indicating strong antioxidant profile (Fig. 7A, C). Groups 4 and 5 showed mild to moderate positive immunoreactivity for Nrf2 protein, indicating a dose dependent enhancement in antioxidant status. Treatment group 6 exhibited a similar expression pattern as seen in high-dose VIS-treated group 5 (Fig. 7D-F).

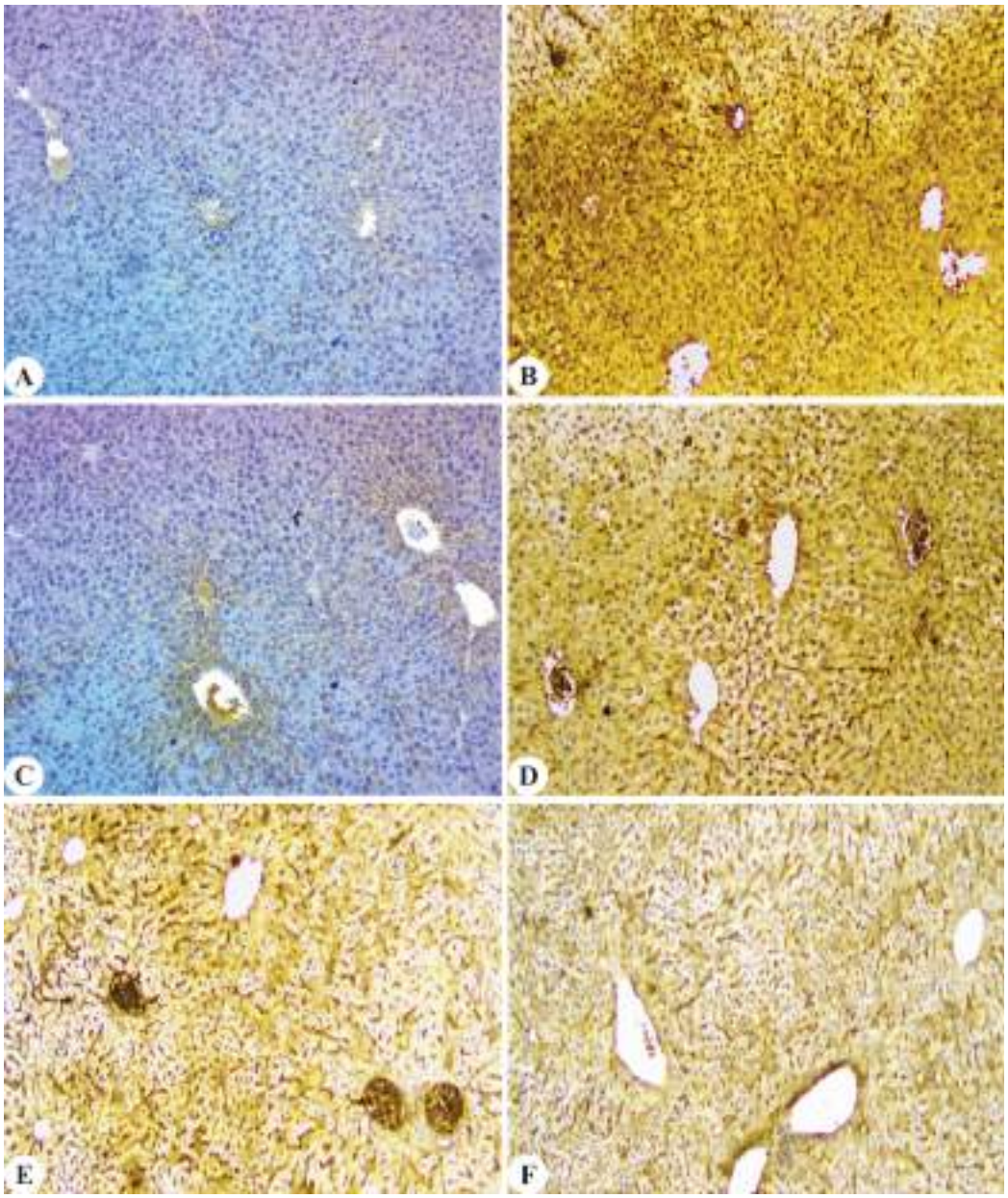


**Fig. 6.** Effect of VIS on immunochemistry of NF-κB marker in liver tissue. **A.** Control mice (G-1). **B.** DSS treated group (G-2). **C.** Ameliorative group (G-3). **D.** Low dose (G-4). **E.** High dose (G-5). **F.** Standard drug (G-6) (IHC X10).

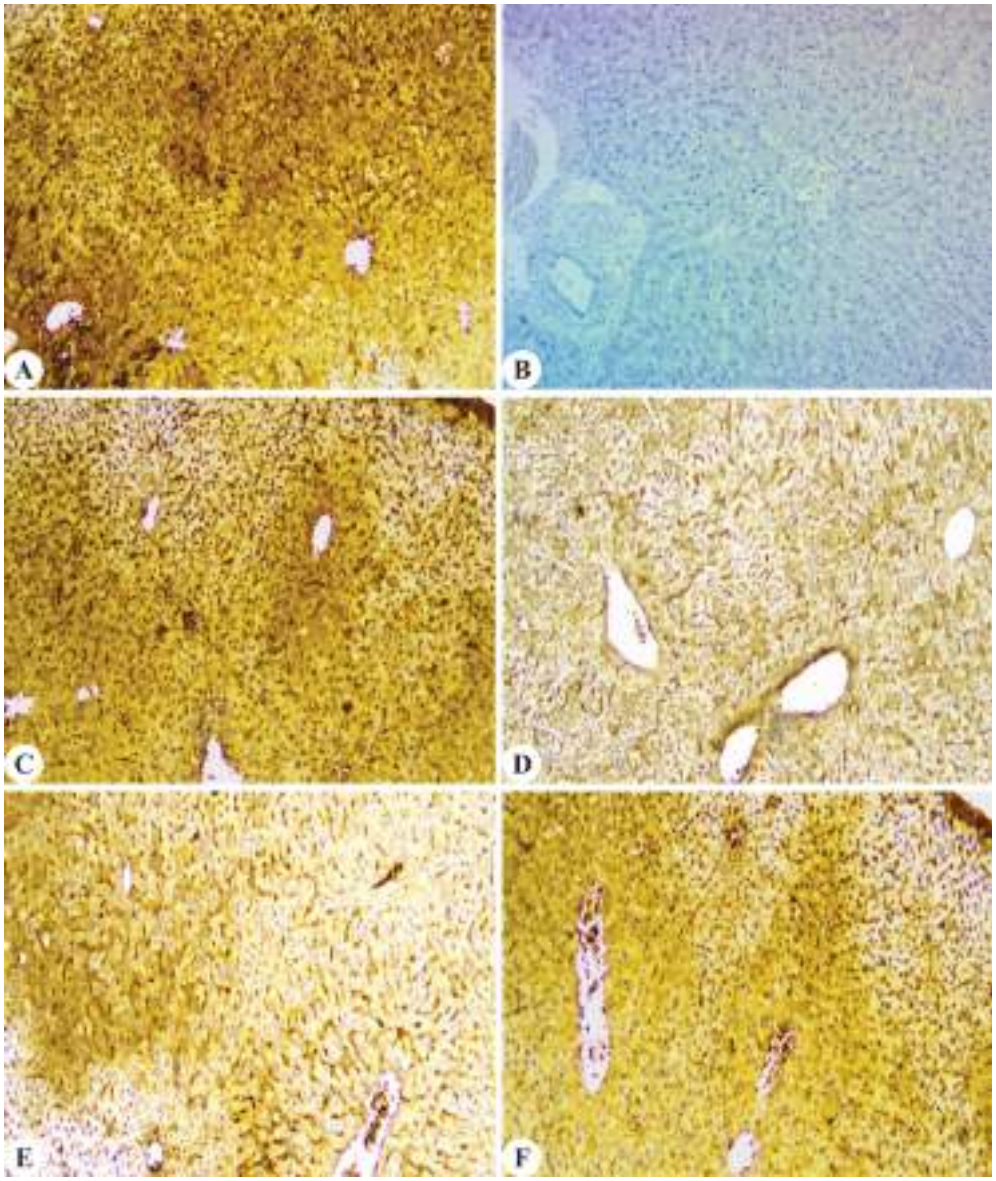


**Fig. 7.** Effect of VIS on immunochemistry of Nrf2 marker in liver tissue. **A.** Control mice (G-1). **B.** DSS treated group (G-2). **C.** Ameliorative group (G-3). **D.** Low dose (G-4). **E.** High dose (G-5). **F.** Standard drug (G-6) (IHC X10).

## DISCUSSION

This study, investigates hepatotoxicity as anextra-intestinal manifestation of ulcerative colitis (UC) in mice and potential amelioration effect of VIS. The induction of UC in the mice was confirmed by a marked increase in the Disease Activity Index (DAI), along with significant cellular damage and inflammatory infiltration in the colon. Chronic UC is known to cause bacterial translocation to the liver, resulting in hepatic damage, which can be mitigated by use of natural plant products[16]. Previous studies have confirmed significant increased endotoxins levels and subsequently increased hepatic inflammation in mice with DSS-induced UC. The influx of by products of gut microbiota like LPS into the liver occurs due to compromised gut wall integrity and permeability. This activates liver derived inflammatory factors mainly toll-like receptor-4, which in turn activates NF-κB and triggers the secretion of pro-inflammatory cytokines ultimately leading to hepatic damage[16,17]. While several studies have examined the protective effects of natural agents against hepatotoxicity, we believe this study is first to investigate VIS potential to mitigate UC induced liver damage, focusing on oxidative stress, inflammation, apoptosis and DNA damage.

ALT and AST enzymes present in the hepatocytes are sensitive markers for assessing liver function and diagnosing hepatotoxicity[18]. Typically, absent in the serum, elevated levels of these enzymes in serum are sensitive indicators of liver and intestinal damage. In the present study, there was a significant increase in the levels

of serum ALT and AST in group 2, which might be due to increased bacterial translocation through altered TJ proteins, leading to hepato-biliary damage and impaired hepatic function[16,17].

Estimation of serum TP is a routine test used to assess the toxicological nature of the various xenobiotics. A significant reduction in TP and albumin levels in group 2 may be due to DSS-induced hepatocellular damage, resulting in changes in protein and free amino acid metabolism and their synthesis in the liver compared to control group 1. The reports of the present study were corroborated by previous reports[18]. Trivedi and Jena, 2013 studied DSS-induced liver injury and reported that destruction of the gut barrier results in increased bacterial translocation, which is associated with a significant increase in LPS into the portal vein blood flow and systemic circulation[17,19]. This, in turn, is reported to promote the release of pro-inflammatory cytokines, cellular damage and loss of functional integrity of hepatocytes, resulting in liver injury accompanied by significantly elevated levels of these enzymes. Conversely, VIS exhibited dose-dependent significant decline in these liver enzymes in groups 4 and 5 and in the standard group 6, with a significant improvement in TP and albumin levels compared to group 2. There was significant improvement observed in group 5 compared to group 4. However, group 5 and group 6 showed no significant difference. This might be due to the protective effect of VIS on damaged liver cells induced by toxic substances through its antioxidant properties, which help to neutralize free radicals and reduce oxidative stress in liver cells. This reduction leads to decreased hepato-cellular injury and hence lower levels of ALT and AST, and higher levels of TP and albumin suggesting hepatoprotective effects of VIS[20].

Systemic inflammation associated with UC is also responsible for causing oxidative stress in the liver due to the extra-intestinal manifestation of systemic circulatory mediators[21]. To examine the role of oxidative stress in hepatocellular damage, MDA and nitrite levels were measured showing a significant increase in oxidative stress in DSS induced group 2, potentially contributing to the hepatic damage and linked with severe tissue damage in previous studies. Additionally, oxidative stress has been implicated in both local and systemic DNA damage associated with UC. Excessive ROS levels can be nutritionally modulated by the supply of antioxidant substances that fuel the cellular antioxidant machinery, which comprises SOD, CAT and glutathione enzymes[22]. Antioxidant profile modulation is regulated by nuclear erythroid related factor-2 (Nrf2) protein, which helps to maintain the cellular homeostasis. Treatment with VIS significantly reduced lipid peroxidation and nitrosative stress by restoring antioxidant enzyme levels through Nrf2 signalling pathway[23].

The TLR4/NF-κB signaling pathway plays a critical role in the immune response, particularly in the development of immune-related liver injury[16,17]. Toll-like receptor 4 (TLR4), a key member of the toll-like receptor (TLR) family, play an important role in initiating inflammatory processes. LPS and cytokines can induce inflammation by activating TLR4 on macrophages, thereby exacerbating hepatic disorders. Additionally, TLR4 activation triggers the NF-κB signaling pathway, leading to the phosphorylation of p65 and IκBα in liver tissues, which in turn stimulates an inflammatory response that contributes to liver injury[18,19]. These insight combined with and research, reveals that VIS significantly reduces the expression of inflammatory proteins, and inhibits the phosphorylation of NF-κB pathway. This suggests that VIS may mitigate colitis-induced liver injury by modulating the TLR4/NF-κB/Nrf2 signaling pathway.

A significant elevation in pro-inflammatory cytokines levels in the liver of animals with UC indicates the role of inflammation in UC-associated liver damage contributing to oxidative stress and apoptosis in the liver. Additionally, NF-κB expression is significantly increased in DSS-treated group which is involved in expression of various inflammatory cytokines. IL-10, an anti-inflammatory cytokine suppresses T lymphocytes and mononuclear cells, reducing pro-inflammatory cytokines by inhibiting suppressor of cytokine signaling-3 and IκB kinases, thus blocking the NF-κB signaling pathway. A significant reduction in IL-10 levels was observed due to severe oxidative stress and release of pro-inflammatory cytokines from damaged tissue. Our results were in agreement with the previous studies showing significant down-regulation of IL-10 cytokine expression in experimental colitis of group 2 mice[17,18].

Administration of both low and high doses of VIS in groups 4 and 5 showed a significant increase in IL-10 levels and significant reduction in pro-inflammatory cytokines compared to group 2, indicating the anti-inflammatory effect of VIS, which is mediate by reducing NF-κB activation. Our findings further support this, as decreased NF-κB levels were observed. These results suggest that VIS effectively suppress inflammation in DSS induced liver injury[24].

Histopathological evaluation was done in order to assess DSS-induced hepatic damage at cellular level. Previous studies have shown that chronic inflammation of colon results into abnormal hepatic damage and degenerative changes[16,18]. Increased oxidative stress and inflammation are responsible for hepatic damage in DSS-induced UC. The liver sections of VIS treated groups 4 and 5 revealed moderate to mild degenerative changes

indicating the restoration of damaged hepatocytes in a dose-dependent manner. Further, the liver sections of group 6 mice showed normal hepatic parenchyma with only mild CV congestion.

NF-κB is a crucial gene, in the transcription of various pro-inflammatory mediators, involved in the development of hepatocellular damage. The DSS treated liver showed increased intensity of immunoexpression of NF-κB and decreased expression of Nrf2 likely due to the activation of inflammatory signaling pathway[15]. However, group 4 and group 5 showed moderate to mild expression suggesting increased activation of antioxidant pathway by VIS and group 6 also showed mild expression due to anti-inflammatory effect of dexamethasone.

In summary, the study concludes that DSS induced hepatic damage is marked by alteration in intestinal barrier integrity and a pronounced increase in the expression of pro-inflammatory cytokines, facilitated through the upregulation of the NF-κB. Additionally, there was a notable alteration in oxidative stress parameters attributed to downstream regulation of the Nrf-2 pathway. Administration of VIS suppresses oxidative stress and inflammation through the downstream regulation of NF-κB and upstream regulation of the Nrf-2 pathway in a dose-dependent manner. Additionally, the higher VIS dose produced results comparable to standard drug-dexamethasone suggesting that VIS may offer therapeutic potential for UC related hepatic injury. Further, molecular studies are needed to further elucidate the mechanism of extra-intestinal manifestations of UC and the protective action of various phytochemicals.

## ACKNOWLEDGEMENTS

We would like to express our gratitude to PV Narsimha Rao Telangana Veterinary University.

## REFERENCES

1. Kwon J, Lee C, Heo S, Kim B and Hyun CK. 2021. DSS-induced colitis is associated with adipose tissue dysfunction and disrupted hepatic lipid metabolism leading to hepatosteatosis and dyslipidemia in mice. *Sci Rep* **11:** 5283.
2. Huang J, Zhang J, Wang F and Tang X. 2024. Exploring the immune landscape of disulfidptosis in ulcerative colitis and the role of modified gegen qinlian decoction in mediating disulfidptosis to alleviate colitis in mice. *J Ethnopharmacol* **334:** 118-527.
3. Xu F, Yu P, Wu H, Liu M, Liu H, Zeng Q, Wu D and Wang X. 2024. Aqueous extract of Sargentodoxa cuneata alleviates ulcerative colitis and its associated liver injuries in mice through the modulation of intestinal flora and related metabolites. *Front Microbiol* **15:** 1295822.
4. Duan S, Du X, Chen S, Liang J, Huang S, Hou S, Gao J and Ding P. 2020. Effect of vitexin on alleviating liver inflammation in a dextran sulfate sodium (DSS)-induced colitis model. *Biomed Pharmacother* **121:** 109-683.
5. Liu H, Chen R, Wen S, Li Q, Lai X, Zhang Z, Sun L, Sun S and Cao F. 2023. Tea (Camellia sinensis) ameliorates DSS-induced colitis and liver injury by inhibiting TLR4/NF-κB/NLRP3 inflammasome in mice. *Biomed Pharmacother* **158:** 114-136.
6. Yadav P, Singh SK, Datta S, Verma S, Verma A, Rakshit A, Bali A, Bhatti JS, Khurana A and Navik U. 2024. Therapeutic potential and pharmacological mechanism of visnagin. *J Integr Med* 1-14.
7. Fu HR, Li XS, Zhang YH, Feng BB and Pan LH. 2020. Visnagin ameliorates myocardial ischemia/reperfusion injury through the promotion of autophagy and the inhibition of apoptosis. *Eur J Histochem* **64:** 48-54.
8. Yang X, Yang C, Lu W and Yang X. 2023. Visnagin Attenuates Gestational Diabetes Mellitus in Streptozotocin-induced Diabetic Pregnant Rats via Regulating Dyslipidemia, Oxidative Stress and Inflammatory Response. *Pharmacogn Mag* **19:** 31-40.
9. Pasari LP, Khurana A, Anchi P, Saifi MA, Annaldas S and Godugu C. 2019. Visnagin attenuates acute pancreatitis *via* Nrf2/NFκB pathway and abrogates associated multiple organ dysfunction. *Biomed Pharmacother* **112:** 108-629.
10. De Leon JA and Borges CR. 2020. Evaluation of oxidative stress in biological samples using the thiobarbituric acid reactive substances assay. *J Vis Exp* **12:** e61122.
11. Zhang J, Chen R, Yu Z and Xue L. 2017. Superoxide dismutase (SOD) and catalase (CAT) activity assay protocols for Caenorhabditis elegans. *Bio Protoc* **7:** e2505.
12. Barros L, Cabrita L, Boas MV, Carvalho AM and Ferreira IC. 2011. Chemical, biochemical and electrochemical assays to evaluate phytochemicals and antioxidant activity of wild plants. *Food Chem* **27:** 1600-1608.
13. Luna GLHT. 1968. Manual of histological and special staining techniques. 2nd edn. The Blakistone Divison McGraw-Hill Book Company, Inc. NewYork, Toronto London: 1-5 and 9-34.
14. Kumar A, Rao A, Bhavani S, Newberg JY and Murphy RF. 2014. Automated analysis of immunohistochemistry images identifies candidate location biomarkers for cancers. *Proc Natl Acad Sci* **111:** 18249-18254.
15. Snedecor GW and Cochran G. 1994. Statistical methods, 8th edn. IOWA State University Press, America, USA: 64-67.
16. Dai W, Zhan X, Peng W, Liu X, Peng W, Mei Q and Hu X. 2021. Ficus pandurata Hance Inhibits Ulcerative Colitis and Colitis-Associated Secondary Liver Damage of Mice by Enhancing Antioxidation Activity. Oxid Med Cell Longev **1:** 2617881.
17. Trivedi PP and Jena GB. 2013. Ulcerative colitis-induced hepatic damage in mice: studies on inflammation, fibrosis, oxidative DNA damage and GST-P expression. *Chem Biol Interact* **201:** 19-30.
18. Lv Q, Wang J, Yang H, Chen X, Zhang Y, Ji G, Hu L and Zhang Y. 2024. Didymin ameliorates ulcerative colitis-associated secondary liver damage by facilitating Notch degradation. *Phytomed* 155-561.
19. Wang Q, Liu Y, Gao L, Zhang L and Wang J. 2024. Study on the Protective Effect and Mechanism of Umbilicaria esculenta Polysaccharide in DSS-induced mice colitis and secondary liver injury. *J Agric Food Chem* **72:** 10923-10935.
20. Wan J, Xu Q, Alahmadi TA, Ds P and Liu M. 2023. Visnagin Mitigates Glycerol-induced Acute Kidney Injury in Rats through Decreasing Inflammation, Oxidative Stress and Renal Dysfunction Markers. *Indian J Pharm Educ Res* **57:** 134-140.
21. Yadav P, Singh SK, Datta S, Verma S, Verma A, Rakshit A, Bali A, Bhatti JS, Khurana A and Navik U. 2024. Therapeutic potential and pharmacological mechanism of visnagin. *J Integr Med* 1-14.
22. Liu H, Chen R, Wen S, Li Q, Lai X, Zhang Z, Sun L, Sun S and Cao F. 2023. Tea (Camellia sinensis) ameliorates DSS-induced

colitis and liver injury by inhibiting TLR4/NF-κB/NLRP3 inflammasome in mice. *Biomed Pharmacother* **158:** 114-136.
23. Sahoo DK, Heilmann RM, Paital B, Patel A, Yadav VK, Wong D and Jergens AE. 2023. Oxidative stress, hormones and effects of natural antioxidants on intestinal inflammation in inflammatory bowel disease. *Front Endocrinol* **14:** 1217165.
24. Ajarem JS, Hegazy AK, Allam GA, Allam AA, Maodaa SN and Mahmoud AM. 2021. Effect of visnagin on altered steroidogenesis and spermatogenesis and testicular injury induced by the heavy metal lead. *Comb Chem High Throughput Screen* **24:** 758-766.
25. Asnani A, Zheng B, Liu Y, Wang Y, Chen HH, Vohra A, Chi A, Cornella-Taracido I, Wang H, Johns DG and Sosnovik DE. 2018. Highly potent visnagin derivatives inhibit Cyp1 and prevent doxorubicin cardiotoxicity. *JCI Insight* **3:** e96753.

*Indian J. Vet. Pathol., 49(2) : 154-159, 2025: DOI: https://doi.org/10.56093/kqvtzc46*

RESEARCH ARTICLE

# Folic acid induced nephropathy in BALB/C mice

**Ritika Tater[1,3], B.S.V. Vinod[1,2], Shobhit Verma[1,2], Kamini Kumari[1], Vanshika Ojha[1], Sargam Srivastava[1,3], Madhav Nilkant Mugale[1,2] and V.M. Prajapati[1,2*]**

[1]Division of Toxicology & Experiment Medicine, CSIR-Central Drug Research Institute, Lucknow-226 031, Uttar Pradesh, [2]Academy of Scientific and Innovative Research (AcSIR), Ghaziabad-201 002, [3]Department of Forensic Science, Parul Institute of Applied Science, Parul University, Vadodara-391 760, Gujarat, India

**Address for Correspondence**

*V.M. Prajapati, Senior Scientist, Division of Toxicology & Experiment Medicine, CSIR-Central Drug Research Institute, Sector-10, Jankipuram Extension, Sitapur Road, Lucknow-226 031, India, E-mail: viren.prajapati.cdri@csir.res.in*

*Received: 19.3.2025; Accepted: 29.4.2025*

## ABSTRACT

The present study was conducted to learn about the various pathological changes due to folic acid-induced Renal changes in mice, which is a widely used experimental model to study the mechanisms underlying kidney fibrosis. Following high-dose folic acid administration, acute kidney injury is rapidly induced, primarily affecting the tubular epithelium. Clinical pathology, macroscopic, and microscopic changes with Hematoxylin & Eosin and special stains such as Masson Trichrome Stain fibrous tissue proliferation. Along with fibronectin, α-SMA, and Smad expression in the progression of Kidney fibrosis. Taken together, our findings might serve as a rationale for developing prospective innovative renal fibrosis. This present study's finding serves as a pathological change with the marker identification, affecting Renal disease progression.

**Keywords:** Acute kidney injury, chronic kidney disease, folic acid, nephropathy, renal fibrosis

## INTRODUCTION

The kidneys perform a crucial homeostatic function in the maintenance of bodily fluid composition and the elimination of waste materials[1]. Kidney failure is a global public health issue with rising frequency and severity, significant expenditures, and poor results[2]. Kidney disease indicates that your kidneys have been damaged and cannot filter blood as effectively as they should. Clinically, Kidney disease is classified into two types: acute kidney injury (AKI) and chronic kidney disease (CKD), which are closely linked[3-5]. These diseases can be caused by various reasons, including ischemia, sepsis, drug toxicity, overdose, heavy metal exposure, and diabetes[6]. AKI is asymptomatic in mild to moderate cases, and patients are recognized through laboratory tests. On the other hand, patients with severe AKI frequently exhibit symptoms such as lethargy, anorexia, nausea, vomiting, restlessness, confusion, fluid retention, and weight gain. Severe and persistent AKI can result in central nervous system symptoms such as uremic encephalopathy, which includes asterixis, confusion, seizures, and a bleeding tendency due to platelet malfunction and severe anemia. Patients suffering from AKI sometimes have regular urine production, oliguria (less than 400 mL/24 h), or anuria (less than 100 mL/24 h) urine output[7].

Nearly 10% of adults worldwide have been diagnosed with CKD, which is linked to significantly elevated risks for cardiovascular events, development of end-stage renal disease (ESRD), which necessitates dialysis or transplantation, hospital problems, and early mortality[8]. The histological lesion of Kidney function deterioration is Renal fibrosis[9], which is defined by the formation of a matrix as a result of fibroblast trans-differentiation and proliferation[10].

Renal fibrosis is a significant indication of all stages of CKD where there is an excess of ECM build-up and deposition. The pathological fibrillar matrix that forms in the potential space between tubules and peritubular capillaries is characteristic of CKD[11]. Fibrosis and fibrogenesis have been recognized as essential amplifiers of CKD progression rather than a bystander process, according to new findings from animal models of renal disease[12]. Animal models have been employed to solve a wide range of scientific problems from basic research to the development and testing of new vaccines and medications[13]. Scientists have investigated various systems and tested new therapies in animal models before translating their findings to humans due to the striking anatomical and physiological similarities between humans and mammals[14].

**How to cite this article :** Tater, R., Vinod, B.S.V., Verma, S., Kumari, K., Ojha, V., Srivastava, S., Mugale, M.N. and Prajapati, V.M. 2025. Folic acid induced nephropathy in BALB /C mice. Indian J. Vet. Pathol., 49(2) : 154-159.

Here we make possible ways to create a FA nephropathy in mice model that reflects human pathophysiology. The main benefit of the FA model is the one-time administration of a high FA concentration, which ensures repeatability[15]. Urinary volume, GFR, and filtration fraction all decrease after FA injection. This is followed by an increase in blood urea nitrogen and creatinine

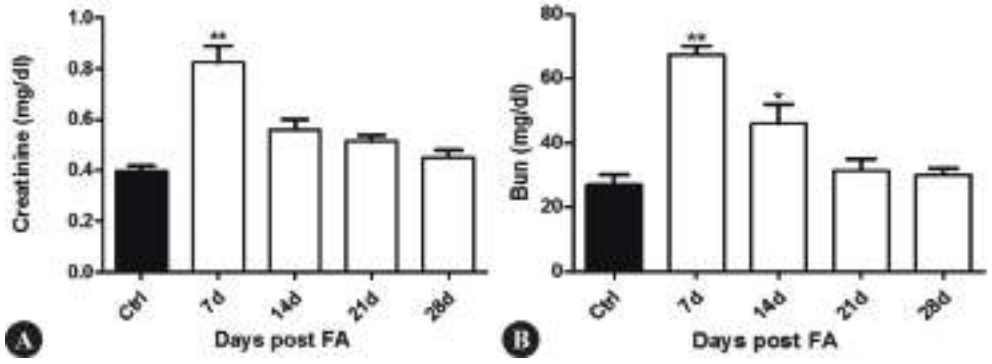


**Fig. 1.** The time course of the standard renal damage indicators. **A.** Creatinine. **B.** Blood urea nitrogen (BUN). Data represent mean +/- SEM for at least three independent experiments (P<0.05 Dunnet's vs treated).

concentrations[16].

In the present study, we explore various biomarkers that would allow early detection of fibrosis, and also this model has undergone extensive histopathology and renal function analysis. This FA nephropathy mice model, which causes renal fibrosis within 2 weeks of FA injection, should be precious for future renal damage and CKD studies.

## MATERIALS AND METHODS

### Chemicals and Reagents

Fibronectin (AF5335) and Smad 3 (AF6362) antibodies were purchased from Affinity Biosciences. Smad 2/3 (D7G7) XP® Rabbit mAb #8685, Phospho-Smad 2 (Ser465/467) Smad 3 (Ser423/425) (D27F4) Rabbit mAb #8828 were purchased from Cell Signaling technology. β-actin (sc-4778) were purchased from Santacruz. Anti-mouse (ab6728) and Anti-rabbit (ab6721) were purchased from Abcam (USA). ECL (Enhanced Chemiluminescence), Cytosolic Buffer, Protease inhibitor (PI), Phosphate Kinase inhibitor (PKI) were purchased from Sigma Aldrich.

### Animals

Male Balb/c mice, aged 3-5 weeks and weighed 15-30 gm, were obtained from the National Laboratory Animal Facility (NLAF), CSIR-Central Drug Research Institute, Lucknow, Uttar Pradesh, India. Animal husbandry procedures were followed by the recommendations of the institutional animal ethical committee and the Committee for the Purpose of Control and Supervision of Experiments on Animals (CPCSEA). Throughout the investigation, mice were maintained in polypropylene cages at ambient temperature (23±2$^{O}$C) and relative humidity (55±20%), with a 12-hour light/dark cycle. Access to food and water was unrestricted for all mice. The study was approved by the Institutional Animal Ethics Committee (IAEC) with approval Certificate Reference No. IAEC/2022/43/Renew-0/sl no. 28.

### Induction of Renal Fibrosis

Fibrosis was induced by a single injection of folic acid at the dose of 250 mg/kg intraperitoneal (dissolved in Sodium bicarbonate in Mill Q water).

### Experimental Design

The total number of animals (n=15) was divided into 2 groups.

Group 1: Normal control mice without FA administration (n=3).

Group 2: Treated mice with FA administration at 250

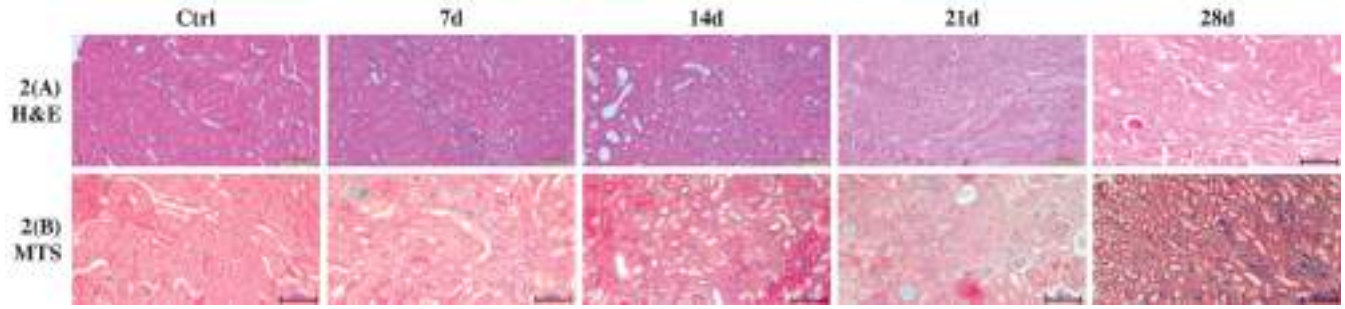


**Fig. 2.** Evaluation of the renal cortex's damaged region based on histopathology. **A.** Renal damage stage showed with hematoxylin-eosin staining. Normal histology kidney structure is seen in the control group (Ctrl). In contrast, mice treated with FA showed mild interstitial fibrosis and tubular dilation to severe interstitial fibrosis and tubular dilation with localized global and segmental glomerulosclerosis. **B.** Masson trichrome staining with the original magnification at 20x of control (Ctrl), 1 week after FA treatment (7 days), 2 weeks after FA treatment (14 days), 3 weeks after FA treatment (21 days), 4 weeks after FA treatment (28 days). The prominent blue-stained regions in the sections from mice treated with FA Spotted the presence of fibrosis.

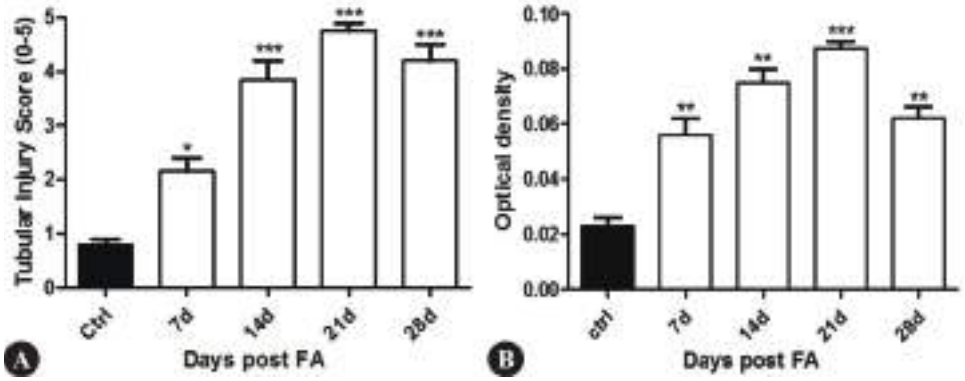


**Fig. 3A.** Tubular injuries were scored as follows: 0, no tubular injury; 1, <10% tubular damage; 2, 10-25% tubular damage; 3, 26-50% tubular damage; 4, 51-74% tubular damage; and 5, >75% tubular damage. Data represent mean +/- SEM for at least three independent experiments (***P<0.05 Dunnet's vs treated mice). **B.** Quantification of Masson Trichome Positive stained areas. Data represent mean +/- SEM for at least three independent experiments (*P<0.05 Dunnet's vs treated mice).

mg/kg dose.

The study was conducted on days 7, 14, 21 and 28 after folic acid administration (n=3 per group).

**Tissue Preparation and Histology**

Tissues were fixed in 10% neutral formalin and embedded in paraffin for haematoxylin & Eosin, Masson's trichome, and immunohistochemical staining. Another portion of tissues was stored at -20$^{O}$C for western blot[17].

**Hematoxylin & Eosin (H&E)**

H&E staining was performed using a kit from Sigma-Aldrich as per the manufacturer's protocol. The sections were stained with hematoxylin and an eosin stain to observe the structure.

**Masson's Trichome**

Masson's trichrome staining was executed using a kit from Polysciences (Catalog No. 25088F-100) as per the manufacturer's instructions. The positive area was determined using a bright field microscope (Zeiss).

**Immunohistochemistry (IHC)**

IHC was performed using an IHC Detection Systems & Kits from Thermo Fisher Scientific (Cat. No. TA-100-DHBH) as per the manufacturer's protocol. The tissue section was incubated in primary antibodies Fibronectin and Smad 3 from Affinity Biosciences overnight at 4$^{O}$C. Then the sections were incubated in secondary antibody for 3 hrs at room temperature. After washing, the section was incubated with DAB substrate liquid, and the slide was then counter stained with hematoxylin[17].

**Western Blot Analysis**

Tissues were lysed in cytosolic buffer containing Protease inhibitor (PI) and Phosphate Kinase inhibitor (PKI). The lysates were homogenized (2 Minutes) and then centrifuged (12000 rpm) for 15 minutes at 4$^{O}$C, and protein estimation was done using the Bradford method. The mixture of protein lysate 40 ug and 2X Laemmli sample buffer was heated for 5 min in a boiling water bath. On SDS-polyacrylamide gel electrophoresis, proteins were resolved using 1X Tris-Glycine-SDS buffer. These resolved or separated proteins were transferred onto a polyvinylidene difluoride membrane (PVDF from Millipore) in a semi-dry transfer unit (BIO-RAD). The membrane was blocked for 1 hour at room temperature in blocking buffer (5% BSA in 0.1% PBST), then incubated with the primary antibody (1:1000) in 2% BSA containing PBST buffer (pH 7.4) overnight at 4$^{O}$C. After washing with 0.1% PBST buffer (pH 7.4), for 10 min each, the blot was incubated with secondary antibody (1:500) in 2% BSA in PBST buffer (pH 7.4) (dilutions according to manufacturer's instructions) for 2 hrs at room temperature with gentle shaking. After washing with

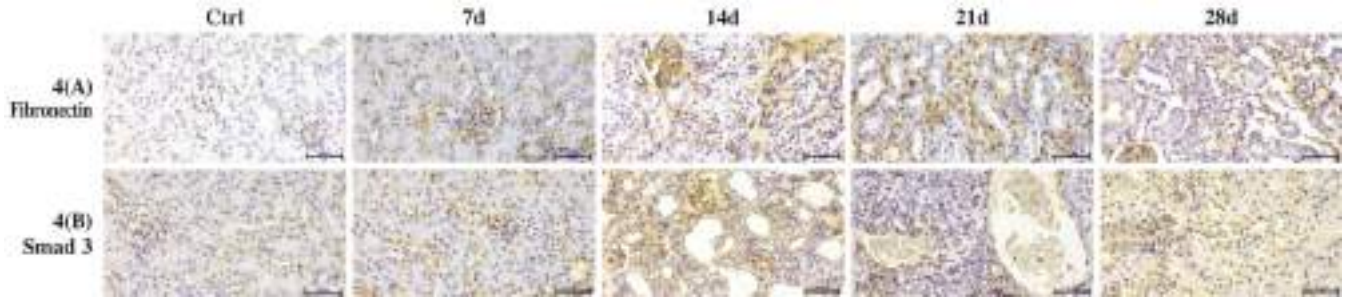


**Fig. 4.** Chronic renal fibrosis marker proteins: The immunohistochemistry showed the gradual deposition of fibrosis marker proteins. **A.** Fibronectin. **B.** Smad 3 in FA-induced mice from day 7 to day 28 compared with uninduced control group mice.

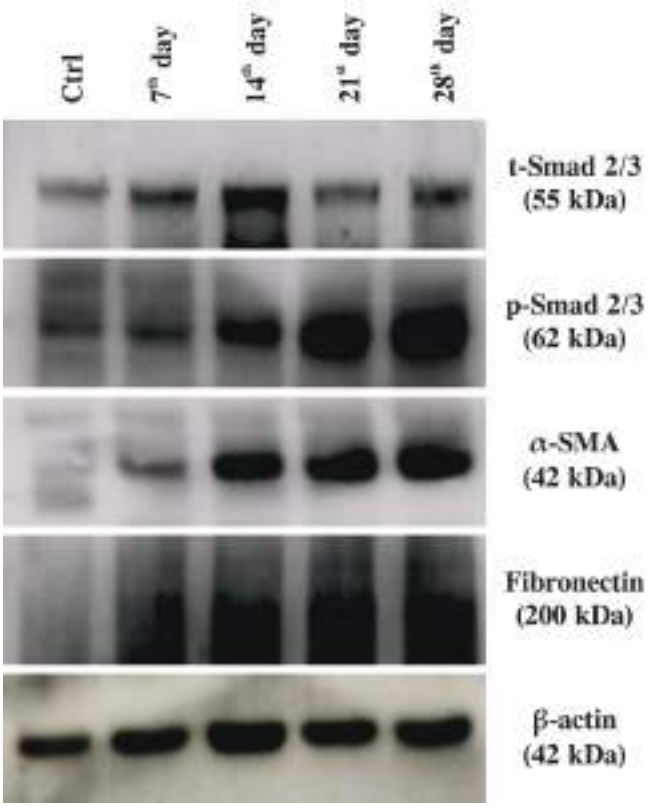


**Fig. 5.** Expression of renal fibrosis marker proteins in FA-injected mice: The above representative western blot depicts the exponential increase of the early fibrosis marker proteins p-smad 2/3, α-SMA, and fibronectin in the FA-treated group mice (Day 7 to day 28) compared with the control group.

0.1% PBST buffer (pH 7.4), for 10 min each, the protein bands were obtained using Chemidoc Image uant 4000 software.

**Statistical Analysis**

The data was statistically analysed using the Graph pad prism 5 software package. Each class was examined separately. The unpaired student's test was used to determine statistical significance of numerical data. Differences were deemed significant at $p<0.05$ (*), very significant when $p \leq 0.01$ (**), and extremely significant when $p \leq 0.001$ (***).

## RESULTS


**Body Weight**

We observed that the induced group had less body weight than the control group, and the mice's body weight of the induced group progressively declined over time. We used repeated measures ANOVA to test the bodyweight difference at different time points, and it was found to be significantly different ($p=0.005$). We used the Dunnett test for post hoc comparison and found a significant difference in (induced Day 21) vs (Control Baseline), (Induced Day 28) vs (Control Baseline).

**Renal damage Markers**

FA significantly affected renal function, as evidenced by elevated plasma levels of BUN and creatinine on day 7 following administration against the control group. A time course analysis showed that the increase in BUN and plasma creatinine levels peaked at 7 days post-FA administration and gradually declined over the subsequent days (Fig. 1A & B).

**Renal damage Progression by Histological examination**

The renal histopathology of mice induced with FA at weekly intervals was examined using H&E and Masson trichome staining. Minimal interstitial fibrosis, mild tubular dilation, and regenerative tubular cells were observed in the stained section on day 7. On day 14, moderate regenerative tubular cells and tubular dilation were seen in some places with increased interstitial fibrosis and localized global and segmental glomerulosclerosis. Severe tubular dilation and regenerative tubular cells with severe interstitial fibrosis and localized severe glomerulosclerosis were observed on day 21. Mild interstitial fibrosis with minimal regenerative tubules and mild tubular dilation were seen on day 28 (Fig. 2A). The study demonstrated that a single injection of FA increased tubular cell injury compared with the control group.

Masson trichrome staining revealed extensive blue areas on days 14th and 21st, indicating severe fibrosis. Sections with small blue regions on days 7th and 28th showed mild fibrosis (Fig. 2B). These results suggest that FA injection causes progressive renal damage and fibrosis over time, with the most severe damage observed on day 21. These findings may have implications for the management and treatment of FA-induced nephrotoxicity.

As shown in Fig. 3A, there is a progressive increase in tubular injury from day 7 to day 21st and decreased on day 28th. The mean optical densities of the induced group are higher than the Control Group Fig. 3B.

**Expression of renal fibrosis marker proteins in FA-induced mice model**

The treated group showed positive staining in the nuclei, which was absent in the control group. Fig. 4A & B shows that the staining levels were low in both the control

and 7th day groups. However, there was a significant increase in staining levels in the tubulointerstitial, glomeruli, and extracellular matrix on the 14th, 21st, and 28th days.

**FA nephropathy Progression by Western blot**

The results showed upregulated expression of p-Smad2/3, $\alpha$-SMA, and Fibronectin in the FA-induced group, as demonstrated in Fig. 5. Specifically, on day 28th, there was a rise in p-Smad2/3 and $\alpha$-SMA expression. These findings suggest that Folic acid administration may lead to increased expression of early fibrosis markers, potentially contributing to the development of fibrosis. Our results provide essential insights into the potential mechanisms underlying the observed changes and highlight the need for further investigation into the effects of Folic acid on fibrosis development.

## DISCUSSION

It is evident from Fig. 1 that after FA administration, Bun and creatinine levels increase which has also been reported in previous studies[18].

Moreover, the histological alternations associated with renal fibrosis, like tubular dilation, interstitial fibrosis, and glomerulosclerosis, are seen in Fig. 2A, demonstrating the development of FA nephropathy in the FA-induced group (Fig. 3A). The deterioration in Kidney function and progression from AKI to Fibrosis in 2 weeks after FA administration has been reported[19].

A study has already shown that the delivery of FA to mice led to significant tubulointerstitial damage, the establishment and progression of tubulointerstitial fibrosis, and inflammation, as depicted by Masson trichrome staining[20]. This type of outcome was also seen in the present study.

As we know, Smad plays a vital role in renal fibrosis. TGF-$\beta$ and smad-dependent mechanisms control a wide range of known factors that participate in tissue homeostasis and repair[21-22]. In the present study, IHC showed the deposition of Smad 3 and Fibronectin. The present data demonstrated that FA contributed to the development and progression of FA-induced renal fibrosis.

FA-related AKI is a well-accepted example of nephrotoxic AKI and a widely used model for studies on the processes underlying AKI. Because the FA-induced impairment is restricted to the kidney, extrarenal confounding variables are removed. FA injection causes a local inflammatory response in the kidney that recapitulates upstream signaling of various cellular responses linked to inflammatory conditions critically crucial for tissue remodelling found in many other types of organ damage[23]. The levels of renal damage markers revealed the upregulated expression of p-Smad2/3, $\alpha$-SMA, and Fibronectin (Fig. 5).

Smad signalling is the primary mechanism by which TGF exerts its biological activity, as well as Smad family members serve specific functions in renal fibrosis. Smad 3 has been reported to have a significant pathogenic role, whereas Smad 7, an inhibitory Smad super family member, counter acts Smad 3's effects[24,25].

## CONCLUSION

Our studies have shown that FA elevated the plasma levels of BUN and creatinine on days 7, 14, 21, and 28 following its administration, compared to the control group. Renal histopathology of the treated group showed interstitial fibrosis, regenerative tubular cells, and tubular dilation. In IHC, the mean optical densities of fibronectin and Smad 3 in the treated group were significantly higher than those of normal controls. Based on Western blot analysis, in FA-induced groups, the expression of p-Smad 2/3, Fibronectin, and $\alpha$-SMA was upregulated in kidneys, indicating the severity of the renal injury. These findings help to understand the pathogenesis of the FA-induced nephropathy mice model and inspire potential therapeutic targets in further studies.

## ACKNOWDGEMENTS

The authors want to express their deepest gratitude to the CSIR-CDRI for the research facilities and the necessary resources. The CSIR-CDRI communication number is 10994.

## REFERENCES

1. Davidson AJ. Mouse kidney development. Stembook. 2009.
2. Eknoyan G, Lameire N, Barsoum R, Eckardt KU, Levin A and Levin N. 2004. The burden of kidney disease: improving global outcomes. *Kidney Internat* **66:** 1310-4.
3. Fiorentino M, Grandaliano G, Gesualdo L and Castellano G. 2018. Acute kidney injury to chronic kidney disease transition. Acute Kidney Injury-Basic Research and Clinical Practice **193:** Karger Publishers; p. 45-54.
4. He L, Wei Q, Liu J, Yi M, Liu Y and Liu H. 2017. AKI on CKD: heightened injury, suppressed repair and the underlying mechanisms. *Kidney Internat* **92:** 1071-83.
5. Jiang M, Bai M, Lei J, Xie Y, Xu S and Jia Z. 2020. Mitochondrial dysfunction and the AKI to CKD transition. *American J Physiol Renal Physiol* **319:** F1105-F16.
6. Huang J, Bayliss G and Zhuang S. 2021. Porcine models of acute kidney injury. *American J Physiol Renal Physiol* **320:** F1030-F44.
7. Alkhunaizi AM. 2018. Acute Kidney Injury. Aspects in Continuous Renal Replacement Therapy: Intech Open.
8. Lamprea Montealegre JA, Joshi P, Shapiro AS, Madden E, Navarra K and Potok OA. 2022. Improving chronic kidney disease detection and treatment in the United States: the chronic kidney disease cascade of care (C3) study protocol. *BMC Nephrol* **23:** 1-10.
9. Edeling M, Ragi G, Huang S, Pavenstädt H and Susztak K. 2016. Developmental signalling pathways in renal fibrosis:

the roles of Notch, Wnt and Hedgehog. *Nature Rev Nephrol* **12:** 426-39.
10. Kaissling B, LeHir M and Kriz W. 2013. Renal epithelial injury and fibrosis. *Biochimica et Biophysica Acta (BBA)-Molecular Basis Dis* **1832:** 931-9.
11. Yoshioka K, Takemura T, Tohda M, Akano N, Miyamoto H and Ooshima A. 1989. Glomerular localization of type III collagen in human kidney disease. *Kidney Internat* **35:** 1203-11.
12. Duffield JS. 2014. Cellular and molecular mechanisms in kidney fibrosis. *J Clin Invest* **124:** 2299-306.
13. Alberti KGM and Bailey C. 2022. The discovery of insulin. *British J Diab* **22:** S3-S5.
14. Barré-Sinoussi F and Montagutelli X. 2015. Animal models are essential to biological research: issues and perspectives. *Future Sci* **OA1**.
15. Fu Y, Tang C, Cai J, Chen G, Zhang D and Dong Z. 2018. Rodent models of AKI-CKD transition. *American J Physiol Renal Physiol* **315:** F1098-F106.
16. Rattanasinganchan P, Sopitthummakhun K, Doi K, Hu X, Payne DM and Pisitkun T. 2016. A folic acid-induced rat model of renal injury to identify biomarkers of tubulointerstitial fibrosis from urinary exosomes. *Asian Biomed* **10:** 491-502.
17. Ram C, Gairola S, Syed AM, Verma S, Mugale MN and Sahu BD. 2022. Carvacrol preserves antioxidant status and attenuates kidney fibrosis via modulation of TGF-β1/Smad signaling and inflammation. *Food & Function* **13:** 10587-600.
18. Aparicio-Trejo OE, Avila-Rojas SH, Tapia E, Rojas-Morales P, León-Contreras JC and Martínez-Klimova E. 2020. Chronic impairment of mitochondrial bioenergetics and β-oxidation promotes experimental AKI-to-CKD transition induced by folic acid. *Free Radical Biol & Med* **154:** 18-32.
19. Yuan HT, Li XZ, Pitera JE, Long DA and Woolf AS. 2013. Peritubular capillary loss after mouse acute nephrotoxicity correlates with down-regulation of vascular endothelial growth factor-A and hypoxia-inducible factor-1α. *American J Pathol* **163:** 2289-301.
20. Jiang M, Fan J, Qu X, Li S, Nilsson SK and Sun YBY. 2019. Combined blockade of Smad 3 and JNK pathways ameliorates progressive fibrosis in folic acid nephropathy. *Front Pharmacol* **10:** 880.
21. Sureshbabu A, Muhsin SA and Choi ME. 2016. TGF-β signaling in the kidney: profibrotic and protective effects. *American J Physiol Renal Physiol* **310:** F596-F606.
22. Casalena G, Daehn I and Bottinger E. 2012. Transforming growth factor-β, bioenergetics and mitochondria in renal disease. Seminars in nephrology, Elsevier.
23. Zheng TS and Burkly LC. 2008. No end in site: TWEAK/Fn14 activation and autoimmunity associated-end-organ pathologies. *J Leukocyte Biol* **84:** 338-47.
24. Meng XM, Chung AC and Lan HY. 2013. Role of the TGF-β/BMP-7/Smad pathways in renal diseases. *Clinical Sci* **124:** 243-54.
25. Loeffler I and Wolf G. 2014. Transforming growth factor-β and the progression of renal disease. *Nephrol Dial Trans* **29:** 37-45.

*Indian J. Vet. Pathol., 49(2) : 160-163, 2025: DOI: https://doi.org/10.56093/bg4yd580*

SHORT COMMUNICATION

# Pathomorphological and immunohistochemical studies on melanocytic tumors in cattle

**G. Poojitha, CH. Sudha Rani Chowdary*, V. Rama Devi and C. Sreedevi[1]**
Department of Veterinary Pathology, NTR College of Veterinary Science, Sri Venkateswara Veterinary University, Gannavaram-521 102, Andhra Pradesh, India, [1]Department of Veterinary Parasitology

**Address for Correspondence**
*CH. Sudha Rani Chowdary, Assistant Professor, Department of Veterinary Pathology, NTR College of Veterinary Science, Sri Venkateswara Veterinary University, Gannavaram-521 102, Andhra Pradesh, India, E-mail: drsudha84@gmail.com*

*Received: 11.12.2024; Accepted: 21.1.2025*

## ABSTRACT

The present study was carried out to know the occurrence and pathomorphology of melanocytic tumors *viz.* melanocytoma and malignant melanoma in cattle. Out of 29 tumors of cattle collected during a period of 2 years, five melanocytic tumors (17.4%) were recorded in the present study. Grossly, the tumors were 3 to 10 cm in diameter, solitary, circumscribed to multinodular, sessile to pedunculated, soft to firm with variegated greyish white to black appearance. Cytology revealed clusters of pleomorphic melanocytes containing large nuclei and variable amounts of melanin granules in the cytoplasm. Histologically, melanocytoma revealed sheets of neoplastic melanocytes containing variable amounts of melanin granules obscuring the nuclear morphology while, malignant melanomas were characterized by the presence of nests of amelanotic to melanotic cells separated by a thin fibrovascular stroma located in the dermis. On IHC, all the melanocytic tumors were positive to S100.

**Keywords:** Cattle, melanocytoma, melanoma, S100

Melanocytomas and melanomas are tumors arising from neuroectodermal melanoblasts or melanocytes. Benign forms of the neoplasm are referred to as melanocytoma in animals and the malignant forms are called melanoma or malignant melanoma[1]. Melanocytic neoplasms are frequently encountered within both veterinary and human medicine. Cattle develop melanocytomas infrequently but congenital tumors and tumors in young animals have been reported[2]. Melanocytic tumors usually account for 5-6% of all tumors in surveys of bovine neoplasms and occur most commonly in the skin or subcutis and constitute 0.3% to 17% of integumentary tumors[1-3]. Since the terminology for these tumors is not consistent in human and veterinary literature, it has become usual to use the term "melanoma" for all malignant melanocytic tumors, whereas "melanocytoma" refers to the benign forms. Descriptive terms of melanocytic neoplasms include 'junctional' that refers to the proliferation of neoplastic melanocytes often as small nests at the epidermal - dermal junction, 'compound' indicating both epidermal and dermal components to the tumor and 'dermal' indicating that the tumor is only intradermal with no epidermal component[3]. In a very few cases, melanomas invade deeper than subcutis or metastasized[2].

Cytological assessment through techniques like fine needle aspiration cytology (FNAC) and impression smears offers a quick and cost-effective way to obtain an initial diagnosis regarding the tumor's origin and malignant potential[4]. Although, there are several diagnostic techniques available, histopathological examination accompanied by histochemical staining found to be the best and most reliable method for appropriate diagnosis of cutaneous neoplasms[5]. Tumor markers such as S100 and Melan A are used to provide the gold standard in the diagnosis of malignant melanomas[6].

The samples for the present study consisted of biopsy samples sent to the Department of Veterinary Pathology, NTR College of Veterinary Science, Gannavaram during the period from April 2023 to November 2024. The total samples screened included 29 cutaneous and ocular tumors of cattle. The tumor samples were examined for gross morphology and the cytological smears were prepared and subsequently stained with Leishman's stain.

**How to cite this article :** Poojitha, G., Chowdary, C.S.R., Devi, V.R. and Sreedevi, C. 2025. Pathomorphological and immunohistochemical studies on melanocytic tumors in cattle. Indian J. Vet. Pathol., 49(2) : 160-163.

Representative tissue samples were collected in 10% neutral buffered formalin. The samples were subjected to routine tissue processing by paraffin embedding technique and stained with haematoxylin and eosin method[7].

The duplicate paraffin tissue sections were immuno stained using ready to use antibodies and super sensitive polymer-HRP detection system (Bio Genex, USA). Four microns thick tissue sections were mounted on positively charged slides and baked for 1 hour at 60°C prior to test. The sections were dewaxed

**Fig. 1.** Melanocytoma - A black, spherical, pedunculated tumor mass on the face of a cattle; **Fig. 2.** Melanocytoma - Impression smear showing amelanotic to melanotic melanocytes amidst brownish black melanin granules (Leishman's stain X1000); **Fig. 3.** Melanocytoma - Section showing sheets of oval to polygonal melanocytes with abundant melanin pigment arranged around a blood vessel (H&E X400); **Fig. 4.** Malignant melanoma - A solitary, round tumor mass on the fetlock region of a cattle.

in xylene, hydrated through a graded series of ethanol solutions and washed three times in 0.1 M phosphate buffered saline (PBS; pH 7.4). Antigen retrieval was undertaken by heat treating sections in 0.01M citrate buffer at pH 6.0 in a pressure cooker for 20 min and were allowed to cool down to room temperature. Sections were rinsed in PBS for 10 min. The sections were placed in a humidifying chamber to carry out further steps at room temperature. Peroxide block™ (HK111-5K, Bio Genex), containing 3% hydrogen peroxide was applied to cover the sections and incubated for 20 min for quenching endogenous peroxidase activity. The sections were then washed in PBS three times. Power block™ (HK083-5K, Bio Genex), a protein aceous blocking agent containing casein was applied to the sections and incubated for 10 min to prevent nonspecific binding of antibodies to highly charged sites. The power block was then tipped off and incubated with S100 primary antibody (S100B/1012 rabbit polyclonal antibodies) for 60 min. The sections were rinsed in PBS and Super enhancer™ (HK518-06K, Bio Genex) was added to the slides and incubated for 20 min to enhance the signals. The sections were then rinsed in PBS buffer and were covered with Polymer-HRP reagent (HK519-06K, Bio Genex) containing anti mouse and anti-rabbit IgG labelled with enzyme polymer in phosphate buffered saline for 30 min. Sections were rinsed in PBS buffer. The sections were then incubated with solution prepared by adding one drop of liquid DAB chromogen i.e. 3,3'-Diamino benzidine mixed with 1 ml of DAB buffer for 5 min. Sections were rinsed with PBS, washed with distilled water, counter stained with Harri's Haematoxylin and mounted with DPX mountant. Negative control sections were also included in the staining procedure by omitting the primary antibody[8].

Out of 29 cutaneous and ocular tumors of cattle, 5 melanocytic tumors were recorded accounting to an occurrence of 17.24%. The occurrence of melanocytic tumors was recorded in Ongole and non-descript breeds of cattle in the age group of 2 - 7 years. The melanocytic tumors included two cases of melanocytomas and three cases of malignant melanomas.

In the present study, the melanocytomas were located on the thigh and face of cattle (Fig. 1). Grossly,

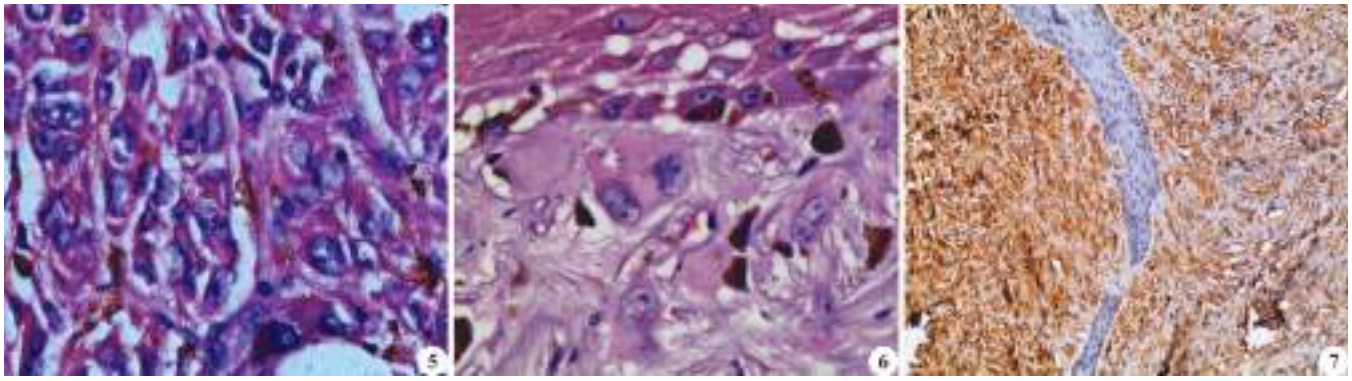

**Fig. 5.** Malignant melanoma - Section showing amelanotic to melanotic neoplastic cells with vesicular nuclei and prominent nucleoli (H&E X400); **Fig. 6.** Malignant melanoma - Section showing mononucleated to binucleated giant cells with abundant eosinophilic cytoplasm, vesicular nuclei and prominent nucleoli along with junctional activity (H&E X400); **Fig. 7.** Malignant melanoma: IHC-S-100 - Note intense cytoplasmic expression in the melanocytes invading the dermis X100.

the tumors were pedunculated to sessile, spherical to irregular in shape, brownish black in color and firm in consistency measuring about 6-10 cm in diameter. Cut sections revealed fleshy, dark brown to black colored surfaces. Cytological studies revealed the presence of clusters of round to oval and spindle shaped melanocytes with intracytoplasmic golden yellow melanin granules and round vesicular nuclei (Fig. 2). Histologically, melanocytomas were characterized by sheets of neoplastic melanocytes in the dermis. The cells were moderately pleomorphic, spindle to epithelioid in shape with variable amounts of melanin granules in the cytoplasm, obscuring the nuclear morphology. The tumor showed significant neovascularization with sheets of melanocytes encircling the capillaries (Fig. 3).

The malignant melanomas in the present study were located on the fetlock region (Fig. 4) and eyelids of cattle. Grossly, the tumors were solitary, circumscribed to multinodular, measuring about 3-5 cm in diameter with a variegated appearance. Cut sections were fleshy to firm and greyish white in color. Cytology revealed clusters of pleomorphic melanocytes containing large nuclei. The cells were amelanotic or contained variable amounts of melanin granules in the cytoplasm. Histologically, malignant melanomas were characterized by junctional activity and presence of nests of melanocytes separated by a thin fibrovascular stroma located in the dermis. The neoplastic melanocytes were epithelioid to spindloid and exhibited high nuclear to cytoplasmic ratio, scant cytoplasm that was frequently amelanotic and the nuclei were vesicular with prominent nucleoli (Fig. 5). The tumor also revealed a large number of giant cells with abundant eosinophilic cytoplasm, marked anisokaryosis, nuclear molding, single to multiple nuclei and nucleoli (Fig. 6).

On immunohistochemistry, melanocytomas and melanomas revealed intense cytoplasmic positivity to S-100 (Fig. 7).

In the present study, melanocytomas occurred on the thigh and face while malignant melanomas were located on fetlock and eyelids of cattle. In the previous studies, melanocytic tumors were reported on jaw, scapular, dewlap, trunk, limbs and conjunctiva of cattle similar to the earlier reports[3,9-15]. Causes for the development of melanoma are unknown. Excessive exposure to sunlight is noted to be risk factor in humans[16]. UV photons can affect the DNA integrity, cell and tissue homeostasis, and induce mutations or affect expression of a plethora of genes including oncogenes and tumor suppressor genes[17]. In the present study, melanocytic tumors occurred in the age group of 2-7 years in accordance to the findings of a previous study[2]. However, they have also reported congenital melanomas in their study. The gross findings of the present study are in line with the earlier findings[10,13-15] *viz.* brownish black melanocytomas and greyish white to variegated malignant melanomas. In the present study, cytology of melanocytic tumors revealed presence of a large number of pleomorphic, polyhedral to spindle shaped cells with intracytoplasmic golden yellow melanin granules and round vesicular nuclei consistent to the findings in earlier studies[10,15,16]. In the present study, benign melanocytomas were composed of sheets of neoplastic melanocytes in the dermis with moderate cellular pleomorphism and variable amounts of melanin obscuring the nuclear morphology. These findings corresponded with the results of earlier reports[6,9,10,16,18]. Histologically, malignant melanomas in the present study were characterized by the presence of nests of pleomorphic, melanotic to amelanotic melanocytes invading the dermis. The presence of amelanotic melanocytes indicate that the cells are poorly differentiated, a feature of anaplasia. The melanocytes were epithelioid and appearance of giant cells was frequent similar to the previous findings[12,14]. In the present study, immunohistochemistry revealed intense cytoplasmic immunopositivity to S-100 in melanotic to amelanotic melanocytes corroborating

earlier findings[6,13]. S-100 protein has a remarkable role in melanocytic tumor diagnosis especially for differential diagnosis of amelanotic melanomas[6]. The S-100 protein family contains a large number of related calcium binding proteins, and are largely found in skin melanocytes and immunoreactivity for such proteins have been carried out as a diagnostic criterion for melanoma in humans and lab animals[6].

## REFERENCES


1. Smith SH, Goldschmidt MH and McManus PM. 2002. A comparative review of melanocytic neoplasms. *Vet Path* **39:** 651-678.
2. Miller MA, Weaver AD, Stogsdill PL, Fischer JR, Kreeger JM, Nelson SL and Turk JR. 1995. Cutaneous melanocytomas in 10 young cattle. *Vet Path* **32:** 479-484.
3. Meuten DJ. 2017. Tumors of skin, hemolymphatic system. In: Tumors in Domestic Animals, 5th edition, Iowa: John Wiley & Sons, USA.
4. Castro MR and Gharib H. 2003. Thyroid fine-needle aspiration biopsy: progress, practice and pitfalls. *Endocr Pract* **9:** 128-136.
5. Vijayakumar S, Lakkawar AW, Kumar R, Alphonse RMD and Nair MG. 2020. Pathomorphological studies on mesenchymal and melanocytic neoplasms of cattle. *Vet Med Public Health J* **1:** 102-107.
6. Javanbakht J, Sasani F, Adibhashemi F and Hemmati S. 2014. Comparative histopathological diagnosis of cutaneous melanoma by H&E, special staining and immunohistochemical methods against cutaneous squamous cell carcinoma in horse and bovine. *J Bioanal Biomed* **6:** 19-23.
7. Luna LG. 1968. Manual of Histologic Staining Methods of the Armed Forces Institute of Pathology, 3rd Edn., The Blakiston Div, McGraw-Hill Book company, New York.
8. Pieper JB, Stern AW, Clerc SM and Campbell KL. 2015. Co-ordinate expression of cytokeratins 7 and 14, vimentin and Bcl-2 in canine cutaneous epithelial tumors and cysts. *J Vet Diag Inves* **27:** 497-503.
9. Sreenu M, Srinivas M and Nagaraj P. 2003. Melanoma of the shoulder region in an Ongole Bullock. *Indian Vet J* **80:** 294-295.
10. Pazhanivel N, Napolean RE, Manohar BM and Ravi U. 2003. A case of cutaneous melanoma in a bull. *Indian J Anim Res* **37:** 151-152.
11. Rama T, Thangapandiyan M, Vigneshwaran S, Chandrasekaran D, Vijayarajan A and Pazhanivel N. 2023. Solitary cutaneous melanoma in a crossbred jersey heifer. *IJAVSR* **52:** 112-116.
12. Chaves Velasquez CA, Astaíza Martínez JM, Benavides Melo CJ and Vallejo Timarán DA. 2015. Malignant tumor derived from skin melanocytes of a bovine of unusual presentation: a case study. *Revista de Medicina Veterinaria* **29:** 63-68.
13. Kapoor Jasmine, Banga Harmanjit, Singh Nittin and Deshmukh Siddhartha. 2020. Studies on pathology of ocular tumors in bovine. *Indian J Vet Path* **44:** 65.
14. Karakurt E, Aydın U, Beytut E, Kılıç E, Dağ S, Nuhoğlu H and Kurtbaş E. 2021. Immunohistochemical assessment of S100, Vimentin, PCNA, p53 and MMP-9 expressions in bovine melanomas. *Harran Üniversitesi Veteriner Fakültesi Dergisi* **10:** 43-49.
15. Sabri MA, Shahzad M and Qayyum A. 2010. Ocular melanoma in a buffalo. A clinical case recorded under field conditions. *Buffalo Bulletin* **29:** 235-237.
16. Garma-Aviña A, Valli VE and Lumsden JH. 1981. Cutaneous melanomas in domestic animals. *J Cutan Pathol* **8:** 3-24.
17. Anna B, Blazej Z, Jacqueline G, Andrew CJ, Jeffrey R and Andrzej S. 2007. Mechanism of UV-related carcinogenesis and its contribution to nevi/melanoma. *Expert Rev Dermatol* **2:** 451-469.
18. Shruthi P. 2014. Pathomorphological studies on Bovine Tumors Doctoral dissertation, Sri Venkateswara Veterinary University, Tirupati-517 502, AP.

*Indian J. Vet. Pathol., 49(2) : 164-165, 2025: DOI: https://doi.org/10.56093/1j9wvj68*

SHORT COMMUNICATION

# Congenital Teratoma in a crossbred Jersey calf

**I. Hemanth*, K. Manoj Kumar[1] and B. Prakash Kumar[1]**
Department of Veterinary Pathology, College of Veterinary Science, Garividi, Sri Venkateswara Veterinary University, Andhra Pradesh, India, [1]Department of Veterinary Clinical Complex

**Address for Correspondence**
*I. Hemanth, Assistant Professor, Department of Veterinary Pathology, College of Veterinary Science, Garividi, Sri Venkateswara Veterinary University, Andhra Pradesh, India, E-mail: hemanthimmanni@gmail.com*

*Received: 21.1.2025; Accepted: 20.2.2025*

## ABSTRACT

Teratomas are unique neoplastic conditions in different animal species including humans, by virtue of their origin from multiple germinal layers. A condition of congenital teratoma was observed in a 3 days old crossbred Jersey female calf. Clinically, a round growth was noticed on dorsal aspect of the neck and it was removed surgically under local anaesthesia. Upon incision, the growth revealed multiple cavities within the whitish stroma surrounded by a tough capsule. Histopathological evaluation revealed areas of different tissue components *viz.* stratified and simple epithelium lining the cavities, respiratory tissue with bronchial components of cartilage and mucosa, nervous tissue with nerve fibres and choroid plexus, few vascular elements of small blood vessels and dense connective tissue with leucocyte infiltration. Based on the presence of tissues that arise from multiple germ layers, the current case was diagnosed as a case of congenital teratoma.

**Keywords:** Calf, congenital, crossbred Jersey, Teratoma

**How to cite this article :** Hemanth, I., Kumar, K.M. and Kumar, B.P. 2025. Congenital Teratoma in a crossbred Jersey calf. Indian J. Vet. Pathol., 49(2) : 164-165.

Congenital tumors are defined as tumors existing at and usually before birth[1] or those detected during pregnancy or within the first 2-3 months of life[2,3]. Various congenital tumors have been reported in calves as like hemangiomas, melanomas, mastocytomas, lipoma and neurofibromatosis[2,4]. Teratomas are rather rare neoplastic conditions, especially in ruminants, that are postulated to arise from neoplastic transformation of pleuripotent cells[3,5]. They are often composed of tissues which originate from more than one germinal layer[6,7] and were often reported to arise from gonads in different animal species[8,9,10]. However, extra-gonadal teratomas also occur in animals[11]. The present case describes the occurrence of congenital teratoma in a new born calf.

A three day old crossbred Jersey female calf was presented to the Veterinary Clinical Complex, College of Veterinary Science - Garividi with the history of a growth on dorsal aspect of the neck since birth. The growth was surgically removed under local anaesthesia and the sample was subjected for routine histopathological processing followed by Hematoxylin & Eosin staining.

Gross examination revealed round, medium sized growth that was hard and tough in consistency. Upon incision, whitish tissue was noticed with multiple cavities of varying sizes within (Fig. 1). Histopathological evaluation revealed different tissue components of variable origin. Multiple cavities/empty spaces were noticed which were distended, thin walled and lined by simple, flattened epithelium. At certain locations, the cavities were found to be lined by stratified epithelium (Fig. 2). These cavities or ducts lined by epithelium suggest endodermal tissue components of digestive system as described earlier[6]. Diffuse fibrous tissue proliferation was evident in between the cavities that revealed haemorrhages at certain locations with infiltration of leucocytes. Small blood capillaries were also noticed with plump endothelial cells within the stroma. Respiratory tissue was noticed as a derivative of mesoderm, characterised by bronchial structures of mucosa and cartilaginous rings (Fig. 3). Multi-focal areas of nervous tissue components suggestive of choroid plexus were noticed. They were characterised by irregular spaces lined by single layer of epithelial/ependymal cells on a fine stroma of loose connective tissue and blood capillaries forming papillary growths into the lumen (Fig. 4). At certain locations, cross sections of nerve fibres were also evident. At the periphery, tissue resembling the keratinised layer of skin was noticed with incompletely differentiated epidermal cells and without any appendageal structures (Fig. 5). Abudunt collagen deposition was noticed below the superficial epithelium. Nervous tissue and keratinised epithelium suggested ectodermal tissue components. Certain vascular structures were also noticed that revealed wavy, reticulin fibres in the wall. However, the epithelial cells were tall and columnar in contrast to the regular flattened endothelial cells. All these findings were in agreement with earlier studies that reported simultaneous occurrence of tissues of different germinal layers as like skin, bone, glands and nervous structures in

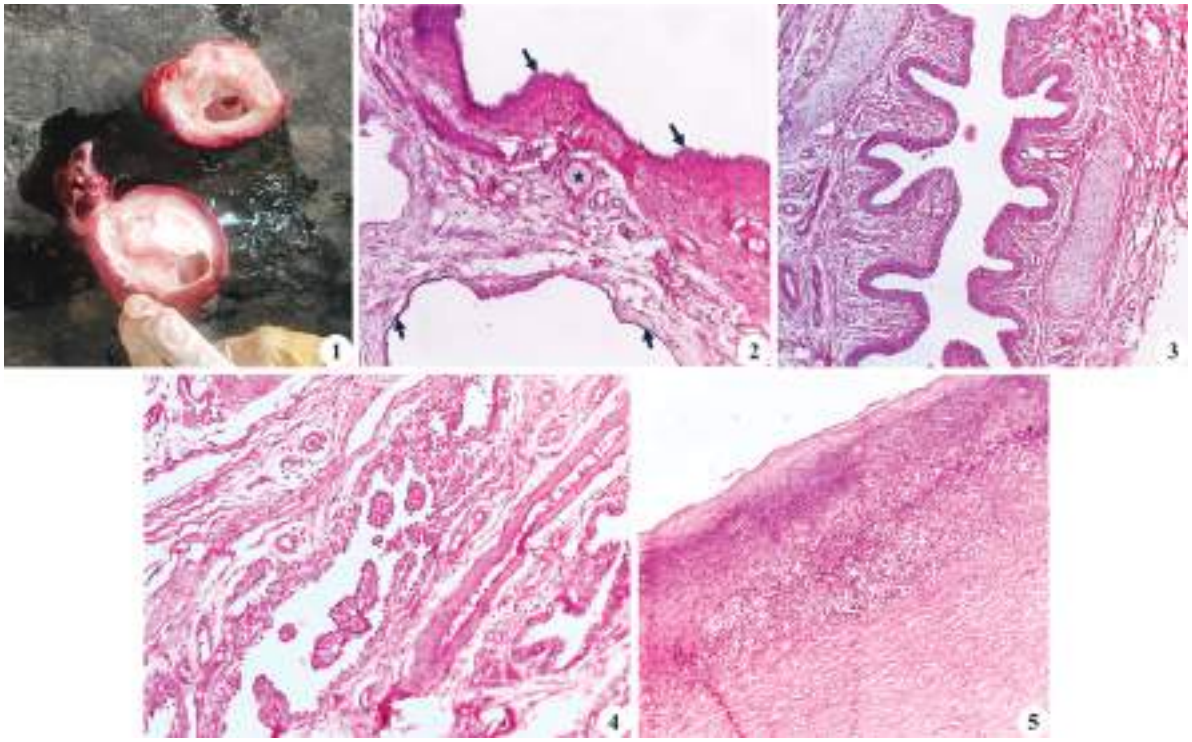

**Fig. 1.** Cut section of tumor mass with multiple cavities inside; **Fig. 2.** Multiple cavities/ducts lined by simple flattened epithelium and stratified epithelium (arrows). Note the section of nerve fiber (asterisk) (H&E x100); **Fig. 3.** Bronchial tissue with mucosa and cartilaginous rings in the wall (H&E x100); **Fig. 4.** Nervous tissue: Choroid plexus forming papillary in growths lined by single layer of ependymal cells with cilia on apical surface (H&E x100); **Fig. 5.** Keratinised epithelium with undifferentiated epidermal cells and dense collagen deposition beneath (H&E x100).

the teratoma[6]. Based on these observations, the present case was diagnosed as congenital teratoma.

Teratomas are often categorised as mature and immature variants. While mature teratomas are often benign and composed of well-differentiated cells of two or three germ cell layers, immature teratomas are malignant with poorly differentiated embryonal components[12]. However, the tissue components in the present case were well differentiated suggestive of a mature, differentiated and benign teratoma.

## ACKNOWLEDGEMENTS

The authors are thankful to Sri Venkateswara Veterinary University, Tirupati for facilities to carry out the study.

## REFERENCES

1. Dorland's Illustrated Medical Dictionary, 27th Edn. WB Saunders Company, Philadelphia London Toronto Montreal Syndney Tokya, 1988.
2. Misdorp W. 2002. Congenital tumours and tumour-like lesions in domestic animals. Cattle - A review. *Vet Quar* **24:** 1-11.
3. Jacinto JGP, Bolcato M, Sheahan BJ, Muscatello LV, Gentile A, Avallone G and Benazzi C. 2021. Congenital Tumours and Tumour Like Lesions in Calves: A Review. *J Com Pathol* **184:** 84-94.
4. Yeruham I, Perl S and Orgad U. 1999. Case report congenital skin neoplasia in cattle. *Vet Dermatol* **10:** 149-156.
5. Becker S, Schön R, Gutwald R, Otten JE, Maier W, Hentschel R, Jüttner E and Gellrich NC. 2007. A congenital teratoma with a cleft palate: Report of a case. *British J Oral Maxil Sur* **45:** 326.
6. Meuten DJ. 2002. Tumors in Domestic Animals. Iowa State Press, Ames, Iowa, USA.
7. Wetherell D, Weerakoon M, Williams D, Beharry BK, Sliwinski A, Ow D, Manya K, Bolton D and Lawrentschuk N. 2014. Mature and Immature Teratoma: A Review of Pathological Characteristics and Treatment Options. *Med Surg Urol* **3:** 124.
8. Carluccio A, Zedda MT, Contri A, Gloria A, Robbe D, Amicis ID and Pau S. 2017. *Vet Ital* **53:** 327-330.
9. Kavitha K, Poornachandhar I, Thangapandiyan M and Sarath T. 2019. Benign cystic ovarian teratoma in a crossbred cattle. *Indian J Anim Rep* **40:** 55-57.
10. Makovicky P, Makarevich AV, Makovicky P, Seidavi A, Vannucci L and Rimarova K. 2022. Benign ovarian teratoma in the dog with predominantly neuronal tissue: A case report. *Veterinární Medicína* **67:** 99-104.
11. Pegas GRA, Monteiro LN and Cassali GD. 2020. Extragonadal malignant teratoma in a dog-Case report. *Arquivo Brasileiro de Medicina Veterinária Zootecnia* **72:** 115-118.
12. Sirivisoot S, Siripara N, Arya N, Techangamsuwan S, Rungsipipat A and Kasantikul T. 2022. Case report: Mature extragonadal teratoma at the proximal part of the tail in a kitten. *Front Vet Sci* **9:** 1003673.

*Indian J. Vet. Pathol., 49(2) : 166-167, 2025: DOI: https://doi.org/10.56093/yvj65s13*

SHORT COMMUNICATION

# A case of congenital goitre in goat kids

**Yatin, Gurtaj Singh[1], Geeta Devi Leishangthem[*] and Bilawal Singh[1]**
Department of Veterinary Pathology and [1]Department of Veterinary Gynaecology and Obstetrics, College of Veterinary Science, Guru Angad Dev Veterinary and Animal Sciences University, Ludhiana, Punjab, India

**Address for Correspondence**
*Geeta Devi Leishangthem, Department of Veterinary Pathology, College of Veterinary Science, Guru Angad Dev Veterinary and Animal Sciences University, Ludhiana, Punjab, India, E-mail: drgeetapatho@gmail.com*

*Received: 14.1.2025; Accepted: 14.2.2025*

## ABSTRACT

A 6 year old pregnant goat was presented with the complaint of straining for one day. The animal has completed the gestation period. The c-section was performed and three kids were delivered, out of which one was alive and two were dead. The dead kids were brought to postmortem and necropsy was conducted. The animals showed pale, thickened skin with myxedema and devoid of hair from the body. The thryoid glands of both animals were enlarged bilaterally. Grossly the enlarged thyroid gland was red and hard in consistency and free from any attachment in the neck region. Histopathologically, various sizes of thyroid follicles filled with colloid and hyper cellularity or c-cell hyperplasia and complete absence of absorption vacuoles were observed. On the basis of gross and histopathology, the case was diagnosed as bilaterally diffused congenital goitre in kids.

**Keywords:** Congenital goitre, goat, thyroid gland

Thyroid gland plays an important role in goats by contributing in reproduction, growth and productivity[1]. Goitre is a non-neoplastic growth of thyroid gland which generally occurs because of lack of iodine in body and as result there is hyperplastic growth of thyroid gland. Among domestic animals, goat kids are most susceptible for congenital goitre. Congenital goitre also leads to prolongation of gestation and dystocia. Iodine plays an important role in production of 3, 3, 5-Triiodothyronine (T3) and tetra-iodothyronine or thyroxine (T4)[2], thus lack of iodine caused improper thyroxin production which sends a negative feedback to pituitary and hypothalamus leading to increase thyroid stimulating hormone (TSH) release, that in turn cause diffused hyperplastic growth of thyroid gland.

In the present study, a pregnant female goat of age 6 years with history of straining and inappetance for 1 day was brought to Multispecialty Veterinary Hospital, Guru Angad Dev Veterinary and Animal Sciences University, Ludhiana. The gestation of dam was completed and was put on induction protocol but unable to deliver, so C-section was performed and 3 kids were delivered out of which two were dead and one alive. Postmortem of both the dead kids was conducted. On through physical examination of carcasses, both the animals had pale, thickened skin with myxedema and devoid of hair from body (Fig. 1). There was bilateral enlargement at cranio-ventral region of both kids which were very easily visible and palpable on physical examination of carcasses. Thyroid gland were extracted, grossly both were diffusely enlarged and dark red in color (Fig. 2). The affected animals show enlargement of thyroid gland, myxedema and alopecia[3]. The thyroid samples collected in 10% neutral buffered formalin were processed, sectioned to 5 micron for routine histopathology and stained hematoxylin and eosin stain[4].

On histopathological examination, variable sized follicles containing colloid with single to multiple layers of follicular cells indicating follicular cell hyperplasia and severe congestion in vessels were observed (Fig. 3). In some areas, C-cell hyperplasia was also appreciated (Fig. 4). Further, the periphery of colloid follicle towards the lumen was wavy in appearance which may be due to formation of endocytic resorption vacuoles at apical surface of follicular cells and follicular cells were also observed forming papillary projections into colloid. Thus, on the basis of gross and histopathological examination, it was concluded that both kids were suffering from diffuse hyperplastic congenital goitre.

**How to cite this article :** Y., Singh, G., Leishangthem, G.D. and Singh, B. 2025. A case of congenital goitre in goat kids. Indian J. Vet. Pathol., 49(2) : 166-167.

Similar hyperplastic goitre in kids has been reported by other workers[3,5-7]. Deficiency of iodine in dam lead to goitre in kids which may be due to dietary iodine deficiency, ingestion of goitrogens such as plants of *Brassica* family or any hereditary condition like congenital dyshormonogenetic goitre. Congenital bilateral goitre is mostly associated with abortions in late gestation, still births or early neonatal death. The affected animal exhibit alopecia and myxoedema[7]. Foetal development retardation and goitre associated weak or dead

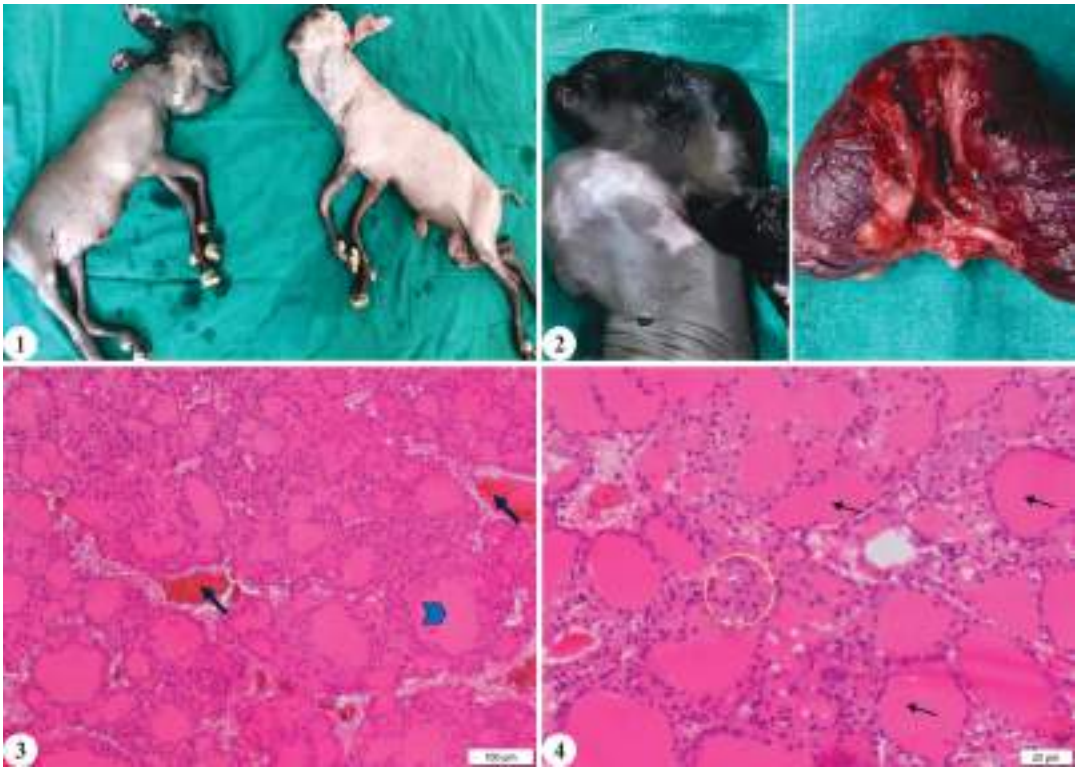

**Fig. 1.** Goat kids with enlarged thyroid gland and myxedema and alopecia; **Fig. 2.** Bilaterally enlarged thyroid gland; **Fig. 3.** Photomicrograph showing follicles of various sizes filled with colloids (arrow head) along with congested blood vessels (arrow) (H&E, Bar = 100µm); **Fig. 4.** Photomicrograph showing follicles of various sizes filled with colloids (arrow) along with congested blood vessels. Follicular and para-follicular cells hyperplasia (circle) was also observed (H&E, Bar = 20µm).

neonates were the adverse effect of iodine deficiency during pregnancy[8]. Wassner and Brown[9] stated that in newborns iodine deficient enlarged thyroid glands were associated with high mortalities. Mostly hyperplastic congenital goitre was characterized by excessive thyroid secretory epithelium growth forming solid clusters and slit-like follicles[10].

## REFERENCES


1. Todini L. 2007. Thyroid hormones in small ruminants: effects of endogenous, environmental and nutritional factors. *Anim* **1:** 997-1008.
2. Smith MC and Sherman DM. 2009. Goat medicine. John Wiley & Sons.
3. Nourani H and Sadr S. 2023. Case report of congenital goitre in a goat kid: Clinical and pathological findings. *Vet Med Sci* **9:** 2796-2799.
4. Luna LG. 1968. Manual of histologic staining methods of the Armed Forces Institute of Pathology. 3rd Edition, McGraw-Hill, New York. Bhardwaj RK. 2018. Iodine deficiency in goats. In S. Kukovics (Ed.), Goat science.
5. Ankita KR, Jamwal S, Verma A, Choudhary S, Patil RD and Asrani RK. 2023. Pathology of congenital goitre in a goat kid. *Haryana Vet* **62:** 174-175.
6. Davoodi F, Zakian A, Rocky A and Raisi A. 2022. Incidence of iodine deficiency and congenital goitre in goats and kids of Darreh Garm region, Khorramabad. *Iran J Vet Res* **8:** 336-342.
7. Zimmermann MB. 2020. Iodine and the iodine deficiency disorders, Editor(s): Bernadette P Marriott, Diane F Birt, Virginia A Stallings, Allison A Yates, Present Knowledge in Nutrition (Eleventh Edition), Academic Press.
8. Wassner AJ and Brown RS. 2015. Congenital hypothyroidism: Recent advances. *Curr Opin Endocrinol Diabetes Obes* **22:** 407-412.
9. Jamshidi K. 2022. Occurrence of congenital goitre in a goat flock, Garmsar. *Iran J Vet Res* **77:** 55-61.

*Indian J. Vet. Pathol., 49(2) : 168-171, 2025: DOI: https://doi.org/10.56093/tg6m6742*

SHORT COMMUNICATION

# A Concurrent tuberculosis and paratuberculosis in a beetal goat

**Geeta Devi Leishangthem*, Tanu Sharma, Sonam Sarita Bal, Nittin Dev Singh and Gursimran Filia**
Department of Veterinary Pathology and Animal Disease Research Centre, Guru Angad Dev Veterinary and Animal Sciences University, Ludhiana, Punjab, India

**Address for Correspondence**
*Geeta Devi Leishangthem, Department of Veterinary Pathology and Animal Disease Research Centre, Guru Angad Dev Veterinary and Animal Sciences University, Ludhiana, Punjab, India, E-mail: drgeetapatho@gmail.com*

*Received: 15.1.2025; Accepted: 14.2.2025*

## ABSTRACT

A two year old female beetal goat was presented with history of diarrhea and progressive weight loss. On hematology, severe anaemia (Hb = 2.9g/dl) and neutrophilic leukocytosis were observed. Ante-mortem fecal examination revealed positive for acid fast bacilli. The animal succumbed to death. On postmortem examination, the carcass showed emaciation and diarrhoeic feces found to be adhered in the perineal and tail region. Grossly, lung revealed edema, congestion along with hard caseated nodules in focal areas and trachea was frothy. Intestine revealed catarrhal enteritis, and also showed thickening of the intestinal mucosa at the caeco-iliac junction. Mesenteric lymph nodes were swollen and caeseated. Impression smear from intestine and lung were positive for acid fast bacilli. Histopathologically lung exhibited focal to multifocal necrotizing lesion at the centre and surrounded by epitheloid cells and Langhan's giant cell, indicating typical TB granuloma. Further, immunohistochemistry and PCR using specific primers for *Mycobacterium tuberculosis* complex and *Mycobacterium avium* subsp paratuberculosis confirmed the presence of tuberculosis and paratuberculosis respectively.

**Keywords:** Acid fast bacilli, beetal goat, johne's disease, tuberculosis

Tuberculosis and paratuberculosis are mycobacterial diseases where in goat tuberculosis is caused by *Mycobacterium bovis* and *Mycobacterium caprae* and paratuberculosis is caused by *Mycobacterium avium* subsp paratuberculosis (MAP)[1]. Both diseases have serious impact on production and economic losses. Having a wide host range *M. bovis* is a huge concern as a zoonotic agent[2]. Tuberculosis transmission occurs primarily through inhalation but can also spread via ingestion of contaminated substances, secretions, and through the placenta to the fetus[3]. However, Paratuberculosis is mainly transmitted via the fecal-oral route, with animals getting infected by grazing on contaminated pasture or sucking contaminated teats[4]. Both the diseases are more associated with crowded population of animals or animals kept under stressful conditions. Tuberculosis causes emaciation, fever, inappetance, and chronic moist cough, while paratuberculosis features are persistent diarrhea, submandibular edema, and emaciation, both leading to significant economic losses to the farmers[5,6]. Mycobacterial diseases are diagnosed through clinical signs, gross observation, histopathology, microscopic examination on sputum, fecal sample or any other secretion with Z-N staining, and molecular assays like PCR, immunohistochemistry.

A two year old female beetle goat was presented to Guru Angad Dev Veterinary and Animal Sciences, Hospital with the history of diarrhea and progressive weight loss. Haematological and faecal smear examination using Ziehl-Neelsen staining was done. Animal was treated symptomatically but could not survive and after death, it was presented for post-mortem examination. Systemic necropsy examination was conducted and gross findings were recorded. Impression smear of the lungs and intestine were prepared and stained with Modified Ziehl-Neelsen staining for detection of acid fast bacilli. For histopathology, lungs, lymph nodes and intestine were collected in 10% neutral buffered formalin. The fixed tissue was embedded with paraffin and 4-µm thickness tissue sections were cut and then stained with routine hematoxylin and eosin (H&E). Stained sections were viewed under microscope (Olympus BX 61) and photomicrographs were taken. Immunohistochemical staining and PCR were done for additional confirmation.

**How to cite this article :** Leishangthem, G.D., Sharma, T., Bal, S.S., Singh, N.D. and Filia, G. 2025. A Concurrent tuberculosis and paratuberculosis in a beetal goat. Indian J. Vet. Pathol., 49(2) : 168-171.

Hematological investigation revealed presence of severe anaemia (with Hb = 2.9g/dl) and neutrophilic leukocytosis with TLC = 15800/ul. Faecal sample stained with Ziehl-Neelsen stain showed positive result for acid fast bacilli. On external examination, the carcass showed emaciation (Fig. 1) and the anal area was soiled with faeces. Upon doing systemic necropsy examination, caseous nodules were observed on the lungs along with congestion and edema (Fig. 2). The trachea was filled with frothy exudates (Fig. 3). Intestine

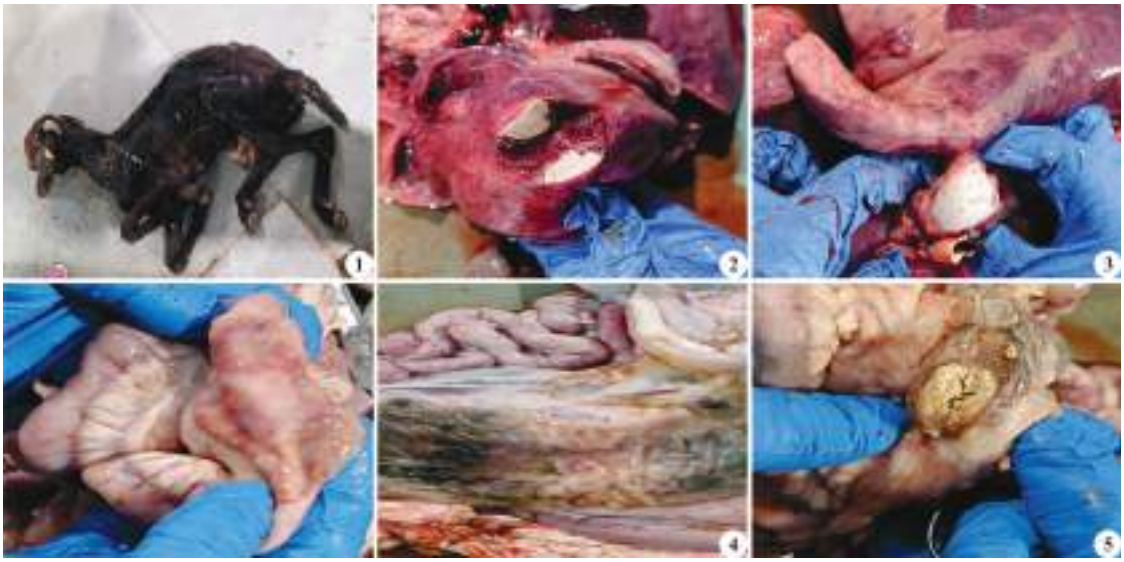

**Fig. 1.** Goat: Emaciated carcass of Beetal goat; **Fig. 2.** Lung showing caseous nodule; **Fig. 3.** Trachea filled with froth; **Fig. 4A & B.** Intestine with thickened and corrugated mucosa; **Fig. 5.** Mesenteric lymphnode showing caseation and mineralization.

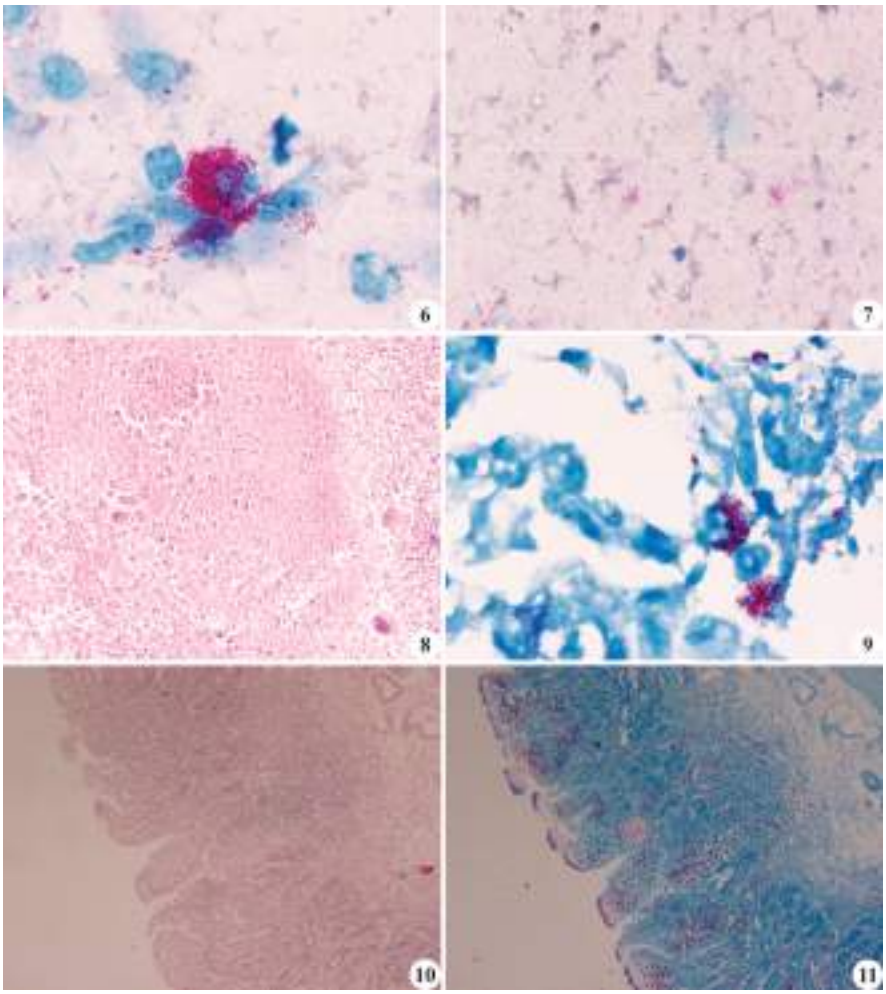

**Fig. 6.** Intestine: Impression smear showing acid fast bacilli with Ziehl-Neelsen stain; **Fig. 7.** Lungs: Impression smear showing acid fast bacilli within the inflammatory cell with Ziehl-Neelsen stain; **Fig. 8.** Lungs: Granuloma showing caseous necrotic area surrounded by inflammatory cells and giant cells (H&E x200); **Fig. 9.** Lungs: Acid fast bacilli within the inflammatory cells (ZN stain x1000); **Fig. 10.** Intestine: Thickened intestinal mucosa with mononuclear cells infiltration within the mucosa and sub-mucosa (H&E x100); **Fig. 11.** Intestine: Acid-Fast bacilli in the mucosa as well as within the mononuclear infiltrating cells (ZN x100).

showed generalized congestion and the mucosa of the intestine was thickened and corrugations at the ileo-caecal junction were observed (Fig. 4). Mesenteric lymph nodes were diffusely swollen and had pale and thick capsule and it had firm consistency along with caseous necrosis and mineralized matrix (Fig. 5). Microscopically, examination of impression smear prepared from intestine and lung showed positive for acid fast bacilli when stained with Ziehl-Neelsen stain (Fig. 6, 7). Histopathologically, lung showed typical tuberculous granuloma with central caseous necrosis surrounded by inflammatory cells and Langhan's giant cells (Fig. 8). Acid fast bacilli were present within the inflammatory cells and necrotic area (Fig. 9). In intestine the thickened intestine mucosa and sub-mucosa had diffused infiltration of mononuclear cells along with congestion (Fig. 10). Upon doing Z-N staining, acid fast bacilli were also appreciated within mononuclear cells of the intestinal mucosa (Fig. 11). In lymph node, there was caseous necrosis with infiltration of giant cells and mononuclear cells (Fig. 12). Similar to the intestine in the lymph node acid fast bacilli were observed within mononuclear cells and necrosed area (Fig. 13).

Additionally, DNA was extracted from tissue samples using a commercial kit (Applied Biosystems™ High-Capacity cDNA Reverse Transcription Kit) for amplification of IS*6110* PCR for detection of *Mycobacterium tuberculosis complex* (MTC) and IS900 PCR for detection of *Mycobacterium avium* subsp. paratuberculosis (MAP) (Table 1). PCR was performed for these 2 genes with cycling parameter of 94°C for 5 min (initial denaturation) followed by 30 cycles of 1 min at 94°C, 1 min at 60°C and 1 min at 72°C followed by final extension of 7 min at 72°C. Thermal cycling was performed in Gradient

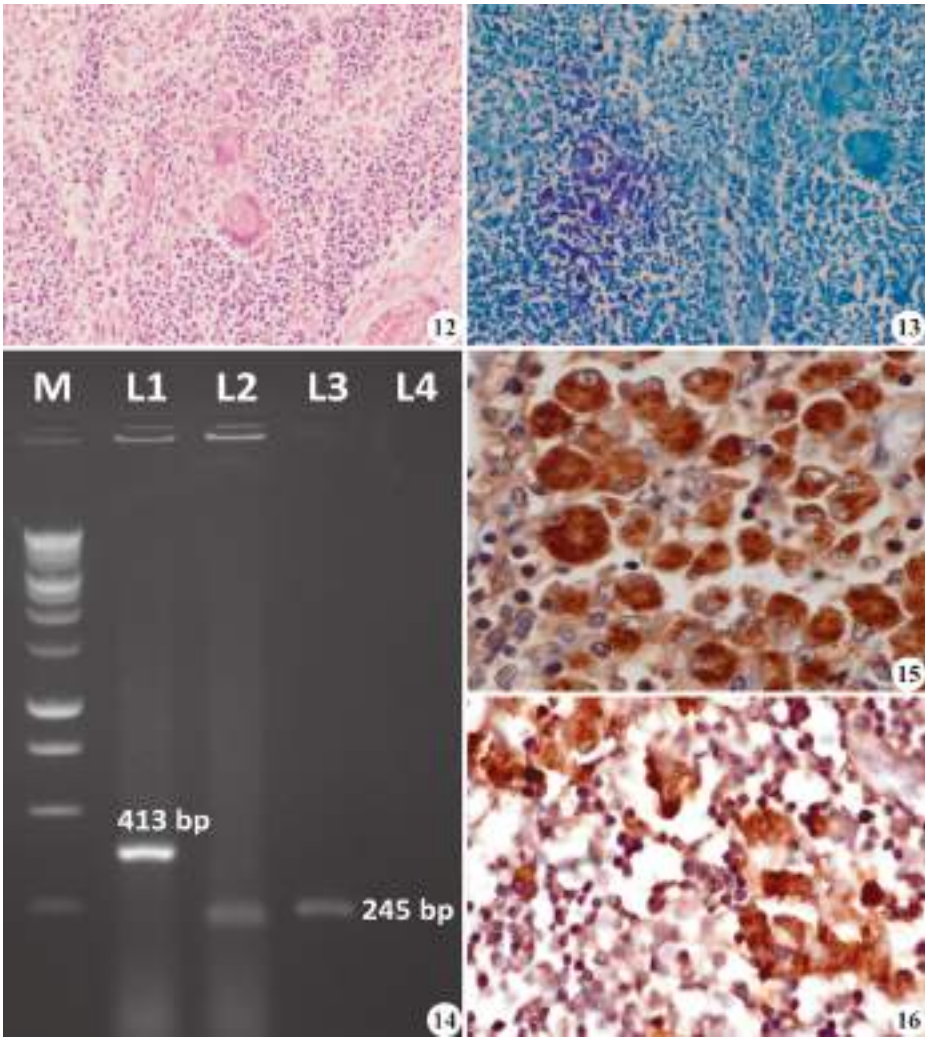


**Fig. 12.** Lymph node showing giant cells and lymphocytes (H&E 20X); **Fig. 13.** Acid-Fast bacilli within the mononuclear cells in lymph node (ZN x200); **Fig. 14.** Gel electrophoresis of PCR product showing 413 bp for MAP in intestine sample and 245 bp for MTC in lung sample. M = DNA ladder (1Kb); L1 = Intestine sample; L2, 3 = Lung sample; **Fig. 15.** Immunolocalization of *Mycobacterium* antigen within the mononuclear cells (IHC, DAB, x1000); **Fig. 16.** Immunolocalization of *Mycobacterium* antigen within the mononuclear cells in lymph node (IHC, DAB, x1000).

**Table 1.**

| Organism | Primer | Sequence | Gene | Product size | Reference |
|---|---|---|---|---|---|
| *Mycobacterium tuberculosis complex* (MTC) | INS1 (forward) | 5′-CGT GAG GGC ATC GAG GTG GC-3' | IS6110 | 245 bp | Filia *et al.*[9] |
| | INS2 (reverse) | 5′-GCG TAG GCG TCG GTG ACA AA-3' | | | |
| *Mycobacterium avium* subspecies paratuberculosis (MAP) | P90B (forward) | 5′-GAA GGG TGT TCG GGG CCG TCG CTT AGG-3' | IS900 | 413 bp | Millar *et al.*[10] |
| | P91B (reverse) | 5′-GGC GTT GAG GTC GAT CGC CCA CGT GAC-3' | | | |

Thermocycler (Thermo Scientific). The presence of amplified DNA was visualized by agarose gel electrophoresis. Gel electrophoresis of PCR product showing 413 bp for MAP in intestine sample and 245 bp for MTC in lung sample (Fig. 14). The animal was found to be positive for both the diseases. Immunohistochemical characterization of the acid fast bacteria was done in the lungs, intestine, lymphnode sample using *Mycobacterium bovis* antigen and positive immunolocalization of *Mycobacterium bovis* antigen found within the mononuclear cells (Fig. 15, 16). Thus, based on gross, cytology, histopathology, IHC and PCR, the case was confirmed as concurrent tuberculosis and paratuberculosis infection.

Mycobacterial diseases are chronic diseases and they have long asymptomatic period and even before manifesting clinical signs they start shedding organism, making it difficult to eliminate the disease[7]. Animals kept in crowded space with poor ventilation are more prone. Tuberculosis commonly presents with emaciation, fever, inappetance, and a chronic moist cough, while paratuberculosis is marked by persistent diarrhea, protein loss, sub-mandibular edema, and emaciation[5,6]. In advanced cases, affected animals may become reluctant to move and may die. Both diseases cause significant economic losses due to reduced weight gain, lower milk production, decreased fertility, and they also costs associated with diagnosis and treatment. Tuberculosis and paratuberculosis are very common diseases; however, concurrent infection of both diseases is rare. In India, goats are reared by poor people who usually are nomads and due to negligence the disease is often not properly reported and diagnosed so making it difficult to eradicate. Diagnosis of mycobacterial diseases can be made by observing clinical signs, gross observation and histopathology. Also, the same can be done by performing microscopic examination on sputum, fecal sample or any other relevant secretion using Z-N staining procedure and molecular assay like PCR which increases the sensitivity for diagnosis of the disease[8]. Mycobacterial disease are highly infectious so while diagnosing screening should be done for whole herd. Animals in crowded, poorly ventilated spaces are more susceptible, so proper hygiene, ventilation, and biosecurity measures are crucial. Sick animals should be isolated, and farmers, especially nomadic goat herders, need education on disease signs and reporting. Early detection tests are essential to control mycobacterial diseases effectively.

## REFERENCES


1. Álvarez J, de Juan L, Bezos J, Romero B, Sáez JL, Gordejo FR, Briones V, Moreno MÁ, Mateos A, Domínguez L and Aranaz A. 2008. Interference of paratuberculosis with the diagnosis of tuberculosis in a goat flock with a natural mixed infection. *Vet Micro* **128:** 72-80.
2. Lema AG and Dame IE. 2022. Bovine tuberculosis remains a major public health concern: A review. *AJVS & AH* **9:** 1085.
3. Vidal E, Grasa M, Perálvarez T, Martín M, Mercader I and de Val BP. 2018. Transmission of tuberculosis caused by Mycobacterium caprae between dairy sheep and goats. *Small Rumin Res* **158:** 22-25.
4. Sweeney RW. 1996. Transmission of paratuberculosis. *Vet Clin North Am Food Anim Pract* **12:** 305-312.
5. Quintas H, Pires I, Prada J, da Conceição Fontes M and Coelho AC. 2017. Diagnosis of Mycobacteriosis in Goats: Tuberculosis and Paratuberculosis. In Sustainable Goat Production in Adverse Environments: Volume I: Simões J, Gutiérrez C, Eds.; Springer International Publishing: Cham, Switzerland, pp. 247-266.
6. Quintas H, Reis J, Pires I and Alegria N. 2010. Tuberculosis in goats. *Vet Rec* **166:** 437.
7. Cosma CL, Sherman DR and Ramakrishnan L. 2003. The secret lives of the pathogenic mycobacteria. *Annu Rev Microbiol* **57:** 641-676.
8. Bates Mand Zumla A. 2016. The development, evaluation and performance of molecular diagnostics for detection of Mycobacterium tuberculosis. *Expert Rev Mol Diagn* **16:** 307-322.
9. Filia G, Leishangthem GD, Mahajan V and Singh A. 2016. Detection of *Mycobacterium tuberculosis* and *Mycobacterium bovis* in Sahiwal cattle from an organized farm using antemortem techniques. *Vet World* **9:** 383-387.
10. Millar D, Ford J, Sanderson J, Withey S and Tizard Mand Doran T. 1996. IS900 PCR to detect Mycobacterium paratuberculosis in retail supplies of whole pasteurized cow's milk in England and Wales. *Appl Environ Microbiol* **62:** 3446-3452.

*Indian J. Vet. Pathol., 49(2) : 172-174, 2025: DOI: https://doi.org/10.56093/3ys5r140*

SHORT COMMUNICATION

# Cytological diagnosis of transmissible venereal tumour in a dog - A report

**S. Ramesh*, Vinitha Vijayendran, A. Balakumar and S. Preetha**
Sanchu Animal Hospital, Chennai-600 020, Tamil Nadu, India

**Address for Correspondence**
*S. Ramesh, Sanchu Animal Hospital, Chennai-600 020, Tamil Nadu, India, E-mail: rameshlibya2010@gmail.com*

*Received: 23.1.2025; Accepted: 26.2.2025*

## ABSTRACT

A six months old mongrel dog was presented at Sanchu Animal Hospital, Velachery, Chennai for diagnosis and treatment with a history of bleeding from the prepuce and presence of cauliflower like growth on the penile region. Physical examination of the affected dog showed numerous cauliflower growths around the bulbus glandis of the penis. Haematological examination revealed mild leukocytosis accompanied by mild neutrophilia and eosinophilia. Cytological examination of impression smears taken from the mass revealed the presence of numerous discrete round cells with characteristic cytoplasmic vacuolations, suggestive of transmissible venereal tumour. Based on the laboratory findings, the affected dog was treated with vincristine sulphate along with multivitamin syrup and herbal liver tonic. The treated dog showed marked regression in growth after two weeks of treatment. Thus, the present study reports a case of transmissible venereal tumour based on the cytological examination of nodules present on the penile region of a dog.

**Keywords:** Cytology, mongrel dog, TVT, vincristine

**How to cite this article :** Ramesh, S., Vijayendran, V., Balakumar, A. and Preetha, S. 2025. Cytological diagnosis of transmissible venereal tumour in a dog - A report. Indian J. Vet. Pathol., 49(2) : 172-174.

Canine transmissible venereal tumor (TVT), also known as Sticker's sarcoma is a highly contagious venereal tumor of mesenchymal origin affecting dogs and other canine species including foxes, coyotes and wolves. TVT has been reported in dogs since many decades and it is mostly recorded in sexually active free-roaming dogs in tropical and subtropical regions. It's incidence is more common in dogs belonging to the age group of 1-5 years. Venereal transmission is most common but transmission also occurs through licking, biting, and sniffing the affected areas[1,2].

The clinical finding recorded in dogs affected with TVT includes presence of a solitary or multiple cauliflower-like growths with the size measuring from 5 mm to more than 10 cm in diameter. Though these lesions are mostly restricted to the external genitalia, they are also seen on the extragenital areas namely skin, nostrils, oral cavity, eye ball, eyelids and anus. The other clinical findings are oozing of blood from the affected area, serosanguineous secretions with intense odor, deformity, ulceration, and possibly areas of necrosis. Usually, the tumor does not metastasize to distant organs except in young and immune incompetent animals[3]. However, in some cases, metastasis can occur to the skin, inguinal lymph nodes, liver, kidneys, spleen, intestine, heart, brain, lungs, and other organs. Diagnosis is usually made based on the clinical, cytological and histological findings[3,4]. Of various therapeutic measures adopted namely complete surgical excision of the mass, radiotherapy, and chemotherapy, latter has been shown to be the most effective and easily available. Among various chemotherapeutic agents used, vincristine sulphate has been found to be highly effective in majority of cases and complete regression of tumour occurs in two to four doses[5]. However if chemotherapy is not effective, radiotherapy has been reported to give successful results[6,7,8]. Though numerous reports are available on incidence of TVT in young and adult dogs, it's incidence in dogs which are less than one year old is scanty. Hence the present paper reports an incidence of TVT diagnosed on cytological examination in a six months old mongrel dog.

A six months old male mongrel dog was presented at Sanchu Animal Hospital, Velachery, Chennai for diagnosis and treatment with a history of bleeding from the penis and presence of growths on the penile region. A thorough physical examination was carried out on ailing animal and blood samples were collected in vacutainers containing EDTA as anticoagulant for haematological studies. In addition, impression smears were prepared from the mass, air dried, and stained with Leishman and Giemsa cocktail stain for cytological examination[9]. Based on the laboratory findings, the case was diagnosed as TVT and the dog was treated intravenously with vincristine sulphate @ 0.025 mg/kg body weight at weekly intervals for two weeks. In addition, multivitamin syrup (Hemobest syrup®) and herbal liver tonic (Revell syrup®)

were prescribed to administer orally twice daily for four weeks.

Physical examination of the affected animal revealed presence of pinkish multiple cauliflower like growths which were friable with the size measuring from 5 mm to 2 cm in diameter around the bulbus glandis of the penis (Fig. 1). Haematological examination revealed mild leukocytosis accompanied by mild neutrophilia and eosinophilia (Table 1-3). Cytological examination of the smears were suggestive of transmissible venereal tumour which revealed numerous discrete round cells containing moderate amount of pale bluish granular cytoplasm with distinct borders. The cytoplasm of few cells showed characteristic punched out vacuolations. The nuclei which were coarse and round to oval in shape were placed either at centre or slightly at the periphery of the cells. The treated dog showed marked regression in growths after two weeks of treatment.

The present clinical findings which revealed multiple cauliflower like friable growths on the penile region of a non descript dog affected with TVT were in accordance with that of previous workers[10,11] who also reported cauliflower like growth in the penile region in non descript dogs affected with TVT.

**Table 1.** Erythrogram.

| Parameters | Results | References[19] |
|---|---|---|
| Haemoglobin (g/dl) | 16.70 | 11.90-18.90 |
| Packed cell volume (%) | 51.00 | 35-57 |
| Red blood cells (x$10^6$/mcL) | 7.56 | 4.95-7.87 |
| MCV (fl) | 67.50 | 66-77 |
| MCHC (g/dl) | 32.70 | 21.0-26.2 |
| MCH (pg) | 22 | 32.0-36.3 |

**Table 2.** Leukogram.

| Parameters | Results | References[19] |
|---|---|---|
| Total leukocyte count (x$10^3$/mcL) | 16.90 | 5-14.1 |
| Differential leukocyte count (%) | | |
| Neutrophil | 77 | 58-85 |
| Lynphocyte | 17 | 8-21 |
| Monocyte | 05 | 2-10 |
| Eosinophil | 15 | 0-9 |

**Table 3.** Thrombogram.

| Parameters | Results | References[19] |
|---|---|---|
| Thrombocyte count (x$10^3$/mcL) | 476 | 211-621 |

The haematological alterations which include mild leukocytosis accompanied by mild neutrophilia recorded during the present study was in agreement with that of earlier workers[12] who also observed leukocytosis accompanied by neutrophilia in dogs affected with TVT. They opined that the abnormal findings in haematological parameters are one of the common paraneoplastic syndromes which result from neoplastic infiltration of bone marrow, dysfunctioning of spleen or from immune mediated abnormalities.

The cytological findings of numerous discrete round cells with moderate amount of pale cytoplasm with vacuolations and eccentrically placed nucleus recorded during the present study were in accordance with that of previous workers[10] who noticed similar observations in an adult non-descript dog affected with TVT. Similar findings were also reported in a 4 years old intact Pit Bull dog[13] and in a three year old male mongrel dog[11] affected with TVT. The presence of characteristic multiple cytoplasmic vacuoles with large foamy nuclei are the common features of TVT cells on cytological examination[14] as noticed in the present study.

Cytological examination revealed characteristic round cells with slightly acidophilic cytoplasm containing finely granular and delicate vacuoles. The cytoplasmic borders were distinct containing centrally placed nuclei which

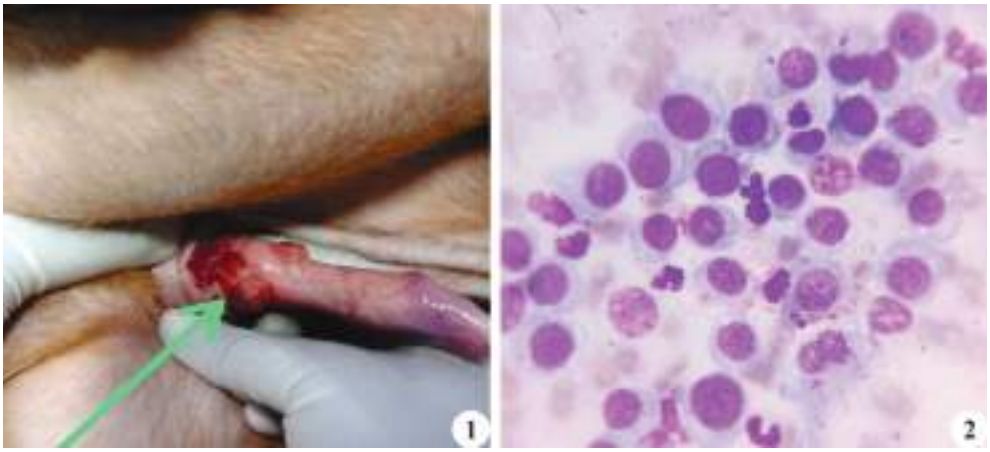


**Fig. 1.** Mongrel Dog - TVT showing cauliflower like growths at the base of the penis after one week of treatment with vincristine; **Fig. 2.** Impression smear of a mongrel dog - TVT showing numerous round cells containing oval to round nuclei with punched out vacuolations in few cells (L&G stain X100).

were oval or round in shape with delicate chromatin and large nucleoli. In addition, cells displayed anisokaryosis, anisocytosis, hyperchromasia or nuclear macrokaryosis and frequent typical or atypical mitoses which were indicative of tumour cells proliferation[15,16]. Numerous apoptotic bodies were also observed in the regression phase. Inflammatory cells such as lymphocytes, plasma cells, macrophages and neutrophils were noticed irrespective of stages of neoplastic development[17].

During the present study, administration of vincristine sulphate @ 0.025 mg/kg body weight intravenously at weekly intervals resulted in marked regression of tumour after two weeks of treatment. A complete regression of growth after four weeks of treatment with vincristine was recorded in three German Shepherd dogs affected with TVT[5]. However, complete regression of tumour was noticed only after six weeks of treatment with vincristine in a two years old male Doberman dog[18] and after five weeks of treatment in a 4 years old Pit Bull dog[11] affected with TVT. Thus, the present study confirms a case of TVT in a six months old mongrel dog based on cytological diagnosis and its successful treatment with vincristine.

## REFERENCES


1. Cohen D. 1985. The canine transmissible venereal tumor: a unique result of tumor progression. *Adv Cancer Res* **43:** 75-112.
2. Claudio Murgia, Jonathan K Pritchard, Su Yeon Kim, Ariberto Fassati and Robin A Weiss. 2006. Clonal Origin and Evolution of a Transmissible Cancer. *Cell* **126:** 477-487.
3. Yimesgen Tarekegn Abeka. 2019. Review on Canine Transmissible Venereal Tumor (CTVT). *Canc Therapy Oncol Int J* **14:** 555-895.
4. Alexandre Jose Rodrigues Bendas, Pablo Luiz das Neves Moreto, Adriano Baldaia Coxo, Paula Gaze Holguin and Denise do Vale Soares. 2022. Intra-abdominal transmissible venereal tumor in a dog: a case report. *Braz J Vet Med* **44:** e001422.
5. Murad A Hiblu, Nizar M Khabuli and Abdurraouf O Gaja. 2019. Canine transmissible venereal tumor: First report of three clinical cases from Tripoli, Libya. *Open Vet J* **9:** 103-105.
6. Chhavi Gupta, Satheshkumar, Ganesan A, Kumar V and Ramprabhu R. 2020. Retrospective analysis of canine transmissible venereal tumour cases in Tirunelveli region of Tamil Nadu. *Indian J Can Prac* **6:** 3-5.
7. Sagar Regmi, Premlal Mahato, Iebu Devkota, Raju Prasad Neupane, Asmin Khulal and Anil Kumar Tiwary. 2020. A Case Report on Canine Transmissible Venereal Tumor. *J Zoolog Res* **2:** 12-14.
8. Navrose Sangha and Barinder Singh. 2023. Canine transmissible venereal tumor. *Pharma Innov J* **12:** 949-954.
9. Garbayl RS, Agarwal N and Kumar P. 2006. Leishman-Giemsa Cocktail, An Effective Romanowsky stain for air dried cytologic smears. *Acta Cytologica* **50:** 403-406.
10. Muhammad Shafiqul Islam, Shubhagata Das, Muhammad Abdul Alim, Muhammad Mohi Uddin, Muhammad Hazzaz Bin Kabir, Muhammad Tariqul Islam, Kazal Krishna Ghosh and Muhammad Masuduzzaman. 2014. Progressive Type of Canine Transmissible Venereal Tumor (CTVT) in a Male Stray Dog: a Case Report. *Res J Vet Pract* **2:** 70-72.
11. Sasikala K, Amaravathi K and Madheswaran R. 2022. Concomitant occurrence of cutaneous form of transmissible venereal tumour and lymphadenopathy in a mongrel dog. *Pharma Innov J* **11:** 30-32.
12. Priyadarshini N, DP Das, SK Panda and L Samal. 2021. Transmissible venereal tumours (TVT) in bitches: A haematological, biochemical and histopathological study. *J Entomol Zool Stud* **9:** 490-493.
13. Gurpreet Singh Preet, Shabnam Sidhu, Kuljeet Singh Dhaliwal, Jasnit Singh and Jasleen Kaur. 2021. Atypical cutaneous transmissible venereal tumour in a dog - a case report. *Haryana Vet* **60:** 317-318.
14. Tasqueti UI, Martins MIM, Boselli CC, Muhammad Shafiqul Islam, Shubhagata Das, Muhammad Abdul Alim, Muhammad Mohi Uddin, Muhammad Hazzaz Bin Kabir, Muhammad Tariqul Islam, Kazal Krishna Ghosh and Muhammad Masuduzzaman. 2014. *Res J Vet Pract* **2:** 70-72.
15. Santos J, Barbosa M, Tenorio A, Coelho M and Rolim M. 2008. Transmissible venereal tumor disease in a dog with involvement of the skin. *Arq Bras Med Vet Zootec* **2:** 39-43.
16. Amaral A, Gaspar L, Silva S and Rocha N. 2004. Cytological diagnostic of transmissible venereal tumor in the Botucatu region, Brazil (descriptive study: 1994-2003). *PCV* **99:** 167-171.
17. Denicola D, Cowell R, Tyler R, Meinkoth J, Denicola D. 2007. Diagnostic cytology and hematology of the dog & cat, 3rd Edition, St. Louis, Mosby: 68-69.
18. Kumar A, Gupta G, Malik H and Vala J Rachna. 2010. Regression of transmissible venereal tumour in a dog treated with vincristine sulphate: a case report. *Haryana Vet* **49:** 76-77.
19. MSD Manual Veterinary Manual. 2025. Merck & Co., Inc., Rahway, NJ, USA.

*Indian J. Vet. Pathol., 49(2) : 175-178, 2025: DOI: https://doi.org/10.56093/ch9s7p24*

SHORT COMMUNICATION

# Pathomorphological findings of gastrointestinal pythiosis in a dog

**K. Sowmya, K. Gopal*, S. Sivaraj, S. Kokila, P. Balachandran and P. Srinivasan**
Department of Veterinary Pathology, Veterinary College and Research Institute, Namakkal-637 002, Tamil Nadu Veterinary and Animal Sciences University, Chennai-600 051, India

**Address for Correspondence**
*K. Gopal, Assistant Professor, Department of Veterinary Pathology, Veterinary College and Research Institute, Namakkal-637 002, Tamil Nadu Veterinary and Animal Sciences University, Chennai-600 051, India, E-mail: drvetpal@gmail.com*

*Received: 19.2.2025; Accepted: 8.3.2025*

## ABSTRACT

Intestinal pythiosis is a life threatening disease in dogs caused by fungus like organism called *Pythium insidiosum*. Gross examination revealed thickened intestinal wall with firm irregular masses on the serosal surface. Histopathological analysis revealed that the mass primarily consisted of fibrous tissue with multiple necrotic areas which were surrounded by macrophages, epithelioid cells, giant cells, lymphocytes and few plasma cells. In haematoxylin and eosin, both the longitudinal and transverse sections of tubuliform structures were observed within the necrotic areas. Periodic Acid-Schiff staining revealed pink fungal elements scattered in necrotic areas, while Grocott methenamine silver nitrate staining highlighted the fungal hyphae in the periphery of the necrotic regions with dark staining. Based on the histopathological and histochemical findings, it was concluded as gastrointestinal pythiosis in a dog.

**Keywords:** Dog, fungal hyphae, intestine, *Pythium insidiosum*

Pythiosis is a granulomatous disease caused mainly by *Pythium insidiosum*, an oomycete, belonging to the kingdom Stramenopila, affects several species of humans and animals[1]. Equines were mostly affected, followed by the dogs[2]. In dogs, the disease involves the skin[3] and gastro intestinal tract[4]. Initial studies on the life cycle of this oomycete have shown that *P. insidiosum* is present in stagnant waters and may possibly require the Australian water lily or other plants to complete its life cycle[5]. It was also found that its zoospores may play an important role in the propagation of infections amidst plants and animals. Infection picked up through minor wounds which came in contact with water or by drinking the water contaminated with motile zoospores[2].

Intestinal pythiosis commonly cause the granulomatous nodules on the serosal surface with involvement of mesentery which affect the normal function of intestine due to pressure and thickening of intestinal wall[6]. The affected dogs show the common non specific clinical signs like vomition, diarrhoea, weight loss and chronic anorexia[4]. Histologically, three different types of lesions were described. First type showed large irregular areas of necrosis surrounded by giant cells, epitheliod cells, macrophages and abundant neutrophils, eosinophils, and few plasma cells in the necrotic areas. Second type showed small, well-differentiated granuloma with small necrotic centers containing numerous neutrophils and few eosinophils. The third type contained mixture of focal granulomas and areas of necrosis followed by macrophages, with excessive connective tissue in the areas of inflammation[7].

The diagnosis of intestinal pythiosis is always challenging due its non specific clinical signs. Histological lesions associated with pythiosis in dogs were similar with other pyogranulomatous lesions so it is necessary to confirm the diagnosis other than the routine haematoxylin and eosin. The present study describes pathomorphological findings of gastrointestinal pythiosis in a dog.

A five year old dog was brought for treatment with the history of anorexia, chronic vomition and weight loss. On clinical examination, there was palpable mass in the abdominal cavity and the mass was removed surgically.

**How to cite this article :** Sowmya, K., Gopal, K., Sivaraj, S., Kokila, S., Balachandran, P. and Srinivasan, P. 2025. Pathomorphological findings of gastrointestinal pythiosis in a dog. Indian J. Vet. Pathol., 49(2) : 175-178.

The mass was fixed in 10 per cent neutral buffered formalin. Paraffin embedded tissue sections of 4 micron thickness was cut and stained with Haematoxylin and Eosin (H&E). Additionally, histochemistry techniques like Grocott Methenamine Silver Nitrate (GMS) and Periodic Acid-Schiff (PAS) were also performed for visualization of fungal hyphae.

Grossly, the irregular thickening of intestine with appreciable firm multiple nodules on the serosal surface were observed. On incision, the nodules were resisting to cut and grey to yellowish in colour. Each nodule was surrounded by thick fibrous connective tissue indicating multiple areas of necrosis and fibrosis (Fig. 1).

Histologically, the granulomatus reactions were extending

from the serosa to mucosa. The luminal surface was free of lesions. Diffuse fibrous connective tissue with multiple areas of liquefactive necrosis surrounded by varying degrees of inflammatory cells was observed on the serosal surface of intestine (Fig. 2). The granulomas were characterized by necrosis in the centre infiltrated by neutrophils (Fig. 3), surrounded by epithelioid cells, giant cells, discrete lymphocytes, plasma cells and moderate fibrosis (Fig. 4). The sections stained with sirius red revealed collagen fibres appearing bright red while the necrotic areas showing yellow colour (Fig. 5). Accompanied with these necrotic areas, unstained tubuliform structures were observed with haematoxylin and eosin (Fig. 6). Both longitudinal and transverse

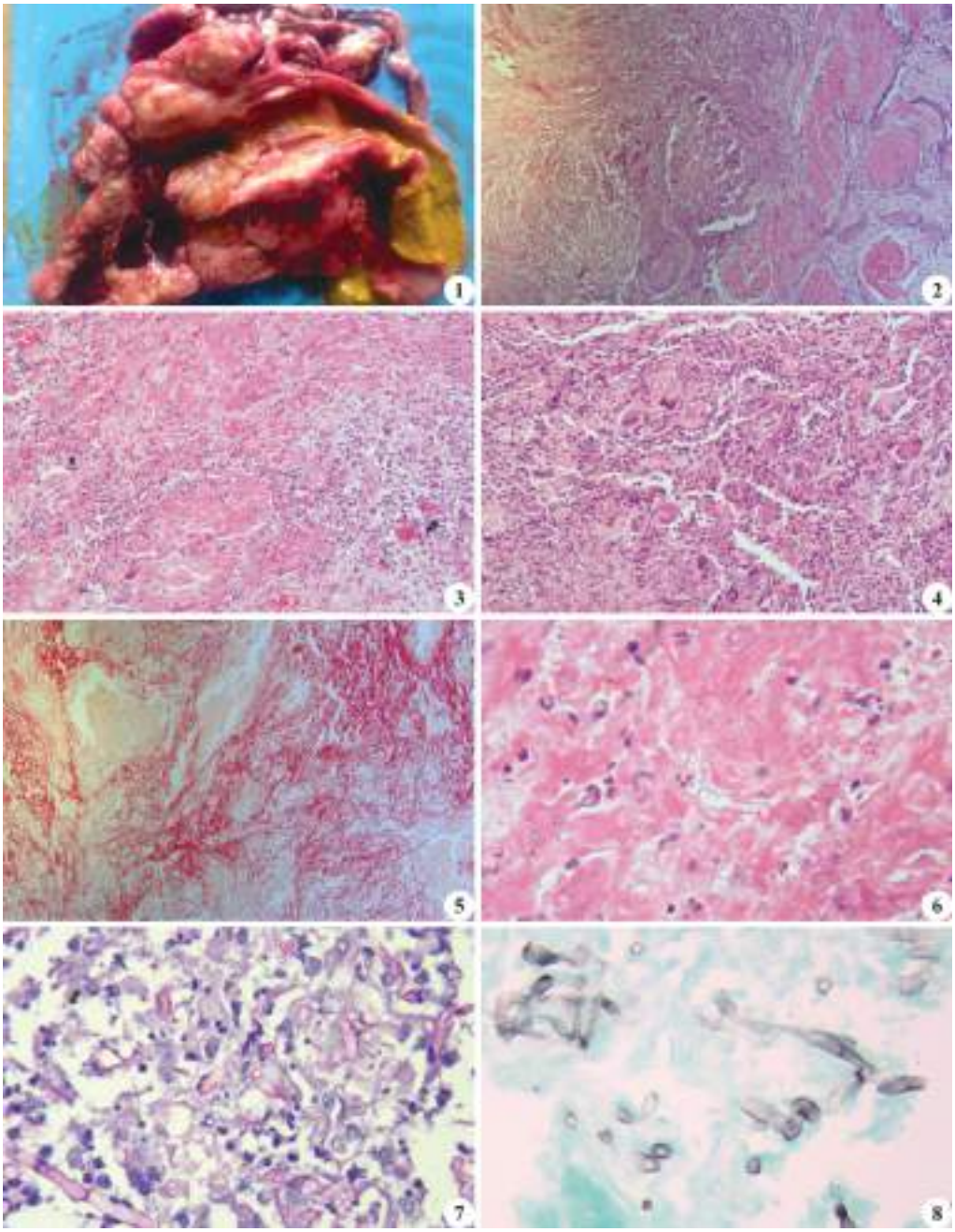


**Fig. 1.** Thickened intestinal wall with firm irregular masses and areas of grey to yellowish nodules on the serosal surface; **Fig. 2.** Multiple necrotic foci with fibrous tissue on the serosal surface of intestine (H&E x40); **Fig. 3.** Infiltration of neutrophils, necrotic debris in the necrotic area with fibrosis (H&E x100); **Fig. 4.** Fibrous tissue around the necrotic foci with infiltration of giant cells, macrophages and plasma cells (H&E x100); **Fig. 5.** The area of fibrosis and collagen deposition are stained red and necrotic area yellow in picro-sirius red x100; **Fig. 6.** Longitudinal and transverse sections of tubuliform structures were observed within the necrotic areas (H&E x400); **Fig. 7.** Both longitudinal and transverse sections of pink stained fungal hyphae were observed (PAS x400); **Fig. 8.** Fungal hyphae were stained black (GMS x400).

sections of pink coloured fungal hyphae structures and weakly stained hyphal walls were observed in the histological sections stained with PAS (Fig. 7). The GMS-stained sections showed that the hyphal walls were weakly stained black (Fig. 8). The weak staining could be due to the specific characteristics of the fungal species, as variations in the composition and thickness of cell wall can affect the intensity of stain.

Canine infections were first reported in dogs with cutaneous and gastrointestinal lesions from the Gulf of Mexico in the USA[5]. Subcutaneous pythiosis lesions have been recorded also on the legs, face and tail in dogs[8]. Disseminated pythiosis with involvement of internal organs like lung and liver has also been reported in dogs[8,9]. In the present study, lesions were confined to small intestinal serosal surface with involvement of mesentery. There were clinical cases caused by an unidentified species in the genus *Lagenidium* which were comparable to those observed in canine pythiosis[10] must be differentiated from canine cases.

The recent studies indicating that from 1980 to 2021, 4203 cases of pythiosis in humans (n = 771; 18.3%) and animals (n = 3432; 81.7%), with an average of 103 cases/year, were reported worldwide[11]. The number of pythiosis cases was significantly increased in the recent past and more importantly, 94.3% of human cases were recorded in India and Thailand, while 79.2% animal cases were reported in the USA and Brazil[11]. The canine pythiosis in India was not reported up to the year 2022[11] and the first case of canine intestinal pythiosis reported in the year 2023 in India[12].

There are several potential mechanisms by which environmental changes related to water may contribute to an increased incidence of pythiosis[1]. In the present study, the history of dog played in the stagnated water or any other water based activities were not available to trace the possible route of infection. In dogs, digestive lesions are more frequently observed in the stomach and small intestine. These lesions can sometimes spread via the serosa to neighbouring structures such as pancreas, uterus, mesenteric lymph nodes, lymphatics and frequently causing the omentum to adhere to the inflamed peritoneum[6].

Both granulomatous/pyogranulomatous and necrotizing eosinophilic inflammatory reactions were recorded in affected dogs[13] but only granulomatous pattern was observed in the present case. Extensive Hoeppli-Splendore-like phenomenon from degranulated eosinophils scattered over the hyphal elements in the sections stained with H&E were recorded in canine cases[9], where as extensive necrosis with unstained tubuliform structure without any eosinophilic infiltration around the fungal hyphae were recorded in the current case.

Some authors have suggested that the histological lesions of pythiosis in dogs were very comparable to those seen in the infections caused by other oomycetes and zygomycetes[14]. Therefore, other diagnostic methods should be considered, including culture, immunohistochemistry, serological tests and DNA amplification using PCR[2]. Ultrasound and X-ray examination were used to evaluate the intestinal lesions and the wall thicknesses exceeding 7 mm in the stomach and 5 mm in the small intestine are considered pathological[15,16]. In immunohistochemistry, hyphae give strong immune reactivity to a polyclonal anti-*Pythium insidiosum* antibody in the cutaneous and intestinal lesions[14]. Another differentiating feature is the diameter of fungal hyphae in the tissue sections. The hyphae diameter of *Pythyium insidiosum* is ranging from 5-7 micron[7] whereas zygomycete fungi diameter ranging from 7-25 micron[10]. In the present case the diameter of fungal hyphae was 4-6 micron. Using antifungal drugs and surgical removal of masses have shown good results in some cases[17].

Based on the histological, histochemical and morphological analysis this case was confirmed as gastro intestinal pythiosis in a dog.

## REFERENCES


1. Berryessa NA, Marks SL, Pesavento PA, Krasnansky T, Yoshimoto SK, Johnson EG and Grooters AM. 2008. Gastrointestinal Pythiosis in 10 Dogs from California. *J Vet Intern Med* **22:** 1065-1069.
2. Gaastra W, Lipman LJA, de Cock AWAM, Exel TK and Pegge RBG. 2010. Pythium insidiosum: An overview. *Vet Microbiol* **146:** 1-2.
3. Hensel P, Greene CE, Meleau L, Latimer KS and Mendoza L. 2003. Immunotherapy for treatment of multicentric cutaneous pythiosis in a dog. *J Am Vet Med Assoc* **223:** 215-8.
4. Fischer JR, Pace LW, Turk JR, Kreeger JM, Miller MA and Gosser HS. 1994. Gastro-intestinal pythiosis in Missouri dogs: eleven cases. *J Vet Diagn Invest* **6:** 380-2.
5. Miller R. 1983. Investigation into the biology of the three phycomycotic agents pathogenic for horses in Australia. *Mycopathol* **81:** 23-8.
6. Rodrigues A, Graça DL, Fontoura C, Cavalheiro AS, Henzel A, Schwendler SE, Alves SH and Santurio JM. 2006. Intestinal dog pythiosis in Brazil. *J Mycol Med* **16:** 37-41.
7. Miller RI. 1985. Gastro-intestinal phycomycosis in 63 dogs. *J Am Vet Med Assoc* **186:** 473-8.
8. Foil CSO, Short BG, Fadok VA and Kunkle GA. 1984. A report of subcutaneous pythiosis in five dogs and a review of the etiologic agent Pythium spp. *J Am Anim Hosp Assoc* **20:** 959-966.
9. Reis Jr JL, de Carvalho ECQ, Nogueira RHG, Lemos LS and Mendoza L. 2003. Disseminated pythiosis in three horses. *Vet Microbiol* **96:** 289-295.
10. Grooters AM. 2003. Pythiosis, lagenidiosis, and zygomycosis in small animals. *Vet Clin Small Anim* **33:** 695-720.
11. Yolanda H and Krajaejun T. 2022. Global distribution and clinical features of pythiosis in humans and animals. *J Fungi* **8:** 182.
12. Rani RU, Arun R, Sowbharenya C, Vishnurahav VB, Arulanan-

dam K and Pazhanivel N. 2023. Clinicopathological findings of intestinal granulomatous pythiosis in a dog. *Indian J Vet Pathol* **47:** 253-256.
13. Martins T, Kommers G, Trost M, Inkelmann M, Fighera R and Schild A. 2012. Comparative study of the histopathology and immunohistochemistry of pythiosis in horses, dogs and cattle. *J Comp Pathol* **146:** 122-131.
14. Pereira DIB, Schild AL, Motta MA, Fighera RA, Sallis ESV and Marcolongo-Pereira C. 2010. Cutaneous and gastrointestinal pythiosis in a dog in Brazil. *Vet Res Commun* **34:** 301-306.
15. Fernandesa CPM, Giordania C, Greccob FB, Sallisb ESV, Stainkic DR, Gasparc LFJ, Ribeiroc CLG and Nobre MO. 2012. Gastric pythiosis in a dog. *Rev Iberoam Micol* **29:** 235-23.
16. Graham JP, Newell SM, Roberts GD and Lester NV. 2000. Ultrasonographic features of canine gastrointestinal pythiosis. *Vet Radiol Ultra* **41:** 273-277.
17. Pereira DI, Botton SA, Azevedo MI, Motta MA, Lobo RR, Soares MP, Fonseca AO, Jesus FP, Alves SH and Santurio JM. 2013. Canine gastrointestinal pythiosis treatment by combined antifungal and immunotherapy and review of published studies. *Mycopathol* **176:** 309-315.

*Indian J. Vet. Pathol., 49(2) : 179-182, 2025: DOI: https://doi.org/10.56093/614tq023*

SHORT COMMUNICATION

# Pathology and molecular characterization of Inclusion Body Hepatitis-Hydropericardium Syndrome complicated with coccidiosis in broilers: A report

**Sukirti Sharma, S. Chaitanya, Madhuri Hedau*, Jaya Singh, Megha Kaore and P.M. Sonkusale**
Department of Veterinary Pathology, Nagpur Veterinary College, Maharashtra Animal and Fishery Sciences University, Nagpur-440 006, Maharashtra, India

**Address for Correspondence**
*Madhuri Hedau, Department of Veterinary Pathology, Nagpur Veterinary College, Maharashtra Animal and Fishery Sciences University, Nagpur-440 006, Maharashtra, India,E-mail: drmshedau1@gmail.com*

*Received: 21.3.2025; Accepted: 9.4.2025*

## ABSTRACT

Inclusion body hepatitis (IBH) is a viral disease caused by Fowl adenovirus (FAdV) affecting poultry mainly, broilers. IBH has a worldwide distribution and is endemic in many states of India. Present investigation was carried out on a flock of 27 days old commercial broiler chickens from the Nagpur region with history of yellow mucoid to red diarrhea and an overall mortality of 25%. Grossly, liver revealed pale colour, friable with pinpoint to ecchymotic haemorrhages and necrotic foci. Microscopically, the liver revealed hepatic degeneration with intranuclear dense basophilic inclusion bodies, vacuolation, and rounding of hepatocytes and hemorrhages. The collected samples were screened for the hexon gene of fowl adenovirus through PCR. Phylogenetic analysis revealed that the current FAdV is closely related to the strain isolated from Pantnagar, India.

**Keywords:** Broiler, coccidiosis, IBH, molecular characterization, pathology, PCR

Fowl adenovirus is known to cause important diseases in poultry birds such as inclusion body hepatitis, hepatitis hydropericardium syndrome, and gizzard erosion and ulceration[1]. Among these conditions, Inclusion body hepatitis has a worldwide distribution and is endemic in many states of India[2]. FAdV has 5 species A to E and 12 serotypes[3]. All 12 serotypes of the group-I FAdVs have been incriminated in the field outbreaks of IBH-HPS, however, FAdV serotype 4 (FAdV-4) had been mostly implicated. Inclusion body hepatitis is characterized by sudden onset of mortality, severe anemia and enlarged, pale, friable fatty liver with hemorrhages with basophilic or eosinophilic intranuclear inclusion bodies in hepatocytes. In recent years, IBH-HPS has become one of the more common impediments with mortality ranging from 10-30% by virulent strains[4]. Coccidiosis, on the other hand, is associated with poor management practices and results in economic losses due to hemorrhagic enteritis. This case report describes the pathology and molecular characterization of IBH-HPS complicated with coccidiosis in broilers.

Ten numbers of 27 days old commercial broiler chickens from the Nagpur region were brought for post-mortem examination to the Department of Veterinary Pathology, Nagpur Veterinary College, Nagpur during March 2023. The flock had a history of yellow mucoid to red diarrhea and an overall mortality of 25%. A detailed post-mortem examination was conducted. Tissues comprising the liver, kidney, heart, intestine, pancreas, spleen and bursa were collected for histopathological examination in 10% neutral buffered formalin. The samples of liver were stored at -20$^{O}$C for molecular detection of Fowl Adenovirus-I. After fixation, these tissues were processed using xylene and alcohol followed by impregnation in paraffin wax (Qualigens) as per routine method and 5µ sections were cut and stained with H&E stain for recording histopathological observations under light microscopy (Nikon)[5]. The genomic DNA from the liver was isolated using Hi-media DNA purification kit as per manufacturer's protocol. The hexon gene was amplified using published forward primer F-CAARTTCAGRCAGACGT and reverse primer R-TAGTGATGCGSGACATCAT[6]. PCR reaction of 20 µl containing 10 µl of 2X master mix (Promega, USA), 1µl each of forward and reverse primers (10 pmol), 3µl of DNA, and 5µl of Nuclease free water was set for amplification of hexon gene. PCR was performed in an automated thermal cycler (Hi-media) under following conditions: initial denaturation at 95$^{O}$C for 5 min, followed by 30 cycles of denaturation at 94$^{O}$C for 45 sec, annealing at 60$^{O}$C for 1 min and extension at 72$^{O}$C for 1 min. Final extension was conducted at 72$^{O}$C for 10 min. A volume of 10 µl of the PCR product was separated in 1% agarose gel

**How to cite this article :** Sharma, S., Chaitanya, S., Hedau, M., Singh, J., Kaore, M. and Sonkusale, P.M. 2025. Pathology and molecular characterization of Inclusion Body Hepatitis-Hydropericardium Syndrome complicated with coccidiosis in broilers: A report. Indian J. Vet. Pathol., 49(2) : 179-182.

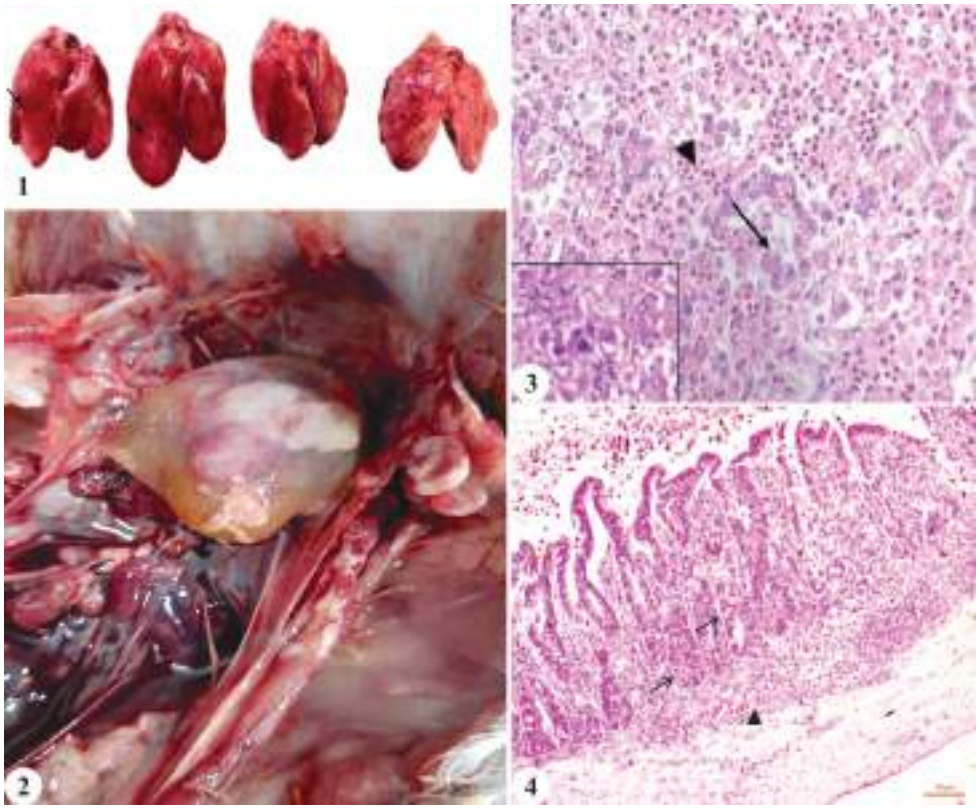


**Fig. 1.** Enlarged pale liver with haemorrhages and necrotic foci; **Fig. 2.** Hydropericardium; **Fig. 3.** Basophilic inclusion bodies inside hepatocytes (inset) and hepatic degeneration (H&E x200); **Fig. 4.** Sporocysts of coccidia in intestinal mucosa (H&E x200).

by electrophoresis. PCR amplicons of the hexon gene segments of the pathogen was sequenced commercially. The gene segments were trimmed and contig sequences were prepared in Bioedit software. These contig sequences were aligned and the phylogenetic tree was constructed using the Neighbor-joining method using Kimura 2 parameter model using MEGA 7 software[7]. The sequence was submitted in GenBank having accession number OR858637.

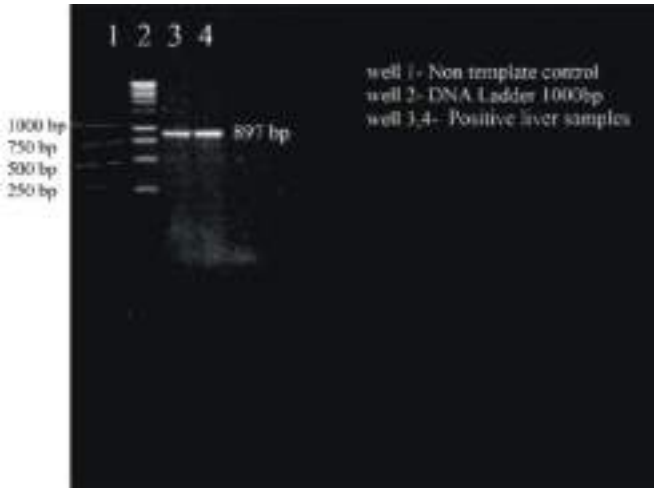


**Fig. 5.** Gel electrophoresis of hexon gene of fowl adenovirus. Lane 1: Non Template Control; Lane 2: Ladder; Lane 3 & 4: Sample.

Grossly, on post mortem, liver revealed pale colour, friable with pinpoint to ecchymotic haemorrhages and necrotic foci (Fig. 1). The heart revealed hydropericardium, and erosions of mucosa in gizzard, congested, enlarged, and mottled kidneys and haemorrhagic typhlitis was also observed (Fig. 2). Moreover, the spleens were slightly enlarged and had necrotic foci and the pancreas was swollen and had hemorrhagic spots.

Microscopically, the liver revealed hepatic degeneration with intranuclear dense basophilic inclusion bodies, vacuolation and rounding of hepatocytes and hemorrhages (Fig. 3). Degenerative changes along with lymphocytic infiltration in cardiac muscle were observed. Kidneys revealed tubular necrosis along with hemorrhages. Loss of acinar arrangement and shrinkage of acinar cells was evident in the pancreas. Caecum revealed numerous developmental stages of *Eimeria spp*. in mucosa along with hemorrhages in muscularies layer (Fig. 4). Microscopic examination of intestinal scrapping revealed oocysts of *coccidia spp.* in a wet smear at 200x magnification.

The primer specific for hexon gene of fowl adenovirus yielded amplicons of 897 bp (Fig. 5). The BLAST hit result of the nucleotide sequence revealed the closest identity of the isolate with IBH previously isolated in India (Fowl adenovirus D isolate Pantnagar/H-15/R-37/Hexon protein

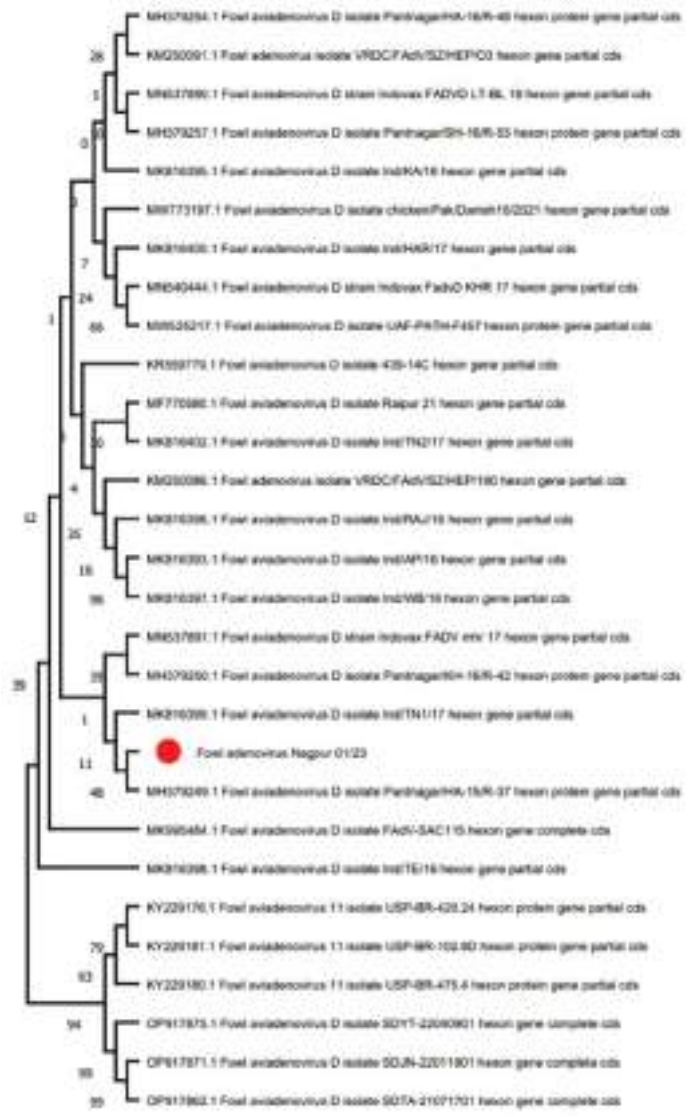


**Fig. 6.** Phylogenetic tree of nucleotide sequences of the hexon gene of PCR fragments of fowl adenovirus.

gene; MH379249) (Fig. 6).

IBH outbreaks caused by different FAdV serotypes have been described in different countries including India in recent years[8]. IBH can affect broilers of all ages, young chicks are found to be more susceptible during the first two weeks. There is a clear age effect with avian adenoviruses, as the age of the host increases, the degree of multiplication of the viruses within the host is restricted and the mortality decreases[9]. In this study, mortality of about 25% started at 24$^{th}$ day of age and peaked at 27$^{th}$ day in affected broilers. Mortality during IBH outbreaks is normally between 2% and 10% of the flock, but up to 30% has been described in case of co-infection with other immunosuppressive agents[10]. In the present study, coccidiosis was also evident which can easily occur in birds with concurrent disease further worsening the economics of farms.

The gross lesions observed in this study like pale, friable liver with pinpoint to ecchymotic haemorrhages and necrotic fociare characteristic of adenoviral infection. Hydropericardium, and erosions of mucosa in gizzard, congested, enlarged, and mottled kidneys were described by many researchers before and correlated with affection of the liver primarily, which results in decreased liver function and thus decreased protein synthesis leading to hydropericardium[11,12].

The reported disease outbreak in broiler birds was diagnosed as inclusion body hepatitis-hydropericardium syndrome complicated with coccidiosis. The strain, causing the disease was phylogenetically closely related to the Indian strain from Pantnagar. More data is required to know the molecular epidemiology of the fowl adenovirus in central India. Understanding the genetic background of circulating fowl adenoviral strains in India will help to formulate control strategies using vaccines and/or the use of therapeutics. These results indicated that preventive measures against FAdV infection on poultry farms should be implemented.

## REFERENCES


1. Cizmecigil UY, Umar S, Yilmaz A, Bayraktar E, Turan N, Tali B, Aydin O, Tali HE, Yaramanoglu M, Yilmaz SG and Kolukisa A. 2020. Characterization of fowl adenovirus (FAdV-8b) strain concerning the geographic analysis and pathological lesions associated with inclusion body hepatitis in broiler flocks in Turkey. *J Vet Res* **64:** 231.
2. Kataria JM, Dhama K, Nagarajan S, Chakraborty S, Kaushal A and Deb R. 2013. Fowl adenoviruses causing hydropericardium syndrome in poultry. *Adv Anim & Vet Sci* **1:** 5-13.
3. Harrach B, Benko M, Both G, Brown M, Davison A, Echavarria M, Hess M, Jones M, Kajon A and Lehmkuhl H. 2012. Virus taxonomy: Family Adenoviridae: Classification and Nomenclature of Viruses. Ninth Report of the International Committee on Taxonomy of Viruses. Elsevier; Amsterdam, The Netherlands 125-141.
4. Hafez MH. 2011. Avian adenoviruses infections with special attention to the inclusion body hepatitis/hydropericardium syndrome and egg drop syndrome. *Pak Vet J* **31:** 85-92.
5. Luna LG. 1968. Manual of histological staining methods of the Armed Forced Institute of Pathology, 3$^{rd}$ ed. McGraw Hill book Co, London: 124-125.
6. Meulemans G, Boschmans M, Van den Berg TP and Decaesstecker M. 2001. Polymerase chain reaction combined with restriction enzyme analysis for detection and differentiation of fowl adenoviruses. *Avian Pathol* **30:** 655-660.
7. Sudhir K, Glen S and Koichiro T. 2015. Molecular Evolutionary Genetics Analysis version 7.0. Molecular Biology and Evolution.
8. Thakor KB, Dave CJ, Fefar DT, Jivani BM and Prajapati KS. 2012. Pathological and molecular diagnosis of naturally occurring inclusion body hepatitis-hydropericardium syndrome in broiler chickens. *Indian J Vet Pathol* **36:** 212-216.

9. Rahimi M and Haghighi ZMS. 2015. Adenovirus-like inclusion body hepatitis in a flock of broiler chickens in Kermanshah province, Iran. *Vet Res Forum* **6:** 95-98.
10. Schachner A, Matos M, Grafl B and Hess M. 2018. Fowl adenovirus-induced diseases and strategies for their control-a review on the current global situation. *Avian Pathol* **47:** 111-126.
11. Philippe C, Grgic H and Nagy E. 2005. Inclusion body hepatitis in young broiler breeders associated with a serotype 2 adenovirus in Ontario, Canada. *J Appl Poult Res* **14:** 588-593.
12. Sawale GK, Gupta SC, Srivastava PK, Sabale SS, Ingole KH, Pawale NH and More BK. 2012. Inclusion body hepatitis-hydropericardium syndrome in commercial broiler chickens. *Indian J Vet Pathol* **36:** 255-257.

*Indian J. Vet. Pathol., 49(2) : 183-184, 2025: DOI: https://doi.org/10.56093/135g9q93*

CASE REPORT

# Onchocercosis in aorta of cattle - A case report

**D. Harshitha*, P. Amaravathi, N. Sailaja, K. Lakshmi Kavitha[1] and A. Anand Kumar**
Department of Veterinary Pathology, College of Veterinary Science, Sri Venkateswara Veterinary University, Tirupati -517 502, Andhra Pradesh, India, [1]Department of Veterinary Microbiology

**Address for Correspondence**
*D. Harshitha, Department of Veterinary Pathology, College of Veterinary Science, Sri Venkateswara Veterinary University, Tirupati-517 502, Andhra Pradesh, India, E-mail: harshithareddy24999@gmail.com*

*Received: 10.12.2024; Accepted: 3.1.2025*

## ABSTRACT

Ten years old cattle carcass was brought for post mortem examination to the Department of Veterinary Pathology, College of Veterinary Science, Tirupati. On necropsy, the aorta showed whitish, hard, elevated areas of irregular shape and varied sizes with 0.5-1 mm diameter. Histopathologically, aorta revealed cut sections of the worms in the tunica media with calcification and eosinophils infiltration surrounding the cut sections were noticed. Based on the gross and histological examination it was confirmed as Onchocercosis in cattle.

**Keywords:** Aorta, calcification, cattle, onchocercosis

Parasitic diseases in cattle are a major concern for the livestock industry, as they can lead to significant economic losses, reduced productivity, and compromised animal welfare. There are several external and internal parasites which affects cattle health. One such internal parasite is the Onchocerca. Onchocerciasis is a parasitic disease caused by a nematode Onchocerca that affects both animals and humans[1]. It is found residing in the aortic walls of the cattle[2,3], buffalo[4], sheep[4], goat[5] and camels[6]. It is also noted in other vessels like brachiocephalic truncus, brachial and cervical arteries and iliac bifurcation of abdominal aorta[2,7]. However, it also affects brain, tendons, skin, testis as well as mammary glands[7]. *Onchocerca armillata* is commonly reported in the southern parts of Asia and Africa[7,8]. The affected animals does not show any prominent clinical symptoms[1]. Grossly the aorta shows nodules, thickening of intimal layers, parasitic tunnels[2]. The eosinophils infiltration is noted surrounding dead parasites or calcified larvae in the granulomatous nodules[7,9]. In aged animals, nodules that are calcified may lead to aneurysms[1,9].

During necropsy, the lesions in aorta were observed and tissue sample of aorta was collected and fixed in 10% neutral buffered formalin. Collected tissues were dehydrated by passing through ascending grades of alcohol, cleared by using xylene and embedded in paraffin. The paraffin embedded blocks were sectioned around 4-6 micron thickness and sections were stained with hematoxylin and eosin and Von kossa's stain[10].

On gross examination, the aorta showed irregular, reddish elevated areas of 0.5-1 cm in diameter in the intima (Fig. 1). These observations were similar to the findings of earlier authors[9,11,12]. The aorta was thickened and flexibility was not observed which may interfere with circulatory functions in the body[13]. Histologically, aorta revealed irregular, large cut sections of the parasite with thin layer of connective tissue in tunica intima and few cut sections of parasite were noted in tunica media (Fig. 2). These findings were in close proximation with earlier workers[8,14]. Some had small round eggs while some had degenerated worms[8]. The surrounding areas of the cut sections of parasite had irregular, bluish areas and infiltration of the eosinophils were predominantly noted along with few mononuclear cells (Fig. 3). These findings were in accordance with the earlier studies[8]. Hyalinization of the smooth muscle cells were also noted. Von kossa's staining revealed black coloured deposits around cut sections of the parasite (Fig. 4). The age of the host and weather conditions are the important determinants for occurrence of the disease[15]. Based on gross and microscopic examination of the aorta the present case was diagnosed as onchocercosis.

**How to cite this article :** Harshitha, D., Amaravathi, P., Sailaja, N., Kavitha, K.L. and Kumar, A.A. 2025. Onchocercosis in aorta of cattle - A case report. Indian J. Vet. Pathol., 49(2) : 183-184.

## ACKNOWLEDGEMENT

I thank the Sri Venkateswara Veterinary University, Tirupati for providing the facilities to carry out the research work.

## REFERENCES

1. Aditi K, Ashok P, Rohit J, Induvyas and Dharampal. 2024. Occurrence and pathology of various parasitic conditions in cattle in Bikaner (Bos indicus). *Int J Vet Sci & Anim Hus* **9:** 301-303.
2. Alibaşoğlu M, Gölesuk K, Erturk E and Güler S. Türkiyedesığırlard-agörülen onchocerciasis olayları (*Onchocerca armillata* Railletve

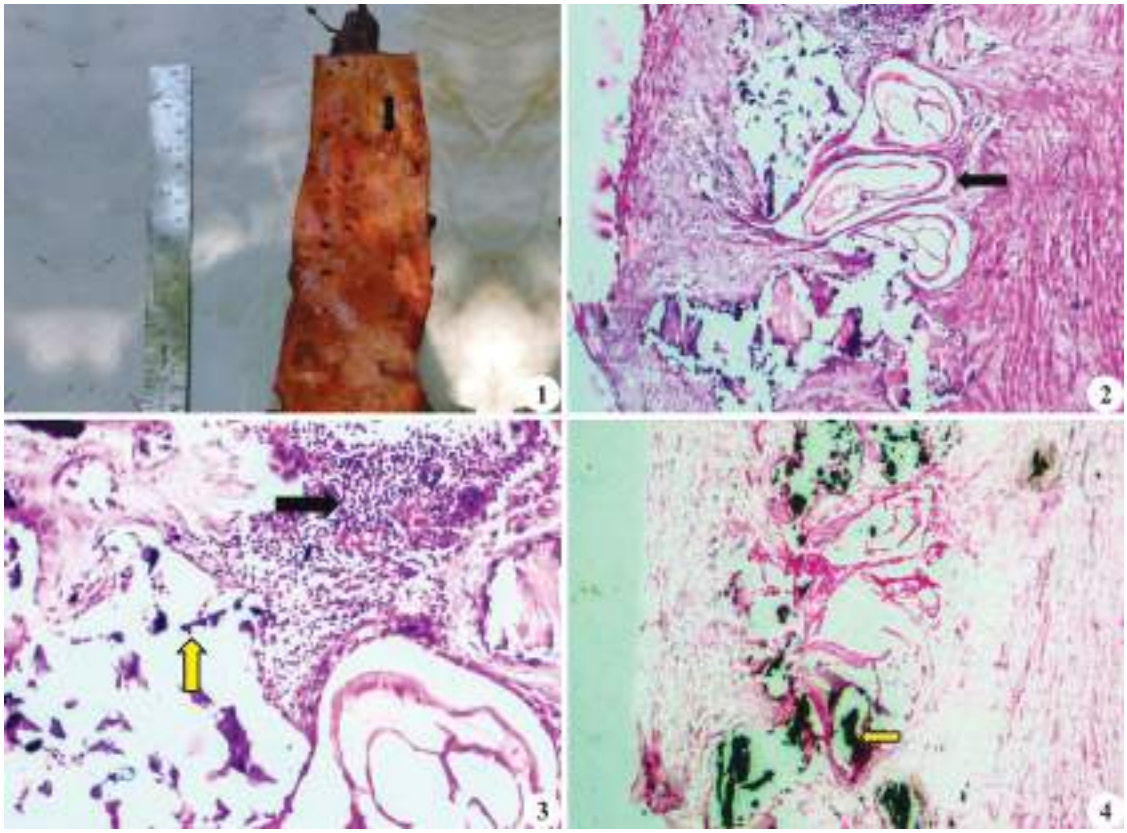

**Fig. 1.** Aorta showing 0.5-1 cm diameter, irregular, elevated areas in intimal surface (arrow); **Fig. 2.** Cut sections of the parasite with degenerated worms in the tunica media of aorta (arrow) (H&E x40); **Fig. 3.** Tunica media showing calcified areas (yellow arrow) and severe infiltration of eosinophils (black arrow) surrounding parasitic cut section (H&E x400); **Fig. 4.** Note black coloured calcium deposits surrounding cut sections of parasite in tunica media of aorta (arrow) (Von kossa's stain x40).


Henry 1909). 1969. *Ankara Üniv Vet Fak Derg* **16:** 50-60.

3. Wildenburg G, Kromer M and Buttner DW. 1996. Dependence of eosinophil granulocyte infiltration into nodules on the presence of microfilariae producing Onchocerca volvulus. *Parasitol Res* **82:** 117-124.
4. Bhatia BB. 1960. *Onchocerca armillata* Railliet and Henry 1909, a study of the infection in Indian sheep with remarks on its bovine hosts. *Ind Vet J* **37:** 394-397.
5. Chowdhury N and Chakraborty RL. 1973. On concurrent and early aortic Onchocerciasis and Spirocerciasis in domestic goats *(Capra hircus)*. *Z Parasitenkunde* **42:** 207-212.
6. Oryan A, Valinezhad A and Bahrami S. 2008. Prevalence and pathology of camel filariasis in Iran. *Parasitol Res* **103:** 1125-1131.
7. Maxie MG and Youssef S. 2007. Diseases of the vascular system. In, Maxie MG, Robinson WF (Eds): Jubb, Kennedy and Palmer's Pathology of Domestic Animals. *Elsevier Science Publishing*, Inc **3:** 91-92.
8. Ogundipe GA, Ogunrinade AF and Akpavie SO. 1984. The prevalence, gross lesions and histopathology of aortic onchocerciasis in Nigerian cattle. *Vet Q* **6:** 85-89.
9. Cheema AH and Ivochli B. 1978. Bovine onchocerciasis caused by *O. armillata* and *O. gutturosa*. *Vet Pathol* **15:** 495-505.
10. Luna LG. 1968. Manual of Histological Staining Methods of the Armed Forces Institute of Pathology.
11. Chodnik KS. 1957. Aortic onchocerciasis due to *Onchocerca armillata* in cattle in Ghana with special references to morphology of the parasite. *Ann Trop Med Parasit* **51:** 216-24.
12. Chodnik KS. 1958. Histopathology of aortic lesions in cattle infected with *Onchocerca armillata* (Filariidae). *Ann Trop Med Parasit* **52:** 145-48.
13. Schillhorn van Veen T and Robl MG. 1975. Aortic onchocercosis in cattle in Zaria. *Pays Trp* **28:** 305-310.
14. SY O and IA O. 2013. Parasitic aortitis due to *Onchocerca armillata* in slaughtered cattle in the southeastern region of Turkey. *Kafkas Üniversitesi Veteriner Fakültesi Dergisi* **19:** 589-594.
15. Asaduzzaman M, Mamun MAA, Anisuzzaman M, Alim MA, Yasin MG and Begum N. 2015. Epidemiology and pathology of onchocerciasis of cattle in Bangladesh. *Progress Agri* **26:** 147 -154.

*Indian J. Vet. Pathol., 49(2) : 185-187, 2025: DOI: https://doi.org/10.56093/ce4msg72*

CASE REPORT

# A rare case of cystic renal cell carcinoma in a sheep

**H. Srinivasa Naik, S.D. Koushar Sahara*, C. Jyothi, C. Yugandhar and V. Gnani Charitha[1]**
Department of Veterinary Pathology, College of Veterinary Science, Proddatur, Sri Venkateswara Veterinary University, Tirupati, [1]Department of Veterinary Parasitology, College of Veterinary Science, Proddatur

**Address for Correspondence**
*S.D. Koushar Sahara, Department of Veterinary Pathology, College of Veterinary Science, Proddatur, Sri Venkateswara Veterinary University, Tirupati, India, E-mail: kousharsahara111@gmail.com*

*Received: 21.3.2025; Accepted: 15.4.2025*

## ABSTRACT

An eight-month-old ram lamb was presented to the Department of Veterinary Pathology, College of Veterinary Science, Proddatur, for necropsy with the history of anorexia, dyspnea, lethargy and emaciation. The post-mortem examination revealed clear serous fluid in the abdominal cavity, pale liver with a distended gall bladder, and enlarged, pale, pulpy kidneys with multi focal white necrotic areas on their surface. Cytological evaluation of kidney impression smears showed clusters of cuboidal epithelial cells, along with degenerative neutrophils, lymphocytes, and a few bipolar microorganisms. The neoplastic epithelial cells exhibited anisocytosis, homogenous bluish cytoplasm and large, pleomorphic nuclei with 3-5 prominent nucleoli. Mitotic figures were observed in the nuclei. Additionally, a few macrophages and multinucleated cells were found within the neoplastic clusters. Histopathological examination revealed diffusely dilated and cystic tubules, proliferation of tubular epithelial cells, infiltration of lymphocytes and degenerated neutrophils. Focal areas of glomerular dilatation were also observed. The tubular epithelial cells appeared polygonal to cuboidal, with basophilic cytoplasm and pleomorphic, dense nuclei containing prominent nucleoli. A few mitotic figures were also noted. Based on the gross, cytological and histopathological findings, the case was diagnosed as "Cystic Renal Cell Carcinoma" which is a rare neoplasm in sheep.

**Keywords:** Carcinoma, kidneys, renal cell carcinoma, sheep

Primary renal neoplasms have been documented in both animals and humans. These tumors are typically classified based on their origin into four categories: epithelial tumors of the renal parenchyma, epithelial tumors of the renal pelvis, nephroblastic tumors and mesenchymal tumors. They can be further categorized by predominant histological patterns; such as solid, tubular, or papillary type. According to their cytological characteristics, they may be clear cell, granular eosinophilic or basophilic and either cuboidal or columnar. The prevalence of primary renal neoplasm in domestic animals is less than one percent of total neoplasm reported. They are usually unilateral and can be of epithelial, mesenchymal or embryonic origin. Adenocarcinoma of the kidney arises from renal tubular epithelium[1]. While some tumors exhibit uniform characteristics, it is common to observe multiple histological patterns within different areas of the same tumor. Among these neoplasms, renal adenocarcinomas are the most prevalent (89%), followed by nephroblastomas (9%) and sarcomas (2%). Most primary tumors are epithelial and they are largely reported as benign in cattle[2] and malignant in horses[3]. Naturally occurring renal adenocarcinomas are quite rare in lower animals but have been reported in rats, mice, guinea pigs, rabbits, monkeys, sheep, cows, pigs, dogs, horses, various fowl and fish[4]. Renal carcinomas are the most common primary renal neoplasm and occur most frequently in older dogs and occasionally in sheep, they must be distinguished from metastatic tumor nodules[1,5]. However, in laboratory animals renal adenocarcinomas are readily induced by a variety of carcinogens including chemical, physical, and viral agents. Although hormones (estrogens) have not been used successfully to induce renal adenocarcinoma in species other than hamsters[6]. Renal carcinomas are the most common primary renal neoplasm and occur most frequently in older dogs[7]. The Ecker rat is a useful model for hereditary renal cell carcinoma[2]. immunosuppression in solid-organ-transplant recipients and obesity have been identified as risk factors for renal cell carcinoma[8]. The purpose of this report is to provide gross, cytology and histopathological descriptions of renal cell carcinoma in Sheep.

**How to cite this article :** Naik, H.S., Sahara, S.D.K., Jyothi, C., Yugandhar, C. and Charitha, V.G. 2025. A rare case of cystic renal cell carcinoma in a sheep. Indian J. Vet. Pathol., 49(2) : 185-187.

An eight-month-old ram lamb was presented to the Department of Veterinary Pathology, College of Veterinary Science, Proddatur, for necropsy following a history of anorexia, dyspnea, lethargy and emaciation. Detailed postmortem was conducted and recorded all gross abnormalities, taken tissue imprints for cytological examination, collected representative tissue pieces in 10% buffered formalin and processed as per the standard histopathological procedure for histopathological examination[8]. Formalin-fixed tissues were embedded in paraffin, sectioned

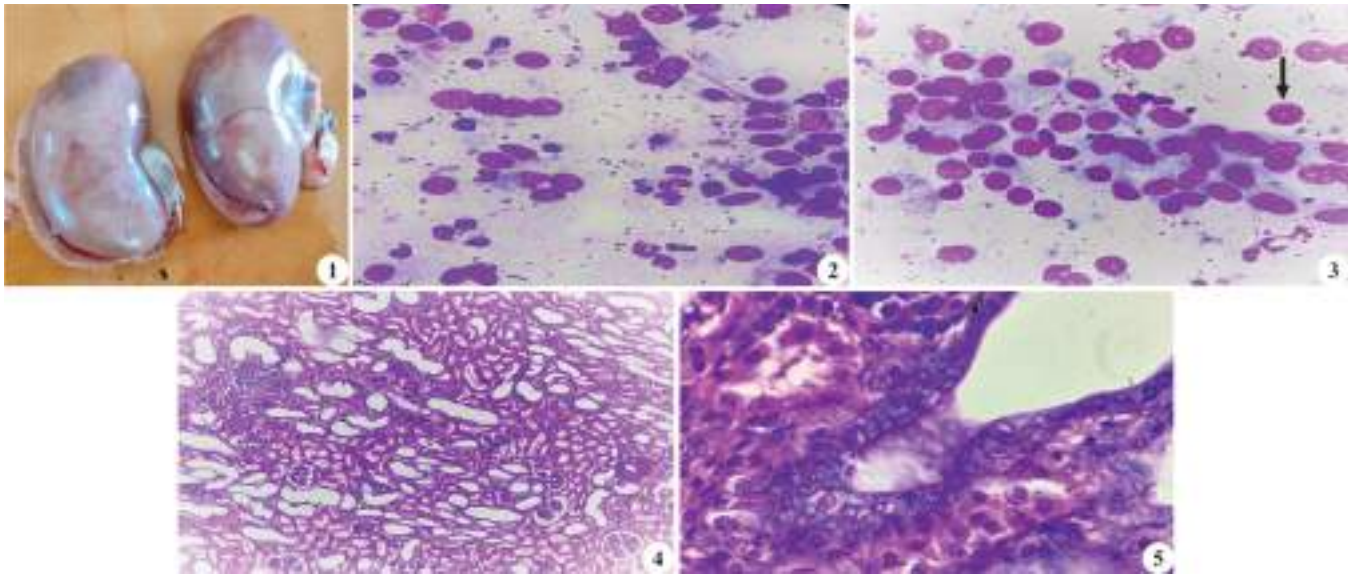

**Fig. 1.** Pale, enlarged pulpy kidneys showing small circumscribed multiple white foci on the surface of the kidney; **Fig. 2.** Cluster of cuboidal epithelial cells along with degenerative neutrophils, lymphocytes, and a few bipolar microorganisms (Giemsa Stain X100); **Fig. 3.** Neoplastic epithelial cells showing anisocytosis, with fairly homogenous bluish cytoplasm, and large, pleomorphic nuclei with 3-5 prominent dark stained nucleoli, and mitotic figures (Giemsa Stain X100); **Fig. 4.** Cystic dilatation of tubules along with proliferation of tubular epithelial cells and dilated glomeruli (H&E X10); **Fig. 5.** Tubular neoplastic epithelial cells showing anisocytosis, with fairly homogenous bluish cytoplasm, and large, pleomorphic nuclei with 3-5 prominent dark stained nucleoli, and mitotic figures (H&E X100).

at 5 μm, stained with Giemsa, examined under light microscopy. Serous fluid from abdominal cavity & 10 ml of urine sample from urinary bladder were collected for further investigation.

The post-mortem examination revealed 500 ml of clear serous fluid in the abdominal cavity. The liver was pale with a distended gall bladder, while the kidneys were enlarged, pale, pulpy with multifocal white necrotic areas on the surface (Fig. 1)[1]. The heart appeared pale, with empty chambers. Both lungs were mildly congested with frothy fluid on cut section of bronchi and bronchioles. The rumen was mildly distended with feed content. No abnormalities were detected in the genital organs, brain or spinal cord. Pale subcutaneous fat was noted. Cytological evaluation of kidney impression smears showed clusters of neoplastic cuboidal epithelial cells, along with degenerative neutrophils, lymphocytes, and a few bipolar microorganisms[3] (Fig. 2). The neoplastic epithelial cells exhibited anisocytosis, with fairly homogenous bluish cytoplasm large, pleomorphic nuclei with 3-5 prominent dark-stained nucleoli and mitotic figures[1,3] (Fig. 3). Histopathological examination of kidney revealed diffusely dilated and cystic tubules, proliferation of tubular epithelial cells, infiltration of lymphocytes and degenerated neutrophils[3] (Fig. 4). Focal areas of glomerular dilatation were also observed. The tubular epithelial cells appeared polygonal to cuboidal with basophilic cytoplasm and pleomorphic, dense nuclei containing prominent nucleoli[3] (Fig. 5). Cell morphology varied from cuboidal, columnar to polyhedral with clear or granular eosinophilic cytoplasm[1]. Nuclei ranged from small, round, and granular to large, oval, vesicular, and pleomorphic. Neoplastic renal parenchyma showed a moderate fibrovascular stroma[1]. The liver showed central venous congestion. Mild pneumonic changes observed in lungs with no evidence of neoplasia. Other organs, including genital organs, brain, rumen, intestines and heart did not show any significant cytological & histopathological changes apart from the kidneys. Urine analysis was negative for glucose. Known causes of renal cell carcinomas in animals include chemical carcinogens such as nitrosamines, nitrosureas, aromatic amines, tri (2,3 dibromopropyl) phosphate, and cadmium[2]. In humans, asbestos, cigarette smoking, coffee consumption, phenacetin and diuretics have been linked to renal cell carcinoma[7]. In cattle, exposure to aflatoxin and lead has been linked to renal carcinoma, both of which are well-documented causes of renal cell carcinoma in rats[2].

Neoplasms in sheep are relatively rare compared to other domestic animals, with most reported cases involving the lymphatic, respiratory, and urinary systems. Commonly observed tumors include enzootic nasal adenocarcinoma, pulmonary adenomatosis (Jaagsiekte), squamous cell carcinoma, lymphosarcoma, and renal cell carcinoma. Among these, enzootic nasal adenocarcinoma and pulmonary adenomatosis are more frequently encountered due to their viral etiology. In contrast, renal cell carcinoma and other epithelial tumors remain rare, often diagnosed incidentally during post-mortem examinations. Environmental factors, genetic

predisposition, and exposure to carcinogens such as aflatoxins and heavy metals may contribute to neoplastic development in sheep. The present case report describes the gross, cytological, and histopathological features of a rare "cystic renal cell carcinoma" in an adult sheep, diagnosed incidentally during post-mortem examination.

## ACKNOWLEDGEMENT

The authors are thankful to the College of Veterinary Science, Sri Venkateswara Veterinary University, Proddatur for providing lab facilities at Department of Veterinary Pathology for carrying above research work.

## REFERENCES

1. Mohajeri D, Ghafour M, Yousef D, Ali R and Asadnasab GHR. 2008. Renal adenocarcinoma in a sheep: surgical and histopathological findings. *Iranian J Vet Surg* **3:** 87-91.
2. Kelley LC, Crowell WA, Puette M, Langheinrich KA and Self AD. 1996. A retrospective study of multicentric bovine renal cell tumors. *Vet Pathol* **33:** 133-141.
3. Sandison AT and Anderson LJ. 1968. Tumors of the kidney in cattle, sheep and pigs. *Cancer* **21:** 727-742.
4. Bennington JL and Kradjian RM. 1967. Renal Carcinoma Philadelphia WB and Saunders Co. 1967.
5. Meuten DJ. (Ed.) 2020. Tumors in domestic animals. John Wiley & Sons. 5th edn. NC USA.
6. Bennington JL. 1973. Cancer of the kidney etiology, epidemiology, and pathology. *Cancer* **32:** 1017-1029.
7. Carlton WW and McGavin MD. 2001. Special veterinary pathology. 3rd edn London: Mosby: 270-275.
8. Mobaraki G, Shi S, Smits KM, Severens K, Lommen K, Rennspiess D and Hausen AZ. 2024. Bovine Meat and Milk Factor-like Sequences Are Frequently Detected in Renal Cell Carcinoma Tissues. *Cancers* **16:** 1746.

*Indian J. Vet. Pathol., 49(2) : 188-191, 2025: DOI: https://doi.org/10.56093/m6nmx749*

CASE REPORT

# Pathological and immunohistochemical characterization of ovarian papillary adenocarcinoma in a spitz dog

**S. Preetha, M. Sasikala*, A. Arulmozhi, A. Kumaresan[1], P. Srinivasan, P. Balachandran, K. Gopal, D. Sumathi[2] and D. Gopikrishnan[3]**

Department of Veterinary Pathology, Veterinary College and Research Institute, Namakkal-637 002, TANUVAS, Tamil Nadu, India, [1]Department of Surgery and Radiology, [2]Department of Veterinary Clinical Medicine, [3]Department of Veterinary Gynaecology and Obstetrics

**Address for Correspondence**

*M. Sasikala, Department of Veterinary Pathology, Veterinary College and Research Institute, Namakkal-637 002, TANUVAS, Tamil Nadu, India, E-mail: vetsasi.pathologist@gmail.com*

*Received: 28.1.2025; Accepted: 2.3.2025*

## ABSTRACT

A case of ovarian papillary adenocarcinoma in a Spitz was reported. Twelve years old female spitz dog was presented to the Veterinary Clinical Complex, Veterinary College and Research Institute, Namakkal with the history of progressive abdominal distension for the past one month. Haematology and serum biochemistry revealed leucocytosis and mild hypercalcemia respectively. Lateral abdominal radiography and transabdominal ultrasonography showed homogenous intra-abdominal mass and irregular mass adjacent to spleen respectively. The computed tomography of abdomen exhibited presence of mass beneath both kidneys extending up to bladder with HU index 60 to 75 suggestive of tumor. The exploratory laparotomy revealed large cauliflower like mass in right ovary and was removed surgically by ovariohysterectomy. The impression smears from the mass showed clusters of cells with indistinct cell border and significant anisokaryosis. Histopathologically, glandular cells were arranged in papillary pattern with irregular branches and the neoplastic cells showed cellular atypia, scanty eosinophilic cytoplasm with hyperchromatic ovoid nuclei. Furthermore, the immunohistochemistry showed moderate to strong expression for pan-cytokeratin and estrogen receptor (ER). Based on histopathology and immunohistochemistry the tumor was confirmed as ovarian papillary adenocarcinoma.

**Keywords:** Dog, histopathology, immunohistochemistry, ovarian adenocarcinoma

Ovarian tumors are most common in bitches and are usually arise from surface epithelium and subepithelial structures of ovaries. The most common epithelial tumors of ovary in canine are papillary adenoma and adenocarcinoma[1]. The ovarian tumors that generally appear as arboriform papillae projecting into the lumen of cystic cavities are subclassified as papillary or cystic adenoma and carcinoma[2]. The clinical features associated with ovarian papillary adenocarcinoma in dogs include ascites, pleural effusion and presence of palpable abdominal mass. Bitches with papillary adenocarcinoma show hormonal imbalances resulting in pyometra and vaginal bleeding[3]. Canine papillary ovarian adenocarcinoma is often associated with extensive peritoneal implantation and formation of malignant effusion[4]. Histopathologically, the ovarian adenocarcinoma is characterized by arrangement of neoplastic epithelial cells in papillary pattern[5]. Immunohistochemical staining provides a more definitive description of morphologically overlapping entities like ovarian epithelial tumors, sex cord-stromal tumours and germ cell tumours[1,6].

The cytokeratin belongs to the family of intermediate filament and are used as the most important marker for the differentiation of various epithelial tumours by immunohistochemistry. Both benign and malignant epithelial tumors show positive immunoreaction for cytokeratin[7,8]. Estrogen from ovaries play a critical role in the regulation of growth and differentiation of normal ovarian follicles and its actions are mediated by estrogen receptor (ER). It is nuclear transcription factors that bind to the estrogen responsive elements present in the target genes and deliver signalling systems for cell division and differentiation. ER expression is seen in 67% of ovarian epithelial tumor cases[9,10,11]. Progesterone is a steroid hormone works together with estrogen and promote follicle maturation, ovulation and corpus luteum formation[10]. Progesterone receptor (PRs) mediates the functions of progesterone and its expression in ovarian tumors, is a good prognostic marker correlated with longer survival period of affected patients[12,13]. The present study was undertaken to unveil the type of tumor and to elucidate the pathology of ovarian adenocarcinoma. Furthermore, the origin of tumor and its hormone dependence

**How to cite this article :** Preetha, S., Sasikala, M., Arulmozhi, A., Kumaresan, A., Srinivasan, P., Balachandran, P., Gopal, K., Sumathi, D. and Gopikrishnan, D. 2025. Pathological and immunohistochemical characterization of ovarian papillary adenocarcinoma in a spitz dog. Indian J. Vet. Pathol., 49(2) : 188-191.

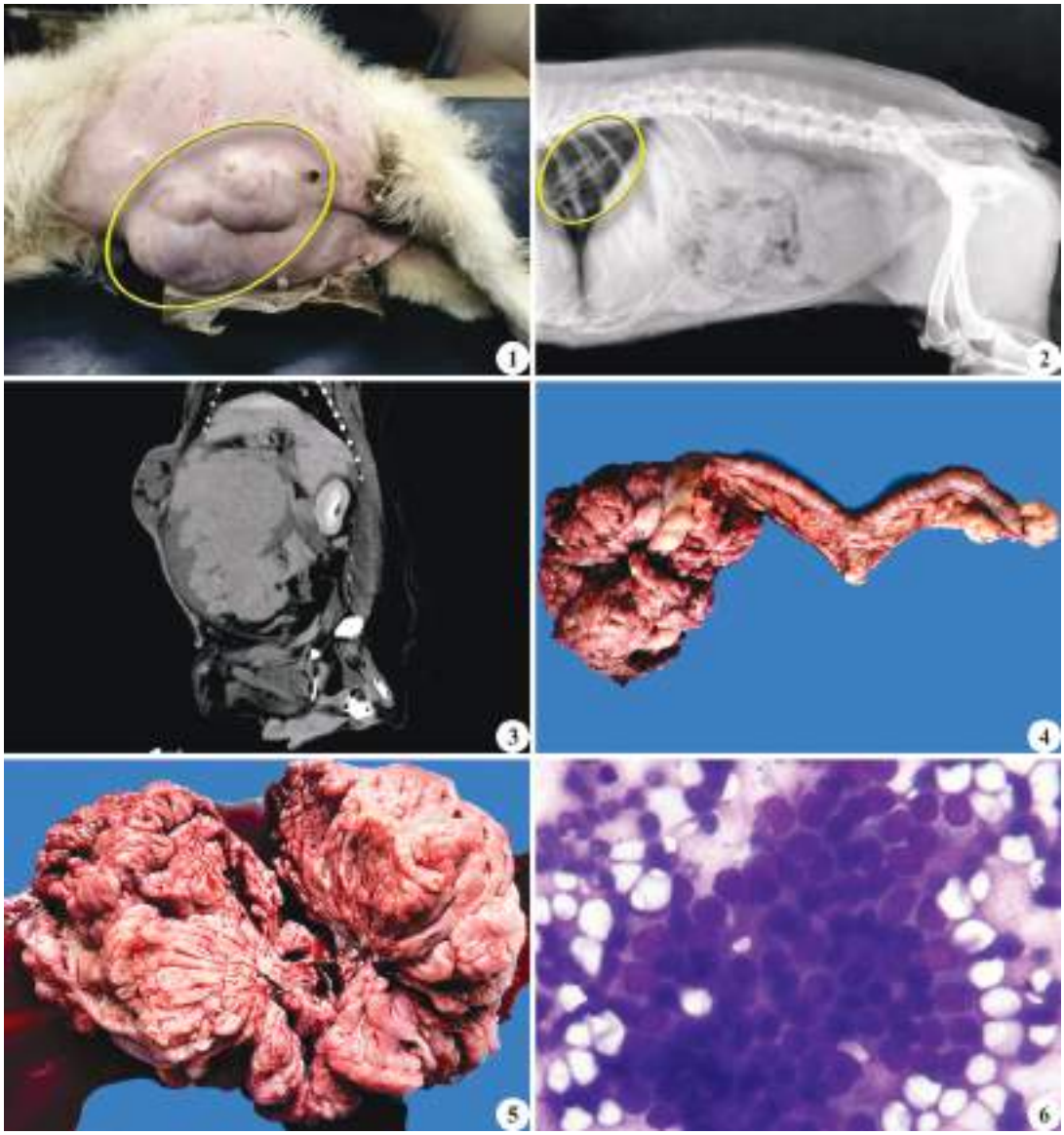

**Fig. 1.** The female spitz dog showing severe abdominal distension; **Fig. 2.** The dog showing radio dense mass caudal to kidney and pulmonary metastases (circle); **Fig. 3.** Computed tomography: Mass beneath both the kidneys extending up to bladder; **Fig. 4.** A huge cauliflower like mass on the right ovary; **Fig. 5.** Cut-section of the tumor mass showing papillary appearance with haemorrhage; **Fig. 6.** Impression smear showing radial arrangement of nuclei with numerous secretory vacuoles and granules in the cytoplasm. (May Grunwald Geimsa x400).

were studied by immunohistochemistry.

A 12 years-old female spitz was presented to the Veterinary clinical complex, Veterinary College & Research Institute, Namakkal with the history of progressive enlargement of ventral abdomen for one month. Detailed clinical examination including abdominal palpation was carried out. Lateral abdominal radiography, abdominal ultrasonography and computed tomography were done to assess the location of the mass and to detect metastasis if any. The blood sample was collected in EDTA coated vacutainer by venipuncture and analysis of blood was done using M/s Rayto RT-7600 haematology analyser, China. Clot activator vials were used for serum samples and biochemical analysis was done using M/s Biosystems A50, India.

Exploratory laparotomy was carried out which revealed presence of huge mass in the right ovary. Ovariohysterectomy was performed to remove the mass surgically and gross morphometry was recorded. Impression smears were taken from the cut surface of the mass and fixed with methanol and stained with Giemsa, May-Grunwald Giemsa and Wright-Giemsa combination for cytological examination. The representative tissue samples from the mass were collected in 10 per cent neutral buffered formalin for histopathology. The tissue samples were processed, embedded in paraffin,

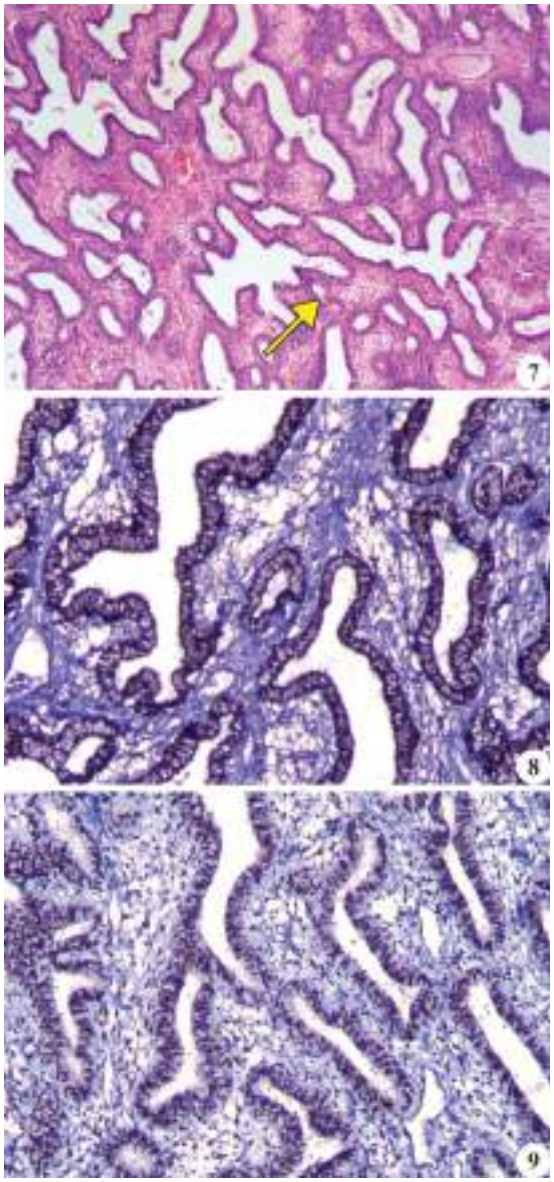

**Fig. 7.** Ovarian mass showing numerous glandular structures with slit like opening and micropapillary growth (arrow) (H&E x40); **Fig. 8.** Papillary ovarian adenocarcinoma showing strong cytoplasmic expression to cytokeratin (IHC AE1/AE3 x100); **Fig. 9.** Papillary ovarian adenocarcinoma showing moderate to strong nuclear expression to estrogen receptor alpha (IHC ER x100).

sectioned at 3-5µm thickness and stained with haematoxylin and eosin (H&E) for histopathological examination.

For immunohistochemistry, the tissue sections were mounted on Poly-L lysine coated slides for demonstration of pan-cytokeratin (CK), estrogen receptor alpha (ER) and progesterone (PR) receptors. Sections were incubated with primary antibodies followed by HRP conjugated secondary antibody and then counter stained with Mayer's haematoxylin.

Clinically, the animal was dull and showed severe abdominal distension with bilateral abduction of forelimbs (Fig. 1). In transabdominal ultrasonography, an irregular mass varying echogenicity adjacent to spleen with high vascularization was observed. Lateral abdominal radiography revealed the radiodense mass caudal to kidney and pulmonary metastases were also noticed in x-ray (Fig. 2). Computed tomography showed a mass beneath the kidneys and extending up to bladder with HU index 60 to 75, suggestive of tumor (Fig. 3). Complete blood count revealed leucocytosis (25.08 x $10^3$ cells/µl) and serum biochemical values showed mild hypercalcemia (15.7 mg/dl).

Grossly, cauliflower like hard mass was present on the right ovary (Fig. 4) measuring about 71.2 mm x 112 mm (length & breadth), weighing around 1.2 kg and the cut surface of the mass showed papillary pattern with haemorrhage (Fig. 5). But the left ovary was normal. The cytological smears prepared from the mass revealed large unified cluster of proliferating epithelial cells were arranged in papillary pattern. The neoplastic epithelial cells exhibited significant anisocytosis with indistinct cell border and anisokaryosis. The cytoplasm was pale blue, contained secretory vacuoles and granules (Fig. 6). The nuclei were uniformly ovoid with hyperchromatia and open chromatin.

On histopathological examination, the tumor mass revealed irregular branching of proliferating epithelial cells in papillary pattern, numerous glandular structures with slit like opening and micropapillary growth (Fig. 7). The numerous papillary projections of surface epithelium appeared as arboriform pattern with micropapillary growth. The multiple layers of pleomorphic cuboidal cells lined the walls of cystic cavities and invasion of neoplastic cells into large stromal core. The neoplastic cells were characterized by scanty eosinophilic cytoplasm, round to ovoid hyperchromatic nucleus with dense chromatin. In addition, the neoplastic cells were invading into the supporting stroma tissue. The immunohistochemical analysis of the ovarian mass demonstrated the positive immunoreaction for pan-cytokeratin (Fig. 8) and estrogen receptor alpha (ER) (Fig. 9). The surface epithelium of ovarian mass revealed moderate to strong cytoplasmic expression of AE1/AE3 and nuclear expression of ER. However, the ovarian mass did not show any expression for progesterone receptor (PR).

The mild hypercalcaemia observed in this study was in accordance with previous workers who also reported the elevated serum calcium in 10-year old Golden Retriever with ovarian serous papillary adenocarcinoma[3]. The gross pathology and cytology observed in the present study were in accordance with the earlier reports[7]. Histopathology of the mass in the present study revealed more micropapillary growth and this observation was in concurrence with the earlier findings[2,6].

AE1/AE3 is a pan cytokeratin marker used to identify the proliferations of epithelial origin. AE1/AE3 expression in this study agreed with the earlier authors[8]. The strong immunoreaction of ER in this study was more evident in this study compared with previous reports. ER expressions in neoplastic cells suggest that

estrogen secreted from the ovaries might have contributed to the proliferation of ovarian papillary adenocarcinoma which clearly indicates the ovarian tumors are estrogen dependent. The negative IHC expression of PR in this study was contrary to the finding of previous workers who encountered positive expression in the subsurface epithelial structures[14]. The negative response to PR in the present study might be of progesterone independent nature of ovarian papillary adenocarcinoma in this bitch.

## REFERENCES


1. Ramos-Vara JA, Beissenherz ME, Miller MA, Johnson GC, Kreeger JM, Pace LW and Yamini B. 2001. Immunoreactivity of A103, an antibody to Melan A, in canine steroid-producing tissues and their tumors. *J Vet Diagnos Invest* **13:** 328-332.
2. Dolensek T, Knific T, Ramírez GA, Erles K, Mallon HE, Priestnall SL and Suárez-Bonnet A. 2024. Canine ovarian epithelial tumours: histopathological and immunohistochemical evaluation with proposed histopathological classification system. *J Comp Pathol* **212:** 42-50.
3. Hori Y, Uechi M, Kanakubo K, Sano T and Oyamada T. 2006. Canine ovarian serous papillary adenocarcinoma with neoplastic hypercalcemia. *J Vet Med Sci* **68:** 979-982.
4. Klein MK. 1996. In: Small Animal Clinical Oncology, 2nd edn. (Withrow SJ and MacEwen EG, eds.), WB Saunders, Philadelphia, pp. 347-455.
5. Meuten DJ. 2017. Tumors in domestic animals. 5th edn. Wiley India Pvt. Ltd., New Delhi, pp. 690-692.
6. Banco B, Antuofermo E, Borzacchiello G, Cossu-Rocca P and Grieco V. 2011. Canine ovarian tumors: an immunohistochemical study with HBME-1 antibody. *J Vet Diagnos Invest* **23:** 977 -981.
7. Kita C, Chambers JK, Tanabe M, Irie M, Yamasaki H and Uchida K. 2022. Immunohistochemical features of canine ovarian papillary adenocarcinoma and utility of cell block technique for detecting neoplastic cells in body cavity effusions. *J Vet Med Sci* **84:** 406-413.
8. Akihara Y, Shimoyama Y, Kawasako K, Komine M, Hirayama K, Kagawa Y, Omachi T, Matsuda K, Okamoto K, Kadosawa T and Taniyama H. 2007. Immunohistochemical evaluation of canine ovarian tumors. *J Vet Med Sci* **69:** 703-708.
9. Bossard C, Busson M, Vindrieux D, Gaudin F, Machelon V, Brigitte M and Lazennec G. 2012. Potential role of estrogen receptor beta as a tumor suppressor of epithelial ovarian cancer. *PLoS ONE* **7:** e44787.
10. Mungenast F and Thalhammer T. 2014. Estrogen biosynthesis and action in ovarian cancer. *Front Endocrinol* **5:** 192.
11. Simpkins F, Garcia-Soto A and Slingerland J. 2013. New insights on the role of hormonal therapy in ovarian cancer. *Steroids* **78:** 530-537.
12. Hill KK, Roemer SC, Churchill ME and Edwards DP. 2012. Structural and functional analysis of domains of the progesterone receptor. *Mol Cell Endocrinol* **348:** 418-429.
13. Lenhard M, Tereza L, Heublein S, Ditsch N, Himsl I, Mayr D, Friese D and Jeschke U. 2012. Steroid hormone receptor expression in ovarian cancer: progesterone receptor B as prognostic marker for patient survival. *BMC Cancer* **12:** 553.
14. Khaki F, Javanbakht J, Sharifzad S, Gharagozlou MJ, Khadivar F, Manesh JYY and Abdi FS. 2016. Metastatic ovarian papillary cystadenocarcinoma to the small intestine serous surface: report of a case of high-grade histopathologic malignancy. *J Ovarian Res* **17:** 33.

*Indian J. Vet. Pathol., 49(2) : 192-195, 2025: DOI: https://doi.org/10.56093/ged2gj88*

CASE REPORT

# Pathology of *Spirocerca lupi* associated oesopageal fibrosarcoma in a dog: A case report

**K. Gopal*, S. Sivaraj, K. Sowmya, K. Dhandapani, P. Balachandran and P. Srinivasan**
Department of Veterinary Pathology, Veterinary College and Research Institute, Namakkal-637 002, Tamil Nadu Veterinary and Animal Sciences University, Chennai-600 051, India

**Address for Correspondence**
*K. Gopal, Assistant Professor, Department of Veterinary Pathology, Veterinary College and Research Institute, Namakkal-637 002, Tamil Nadu Veterinary and Animal Sciences University, Chennai-600 051, India, E-mail: drvetpal@gmail.com*

*Received: 10.2.2025; Accepted: 22.2.2025*

## ABSTRACT

*Spirocerca lupi* is associated with the formation of sarcomas in the oesophagus of canines. A nine-year-old male Labrador carcass was presented for postmortem examination. The necropsy revealed gelatinization of subcutaneous fat and rounded up heart with gelatinization of epicardial fat. The liver was slightly enlarged, mottled in appearance with rounded borders. Kidney showed pitted up appearance on cortex. The prostate showed moderate enlargement. A nodule measuring about 5 × 4 cm in size was observed on the distal oesophagus just proximal to gastric cardia. On incision of nodule, a reddish worm was extracted. Histopathological examination of the nodule revealed spindle to plumpy cells arranged in intertwining whorls with little amount of collagen. Degeneration and necrosis of hepatocytes were observed around the central veins whereas cells around portal triads showing mild fatty changes. Kidney revealed mononuclear cell infiltration in the interstitium along with mild fibrosis. Intestinal mucosa revealed patches of hemorrhages, mucosal necrosis and mononuclear cell infiltration in the sub mucosa. Glandular epithelium of prostate showed papillary like projections into the lumen. Based on gross and histopathological examination, the case was diagnosed as *Spirocerca lupi* induced oesophageal fibrosarcoma.

**Keywords:** Dog, fibrosarcoma, oesophagus, *Spirocerca lupi*

Spirocercosis presents a significant risk as a parasitic ailment affecting both domestic and wild canines and felines caused by the spirurid nematode *Spirocerca lupi*. Although the disease is found worldwide, its highest prevalence is reported in tropical and subtropical regions[1]. Dung beetles or coprophagous beetles, serve as intermediate hosts. Additionally, lizards, snakes, frogs, birds, rodents and rabbits may also act as paratenic hosts for the parasite[2]. Spirocercosis often associated with scarring and aneurysm of the aorta, spondylitis of the thoracic vertebrae, also *Spirocerca lupi*, inhabits the esophageal wall of hosts results in the formation of sizable, thick walled, cystic granulomas in the submucosa of the caudal oesophagus[3] and may prompt malignant alterations in the oesophageal wall, characterized by the development of mesenchymal neoplasms such as fibrosarcoma and osteosarcoma[4]. The present communication reports a fatal case of *Spirocerca lupi* induced oesophageal fibrosarcoma and associated pathological changes in a dog.

A nine-year-old male Labrador carcass was presented for postmortem examination with the history of lateral recumbency for past two weeks. The complete necropsy was carried out and samples were collected in 10% neutral buffered formalin for histopathological examination. Nematodes were extracted from the cavity of the nodule in the oesophagus and preserved in 70% alcohol for identification and confirmation. The formalin-fixed tissue samples being cut into thin sections (4 microns) and placed on glass slides. These slides were then stained with Haematoxylin and Eosin (H&E).

External examination revealed shrunken eyeballs with pale mucous membrane and edema in both hind limbs. The internal examination revealed gelatinization of subcutaneous fat. Serous fluid of about 1 liter and 200 ml was noticed in the abdominal cavity and pericardial sac respectively. A nodule measuring about 5×4 cm in size was observed on the distal oesophagus just proximal to gastric cardia (Fig. 1). The nodule was hard to cut and a reddish coiled worm was extracted. Heart showed rounded appearance with gelatinization of epicardial fat along with thinning of left ventricular wall. The kidneys appeared shrunken and the capsule peeled off with difficulty, revealing a pitted cortex (Fig. 2). Lungs were leathery in appearance and slightly hard in consistency. The liver was slightly enlarged, mottled in appearance with rounded borders. The intestinal lumen contained mucoid contents and the mucosa revealed diffuse haemorrhages with numerous tiny round worms. Multiple

**How to cite this article :** Gopal, K., Sivaraj, S., Sowmya, K., Dhandapani, K., Balachandran, P. and Srinivasan, P. 2025. Pathology of *Spirocerca lupi* associated oesopageal fibrosarcoma in a dog: A case report. Indian J. Vet. Pathol., 49(2) : 192-195.

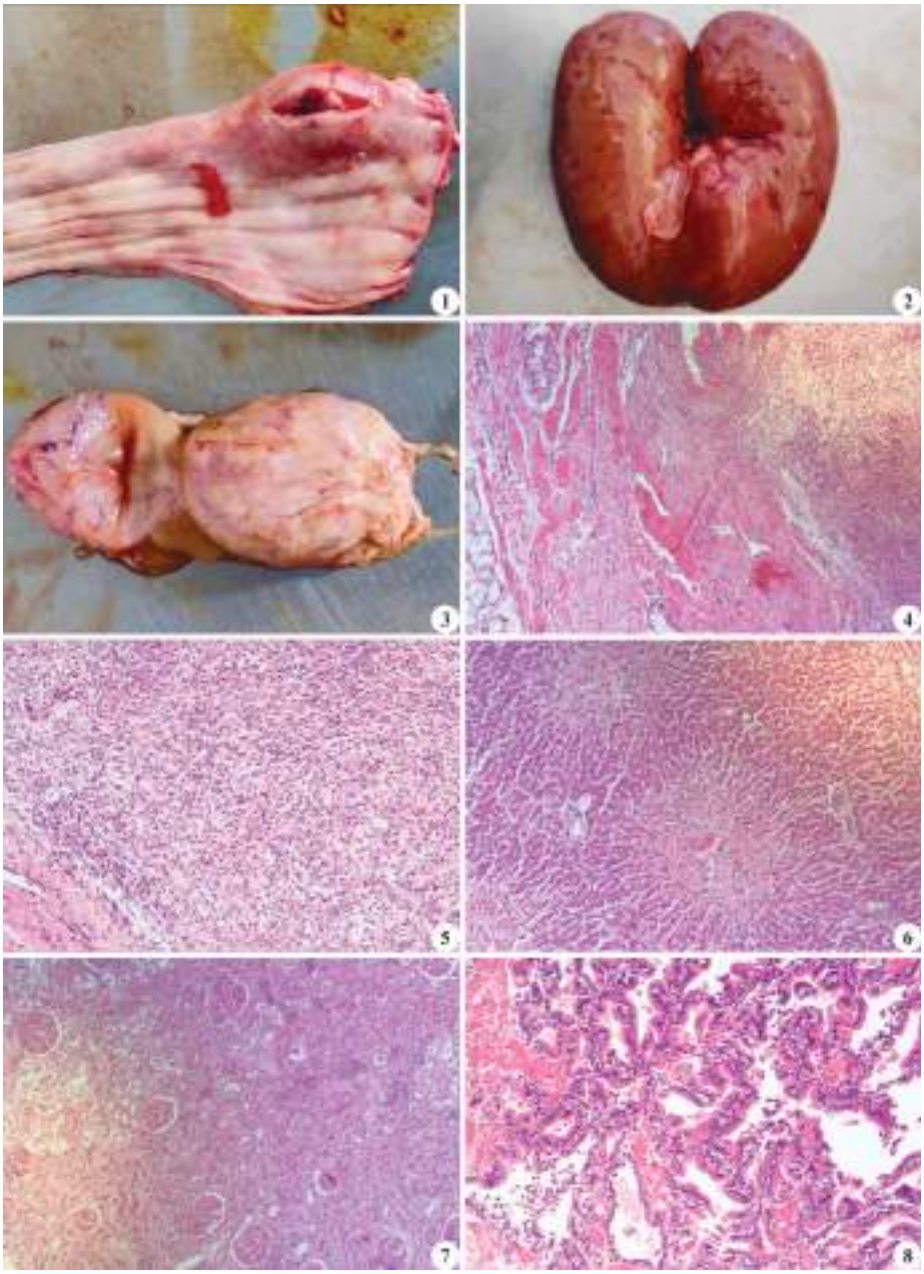

**Fig. 1.** Oesophagus - Nodule in distal oesophagus just proximal to gastric cardia and a mature *S. lupi* on the mucosa; **Fig. 2.** Kidney showing pitted up appearance in the sub capsular area; **Fig. 3.** Prostate showing moderate enlargement; **Fig. 4.** Fibrosarcoma - Exophytic tumour mass raised from the mucosa of oesophagus (H&E x40); **Fig. 5.** Fibrosarcoma showing haphazardly arranged spindle shaped cells with plumpy nucleus (H&E x100); **Fig. 6.** Liver - CVC - Nutmug pattern (H&E x40); **Fig. 7.** Kidney revealed interstitial fibrosis with MNC infiltration (H&E x40); **Fig. 8.** Prostate - Hyperplastic epithelium thrown into papillary folds (H&E x100).

ulcers were observed on thickened intestinal mucosa. The urinary bladder was empty, the lumen contained brownish calculi and the mucosa showed severe congestion. The prostate showed moderate enlargement (Fig. 3).

Parasitological examination revealed a reddish pink, coiled female *Spirocerca lupi* measuring about 5.1 cm in length. The worm had six lips with hexagonal mouth and a dorsally curved tail end.

Histopathology of the oesophagus revealed a well capsulated tumour mass raised from the mucosa (Fig. 4). The tumour mass composed of haphazardly arranged spindle shaped cells. The neoplastic cells contained plumpy elongate nucleus with prominent nucleolus (Fig. 5). Considerable anisocytosis and anisokaryosis were observed in the tumour cell population. Few areas showed metaplasia of fibrous tissue into osteoid tissue. Left ventricle, muscle fibers were small and contained more closely placed nucleus which indicates

the atrophy of the cardiac muscle fibers. This might be due to continuous pressure on the aorta which prevents the complete empting of left ventricle during systole, as a result the stasis of blood occurs in the left ventricles leading to chronic venous congestion that leads to compensatory heart failure, which is evident by the characteristic nutmeg pattern in the liver. The hepatocytes around the central vein showed degeneration and necrosis with more number of RBCs, where as the hepatocytes around the portal triad showed mild fatty changes (Fig. 6). Bile duct hyperplasia was seen in few areas. Lung revealed edema fluid accumulation in the alveoli and inter alveolar space. Kidney showed chronic interstitial nephritis, characterized by fibrous tissue proliferation in the severely affected areas, small glomeruli and plasma cell infiltration in the interstitium (Fig. 7). Patchy areas of necrosis and haemorrhages were observed on the intestinal mucosa. The submucosa was infiltrated with mononuclear cells. The hyperplastic prostate epithelium was thrown into folds and papillary projections into the lumen (Fig. 8). The epithelium was lined by tall columnar cells with centrally placed nucleus.

The diagnosis of spirocercosis is still challenging due to many factors like small or atypically located nodules, presenting the case early disease stages, differentiating the *S. lupi* induced benign nodule and a neoplastic tumuor. Atypical cases or aberrant migration are also diagnostically challenging[5]. Computed tomography (CT) is a particularly useful method for diagnosing tiny intraluminal, mural and extraluminal nodules, abnormally positioned nodules, and dystrophic aortic mineralization[6]. However, CT examination is still not affordable in all developing countries. Ultrasonography is not an effective diagnostic tool for spirocercosis in dogs but the lesions like vascular wall irregularity and thickening in the abdominal aorta or celiac artery might be due to migration of *S. lupi*. Therefore, clinical diagnosis of spirocercosis mostly depends on thoracic radiography, which shows a caudodorsal mediastinal mass, caudal thoracic vertebral spondylitis and aortic undulation from aneurysm formation[7].

In general, postmortem examination reveals the nodules in the oesophagus and other lesions in the aorta. The caudal oesophageal mass and aortic aneurysms are considered to be a pathognomonic to spirocercosis[8]. In the present case, we found a nodule in the oesophagus but there was no aneurysm in the aorta. Most of the time the spirocercosis is subclinical and produce the considerable lesions in the oesophagus including granulomas, sarcomas and other lesions are aortic aneurysms, thoracic discospondylitis or spondylosis, hypertrophic osteopathy[9] and salivary gland necrosis have been occasionally reported[10]. The oesophageal neoplasia is extremely rare where the spirocercosis does not exist, so spirocercosis is the major cause of oesophageal neoplasia in the dog[11] and therefore this is considered as a potential natural model for carcinogenesis study[12]. The nodule in the present case was firm in consistency, thick fibrotic wall; cavity contained a single worm and little quantity of yellow pus[13]. Generally the presence of helminthes leads to formation of high substitution rate granulomas, which were characterized by the presence of macrophages with mitotic division, epithelioid cells, giant cells, lymphocytes and fibrous tissue[13]. But in the present case, there was no granuloma however we observed highly cellular fibrosarcoma with few metaplastic changes.

Spondylitis of the thoracic vertebrae is considerably constant in spirocercosis[14] but in the present study this was the incidental finding during the postmortem examination. Radiographic results were not available to confirm the thoracic spondylitis. Other lesions reported in spirocercosis include pulmonary edema, atelectasis and pneumonia, hyperemia and fatty changes in liver, interstitial nephritis and adhesive cystitis[12,15]. In the present case we observed the pulmonary edema, nutmug pattern in liver, chronic nephritis, uroliths, chronic enteritis and prostate hyperplasia. These lesions might be associated with other diseases. Even in the modern era of diagnostic facility, early diagnosis of infection is still a challenge.

## REFERENCES


1. McGavin DM and Zachary JF. 2007. Pathologic basis of veterinary disease, (4th Edn), Mosby Elsevier, St. Louis. Pp. 322-323.
2. Da Fonseca EJ, Do Amarante EE, de S Abboud LC, Hees SJ, Franco RJ and de A Silva BJ. 2012. Fatal esophageal fibrosarcoma associated to parasitism by spirurid nematode Spirocerca lupi in a dog: a case report. *J Parasit Dis* **36:** 273-276.
3. Rinas MA, Nesnek R, Kinsella JM and DeMatteo KE. 2009. Fatal aortic aneurysm and rupture in a neotropical bush dog (Speothos venaticus) caused by Spirocerca lupi. *Vet Parasitol* **164:** 347-349.
4. Blume GR, Reis Junior JL, Gardiner CH, Hoberg EP, Pilitt PA, Monteiro RV and de Sant'Ana FJ. 2014. Spirocerca lupi granulomatous pneumonia in two free-ranging maned wolves (Chrysocyon brachyurus) from central Brazil. *J Vet Diagn Invest* **26:** 815-817.
5. Dvir E, Kirberger RM, Clift SJ and Van der Merwe LL. 2010. Review: challenges in diagnosis and treatment of canine spirocercosis. *Isr J Vet Med* **65**.
6. Dvir E, Kirberger RM and Malleczek D. 2001. Radiographic and computed tomographic changes and clinical presentation of spirocercosis in the dog. *Vet Radiol Ultrasound* **42:** 119-129.
7. Merhavi N, Segev G, Dvir E and Peery D. 2020. Ultrasonography is insensitive but specific for detecting aortic wall abnormalities in dogs infected with *Spirocerca lupi*. *Vet Rec* **187:** e59-e59.
8. Harrus S, Harmelin A, Markovics A and Bark H. 1996. Spirocerca lupi in the dog: aberrant migration. *J Am Anim Hosp Assoc* **32:** 125-130.
9. Fox SM, Burns J and Hawkins J. 1988. Spirocercosis in dogs. *Compend Small Anim* **10:** 807-822.
10. Schroeder H and Berry WL. 1998. Salivary gland necrosis in

dogs: a retrospective study of 19 cases. *J Small Anim Pract* **39:** 121-125.
11. Porras-Silesky C, Mejías-Alpízar MJ, Mora J, Baneth G and Rojas A. 2021. *Spirocerca lupi* Proteomics and Its Role in Cancer Development: An Overview of Spirocercosis-Induced Sarcomas and Revision of Helminth-Induced Carcinomas. *Pathogens* **10:** 124.
12. Sasani F, Javanbakht J, Javaheri A, Hassan MM and Bashiri S. 2014. The evaluation of retrospective pathological lesions on spirocercosis *(Spirocerca lupi)* in dogs. *J Parasit Dis* **38:** 170-173.
13. Jones TC, Hunt RD and King NW. 1997. Disturbances of growth: aplasia to neoplasia. In: Jones TC, Hunt RD and King NW eds. Veterinary Pathology, (6th Edn), Williams and Wilkins, Baltimore, pp. 110-112.
14. van der Merwe LL, Kirberger RM, Clift S, Williams M, Keller N and Naidoo V. 2008. *Spirocerca lupi* infection in the dog: a review. *Vet J* **176:** 294-309.
15. De Aguiar I, García R, Madriz D, Alfaro-Alarcón A, Montenegro VM, Aizenberg I, Baneth G and Rojas A. 2021. Esophageal spirocercosis with pulmonary egg deposition and secondary hypertrophic osteopathy in a dog from Costa Rica. *Vet Paras Reg Stud Rep* **23:** 100-510.

| | | |
|---|---|---|
| *Title of Thesis* | : | Pathomorphological studies on heart and aorta in different animal species with special reference to atherosclerosis - A comparative study |
| *Name of the Student* | : | **Doddamreddy Harshitha Reddy** |
| *Name of the Advisor* | : | Dr P. Amaravathi |
| *Degree/Year* | : | MVSc/2025 |
| *Name of the University* | : | Sri Venkateswara Veterinary University, Tirupati-517 502, Andhra Pradesh |

The cardiovascular system plays an important role in maintaining physiological wellbeing of the animals. The literature regarding pathomorphology of the heart and aortas in different animals were meagre. So, the present study was conducted to address this gap, which helps in better understanding of heart and aortic lesions in different animals.

The present study involved the collection and examination of the heart and aorta samples of 120 animals which included cattle, sheep, goat, pigs and dogs. Among the hearts of different animals, degenerative changes in hearts of goats had highest prevalence of 83% whereas in aorta it was noted in dogs (83%). Vascular disturbances with highest prevalence (93%) were noted in hearts of pigs while in aortas of goats had highest prevalence (58%). Growth disturbances were frequently noted in goats with 83% prevalence in goats and 17% prevalence in aortas. Inflammatory changes were highest in hearts of dogs with 83% prevalence whereas in aortas prevalence was more in goats (54%). Highest parasitic conditions in hearts with 73% prevalence was observed in sheep and the aortas of cattle had 7% prevalence. Necrosis of heart was 4% in goats, calcification was noted mostly in 4% hearts and 8% aortas of goats, pigmentation in 8% hearts of goat, tumors in 17% hearts and aortas and miscellaneous conditions were documented.

Macroscopically, in hearts, petechial hemorrhages were observed in cattle. Hydropericardium, serous atrophy of epicardial fat, fat necrosis and fibrinous pericarditis were noticed in sheep and goats. Hypertrophy of ventricles in pigs, congestion and hemorrhages in dogs were recorded. The aortas of one cattle and one sheep showed elevated areas in intima remaining aortas had smooth intimal surface.

Histopathological examination of hearts and aortas of different animals showed various pathological lesions. Degenerative changes like cloudy swelling, vacuolar degeneration, fatty change, hyaline degeneration with homogenous, swollen, cardiac muscle fibres and acidophilic cytoplasm, myxomatous degeneration that had stellate shaped cells with long cytoplasmic processes and bluish cytoplasm and amyloid deposition in between smooth muscle fibres were noticed. Vascular changes like congestion, hemorrhages and growth disturbances like hypertrophy, hyperplasia with increased size and number of smooth muscle cells and metaplasia of connective tissue were noted. Inflammatory cells infiltration in different layers of hearts and aortas were noticed in aortas. Sarcocysts in hearts and cut section of parasite in aortas were observed. Calcification, pigmentation, tumors showed characteristic microscopic features. Sarcolysis, individual bradyzoites in hearts and scar tissue, perinuclear vacuolation, periarteritis in aortas showed distinct patterns.

Immunohistochemical studies revealed immunoreactivity to VEGF and CD31 in endothelial cells and tunica intima of aorta. Positive immune reaction to cytochrome - C in degenerating changes of hearts and aortas were observed. Apoptotic cells in tunica media showed positive reaction for caspase-9 and proliferating smooth muscle cells in angioma showed reactivity for Ki-67. Mild reactivity for collagen-III was noted in proliferating connective tissues in aorta.

| | | |
|---|---|---|
| *Title of Thesis* | : | Pathomorphology of canine epithelial tumors with special reference to perianal gland proliferations |
| *Name of the Student* | : | **S. Preetha** |
| *Name of the Advisor* | : | Dr M. Sasikala |
| *Degree/Year* | : | MVSc/2025 |
| *Name of the University* | : | Tamil Nadu Veterinary and Animal Sciences University |

The present work was conducted to study the pathomorphology of canine epithelial tumors with special reference to perianal gland proliferations. The incidence, haematology, serum biochemistry, radiography, gross pathology, cytology, histopathology and immunohistochemistry were performed in dogs (48 cases) with epithelial tumor. Serum gonadal hormone assay, antioxidant profile and histochemistry were performed only in dogs (22 cases) suspected for perianal gland tumors.

The annual incidence rate of epithelial tumors recorded at Veterinary Clinical Complex, Veterinary College and Research Institute, Namakkal was 58.5 per cent. Among epithelial tumors, the occurrence of perianal gland tumors was 45.83 per cent. The incidence of all the epithelial tumors including perianal gland tumor was highest in non-descript dogs. The mean age of the dogs affected with epithelial tumor was observed as 9.03 years ranging from 4 to 15 years of age. The mean age of the dogs affected with perianal gland tumor was observed as 9.95 years ranging from 4 to 16 years of age. The perianal gland tumors were found only in the intact male dogs and the other epithelial tumors were found predominantly in intact female dogs.

Haematological parameters like TEC and Hb values showed highly significant reduction whereas, the PCV value differed significantly in perianal gland tumor affected dogs compared to control and other epithelial tumor affected dogs. Serum biochemical parameters like ALT and creatinine showed significant increase in the perianal gland tumor affected dogs.

Perianal gland carcinoma cases revealed a highly significant increase in serum testosterone and reduction in estradiol level when compared to control, perianal gland adenoma and epithelioma groups.

A 2.5 fold elevation of SOD, 1.2 fold elevation of CAT, 4.7 fold elevation of GPx and 7.7 fold elevation of GSH was seen in the perianal gland tumor tissues. 5 out of 48 dogs revealed varying degrees of pulmonary metastases in thoracic radiological findings that indicates different stages of tumor progression. The tumors were more localized in perianal region, mammary gland, head, trunk, followed by tail and extremities. In head, the tumors were distributed in ocular region and skin of perioral, forehead and mandibular region. The trunk had distribution of tumors in thorax, ventral abdomen, neck and ovary. In extremities tumors were found in digits.

The generalized clinical signs exhibited by the epithelial tumor affected dogs including perianal gland tumor was similar irrespective of the type of tumors. Otherwise, the affected animals exhibited the specific signs related to the anatomical location that involved in the tumor manifestation. The dogs with perianal gland tumor exhibited constipation, strain during defecation, pruritis and varying sings related to GI tract according to degree of invasion and site of tumor.

Cytological examination of perianal gland and epithelial tumors revealed characteristic epithelial cells arranged in clusters and also in discrete population. The perianal gland tumors displayed both hepatoid and reserve cells in clusters with varied population.

Histopathological examination revealed three types of perianal gland tumors and five different types of epithelial tumors. Out of 48 epithelial tumors, the perianal tumors were more in number followed by mammary gland tumors, squamous cell carcinoma, basal cell carcinoma, anaplastic carcinoma and ovarian adenocarcinoma. Histologically, the perianal gland tumors were classified into perianal gland adenoma, perianal gland carcinoma and perianal gland epithelioma.

Immunohistochemistry revealed immunopositivity to pan-cytokeratin in all the epithelial tumors including perianal gland tumors. Further, the perianal gland tumors showed varying degree of immunopositivity to Ki-67, p63, BCL-2, AR and ER but showed negative expression to HER2.

| | | |
|---|---|---|
| *Title of Thesis* | : | Pathology and Host Immune Response in Pigeons Affected with Newcastle Disease Virus |
| *Name of the Student* | : | **Dr Syedah Asma Andrabi** |
| *Name of the Advisor* | : | Dr Nawab Nashiruddullah |
| *Degree/Year* | : | PhD/2023 |
| *Name of the University* | : | Sher-e-Kashmir University of Agricultural Sciences & Technology, Jammu (J&K) |

With the intent to study the prevalence and pathology of Newcastle disease in pigeons and backyard fowl flocks, localities around Ranbir Singh Pura and Jammu city were investigated for outbreaks of the disease from March 2021 to September 2022. The disease was suspected in sixteen pigeon *(Columba livia domestica)* flocks and five flocks of backyard fowl *(Gallus gallus domesticus)*, with 89.66% and 100% morbidity and approximately 81.8% and 91.5% mortality rates, respectively. Chiefly neurological signs in pigeons, and predominantly respiratory and/or enteric clinical signs in fowls were recorded. Gross lesions in pigeon were subdural haemorrhages, meningeal congestion or haemorrhages in the brain stem and lungs but rarely in the proventriculus. In fowls, gross lesions were mainly manifested by vascular derangement, causing haemorrhages on proventriculus and enteric mucosa and corresponding necrotizing enteritis. Haemorrhages were evident in most of the organs of the respiratory tract, while mild congestion of meninges was noticeable in few birds. Microscopic lesions in both pigeons and fowl validated the gross lesions typical of Newcastle Disease, pertaining to the neurotropic form in pigeons and viscerotropic form in fowls. Preliminary diagnosis was also based on Haemagglutination assay showing 78.7% positivity with clinical samples. Confirmation of the disease in all clinical samples and infected allantoic fluids was done using Reverse Transcriptase PCR (RT-PCR) targeting a partial Fusion protein gene. Six isolates, three from each pigeon and fowl ND outbreaks from different geospatial locations of the region were sequenced and allotted accession numbers from GenBank. Sequence comparison of isolates showed five of the six isolates with close homology (99.6-100%) to each other. Deducted amino acid sequence at the Fusion protein cleavage site showed a $^{112}$R-R-Q-K-R*F$^{117}$ velogenic motif for all pigeon and fowl isolates. Biological characterization also showed velogenic pathotypic traits with indicators like Mean Death Time (MDT <60 hrs), and pronounced cytopathic effect (CPE) in chicken embryo fibroblasts (CEF). Phylogenetic analysis showed that the three pigeon isolates and two fowl isolates clustered within genotype II, and one of the fowl isolate clustered with sub genotype VII.1.1. Experimental trial was conducted in 45 healthy pigeons divided into three groups consisting of pigeons inoculated with genotype II NDV pigeon isolate (Group-I) and genotype VII NDV fowl isolate (Group-II), respectively via intranasal and intraocular route. Control group was mock infected with PBS. Signs, gross and histopathological lesions were recorded on 1$^{st}$, 3$^{rd}$ and 7$^{th}$ day post infection along with mRNA expression of selected innate immune proteins (Pattern Recognition Receptors (PRR's): TLR-7, TLR-3 and RIG-1), anti-viral inflammatory cytokines/ chemokines (CCL-5, IFN-γ, IL-10, IL-6 and IL-1β) and apoptotic factors (BCL-2). Progressive signs and lesions were apparent in both the groups after 3 dpi. Lesions were predominantly associated with nervous system in Group-I birds and respiratory and enteric system in-Group-II birds. In general, increased mRNA expression of PRRs was evident in both groups; and expression of pro-inflammatory cytokines (IL-6, IL-1β, and IFN-γ) and chemokines (CCL-5) in the spleen, lung and brain was fairly up-regulated as compared to the mock-infected control birds in both the groups, signifying a robust innate and anti-viral inflammatory response. Delayed expression of BCL-2, an anti-apoptotic factor was evident in lungs while early expression in spleen in both the groups. Strain homology, unique mutations and establishment of experimental infection in heterologous host could suggest the possible cross-transmission potential between avian species and emerging threats of circulating ND viruses in the region.

# OBITUARY

## Dr L.N. Acharjyo Passes Away

**Dr Lakshmi Narayan Acharjyo** was a renowned expert in zoo and wildlife health, who played a pivotal role in shaping wildlife healthcare in India for over six decades. Dr Acharjyo served as a Veterinarian at Nandankanan Zoological Park from 1967 to 1992. He earned his BVSc and AH at Bihar University during 1955-59 and his MVSc in Pathology at Orissa University of Agriculture and Technology from 1983-1985. He had extensively worked on ecology, biology, behaviour, management, antler cycle of deer, pathology, parasites and diseases of wildlife especially in captivity. He also edited Indian Zoo Yearbooks and authored over 300 scientific articles focused on animal health and wildlife biology. One of the Dr Acharjyo's greatest editorial achievements has been to assemble the publications entitled "A compendium of publications from Indian zoos Vol I, II and III' published by Indian Zoo Directors association and central Zoo authority. He was honoured with numerous national and international awards including an Honorary DSc from OUAT. He was the member of the Technical Committee of Nandankanan Zoological Park from the year 2000 to 2022. He was awarded Fellow IAVP in the year 2002. He passed away from old age on 30$^{th}$ April, 2025. IAVP family extends their condolences to the departed soul.